

Department of Chemical and Process Engineering

**Understanding and mitigating the
consequences of undesired
crystallisation taking place during
washing of active pharmaceuticals**

Muhid Bin Shahid

Thesis submitted at the University of Strathclyde in accordance with
the requirements for the Degree of Philosophy

2023

Declaration of Author's Rights

This thesis is the result of the author's original research. It has been composed by the author and has not been previously submitted for examination which has led to the award of a degree.

The copyright of this thesis belongs to the author under the terms of the United Kingdom Copyright Acts as qualified by University of Strathclyde Regulation 3.50. Due acknowledgement must always be made of the use of any material contained in, or derived from, this thesis.

Signed: *Muhid Bin Shahid*

Date: 10/07/2023

Acknowledgements

First and foremost, I would like to praise and thank Allah SWT for his greatness and for giving me the strength and courage to complete my thesis, Alhamdulillah.

I would like to thank my supervisor, Dr Chris Price, for allowing me the opportunity to undertake this research project and for his endless support and guidance through the last four years. He always provided me with encouragement and freedom to carry out extra work and activities apart from the PhD project, to help build my skills and CV which have been very beneficial so far in my career after this PhD. I would also like to thank him for providing me with a chance to work with some amazing colleagues; Sara Ottoboni, Georgia Sanxaridou and Clarissa Forbes.

I would like to acknowledge Dr Leo Lue, my secondary supervisor, for his technical support throughout with data analysis. I would also like to thank all my colleagues at CMAC and the Chemical engineering department that have helped me throughout with my work and personal life.

To all the people who I have collaborated with over the time of this PhD, thank you, as none of this would be possible without you all. I would like to acknowledge the humongous support of Sara Ottoboni, for her friendship, her helpful discussions, her guidance, and her kind offer to proofread my thesis. Georgia Sanxaridou for her help in the lab and being an instrumental part of the solubility lab work carried out in my first authored paper. Chloé Faure, for her hard work in the lab during her internship which helped provide data for my second authored paper. Colm Cotter, Billy Hicks and James Black for their help and the opportunity to conduct research with AstraZeneca for few months as part of this PhD project.

I would like to sincerely thank my family – mum, brother & wife – for putting up with me over the last few years, for all their patience and constant support.

Finally, I would like to dedicate this thesis to my late father, Dr Mohammad Shahid, who unfortunately won't be able to read this thesis, but played an instrumental part in guiding me throughout my university career and was the main reason for me on taking up this PhD. Himself, a PhD graduate from Strathclyde university, I still remember the tears in his eyes, the day I told him about me getting an offer to carry this PhD at Strathclyde. I know seeing me finish this degree would have meant a great deal to him and not having him there would make the occasion much less joyful.

Abstract

In the pharmaceutical industry, the final drug substance (active pharmaceutical ingredients (API)), and the key synthetic intermediates are mostly isolated as crystalline solids. A considerable amount of effort is spent in the crystallisation process to produce a crystalline solid with the requisite chemical quality together with the right physical properties (filterability, product size, uniformity, etc.), for isolation and further downstream processing to manufacture the drug product. Whilst carefully designed upstream processes may attain the desired crystal properties in suspension, these are often compromised during the isolation of the API by filtration, washing and drying. These isolation processes pose significant challenges to the production of crystals with the desired physical properties; avoiding granulating, or breaking the crystals, or precipitating dissolved product and impurities.

Washing is a key step in pharmaceutical isolation to remove the unwanted crystallisation solvent and dissolved impurities (mother liquor) from the API filter cake to ensure the purity of the product whilst maximising yield. The aim of this thesis is to understand how the physiochemical properties of crystallized material and the wash solvent can affect the characteristic of the API product at the end of the washing process. Strategies for optimal wash solvent selections are explored to help minimise dissolution of API product crystals while preventing precipitation of product or impurities. This is done by taking solubility measurement of commonly used binary solvent mixtures of; paracetamol API, crystallisation solvent and wash solvent. The results of these solubility measurements are presented together with a methodology to analyse anti-solvent effect of different solvent combinations. The data from these results are used for selection of wash solvent to avoid both these phenomena which can be challenging but is essential to maintain yield, purity, and particle characteristics throughout the isolation process.

A major objective of this work aims to improve pharmaceutical product quality, increase sustainability, and reduce manufacturing cost. Constant rate filtration/washing is employed that allows for collection of separate aliquots during all stages of filtration, washing and deliquoring of the API cake. This enables a wash profile to be obtained, as well as providing an overall picture on the mass of API lost during isolation and so can assist in optimizing the washing strategy. This constant rate methodology was tested using paracetamol API together with blue dye used as an impurity to allow for visualization of washing process of a filtered API cake. Analysis of the filtrate collected during this study was found to be useful in determining the endpoint of washing, the amount of API lost during the washing process and the likely extent of agglomeration occurring during washing to be evaluated.

Further work looks at employing particle size distribution measurement techniques to quantify agglomerate formation caused during the washing process. Several different lab-based particle size distribution techniques were employed to analyse washed API cake, however, none of them were found to be successful in providing conclusive results. This work highlighted some of the challenges of characterising API particles obtained from a multi-component system at the end of the washing process. This demonstrates that sizing wet clumped material is even more challenging than sizing dried but agglomerated product.

The final component of this work was the development of a wash process workflow to assist with design and optimisation of an API washing process. This workflow collates all the learning developed throughout the different studies in this PhD project to produce a workflow which provides an optimum strategy for designing of washing processes in pharmaceutical isolation of APIs. This workflow was validated using an industrial compound from AstraZeneca with the constant rate methodology successfully used to investigate optimum washing process parameters for the investigated compound.

Contents

| | |
|--|--------------|
| <i>Declaration of Author's Rights</i> | <i>ii</i> |
| <i>Acknowledgements</i> | <i>iii</i> |
| <i>Abstract</i> | <i>v</i> |
| <i>Contents</i> | <i>viii</i> |
| <i>Papers published and conferences attended</i> | <i>xi</i> |
| <i>List of figures</i> | <i>xiii</i> |
| <i>List of tables</i> | <i>xviii</i> |
| 1. Introduction | 1 |
| 1.1 General Introduction | 2 |
| 1.2 Washing theory | 3 |
| 1.3 Solubility in mixed system | 7 |
| 1.4 Crystallisation kinetic in anti-solvent system | 8 |
| 1.5 Axial dispersion in packed beds | 9 |
| 1.6 Agglomeration | 10 |
| 1.7 Model compounds | 12 |
| 1.7.1 Paracetamol | 12 |
| 1.7.2 AZ200/2 | 14 |
| 1.7.3 Impurities | 14 |
| 1.8 General aims and objectives of research | 15 |
| 1.9 Abbreviations | 17 |
| References | 17 |
| 2. Exploring the role of anti-solvent effects during washing in active pharmaceutical ingredient purity | 22 |
| 2.1 Introduction | 23 |
| 2.2. Materials and Method | 26 |
| 2.2.1 Raw Material | 26 |
| 2.2.2 Sample Preparation | 28 |
| 2.2.3 Anti-solvent screening procedure | 29 |
| 2.2.4 Post anti-solvent procedure analysis | 31 |
| 2.2.5 Gravimetric solubility analysis procedure | 32 |
| 2.3 Results & Discussions | 33 |
| 2.3.1 Anti-solvent effect – Glass vial method | 33 |
| 2.3.2 Anti-solvent effect– Centrifuge vial method | 38 |
| 2.4 Conclusion | 47 |

| | |
|--|------------|
| 2.5 Abbreviations | 50 |
| References..... | 50 |
| 3. Employing constant rate filtration to assess active pharmaceutical ingredient (API) washing efficiency..... | 53 |
| 3.1 Introduction..... | 54 |
| 3.2 Material and Method..... | 56 |
| 3.2.1 Raw Materials | 56 |
| 3.2.2 Suspension Preparation..... | 57 |
| 3.2.3 Experimental Setup & Design..... | 59 |
| 3.2.4 Liquid Filtrate Off-line Post Analysis | 63 |
| 3.2.5 Solid API Cake Off-line Post Analysis..... | 64 |
| 3.3 Results and Discussion..... | 65 |
| 3.3.1 API loss | 68 |
| 3.3.2 Purity..... | 71 |
| 3.4 Conclusion | 78 |
| 3.5 Abbreviations | 79 |
| References..... | 79 |
| 4. Investigating particle size distribution of agglomerates formed during washing process..... | 82 |
| 4.1 Introduction..... | 83 |
| 4.2 PSD analysis of washed API material from Chapter 3..... | 86 |
| 4.3 Material and Method..... | 93 |
| 4.3.1 Raw Materials | 93 |
| 4.3.2 Sample Preparation | 94 |
| 4.3.3 Experimental Procedure..... | 94 |
| 4.3.4 Laser diffraction particle size analysis..... | 96 |
| 4.3.5 Focused Beam Reflectance Measurement (FBRM) analysis..... | 96 |
| 4.4 Results and Discussion..... | 97 |
| 4.4.1 Sample handling..... | 97 |
| 4.4.2 Laser diffraction analysis results..... | 99 |
| 4.4.3 Focused Beam Reflectance Measurement (FBRM) analysis results | 107 |
| 4.4.4 Other particle analysis techniques tested..... | 113 |
| 4.5 Conclusion | 117 |
| 4.6 Abbreviation..... | 119 |
| References..... | 119 |
| 5. Optimising removal of impurity on an industrial active pharmaceutical ingredient (API) using constant rate washing methodology | 121 |

| | |
|--|-----|
| 5.1 Introduction | 122 |
| 5.2 Wash process workflow | 123 |
| 5.3 Material and Method | 128 |
| 5.3.1 Raw Materials | 128 |
| 5.3.2 Suspension Preparation | 129 |
| 5.3.3 Experimental Setup | 132 |
| 5.3.4 Liquid Filtrate Post Off-line Analysis | 134 |
| 5.3.5 Solid API Cake Post Off-line Analysis | 136 |
| 5.3.6 Design of Experiment (DoE) | 136 |
| 5.4 Results and Discussion | 139 |
| 5.4.1 Experimental complications | 139 |
| 5.4.2 DoE results obtained – IC1 impurity | 143 |
| 5.4.3 Experimental result obtained – Red Dye impurity | 150 |
| 5.5 Conclusion | 153 |
| 5.6 Abbreviations | 154 |
| References | 154 |
| 6. Conclusion and Future Work | 156 |
| 6.1 Conclusion | 156 |
| 6.2 Future Work | 159 |
| <i>Appendix A - Exploring the role of anti-solvent effects during washing in active pharmaceutical ingredient purity</i> | 162 |
| <i>Appendix B - Employing constant rate filtration to assess active pharmaceutical ingredient (API) washing efficiency</i> | 175 |
| <i>Appendix C - Optimising removal of impurity on an industrial active pharmaceutical ingredient (API) using constant rate washing methodology</i> | 189 |
| <i>Appendix D - Investigating particle size distribution of agglomerates formed during washing process</i> | |

Papers published and conferences attended

Publications

- Shahid, M.; Sanxaridou, G.; Ottoboni, S.; Lue, L.; Price, C. Exploring the role of antisolvent effect during washing on active pharmaceutical ingredient purity. *Org. Process Res. Dev.* 2021. 25, 4, 969–981 (first author).
- Shahid, M.; Faure, C.; Ottoboni, S.; Lue, L.; Price, C. Employing constant rate of filtration to assess active pharmaceutical ingredient (API) washing efficiency. *Org. Process Res. Dev.* 2022. 26, 1, 97–110 (first author).
- Ottoboni, S.; Shahid, M.; Steven, C.; Coleman, S.; Meehan, E.; Barton, A.; Firth, P.; Sutherland, R.; Price, C. J. Developing a batch isolation procedure and running it in an automated semi continuous unit: AWL CFD25 case study. *Org. Process Res. Dev.* 2020. 24. 4. 520-539 (co-author).

Conference proceedings

- Fluid and impurity transport during online isolation experiments conducted with X-ray tomography. Sara Ottoboni, Muhid Shahid, Alan Martin, Thokozile Kathyola, Gunjan Das, Sven Schroeder, Shashidhara Marathe, Christopher Rau, Kaz Wanelik, Chris John Price. 13th World Filtration Congress. 2021. (co-author).

Conference presentations:

- Understanding and mitigating the consequences of undesired crystallisation taking place during washing of active pharmaceuticals. Muhid Shahid, Georgia Sanxaridou, Sara Ottoboni, Leo Lue, Chris Price. 50th British Association of Crystal Growth Conference, 9th-11th July 2019. Presentation at student conference. Poster at the BACG annual conference.

- Exploring the role of anti-solvent effects during washing on active pharmaceutical product purity. Muhid Shahid, Chloé Faure, Sara Ottoboni, Leo Lue, Chris Price. 13th World Filtration Congress, 5th-9th October 2022, San Diego, USA. Presentation by Sara Ottoboni on my behalf.

Contribution to public engagement

- Explorathon at Glasgow science museum, “Crystal Builder” workshops – 2018 & 2019
- School engagement event at Gorbals Stem Outreach
- Stem Ambassador school visits at Lockerbie primary school, Crookston primary school and St Marnock’s RC primary school

List of figures

| | |
|--|----|
| Figure 1-1: Schematic of a cake washing process | 4 |
| Figure 1-2: Wash curve obtained from measuring the solute concentration of the filtrate ¹⁵ | 5 |
| Figure 1-3: Paracetamol chemical structure | 12 |
| Figure 1-4: Molecular packing diagram of paracetamol - form I ⁵² | 13 |
| Figure 1-5: Paracetamol related impurities - chemical structures | 15 |
| Figure 2-1: SEM image of dried paracetamol agglomerate showing formation of crystal bridges | 25 |
| Figure 2-2: Glass vial precipitation detection method..... | 29 |
| Figure 2-3: Centrifuge vial precipitation detection method..... | 30 |
| Figure 2-4: Ethanol - n-heptane glass vial precipitation qualitative test | 33 |
| Figure 2-5: Quantitative analysis of the ethanol-acetonitrile case. a.) Solubility of paracetamol in ethanol-acetonitrile binary solvent mixture at 22 °C. b.) Percentage of solute precipitating out of solution for different wash solution compositions is shown in the Y axis on the left hand side of the graph, with the supersaturation achieved in the solution when different ratio of wash solution is added to the saturated crystallisation solvent shown on the Y axis on the right hand side of the graph..... | 39 |
| Figure 2-6: Quantitative analysis of the ethanol - n-heptane case. a.) Solubility of paracetamol in ethanol - n-heptane binary solvent mixture at 22 ° | 43 |
| Figure 2-7: XRPD results for raw paracetamol, metacetamol and acetanilide together with the precipitate sample obtained from ethanol – n-heptane sample..... | 46 |
| Figure 3-1: Experimental procedure | 59 |
| Figure 3-2: Experimental setup for constant rate filtration including process flow diagram of the setup used..... | 62 |
| Figure 3-3: Evolution of blue dye impurity concentration in filtrate – EXP 1 | 64 |
| Figure 3-4: a.) Close-up of a few dried filtrate vials showing presence of precipitated material. b.) Collected filtrate vials from experiment 15 showing gradual blue dye impurity removal from the system..... | 67 |
| Figure 3-5: Experiment 15 – paracetamol grade – crystalline, crystallisation solvent: isoamyl alcohol, wash solvent – acetonitrile, filtration & washing rate – 100 rpm, volume of wash | |

| | |
|--|----|
| solvent – 3 cake void volume, number of washes – 3, mass of PCM API lost during wash = 1.48 g..... | 68 |
| Figure 3-6: Experiment 1 – paracetamol grade – crystalline, crystallization solvent – ethanol, wash solvent – n-heptane, filtration & washing rate – 10 rpm, volume of wash solvent – 1 cake void volume, number of washes – 3, mass of PCM API lost during wash = 0.1 g | 68 |
| Figure 3-7: DoE variables that effect API loss during the wash process, R2 = 0.93, Q2 = 0.61, reproducibility = 0.97 | 69 |
| Figure 3- 8: a.) Graph showing cumulative API loss in filtrate samples throughout experiment 8, mass of PCM API lost during wash = 0. b.) Graph showing cumulative API loss in filtrate samples throughout the experiment 13, mass of PCM API lost during wash = 0 | 70 |
| Figure 3-9: DoE variables that affect mother liquor removal during the wash process, R2 = 0.77, Q2 = 0.27, reproducibility = 0.80 | 72 |
| Figure 3-10: DoE variables that affect blue dye impurity removal during washing, R2 = 0.79, Q2 = 0.35, reproducibility = 0.44 | 72 |
| Figure 3-11: Images of all the API washed cakes taken at the end of experiment and sorted in terms of wash solvent, number of washes and void volume of wash solvent | 73 |
| Figure 3-12: a.) Biotage filter tube from experiment 3 after n-dodecane wash solvent addition. b.) Paracetamol API cake obtained at the end of experiment 3 with a layer of the blue dye at the top of the washed cake. | 75 |
| Figure 4-1: DoE variables that affect particle size distribution (D10) of washed cake - change in D10, R2 = 0.80, Q2 = 0.52, reproducibility = 0.97 | 88 |
| Figure 4-2: DoE variables that affect particle size distribution (D50) of washed cake - change in D50, R2 = 0.82, Q2 = 0.58, reproducibility = 0.97 | 88 |
| Figure 4-3: DoE variables that affect particle size distribution (D90) of washed cake - change in D90, R2 = 0.60, Q2 = 0.05, reproducibility = 0.81 | 89 |
| Figure 4-4: a.) PSD of raw micronised PCM and of final washed cakes from EXP 10 (D10: 15.2 µm, D50: 43.8 µm, D90: 638.3 µm) & EXP 18 (D10: 35.1 µm, D50: 72.9µm, D90: 128.2µm). b.) PSD of raw crystalline PCM and of final washed cakes from EXP 4 (D10: 27.8 µm, D50: 76.5 µm, D90: 201.0 µm) & 19 (D10: 26.8 µm, D50: 76.7 µm, D90: 154.4 µm). c.) PSD of raw granular PCM and of final washed cakes from EXP 5 (D10: 292.4 µm, D50: 397.4 µm, D90: 531.8 µm) & EXP 8(D10: 312.8 µm, D50: 437.0 µm, D90: 606.4 µm)..... | 91 |
| Figure 4-5: a. Filtered API cake obtained from a Biotage tube after filtration. b. Vertically sliced API cake, with the other half re-suspended in dispersant..... | 95 |
| Figure 4-6: Filtered and washed crystalline PCM API cake which is not deliquored properly | 97 |

Figure 4-7: Examples of API cakes obtained at the end of washing process. a.) Micronised PCM API cake. b.) Crystalline PCM API cake. c.) Granular PCM API cake..... 98

Figure 4-8: Particle size distribution of PCM API obtained from both dry and wet cell analysis. a.) Micronised PCM PSD obtained; Dry Cell Analysis - D10: 3 µm, D50: 9 µm, D90: 29 µm; Wet Cell Analysis - D10: 30 µm, D50: 75 µm, D90: 152 µm. b.) Crystalline PCM PSD obtained; Dry Cell Analysis - D10: 5 µm, D50: 32 µm, D90: 150 µm; Wet Cell Analysis - D10: 12 µm, D50: 44 µm, D90: 101 µm. c.) Granular PCM PSD obtained; Dry Cell Analysis - D10: 53 µm, D50: 249 µm, D90: 450 µm; Wet Cell Analysis - D10: 247 µm, D50: 361 µm, D90: 518 µm. 100

Figure 4-9: a.) PSD obtained for the two filtration runs for micronised PCM; Breakthrough - D10: 33 µm, D50: 77 µm, D90: 140 µm; Dryland - D10: 32 µm, D50: 78 µm, D90: 150 µm. a.) PSD obtained for the two wash runs for micronised PCM; Bad case - D10: 42 µm, D50: 128 µm, D90: 316 µm; Good case- D10: 42 µm, D50: 119 µm, D90: 226 µm.. 102

Figure 4-10: a.) PSD obtained for the two filtration runs for crystalline PCM; Breakthrough - D10: 101 µm, D50: 1470 µm, D90: 2610 µm; Dryland - D10: 31 µm, D50: 93 µm, D90: 232 µm. a.) PSD obtained for the two wash runs for crystalline PCM; Bad case - D10: 39 µm, D50: 119 µm, D90: 221 µm; Good case- D10: 42 µm, D50: 142 µm, D90: 294 µm. 102

Figure 4-11: a.) PSD obtained for the two filtration runs for granular PCM; Breakthrough - D10: 280 µm, D50: 481 µm, D90: 1292 µm; Dryland - D10: 202 µm, D50: 289 µm, D90: 512 µm. a.) PSD obtained for the two wash runs for granular PCM; Bad case - D10: 246 µm, D50: 367 µm, D90: 535 µm; Good case- D10: 269 µm, D50: 397 µm, D90: 573 µm. 102

Figure 4-12: a.) PSD obtain for micronised PCM during different isolation stages. b.) Percentile particle size values obtained for the distributions shown in a. 105

Figure 4-13: a.) PSD obtain for crystalline PCM during different isolation stages. b.) Percentile particle size values obtained for the distributions shown in a. 105

Figure 4-14: a.) PSD obtain for granular PCM during different isolation stages. b.) Percentile particle size values obtained for the distributions shown in a. 105

Figure 4-15: Images obtained of dispersed filtered/washed API cake samples for mastersizer analysis. a.) Image of dispersed sample in a duran bottle taken from bottom showing the large agglomerates present in the sample. b & c.) Images of API mastersizer samples allowed to settle showing the large agglomerates present within..... 107

Figure 4-16: a.) Example of particle size trend obtained from Mettler Toledo FBRM iC software for micronised PCM obtained at the end of good case of washing. b.) Average chord length distribution obtained for micronised PCM (good washing case) using FBRM..... 108

Figure 4-17: a.) Unweighted CLD obtained for micronised PCM during different isolation stages. b.) Square-weighted CLD obtained for micronised PCM during different isolation stages..... 110

Figure 4-18: Images obtained from PVM probe during the different micronised analysis runs, with FBRM results attached in Figure 5-13. a.) Images of raw micronised PCM dispersed in saturated ethanol. b.) Images of micronised PCM filtered to dryland and then dispersed in saturated ethanol. c.) Images of micronised PCM washed using bad case scenario and then dispersed in isooctane. d.) Images of micronised PCM washed using good case scenario and then dispersed in isooctane. 111

Figure 4-19: a.) Unweighted CLD obtained for crystalline PCM during different isolation stages. b.) Square-weighted CLD obtained for crystalline PCM during different isolation stages..... 111

Figure 4-20: Images obtained from PVM probe during the different crystalline analysis runs, with FBRM results attached in Figure 4-19. a.) Images of raw crystalline PCM dispersed in saturated ethanol. b.) Images of crystalline PCM filtered to dryland and then dispersed in saturated ethanol. c.) Images of crystalline PCM washed using bad case scenario and then dispersed in isooctane. d.) Images of crystalline PCM washed using good case scenario and then dispersed in isooctane. 112

Figure 4-21: a.) Unweighted CLD obtained for granular PCM during different isolation stages. b.) Square-weighted CLD obtained for granular PCM during different isolation stages. 112

Figure 4-22: Images obtained from PVM probe during the different crystalline analysis runs, with FBRM results attached in Figure 4-21. a.) Images of raw granular PCM dispersed in saturated ethanol. b.) Images of granular PCM filtered to dryland and then dispersed in saturated ethanol. c.) Images of granular PCM washed using bad case scenario and then dispersed in isooctane. d.) Images of granular PCM washed using good case scenario and then dispersed in isooctane. 112

Figure 4-23: Images showing PCM API stuck to the wall of the vessel and the probe at the end of analysis. 113

Figure 4-24: Graphs obtained from a micronised PCM measurement carried out using an EasyViewer provided by Mettler Toledo. a.) Trend for turbidity and chord length obtained during the micronised PSD analysis run. b.) Chord length distribution obtained for micronised PCM during the different stages of the run..... 116

Figure 4-25: Images obtained from an EasyViewer for micronised PCM at different stages of the run with results shown in Figure 4-24. a.) Image of micronised PCM particles at the start of analysis dispersed in saturated ethanol. b.) Image of micronised PCM particles at the start of analysis dispersed in saturated ethanol before heptane addition. c.) Image of micronised PCM particles after heptane addition to the slurry mixture, causing aggregation. d.) Image of micronised PCM particles after heptane addition with an increase in stirrer speed to 600 rpm. e.) Images of micronised PCM particles at the end with the increase in stirring causing the aggregate to break up a little..... 117

Figure 5-1: Washing isolation workflow developed..... 124

| | |
|--|-----|
| Figure 5-2: Cooling jacket used for biotage filter tube..... | 131 |
| Figure 5-3: Process flow diagram of the filtration/washing experimental set-up..... | 132 |
| Figure 5-4: Post washing experiment analysis of the filtrate fraction samples (IC1 impurity) | 134 |
| Figure 5-5: Post washing experiment analysis of the filtrate fraction samples (Red Dye impurity) | 134 |
| Figure 5-6: Dry filtrate sample vial take from the vacuum oven..... | 141 |
| Figure 5-7: IC1 concentration in filtrate obtained from experiment 8. The red line shows the 8 ppm limit specification of the HPLC test | 142 |
| Figure 5-8: a.) Coefficient plot of DoE variables that effect API loss during the washing process, R2 = 0.998, reproducibility = 0.996. b.) Contour plot obtained for the API loss | 145 |
| Figure 5-9: a.) Coefficient plot of DoE variable that effect the final washed cake IC1 concentration, R2 = 0.549, reproducibility = 0.546. b.) Contour plot obtained for the IC1 concentration..... | 146 |
| Figure 5-10: a.) Coefficient plot of DoE variable that effect the percentage decrease in IC1 concentration, R2 = 0.529, reproducibility = 0.439. b.) Contour plot obtained for the percentage decrease in IC1 concentration..... | 147 |
| Figure 5-11: a.) Coefficient plot of DoE variables that effect the change in particle size, D10, R2 = 0.573, reproducibility = 0.585. b.) Coefficient plot of DoE variable that effect the change in particle size, D50, R2 = 0.366, reproducibility = 0.122. c.) Coefficient plot of DoE variable that effect the change in particle size, D90, R2 = 0.715, reproducibility = 0.742. | 148 |
| Figure 5-12: Sweet spot plot for reducing IC1 impurity using the DoE result obtained..... | 149 |
| Figure 5-13: a.) Filtrate vial samples obtained for experiment R1. b.) Wash profile curve for red dye impurity concentration and the cumulative API lost graph obtained for experiment R1 | 150 |

List of tables

| | |
|---|-----|
| Table 2-1: Wash solutions of different ratios that were tested for each solvent system..... | 28 |
| Table 2-2: Precipitation caused for different solvent combinations - glass vial method. The crystallisation solvent used is provided on the left side of the table whilst the wash solvent across the top of the table. The ratio of the wash solution at which precipitation is first observed in the solvents system for paracetamol API case is given here. (The bold numbers correspond to the volume ratio of crystallisation solvent in the wash solution, while the italic number corresponds to the volume ratio of wash solvent in the wash solution.) | 36 |
| Table 2-3: Experimental solubility determined of paracetamol in the selected solvent at 22 °C (average lab temperature at which this anti-solvent effect study is conducted) | 37 |
| Table 2- 4: ΔC achieved for the solvent combinations used. Blue cells represent scenarios where nucleation and crystallisation was observed. Orange cell represent scenarios where local supersaturation resulted in nucleation and then dissolution of crystals as bulk saturation is reached. | 37 |
| Table 2- 5: Precipitation caused by different solvent combinations - centrifuge vial method. The crystallisation solvent used is reported on the left side of the table whilst the wash solvent across the top of the table. The ratio of wash solution at which precipitation is first observed in these solvent system for paracetamol as a representative API is reported here. (The bold numbers correspond to the volume ratio of crystallisation solvent in the wash solution, while the italic number corresponds to the volume ratio of wash solvent in the wash solution.) | 38 |
| Table 2-6: Ratio of wash solvent in the final solution mixture..... | 39 |
| Table 2-7: Experimental solubility determined of Metacetamol and Acetanilide in the selected solvent at 25 °C. | 41 |
| Table 2- 8: Mass of API and impurities in the 120 μ l ethanoic solution..... | 44 |
| Table 3-1: Particle size distribution of different PCM grades investigated within this study . | 56 |
| Table 3-2: Solubility measurements determined experimentally at 22oC (lab temperature) .. | 58 |
| Table 3-3: Table of factors, responses and analytical techniques used to quantify the responses in the DoE | 61 |
| Table 4-1: Response used for particle size distribution to quantify in the DoE | 87 |
| Table 4- 2: Factors used for experiments presented in Figure 3-14 | 91 |
| Table 5-1: Table of factors, responses and analytical techniques used to quantify the responses in the DOE | 137 |

| | |
|--|-----|
| Table 5-2: Experiments carried out with IC1 impurity..... | 138 |
| Table 5-3: Experiments carried out with Red Dye impurity..... | 138 |
| Table 5- 4: API loss responses obtained from DoE experiment..... | 145 |
| Table 5-5: API loss and impurity removal results obtained from the red dye impurity experiments..... | 152 |
| Table 5- 6: Change in particle size distribution at the end of the washing process for experiment with 20 mL wash volume. Negative percentage values in the table represent a decrease in the particle size after the washing process..... | 152 |

1. Introduction

1.1 General Introduction

In the pharmaceutical industry, crystallisation is a widely used purification technique employed to obtain active pharmaceutical ingredient particles of the required size, purity and crystal habit.^{1,2} Hence, crystallisation has been extensively researched to establish understanding and control of the key mechanisms that take place during this process to create the desired product with the requisite chemical and physical properties.³

Following crystallisation, filtration, washing and drying are the isolation steps required to separate the active pharmaceutical ingredient (API) crystals from the unwanted, impure mother liquor.⁴ Filtration uses a porous medium to retain the API crystals and separate them from the impure mother liquor which surrounds the crystals at the end of the crystallisation process.⁵

Washing involves using a clean wash solvent to remove the unwanted impurities present within the mother liquors trapped between the API crystals in the filter cake. Drying is the final step required to remove the residual solvent (predominantly the wash solvent as most of the mother liquor will have been displaced during washing) from the API crystals forming the filter cake. The aim of drying is to produce a consistent, stable and free-flowing product ready for secondary processing (formulation).⁶ Ideally, the complete isolation process should be achieved without any changes to the crystals produced during crystallisation. Any breakage or granulation of crystals, or precipitation of dissolved product or impurities from the mother liquor onto the crystal surface should be avoided.⁷ Recently attention has started to be paid to optimising pharmaceutical isolation processes especially filtration and drying. The major objective being to investigate the mechanisms affecting the product crystal attributes during these processes. This includes understanding the key mechanisms controlling filtration and washing, and involves designing continuous and semi-continuous filtration, washing and drying rigs and investigating new analytical methods for effectively measuring the crystal product attributes obtained during and at the end of the isolation processes.⁸⁻¹³

Washing in pharmaceutical manufacturing is still relatively unexplored with very few academic publications.¹⁴⁻¹⁶ Washing plays a vital role in isolation since it is pivotal in the removal of impurities and mother liquor from the API filter cake. Residual impure mother liquor present in the wet filter cake at the end of filtration contains any unreacted starting materials, unwanted side products (impurities of synthesis) and any degradants. If the remaining mother liquor is not removed, then the non-volatile dissolved materials would be deposited on the crystal surfaces during drying increasing the impurity levels in the final isolated cake.¹⁴ This could result in the product failing to meet the purity requirements set out in the International Council for Harmonisation of Technical Requirement for Pharmaceuticals for Human use (ICH) Q6A guideline.¹⁷

This PhD project looks at increasing and adding to the scientific understanding around the API washing process. Some of key mechanisms taking place during the washing process, which can affect its performance, are explored with the aim to provide a guide which assist with designing an optimised washing process.

1.2 Washing theory

Washing displaces the mother liquor present in the filtered cake with a wash solvent. This allows for removal of dissolved raw material and impurities from the API crystal product. Tien (2012), proposes that washing of a filter cake is carried out by three main mechanisms; (1) displacement of mother liquor in the cake, (2) reslurrying of filter cake, (3) consecutive dilution.^{8,15} During washing the wash solvent first displaces the mother liquor from the large pores in the cake; then the mother liquor from the adjacent narrower pores in the cake diffuses into the wash solvent. The resulting solute transport is regarded as axial dispersion. During subsequent washing steps both diffusion and dispersion processes occur in combination. The

schematic of washing process occurring within the cake as proposed by Tien (2012) can be seen in Figure 1-1.

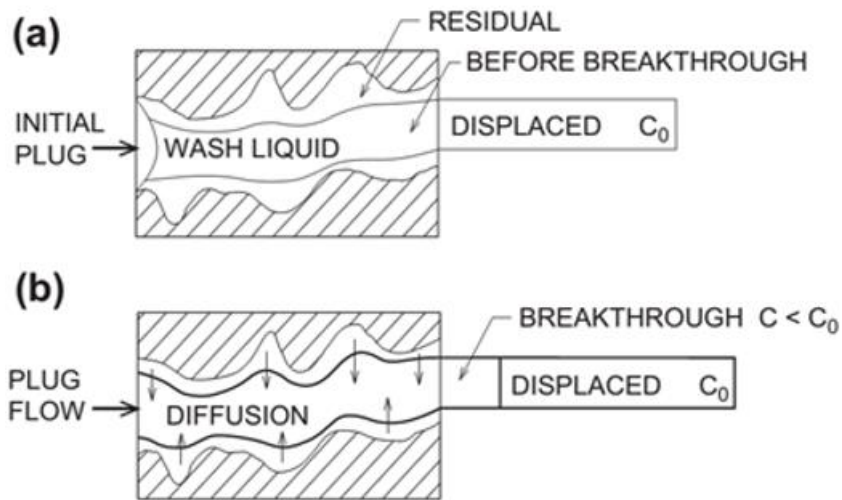


Figure 1-1: Schematic of a cake washing process

One of the ways of measuring the cake washing process is by determining the solute (impurity and API) concentration of the collected filtrate as a function of wash ratio, where wash ratio is defined as volume of wash solvent used divided by volume of mother liquor trapped in the cake at start of the washing process. For solute concentration, remaining impurity concentration ratio, c^* , is used Equation 1:

$$c^* = \frac{c}{c_0} \quad \text{Equation 1}$$

Where, the remaining impurity concentration (c) is related to initial concentration (c_0). Figure 1-2 shows three idealised washing curves obtained which can be divided into three main regions. (I) is the initial displacement region (a plug flow regime) where the residual mother liquor is removed from the larger pores due to wash solvent entrance. (II) is the intermediate stage where direct displacement of mother liquor occurs in the smaller pores and the wash solvent starts to dilute the mother liquor as it passes through the larger pores and hence the mass transfer process starts. (III) is the mass transfer region, where diffusion is the rate-limiting

step as mother liquor diffuses from the fine pore structure into the wash solvent over the entire volume of the cake.¹⁸

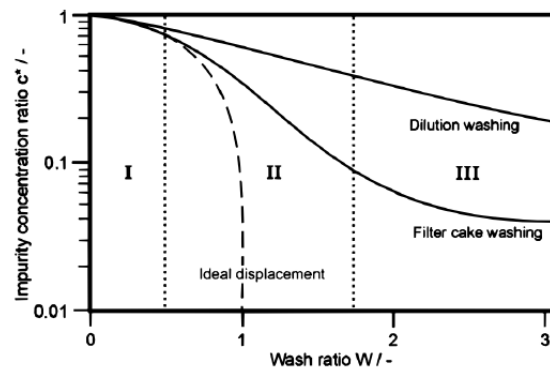


Figure 1-2: Wash curve obtained from measuring the solute concentration of the filtrate¹⁵

In an ideal case, the wash solvent would run in a plug-flow regime displacing all the mother liquor from the cake, as is the case in region I. This is due to the high efficiency of the ideal displacement regime and hence a small amount of wash solvent is required. However, ideal displacement can never be reached in real systems where there is a distribution of particle size rather than a perfect mono size product, in practice a combination of displacement, dilution and diffusion washing mechanism are required for effective washing.

The relative importance of each regime in a given experiment depends on the physical operating conditions, solvent properties, and the microstructure of the pores in the filter cake influencing the local wash liquid flow rate.^{18,19,20} Particle morphology (shape) and size distribution therefore affect washing performance. Cakes formed of larger particles contain larger pores and wider pathways which reduces the specific resistance of the cake and enables higher wash flowrates.²¹ Cakes formed with fine particles and broad particle size distribution have smaller pore networks, lower permeability and hence filtration times are extended. Mass transfer and diffusion mechanisms play a bigger role in the washing regime of such filter cakes. Further negative effects such as local under saturation of wash medium or formation of cracks or craters due to malformation of the cake can lead to liquid by passing or channelling

(especially when high driving force is applied).¹⁵ Chapter 3 in this thesis looks to further investigate the effect of material with different particle size on washing process performance.

Generally, washing is performed immediately after filtration to avoid the cake surface beginning to dry. The ideal starting condition being a well-formed filter cake with a level surface which is fully saturated with mother liquor.^{15,22} Wash solvent is carefully distributed over the top of the cake, preferably using a misting spray, as disturbance to cake surface can lead to thin spots and cracks resulting in the wash bypassing areas as it follows the path of least resistance.

Selection of the wash solvent is an essential part of the API cake washing process. It is important to pick a solvent that will minimise dissolution of the API crystals, whilst also avoiding any precipitation of both dissolved API and impurities when the wash solvent comes into contact with the retained crystallization solvent in the saturated filtered cake. Selecting a wash solvent to avoid both these phenomena can be challenging but is essential to maintain yield, purity, and particle characteristics of the crystals obtained through the crystallization processes.

To be effective the wash solvent should ideally have the following properties:²³

- Sufficient solubility of the unwanted impurities to ensure they remain in solution or dissolve; Low solubility of the API product to minimise product loss during the washing process;
- Miscibility with the mother liquor to allow diffusion and dilution mechanisms;
- The viscosity of the wash solvent should be similar to the crystallisation solvent to allow for appropriately long contact with the crystals to allow removal of impurity from the cake without excessive filtration cycle time;¹⁴

- The API product should have thermal stability in the wash solvent under drying process conditions needed to remove the wash solvents;
- The volatility of the wash solvent should be kept appropriately low to assist with the drying process.

Chapter 2 of this thesis further elaborates and investigates some of these properties of wash solution.

1.3 Solubility in mixed system

Knowing the solubility of the active pharmaceutical ingredient in pure solvents and solvent mixtures is essential for several aspects of pharmaceutical manufacturing. Pure solvents are used in many manufacturing stages such as solubilization, extraction, crystallisation etc. However, solvent mixtures are often employed during manufacturing processes to improve certain physical properties such as solubility and miscibility of the API compound, for example, in anti-solvent crystallisation, or in spray dried formulation, etc.^{24,25}

Solubility of APIs in solvent mixtures are widely investigated and reported in literature. These studies often use gravimetric analysis to experimentally determine solubilities in binary solvent mixture and are often accompanied by a corresponding model developed to correlate and predict solubilities of those API compounds in the different solvent mixtures evaluated.^{26,27,28}

Paracetamol is one of the APIs, which due to its simple molecular structure is widely studied for solubility measurement both in pure and binary solvent mixtures. The hydrogen bonding ability of paracetamol as both donor and acceptor allows it to have high solubility in polar protic solvents. The solubility of paracetamol in mixtures of solvents have shown to have a maximum at a specific solvent composition. This is in accordance with the regular solution theory, where for a given solid in a cosolvent, the solubility curve shows a maximum at a specific solvent composition (the effective solubility parameter of a cosolvent is a function of

the solvent composition), if the solubility parameter of solute is between the solubility parameters of solvents. This phenomenon of solubility maxima have also been observed for other APIs in solvent mixtures in literature.^{29,30,31}

Chapter 2 of this thesis investigates the solubility of Paracetamol API in crystallisation and wash solvent mixtures. The study looks to understand possible solubility maxima formation for the solvent mixture that would be encountered during the washing process in the packed bed of API formed during filtration and tries to understand the effect of this phenomena on the API crystals during isolation.

1.4 Crystallisation kinetic in anti-solvent system

Anti-solvent crystallisation is a separation/purification method used to effectively remove solid from a solution.³² The solid is usually produced in the form of crystals, where an anti-solvent addition into the solution reduces solubility of solute and induces rapid crystallisation. Scientists can develop this process to control crystalline properties such as particle size and morphology. The physical and chemical properties of the anti-solvent can alter the rate of supersaturation generation during mixing within the solution and thereby affect the rate of nucleation and crystal growth.^{33,34}

Formation of a crystalline phase has two main steps: nucleation and crystal growth. Nucleation is the birth of stable crystal nuclei – either spontaneously in the solution (primary nucleation) or in presence of existing crystals in the system, (secondary nucleation). Crystal growth is the addition of solute onto the existing crystals in the system, resulting in an increase in size. The relationship between supersaturation, nucleation and crystal growth was defined by J. Nývlt (1968) using empirical models. Nucleation is frequently describe using power law model:^{35,36}

$$B = k_b \Delta C^b \quad \text{Equation 2}$$

Where B is the nucleation rate, k_b is the nucleation constant, ΔC is the supersaturation, b is the nucleation power.

Similarly, crystal growth is frequently described using an analogous power law model:

$$G = k_g \Delta C^g \quad \text{Equation 3}$$

Where G is the growth rate, k_g is the growth constant, and g is the growth power. The rate constants, in these power law models, are known as Arrhenius rate functions of temperature:

$$k_g = k'_g e^{-E_g/RT} \quad \text{Equation 4}$$

Where k'_g is pre-exponential for the kinetic growth pre-factor, E_g is the activation energy for growth, R is the universal gas constant and T is the temperature. For organic crystallisation systems, the value of growth rate constant, k_g , is typically between 1 and 2 and the value of nucleation rate constant, k_b , is typically between 5 and 10. These equations show the importance of crystal surface area in crystal slurry in determining crystal nucleation and growth kinetics. At the start of crystallisation process when the surface area of crystals present is low and there is likely high supersaturation, crystal nucleation dominates over crystal growth. As the crystallisation process proceeds, the crystal surface area increases and with lower supersaturation, crystals are likely to grow faster than they nucleate. In literature, growth rate parameters have also shown to be dependent on other factors, such as agitation and crystal size.³⁷

1.5 Axial dispersion in packed beds

Axial dispersion in pack beds refers to the phenomenon of incomplete mixing or dispersion of fluid components along the axial direction in a bed of packed particles, as encountered during washing process of API crystal particles. In pack beds, fluid flows through the interstitial voids between the particles and hence mass transfer and any chemical reactions take place between the fluid and the solid phase.³⁸ Axial dispersion leads to variation in concentration along the

bed length, mainly caused due to parameters such as viscosity and density of fluids, length of the packed column, ratio of column diameter and length to particle diameter, particle size distribution, particle shape, effect of fluid velocity and of temperature.^{39,40}

The main mechanisms that contribute to axial dispersion in packed beds include, molecular diffusion, and longitudinal eddy diffusion. Molecular diffusion is the random molecular motion causing the solute/component to spread within the fluid leading to concentration gradient along the flow of direction. At low flowrates, axial dispersion is a function of molecular diffusion coefficient modified by a factor which accounts for tortuosity created from the packing of the bed.⁴¹

Longitudinal eddy diffusion occurs due to eddies/swirling flow occurring in presence of particles. These eddies result in fluid motion due to convection from one part of the packed bed to another contributing to mixing, however cause variation in fluid velocity resulting in axial dispersion. At high flow velocities, spreading becomes less dependent of the properties of the solute/tracer and becomes function of hydrodynamics in the specific particle packaging.

Axial dispersion in porous media has been widely studied in literature due to its importance and use within many industries including water and petroleum.^{39,42} The extent of axial dispersion can be quantified using the dispersion coefficient and several studies attempt to correlate and predict these dispersion coefficients for systems where fluid is flowing through a bed of inert particles. For the system present during the washing process of APIs, where the particles are chemically active and interact with the wash fluid flowing through the packed bed, determining dispersion coefficient is much more difficult.⁴³

1.6 Agglomeration

Solid crystalline particles are often found to form hard, unbreakable lumps at the end of the isolation/drying process. In literature, these lumps/agglomerates are typically reported to occur

in agitated filter dryers when material containing high residual solvent is extensively agitated.⁴⁴ The fundamental mechanism of agglomeration caused during drying process is well understood to involve the deposition of dissolved material at points of contact between crystals when the solvent evaporates, however, little guidance is provided on how to prevent this issue during drying. General approaches involve avoiding agitation during initial stages of the drying process or to use surfactants which act as agglomeration inhibitors. Surfactants act by adsorbing on the solid crystal surface and/or interface and altering the interfacial energies (electrostatic and steric stabilization).⁴⁵ Such additional surfactants can have toxicity associated to them and so may not be acceptable for pharmaceutical products.

Several papers have been published examining the cause of agglomeration in crystalline products. Common hypotheses suggest the polarity of the solvent and solubility of the wash solvent in the API product are main cause, with formation of “sticky spot” due to local API dissolution during drying resulting in solid bridges forming in between particles.

Experimental research conducted by Birch and Marziano demonstrated that the higher the solubility of the product in wash solvent, the greater the chance of solid bridge formation.^{46,47} Different wash solvent combinations were examined in the study with the results indicating strong impact of wash solvent composition (solubility) on the compound tendency to agglomerate. This is also due to increased apparent viscosity of thin liquid layer forming surrounding the particle for system with higher solubility wash solution. Hence tailoring wash solvent composition to minimize presence of solution with highly soluble component during drying process, is one approach to reduce agglomeration.

Another study conducted by Papageorgiou et al. investigated solid particulate to undergo agglomeration and concluded that the moisture content and solvent selection has the biggest impact on particle agglomerating with polar solvent resulting in much harder agglomerate.⁴⁷

Similar analogous observation was also reported by Zhang and Lamberto, and Tamrakar et al.

showing increase solvent polarity resulting in stronger agglomerates.^{48,49} These studies used sieving as the method to quantify the extent of agglomeration for the dried crystalline material at the end of the drying process. However, none of the studies in literature have tried examining or quantifying possible agglomerate formation during the washing process itself. Chapter 4 in this thesis looks to determine possible agglomerate formation during the wash process, such agglomerates are then possibly further strengthened during the drying process.

1.7 Model compounds

1.7.1 Paracetamol

The main compound used within this research is paracetamol, also known as Acetaminophen, (C₈H₉NO₂). This research involved numerous questions related to chemical and physical behaviour and interactions during the washing process. Hence, a well-researched compound like paracetamol is used.

Paracetamol (PCM) is an active pharmaceutical ingredient (API) which acts as an analgesic (painkiller) and antipyretic (fever reducing) drug. It is a relatively safe drug, however, toxic side effects are observed at relatively high dosage of around 10-15 g. These toxic side effects are due to the chemical structure of the compound and the way in which human body breaks it down where it metabolises to a reactive intermediate at high dosage.⁵⁰

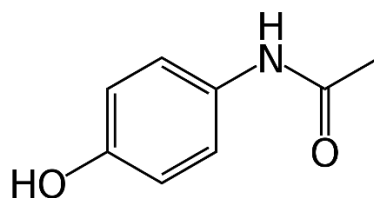
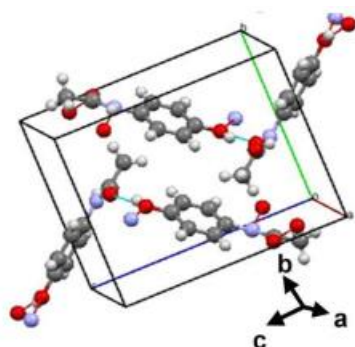


Figure 1-3: Paracetamol chemical structure

Paracetamol consists of a benzene group core, substituted by one hydroxyl group and an amide group present in the para position, Figure 1-3.⁵¹ The presence of carbonyl group acts as an intramolecular hydrogen bond acceptor while the amide and hydroxyl group acts as a hydrogen

bond donor. Combination of these hydrogen bond donor and acceptors form a hydrogen bonded network in crystal structure. The OH...NH and C=O...HO molecules of successive layers form head to tail sequence using hydrogen bonds.⁵² Molecular packing arrangement of a grown monoclinic paracetamol refined from single crystal x-ray diffraction, Figure 1-4.



*Figure 1-4: Molecular packing diagram of paracetamol - form I*⁵²

Paracetamol exists in five polymorphic forms; I, II, III, IV and V. Form I is thermodynamically the most stable form whilst form II is sufficiently similar in stability that it can be isolated and extensively researched, while form IV and V can only be obtained at high pressure.⁵³ Form III has been recrystallized under a microscope but is very unstable to perform any experimental analysis on its crystal structure.⁵⁴ Form I, the monoclinic form, is the thermodynamically stable form of paracetamol while Form II, orthorhombic form, is the metastable form at room temperature. Form I displays a herringbone lattice arrangement, with structure creating difficulties when under compaction leading to problem during compaction into tablets. The structure of Form II enhances physical properties such as compressibility and solubility, which helps in tableting. However, since form I is more stable at room temperature therefore is more widely used than form II.⁵⁵

In paracetamol, there are three polar functional groups; hydroxyl (OH), amide (NH) and carbonyl (CO) and several non-polar CH groups. As a result, paracetamol can dissolve in polar protic solvents (such as ethanol, water, methanol etc.) due to presence of both negative and

positive charged species that participate in intermolecular forces by forming hydrogen bonding. In polar aprotic solvents (such as acetone, acetonitrile, ethyl acetate etc.) only the positive ions can aid dissolution and so no hydrogen bonding takes place.⁵² In non-polar solvents (such as pentane, hexane, toluene etc.) there is a lack of functional groups to form strong bonds and so the weak bonds that form with paracetamol are between similar electronegative C-H groups with lack of partial charge.

1.7.2 AZ200/2

Due to confidentiality reasons, AstraZeneca Compound 1 (AZC1) is the name given to an industrial compound that is used for investigation in chapter 5. The aim of the work is to transfer the methodology of constant rate washing developed in chapter 3 using model compound, paracetamol, onto an industrial API product. This methodology is then used to optimise the AZC1 washing process. The identity of the compound is not relevant for this thesis and its omission should not be disadvantageous to it.

1.7.3 Impurities

An impurity is any component whose chemical entity is not defined as the drug substance and its presence affects the purity of the active ingredient, in accordance with the International Conference on Harmonisation (ICH) Guidelines.⁵⁶ APIs are mostly manufactured by organic chemical synthesis and so any non-API component remaining in the final API product is considered an impurity. These could be unreacted starting material, reaction by-products, residual solvent from API synthesis, etc. In pharmaceutical manufacturing stringent efforts are made to monitor and control impurities in API products.^{57,58}

Impurities with similar solubility to API in specific solvents poses challenge for their removal during the washing process as it affects final process yield.⁵⁹ Designing wash process with

optimal impurity removal while preventing yield loss is investigated in detail in chapters 2 & 3.

In chapter 2, two impurities structurally related to paracetamol (acetanilide and metacetamol, Figure 1-5) are used to investigate the propensity of anti-solvent effects occurring during the washing process. These impurities are produced as by-product of paracetamol synthesis. Acetanilide molecule has a lack of hydroxyl group compared to the paracetamol molecule and metacetamol molecule is the meta-isomer of the acetaminophen molecule (paracetamol).

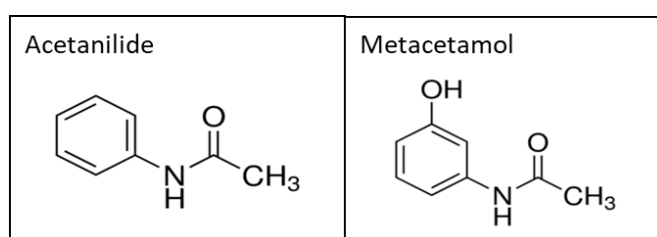


Figure 1-5: Paracetamol related impurities - chemical structures

In chapter 3, an organic dye is used to mimic impurity to better visualise impurity removal during the washing process. This helped with designing constant rate washing process methodology. Further information regarding this work and the dye are reported in chapter 3.

In chapter 5, removal of Impurity Compound 1 (IC1) impurity is investigated in the AZC1 compound. Apart from the solubility of the impurity in the solvent system, no other information was available for this project. The analysis used for IC1 quantification is gone over in detail in chapter 5.

1.8 General aims and objectives of research

This PhD research programme looks at advancing understanding of the API washing process. The work performed looks at understanding the parameters involved in improving the wash process performance and the characteristics of the final washed API product. Paracetamol, a well-researched API model compound was used in this study to allow for focus on specific

research questions targeted in this thesis. Microscopic interactions between different components in a multi-component system, present during the washing process, were investigated to understand:

- How to select a wash solvent that can increase or maintain system purity without causing agglomeration or dissolution of API particles present within the system. Chapter 2 looks at understanding how the wash solvent interacts with the mother liquor present in a saturated PCM filtered cake and how can this affect the API particles present in the system.
- How to design and analyse washing process which can allow for optimisation of the process. Chapter 3 uses the PCM model compound with a constant rate filtration and washing process to evaluate the wash process performance. This work looks to gather data on both the solvent compounds and the solid API present in the system to analyse and monitor the process. The process method and the wash workflow developed, is then utilised to analyse washing performance of an industrial API, AZC1, compound, Chapter 5.
- How to analyse the characteristics of the API particles obtained at the end of the washing process, Chapter 4. Determining the shape and size distribution of the API particles in the washed damp API cake is important to understand any changes occurring during the washing process, such as dissolution, precipitation, or agglomeration taking place during the washing process prior to the further impact of drying on the resulting product.

By the end of the research programme, the aim is to develop an optimum strategy and workflow for washing that allows for pharmaceutical companies to be better equipped to isolate purified

API crystals as individual free flowing particles without agglomeration whilst minimising product loss and solvent waste.

1.9 Abbreviations

International Council for Harmonisation of Technical Requirement for Pharmaceuticals for Human use (ICH); active pharmaceutical ingredient (API); paracetamol (PCM); AstraZeneca Compound 1 (AZC1); Impurity Compound 1 (IC1).

References

1. Mullin, J. W. Crystallisation, Fourth Edition. Chapter 9 – Crystallizer design and operation. Butterworth Heinemann. **2001**.
2. Gao, Z.; Rohani, S.; Gong, J.; Wang, J. Recent developments in the crystallisation process: toward the pharmaceutical industry. *Engineering*. **2017**. 3. 345-353.
3. McWilliams, J. C.; Allian, A. D.; Opalka, S. M.; May, S. A.; Journet, M.; Braden, T. M. The evolving state of continuing processing in pharmaceutical API manufacturing: a survey of pharmaceutical companies and contract manufacturing organizations. *Org. Process Res. Dev.* **2018**. 22. 1143-1166.
4. Am Ende, D. J. *Chemical Engineering in the Pharmaceutical Industry: R&D to Manufacturing*. 1st ed. Hoboken. New Jersey: Wiley. 17. Design of Filtration and Drying Operations. **2011**. 315–347.
5. Svarovsky, L. *Solid-Liquid Separation*. 4th ed. Oxford. UK. Butterworth-Heinemann. **2000**.
6. Guerrero, M., Albet, C., Palomer, A., Guglietta, A. Drying of pharmaceutical and biotechnological industries. *Food Sci. Tech. Int.* **2013**. 237-243.
7. Lim, L. H.; Hapgood, K. P.; Haig, B. Understanding and preventing agglomeration in a filter drying process. *Powder Technol.* **2016**. 300. 146–156.
8. Tien, C. *Principles of Filtration*. 1st ed. Elsevier. 2012.
9. Ottoboni, S.; Shahid, M.; Steven, C.; Coleman, S.; Meehan, E.; Barton, A.; Firth, P.; Sutherland, R.; Price, C. J. Developing a batch isolation procedure and running it in an automated semi continuous unit: AWL CFD25 case study. *Org. Process Res. Dev.* **2020**. 24. 4. 520-539.
10. Birch, M.; Marziano, I. Understanding and avoidance of agglomeration during drying processes: a case study. *Org. Process Res. Dev.* **2013**. 17. 1359–1366.
11. Capellades, G.; Neurohr, C.; Azad, M.; Brancazio, D.; Rapp, K.; Hammersmith, G.; Meyerson, A. S. A compact device for integrated filtration, drying, and mechanical processing of active pharmaceutical ingredients. *J. Pharm. Sci.* **2020**. 109. 1365-1372.

12. Pakowski, Z.; Mujumdar, A. S. Drying of Pharmaceutical Product. Chapter 29. Handbook of Industrial Drying. Fourth Edition. CRC Press. **2007**. 689-712.
13. Conder, E. W.; Cosbie, A. S.; Gaertner, J.; Hicks, W.; Huggns, S.; MacLeod, C. S.; Remy, B.; Yang, B.; Engstrom, J. D.; Lamberto, D. J.; Papageorgiou, C. D. The pharmaceutical drying unit operation: an industry perspective on advancing the science and development approach for scale-up and technology transfer. *Org. Process Res. Dev.* **2017**. 21. 420-429.
14. Kuo, M. T.; Barrett, E. C. Continuous filter cake washing performance. *AIChE J.* **1970**. 16. 633–638.
15. Ruslim, F.; Nirschl, H.; Stahl, W.; Carvin, P. Optimization of the wash liquor flow rate to improve washing of pre-deliquored filter cakes. *Chem. Eng. Sci.* **2007**. 62. 3951–3961.
16. Huhtanen, M.; Salmimies, R.; Kinnarinen, T.; Hakkinen, A.; Ekberg, B.; Kallas, J. Empirical modelling of cake washing in a pressure filter. *Sep. Sci. Technol.* **2012**. 47. 1102-1112.
17. International Conference of Harmonisation of technical requirements for registration of pharmaceuticals for human use. ICH Harmonised Tripartite Guideline. **1999**. Specifications: Test procedures and Acceptance Criteria for New Drug Substances and New Drug Products: Chemical Substances (Q6A).
18. Huhtanen, M.; Salmimies, R.; Kinnarinen, T.; Hakkinen, A.; Ekberg, B.; Kallas, J. Empirical Modelling of Cake Washing in a Pressure Filter. *Sep. Sci. Technol.* Vol. 47, **2012**. p. 1102–1112.
19. Ruslim, F.; Hoffner, B.; Nirschl, H.; Stahl, W. Evaluation of pathways for washing soluble solids. *Chem. Eng. Res. Des.* **2009**, 87, 1075–1084.
20. Tien, C. Introduction to Cake Filtration: Analyses, Experiments and Applications; Elsevier: Amsterdam, The Netherlands. **2006**.
21. Wakeman, R.J. The influence of particle properties on filtration. *Sep. Purif. Technol.* **2007**, 58, 234–241.
22. Perlmutter, B.A. A Treatise of Filter Cake Washing Mechanisms in Pressure and Vacuum Filtration Systems. *BHS Filtration*. [assessed 18/03/2021], Available at: http://www.bhs-filtration.com/A_Treatise_of_Filter_Cake_Washing_Mechanisms.pdf
23. Yazdanpanah, N.; Nagy, Z. K.; Price, C. J.; Barton, A.; Coleman, S. J. The handbook of continuous crystallisation. Chapter 13. RSC. **2020**.
24. Dohrn, S., Luebbert, C., Lehmkemper, K., Kyeremateng, S.O. Solvent mixtures in pharmaceutical development: Maximizing the API solubility and avoiding phase separation. *Fluid Phase Equilibria*. **2021**. 548.
25. Mota, F.L., Carneiro, A.P., Queimada, A.J., Pinho, S.P. Temperature and solvent effects in the solubility of some pharmaceutical compounds: measurements and modelling. *J. Pharm. Sci.* **2009**. 37. 499-507.

26. Qui, J., Huang, H., He, H., Liu, H., Hu, S., Han, J., Yi, D., An, D., Guo, Y., Wang, P. Solubility determination and thermodynamic modelling of edaravone in different solvent systems and the solvent effect in solvents. *J. Chem. Eng. Data.* **2020.** 65, 6, 3240–3251.
27. Mohammadzade, M., Barzegar-Jalali, M., Jouyban, A. Solubility of naproxen in 2-propanol+water mixtures at various temperatures. *Journal of Molecular Liquids.* **2015.** 206. 110-113.
28. Pacheco, D.P., Martinez, F. Thermodynamics analysis of the solubility of naproxen in ethanol + water cosolvent mixtures. *Physics and Chemistry of Liquids.* **2007.** 45:5. 581-595.
29. Hojjati, H., Rohani, S. Measurement and Prediction of Solubility of Paracetamol in Water-Isopropanol Solution. Part 1. Measurement and Data Analysis. *Org Process Res Dev.* **2006.** 10. 1101-1109.
30. Subrahmanyam, C.V.S., Reddy, M.S., Rao, J.V., Rao, P.G. Irregular solution behaviour of paracetamol in binary solvents. *Int. Journal of Pharmaceutics.* **1992.** 78. 17-24.
31. Jouyban, A., Chan, H.K., Chew, N.Y.K., Khoubnasabjafari, M., Acree, W.E. Solubility of prediction of paracetamol in binary and ternary solvent mixtures using Jouyban-Acree Model. *Chem. Pharm. Bull.* **2006.** 54(4). 428-431
32. Xia, D., Quan, P., Piao, H., Sun, S., Yin, Y., Cui, F. Preparation of stable nitrendipine nanosuspensions using the precipitation–ultrasonication method for enhancement of dissolution and oral bioavailability. *European Journal of Pharmaceutical Sciences.* **2010.** 40. 325-334.
33. Giulietti, M., Bernardo, A. Crystallization by antisolvent addition and cooling. *Crystallization - Science and Technology.* **2012.** 379–396.
34. Lee, M.-J., Chun, N.-H., Wang, I.-C., Liu, J. J., Jeong, M.-Y., Choi, G. J. Understanding the Formation of Indomethacin–Saccharin Cocrystals by Anti-Solvent Crystallization. **2013.**
35. Nývlt, J. Kinetics of Nucleation in Solutions. *Journal of Crystal Growth.* **1968.** 377 – 383
36. Myerson, A. S. *Handbook of Industrial Crystallization*, 2nd ed. Butterworth-Heinemann: Woburn, MA. **2002.**
37. Nagy, Z. K., Fujiwara, M., Braatz, R. D. Modelling and Control of Combined Cooling and Antisolvent Crystallization Processes. *J. Process Control.* **2008.** 18. 856–864.
38. Johnson, G.W., Kapner, R.S. The dependence of axial dispersion on non-uniform flows in beds of uniform packing. *Chemical Engineering science.* **1990.** 45. 3329-3339.
39. Delgado, J.M.P.Q. A critical review of dispersion in packed beds. *Heat and Mass Transfer.* **2006.** 42. 279-310.

40. Urban, J.C., Gomezplata, A. Axial dispersion coefficients in packed beds at low Reynold numbers. *The Canadian journal od chemical engineering*. **1969**. 47.
41. Kehinde, A.J., Hudgins, R.R., Silveston, P.L. Measurement of axial dispersion in packed beds at low Reynold numbers by imperfect pulse chromatograph. *Journal of chemical engineering of Japan*. **1983**. 16.
42. Bear, J. *Dynamics of fluids in porous media*. Dover Publications, New York. **1972**.
43. Ottoboni, S., Brown, C.J., Mehta. B., Jimeno, G., Mitchell, N.A., Sefcik. J., Price, C.J. Digital design of filtration and washing of active pharmaceutical ingredients via mechanistic modeling. *Organic Process Research & Development*. **2022**. 26. 3236-3253.
44. Wakeman, R. J., Tarleton, E. S., *Filtration: equipment selection, modelling and process simulation*. 1st ed. Oxford, United Kingdom: Elsevier Science Ltd. **1999**.
45. Chow, G. M., Gonsalwes, G. E. Particle Synthesis by chemical routes. In Edelstein, A. S., Cammaratara, R. C. *Nanomaterials: Synthesis, Properties and Applications*, Second Edition. 1st ed. New York, USA: CRC Press. **1998**. 55–59.
46. Birch, M., Marziano, I. Understanding and Avoidance of Agglomeration During Drying Processes: A Case Study. *Organic Process Research & Development*. **2013**. 17. 1359–1366.
47. Papageorgiou, C. D., Langston, M., Hicks, F., Am Ende, D., Martin, E., Rothstein, S., Salan, J., Muir, R. Development of Screening Methodology for the Assessment of the Agglomeration Potential of APIs. *Organic Process Research & Development*. **2016**. 20. 1500–1508.
48. Zhang, S., Lamberto, D. J. Development of New Laboratory Tools for Assessment of Granulation Behaviour During Bulk Active Pharmaceutical Ingredient Drying. *J. Pharm. Sci*. **2014**. 103. 152–160.
49. Tamrakar, A., Gunadi, A., Piccione, P. M., Ramachandran, R. Dynamic agglomeration profiling during the drying phase in an agitated filter dryer: Parametric investigation and regime map studies. *Powder Technology*. **2016**. 303. 109-123.
50. Ellis, F. *Paracetamol - A Curriculum Resource*. Royal Society of Chemistry. London. **2002**.
51. Finnie, S.; Prasad, K.V.R.; Sheen, D.B.; Sherwood, J.N. Micro-hardness and Dislocation Identification Studies on Paracetamol Single Crystals. *Pharm Res*. 18. 674–681. **2001**.
52. Sudha, C.; Srinivasan, K. Understanding the effect of solvent polarity on the habit modification of monoclinic paracetamol in terms of molecular recognition at the solvent crystal/interface. *Crystal Research and Technology*. 49. 865–872. **2014**.
53. Agnew, L.R.; Cruickshank D.L.; McGlone, T.; Wilson, C.C. Controlled Production of the Elusive Metastable Form II of Acetaminophen (Paracetamol): A Fully Scalable

- Templating Approach in a Cooling Environment. Chem. Commun. Vol 7368. pp 52. **2016**.
54. Di Martino, P.; Conflant, P.; Drache, M.; Huvenne, J.P.; Guyot-Hermann, A.M. Preparation and physical characterization of forms II and III of paracetamol. Journal of Thermal Analysis. Vol 48. No. 3. pp. 447-458. **1997**.
 55. Heng, J.Y.Y.; Williams, D.R. Wettability of Paracetamol Polymorphic Forms I and II. Langmuir. Vol. 22. No. 16. **2006**.
 56. U. S. Department of Health and Human Services, Food and Drug Administration, Center for Drug Evaluation and Research (CDER), Center for Biologics Evaluation and Research (CBER). Q3D Elemental Impurities, Guidance for Industry. ICH. **2015**.
 57. Prabu, S.L.; Suriyaprakash, T.N.K. Impurities and its importance in pharmacy. Int. J. Pharm. Sci. Rev. Res. 66. **2010**.
 58. Witschi, C.; Doelker, E. Residual solvents in pharmaceutical products: acceptable limits, influences on physicochemical properties, analytical methods and documented values. Eur. J. Pharm. Biopharm. 215. **1997**.
 59. Kuvadia, Z.B.; Doherty, M.F. Effect of Structurally Similar Additives on Crystal Habit of Organic Molecular Crystals at Low Supersaturation. Cryst. Growth Des., 1412. **2013**.

2. Exploring the role of anti-solvent effects during washing in active pharmaceutical ingredient purity

[This chapter is published in Organic Process Research and Development;

Shahid, M.; Sanxaridou, G.; Ottoboni, S.; Lue, L.; Price, C. Exploring the role of antisolvent effect during washing on active pharmaceutical ingredient purity. *Org. Process Res. Dev.* 2021, 25, 4, 969–981.]

2.1 Introduction

Washing is a fundamental post-filtration step required for removal of residual mother liquor, unacceptable side-products and/or undesirable insoluble components trapped inside the porous API bed. Washing displaces these components from a filtered cake by introducing a wash solvent on top. This wash solvent then flows through the filtered API bed, as both diffusion and dispersion processes occur in combination, see Chapter 1.

Section 1.2 mentions a few properties of a solvent which an ideal wash solvent should pose for an effective washing. However, some of these wash characteristics are mutually exclusive. Introduction of wash solvent into the mother liquor wet API filter cake can result in several undesirable outcomes. The anti-solvent effect is one of the problems commonly encountered during washing because of the requirement for the API product to have a low solubility in the wash solvent. As the wash solvent comes in contact with the slightly supersaturated mother liquor present within the filter cake, nucleation takes place initiating an anti-solvent crystallisation. Anti-solvent crystallisation, also known as precipitation, is a widely used technique in the pharmaceutical and fine chemical industry to recover product from solution in a solvent in which the product has high solubility.¹ Supersaturation is generated by mixing a concentrated solution of the product with another miscible solvent in which the product has limited solubility. Anti-solvent crystallisation can be well controlled and avoids the need to heat and cool the product stream where this is undesirable.² However, this control of an anti-solvent crystallisation is lacking during washing and is made more difficult in binary solvent mixture systems due to non-linear relationship between solubility and composition. Rather washing with an anti-solvent may lead to uncontrolled anti-solvent crystallisation and can result in product precipitation, leading to severe agglomeration.³ Precipitation occurring in the packed bed of API crystals in the filter cake provides ideal conditions for the formation of solid bridges between crystals and hence agglomerate formation during washing. With high impurity

content present in the mother liquor, the function of the wash as an anti-solvent can have a drastic effect on the purity of the final product as the impurities are potentially subject to anti-solvent crystallisation.

One solution to this problem is to use chilled crystallisation solvent as the first wash solvent, possibly saturating the crystallisation solvent to minimise the extent of dissolution. Alternatively selecting a solvent in which the API has similar solubility as that of the API in the mother liquor to prevent precipitation of material present within the mother liquor solution.⁴ However, these approaches result in a reduction of yield from that obtained during the crystallisation process. In addition, the final crystalline product obtained at the end of the drying process could have a different particle size distribution to the one obtained during crystallisation.

A confounding factor in investigating anti-solvent effect during washing leading to agglomerate formation, is that agglomerates can also be formed during crystallisation and carried into the isolation process and, furthermore, agglomerates can be formed during drying. The presence of dissolved API in the residual wash solvent in the washed cake at the start of the drying process results in agglomeration as crystalline bridges form as the wash solvent evaporates from the porous crystal structure.^{5,6} The capillary forces acting on the retained liquid film in the wet cake tend to concentrate the residual solution at the points of contact between particles favouring agglomerate formation. This effect is illustrated in the SEM image shown in Figure 2-1. This illustrates the presence of crystalline bridges in the API paracetamol at the end of drying (paracetamol API present in ethanol as crystallisation solvent and washed using acetonitrile and dried in vacuum oven). The presence of crystalline bridge formations produced during any of the process steps; crystallisation, washing and drying will increase the particle size of API crystals, which are typically characterised at the end of the drying process.⁷ To

overcome the consequences of agglomeration, milling is often used as a downstream process step in the pharmaceutical industry applied either after drying or immediately prior to formulation. This not only increases the number of process steps and processing time but can also lead to the formation of amorphous material, and can expose new facets of the crystals which may have different characteristics to those formed during the crystallisation and may modify the powder behaviours.⁸

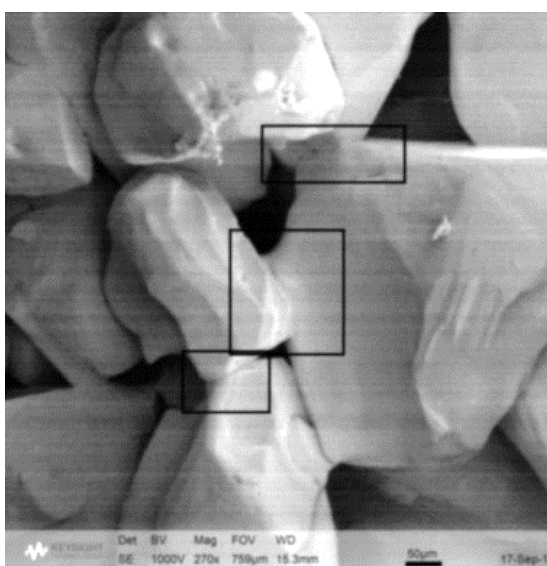


Figure 2-1: SEM image of dried paracetamol agglomerate showing formation of crystal bridges

This suggests that poorly designed washing processes can modify particle properties. This is a potentially important complication in the subsequent drying step which is very likely to further strengthen the agglomerates formed during washing. Therefore, it is important to prevent agglomeration during washing and limit the amount of product in solution at the start of drying by optimising the washing process. This research investigates strategies to follow for optimal selection of the wash solvent. The approach involves minimising dissolution of API crystals, whilst preventing any precipitation of dissolved API and impurities. Selecting a wash solvent to avoid these phenomena, when the wash solvent comes into contact with the retained crystallisation solvent in the saturated filtered cake, can be challenging but is essential to maintain yield, purity, and particle characteristics throughout the isolation process.

This study investigates the effect of wash solvent selection by considering the mechanisms taking place during the interaction between crystallisation and wash solvent in the washing process. In the first instance, the already crystallised API particles in the filter cake present during the washing process are ignored to simplify the system. Once the processes taking place in the liquid solvent mixture, during the washing process, are understood then the API crystals in the cake can be reintroduced and the understanding of the solution side processes can be built upon.

The aim of this work is to develop a quick and simple screening methodology to qualitatively and quantitatively analyse the propensity of different wash solvents to cause precipitation to occur during the washing process. Paracetamol was the API selected for the experimental work in this study as it is a widely researched compound with a significant body of published data which can be drawn upon to facilitate the experimental work.⁹⁻¹²

The approach developed in this study allows quantification of both the amount of paracetamol API precipitating out during washing and the quantity of dissolved impurities that could precipitate out and adversely affect the purity of the final product. The findings from this work allow crystallisation – wash solvent combinations which would prevent / limit any precipitation or dissolution during washing to be identified. This is illustrated with paracetamol as a model compound.

2.2. Materials and Method

2.2.1 Raw Material

Paracetamol (PCM) was selected as a representative test compound with characteristics typical of APIs. It is commercially available, as are its impurities of synthesis. In this study paracetamol of typical crystalline grade was used (Mallinckrodt Inc., UK, batch 637514D001; D10: 12.48 μ m, D50: 43.96 μ m, D90: 101.30 μ m). Acetanilide (Sigma-Aldrich, UK, Lot #

STBF7835V, purity 99%) and Metacetamol (Sigma-Aldrich, UK, Lot # MKBX4643V, purity 97%), two structurally related compounds to paracetamol, were used as representative impurities in this work. These impurities could be present in the mother liquor during the crystallisation step.¹³

To investigate the anti-solvent effect during washing on representative slurry suspensions typical of those formed at the end of a crystallisation, a series of three commonly used crystallisation solvents appropriate for isolating paracetamol were used: ethanol (purity ≥ 99.8 % (GC), from Sigma Aldrich), propan-2-ol (IPA) (purity ≥ 99.5 % (GC), from Sigma Aldrich) and 3-methylbutan-1-ol, (isoamyl alcohol) (purity ≥ 99.5 % (GC), from Sigma Aldrich).¹⁴ As wash solvents; acetonitrile (purity 99+ % from Alfa Aesar), isopropyl acetate (purity 99+ % from Alfa Aesar) and n-heptane (purity 99%, from Alfa Aesar) were selected for this investigation. Acetonitrile was chosen because the API solubility is at the high end of those typically selected as wash solvents and because it is a widely used solvent in industry. n-heptane was selected because the solubility of PCM and the selected impurities is very low, almost negligible. Isopropyl acetate is another commonly used wash solvent in industry and the solubility of API in the isopropyl acetate is in the middle of the two extremes represented by acetonitrile and heptane. A further criterion is that all three wash solvents were chosen to be miscible with the three crystallisation solvents.

To determine the purity of the precipitated material at the end of each experiment, high pressure liquid chromatography (HPLC) was used. The eluents contained water (Water, ultrapure, HPLC Grade, Alfa Aesar) and methanol (Methanol, ultrapure, HPLC Grade, 99.8+%, Alfa Aesar). Methanol was also used as diluent for some samples.

2.2.2 Sample Preparation

Saturated PCM solution, with impurities included where selected, was prepared in two stages based on previously measured solubility of PCM in the selected crystallisation solvents:¹⁵ Firstly 2 % by mass relative to the known PCM solubility of each impurity was added and dissolved in the crystallisation solvent. To ensure complete dissolution of impurities a sonic water bath was used (Elmasonic P300H Ultrasonic, Cole-Parmer Instruments Ltd.). The amount of paracetamol required to saturate the solution was then added and dissolved in similar manner. This two-stage addition prevents any undissolved impurity crystals remaining in the final saturated solution. The saturated solution was also filtered before anti-solvent screening experiments to prevent potential seeding effect.

Wash solutions were prepared using a mixture of the selected wash solvent and crystallisation solvent. For each crystallisation and wash solvent system, a total of 8 different wash solution combinations were investigated. The different ratios, by volume, of wash solution used in each solvent system is reported in Table 2-1.

Table 2-1: Wash solutions of different ratios that were tested for each solvent system

| Wash solvent solution identity | Percentage of crystallisation solvent by volume | Percentage of wash solvent by volume |
|--------------------------------|---|--------------------------------------|
| 1 | 90 % | 10 % |
| 2 | 75 % | 25 % |
| 3 | 50 % | 50 % |
| 4 | 40 % | 60 % |
| 5 | 30 % | 70 % |
| 6 | 20 % | 80 % |
| 7 | 10 % | 90 % |
| 8 | 0 % | 100 % |

2.2.3 Anti-solvent screening procedure

Two anti-solvent screening approaches were developed and evaluated, one based on portion-wise addition of the wash solvent to a saturated solution and monitored by visual observation, the other used centrifugation to separate and recover any precipitated particles.

2.2.3.1 Anti-solvent screening procedure – Glass vial method



Figure 2-2: Glass vial precipitation detection method

Figure 2-2 gives a schematic representation of the glass vial method. This method uses a standard 1.8mL glass HPLC vial. 300 µL of saturated crystallisation solution is first added to the vial using an Eppendorf pipette. Then wash solution is added 2 drops at a time using a 1 mL disposable pipette. After each addition, the vial was shaken and checked for any precipitation of crystals that might have taken place. Wash solvent addition was continued until the total amount of wash solvent added corresponded to 700 µL. Given a typical saturated filter cake contains very approximately 50% by volume API crystals and 50% by volume mother liquor, then a one cake volume wash would broadly match the 2:1 ratio achieved here depending on particle aspect ratio and packing. The amount of wash solvent used is better expressed as a two cake void volume wash.¹⁶ The glass vial was then visually inspected at the end of the drop wise addition to check for any precipitation of crystals. If no crystals were formed, the vials were re-inspected the following day (approximately 24 hours later) to determine whether precipitation was possible but a very slow process under the conditions investigated. Whilst precipitation taking significantly longer than the normal duration of the

washing step may not be of practical significance it is considered to be useful to know whether precipitation is possible under each of the conditions investigated.

2.2.3.2 Anti-solvent screening procedure – Centrifuge vial method

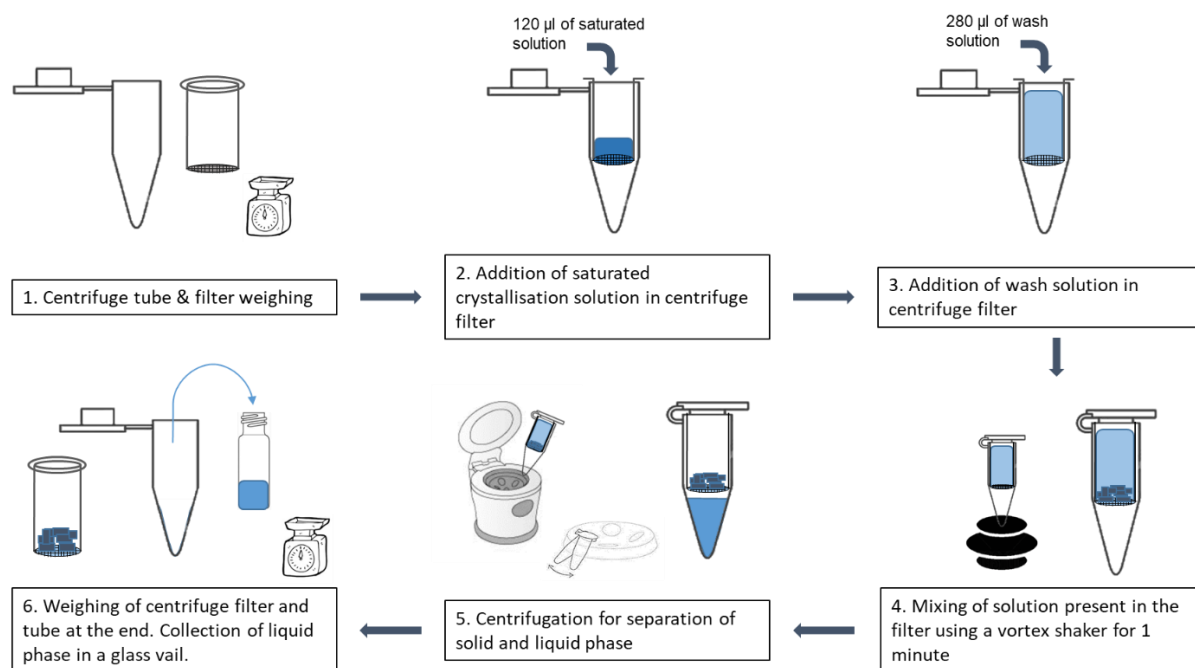


Figure 2-3: Centrifuge vial precipitation detection method

To evaluate the anti-solvent effect during washing using a centrifuge tube setup, centrifuge filter tubes incorporating a basket with 0.2 µm pore size were used (Thermo Scientific National, Scientific F2517-9 D100 PTFE 750 µL Centri Filter 0.2 µm pore size). The small pore size allowed for mixing of the sample solution and the wash solvents to be performed in the filter basket without any solvent leakage into the filter tube.

Figure 2-3 is a schematic representation of the anti-solvent methodology developed using the centrifuge vial. The procedure was divided into six steps, with a mass balance maintained across each step to take into account any material loss. In a pre-weighed centrifuge filter basket and centrifuge tube, the saturated crystallisation solvent was added and the mass of the filled tube was recorded (Figure 2-3).

The centrifuge filter basket had a capacity of 500 μL , thus 120 μL of saturated crystallisation solvent was added using an Eppendorf pipette, this was followed by the addition of 280 μL of the wash solvent. The choice of solvent volumes allowed a small space to remain at the top of the filter basket to prevent any solvent spillage while mixing the sample using a vortex shaker.

After addition of wash solution (step 4 in Figure 2-3) the solvent was kept in the centrifuge tube basket for 2 hours and then the anti-solvent effect was checked (looking for any crystal formation). Longer contact times between mother liquor and wash solvent, e.g. 24 hours, was not investigated as the selected centrifuge vials were found not to seal well enough to completely prevent solvent evaporation occurring if vials were left overnight. Also the filter medium in the baskets eventually allowed solvent to drain onto the centrifuge vial, due to gravity, if left over a long period of time. The compromise of two hours was selected as an appropriate amount of time to represent the practical maximum time for which wash solvent would be present in contact with the saturated crystallisation solution in the API cake.

The separation of any precipitated solid from the mixture of saturated solution and wash solvent takes place in step 5 of Figure 2-3. Centrifugation was carried out for 2 minutes at 6000 rpm. The basis of selection of these conditions is reported in the Appendix A - **Exploring the role of anti-solvent effects during washing in active pharmaceutical ingredient purity**. The chosen conditions were found to be effective in separating the mixed crystallisation and wash solvent from any precipitated solid particles retained in the centrifuge filter basket.

2.2.4 Post anti-solvent procedure analysis

HPLC was used to investigate composition of the liquid and solid phases obtained using the centrifuge vial method. X-ray powder diffraction (XRPD) and differential scanning calorimetry (DSC) was performed on the precipitated solid phase to determine the crystal

structure and to investigate whether the impurities present in the saturated solution were present as separate crystals or incorporated within the paracetamol API crystal lattice.

HPLC was used to determine the concentration of paracetamol and its impurities present in the liquid and solid phases at the end of the anti-solvent screening methods. Water and methanol were used as the eluents in the mobile phase, while methanol was also used as diluent for the samples. Calibration curves for pure paracetamol, metacetamol and acetanilide were gathered using a multilevel calibration method reported in the Appendix A - **Exploring the role of anti-solvent effects during washing in active pharmaceutical ingredient purity**. An Agilent 1260 Infinity II system was used. The column was an Agilent Poroshell 120 EC-C18 4.6 x 100mm 4 μ m operated at 40°C, with a flow rate of 1mL/min. The injection volume was 5 μ L, data was collected at 243 nm wavelength, and the mobile phase was 80% water and 20% methanol.

The XRPD analysis was performed using a D8 (multi-well) powder X-ray diffractometer – Flat plate instrument, Bruker AXS GmbH. The detector rotation (2θ) was set at $2\theta_{min}$ at 4° and $2\theta_{max}$ at 35°. A step size of 0.017° was used and the sec/step was set at 1 second.

DSC analysis was performed using a DSC 214 Polyma, NETZSCH-Gerätebau GmbH. Standard aluminium pans were used. The mass of sample added to the pans was maintained around 2-3 mg. The DSC214 Polyma employed a helium purge (in-line pressure set at 0.5 bar) and as a protective gas during analysis, and flowing through a chiller unit for sample cooling. The initial temperature was set at ambient, 25 °C, and the final temperature was set at 200 °C. The heating rate used was 10 °C /min. A sample was also run with heating rate of 2 °C /min to check the sensitivity looking for peak separation that might be missed at a high heating rate.

2.2.5 Gravimetric solubility analysis procedure

The solubility of paracetamol in the binary solvent mixtures (crystallisation and wash solvents) was determined experimentally by equilibration and gravimetric analysis. A Hailea HC-100A

chiller was used to maintain the temperature at 22 °C (the average temperature of the lab where the anti-solvent screening experiments were conducted). Excess paracetamol was added to 20 mL, clear glass vials together with the binary solvent mixture and a magnetic stirrer bar. The vials were sealed and left on a multi-position stirrer plate inside the water bath for around 48 hours to equilibrate. Samples of the solutions were then taken from the slurry in the vials using a syringe and filtered using a PES syringe filter (Fisherbrand, Cat No. 15206869, 0.2 µm, sterile), and added to a separate glass vial which was weighed and then left to dry. Table 2-1 shows all the ratios of binary solvent mixtures for which solubility was determined.

2.3 Results & Discussions

2.3.1 Anti-solvent effect – Glass vial method



Figure 2-4: Ethanol - n-heptane glass vial precipitation qualitative test

Figure 2-4 shows the results from the anti-solvent screening carried out for the ethanol - n-heptane solvent system using the glass vial method. The 50:50 solvent ratio (first picture on the left in Figure 2-4) represents wash solution made up of 50% by volume ethanol (the crystallisation solvent) with 50% by volume of n-heptane (the wash solvent), respectively. Precipitation was first observed in the ethanol-n-heptane experiments when a wash solution ratio of 40:60 was used (40% ethanol, 60% n-heptane by volume). In this condition of 40:60 wash solution, there was local and rapid precipitation of crystals was observed as the first few drops of wash solution was added to the saturated crystallisation solvent. These crystals subsequently dissolved back into the mixed liquid phase after a few seconds, once all the wash solution was added to the saturated crystallisation solvent. Therefore, the initial precipitation

observed was due to the local supersaturation in a non-mixed environment. As soon as mixing occurred the bulk composition remained undersaturated consequently the crystals dissolved back in solution. However, after leaving the vials for 24 hours, there were three or four small crystals were seen at the bottom of the glass vial, by the naked eye. This delayed precipitation indicates the slow kinetics of the system at this composition.

For the samples with compositions of 30:70 to 0:100 ethanol : n-heptane in Figure 2-4, crystal precipitation occurred as soon as the wash solution was added and mixed with the saturated crystallisation solvent. This was due to the large paracetamol solubility difference between the crystallisation solvent and the wash solutions. The crystals formed can be seen at the bottom of the vials as indicated by red circle in 30:70 solvent ratio vials in Figure 2-4.

There is an increase in crystal concentration in the vials going from compositions of 40:60 to 0:100 ethanol : n-heptane as seen in Figure 2-4. This increase is due to the higher supersaturation achieved in the solvent mixture as the concentration of n-heptane in the wash solution increases, this can be seen in Table 2- 4. Higher supersaturation results in a more thermodynamically unstable solution, which then results in increased precipitation of crystals occurring to allow the solution to return to thermodynamic equilibrium.¹⁷

This anti-solvent effect (crystal formation due to anti-solvent addition) was seen for 5 different cases, for the combination of crystallisation solvent and wash solvents used in this study. The results for this can be seen in Table 2-2. For each solvent combination case, if precipitation of crystals is observed then the solvent composition or the solvent proportions of the wash solution at the point where precipitation is first observed is given in Table 2-2.

In the case of using n-heptane as wash solvent, precipitation was detected in all three different crystallisation solvent systems. The almost negligible solubility of paracetamol in n-heptane combined with its much higher solubility in the crystallisation solvents, results in a

supersaturated solution being formed as the wash solution is added to the saturated crystallisation solvent. Table 2-3 provides the experimentally determined solubility (using gravimetric solubility analysis) of paracetamol in all 6 pure solvents used in this study. Paracetamol has shown to have very low solubility (> 1 g of paracetamol/kg of solvent) in non-polar hydrocarbon such as heptane and the solubility of paracetamol is decreasing with increasing carbon chain going from ethanol to isopropanol (Table 2-3). The results obtained for the solubility (C_s) of paracetamol in isopropanol and acetonitrile ($C_s = 114.1$ g/kg solvent & $C_s = 24$ g/kg solvent at 22 °C) are in good agreement with the values reported by Granberg et al. (1999) ($C_s = 108.8$ g/kg solvent for isopropanol & $C_s = 23.1$ or acetonitrile at 20 °C).¹⁵ The solubility in pure ethanol ($C_s = 186.7$ g/kg solvent at 22 °C) is in good agreement with value reported by Romero et al. (1996) ($C_s = 187.9$ g/kg solvent at 25 °C) but lower than the values reported by Granberg et al. (1999) ($C_s = 190.6$ g/kg solvent at 20 °C).^{15,18} The solubility data reported in literature is mostly present data at either 20 or 25 °C and not the 22 °C used in this work. However, good correlation is present between the results obtained and the data present in literature with the minor differences present, which could be due to purity of solvent or paracetamol used, where it has been shown that small amount of water in ethanol can significantly increase the solubility (Prakongoan and Nagai, 1984).¹⁹ The solubility maxima determined for binary solvent mixtures is comparable to what has been reported in literature for solubility in binary solvent solutions for different APIs including paracetamol.^{20,21}

Table 2- 4 provides the change in saturation (ΔC) in the final solution obtained at the end of washing after all the wash solution is added, for all the different wash ratios used.

There was no anti-solvent effect observed where acetonitrile was used as the wash solvent. Acetonitrile has the highest solubility of all the wash solvents used. Looking at the binary solvent solubility graphs for the acetonitrile cases (see Appendix A - **Exploring the role of anti-solvent effects during washing in active pharmaceutical ingredient purity**), the operating dilution

line is below the solubility curve. This explains why precipitation cannot take place, as the concentration of paracetamol in this system remains below the solubility limit of the solution. The calculated ΔC values for all acetonitrile cases, Table 2- 4, shows that supersaturation is not achieved and so no precipitation should be observed. In fact, any paracetamol crystals present would be subject to dissolution in these unsaturated conditions.

As the calculated ΔC values (Table 2- 4) for all cases with isopropyl acetate as the wash solvent was also found to be < 1 for all the wash solution ratios, hence no precipitation should have been detected. However, during the glass vial experiment, for both ethanol and isopropanol crystallisation solvent cases with isopropyl acetate, a few crystals were seen to form as the first few drops of wash solution was added to the saturated solvents, as reported in Table 2-2. This phenomenon probably occurred due to the local supersaturation effect where the localised environment close to the site of the drop addition would have resulted in nucleation of crystals, due to poor mixing. This then seems to disappear after the whole wash solution was added and the solution in the vial had become fully mixed. This effect if encountered during washing an API filter cake, where solution mixing can be very limited, could have detrimental effect on the purity and particle size distribution of the final isolated product.

Table 2-2: Precipitation caused for different solvent combinations - glass vial method. The crystallisation solvent used is provided on the left side of the table whilst the wash solvent across the top of the table. The ratio of the wash solution at which precipitation is first observed in the solvents system for paracetamol API case is given here. (The bold numbers correspond to the volume ratio of crystallisation solvent in the wash solution, while the italic number corresponds to the volume ratio of wash solvent in the wash solution.)

| | | <i>Wash solvent</i> | | |
|--------------------------------|------------------------|------------------------|---------------------|--------------------------|
| | | <i>n-heptane</i> | <i>Acetonitrile</i> | <i>Isopropyl acetate</i> |
| Crystallisation Solvent | Ethanol | 40 – 60 % (v/v) | No nucleation | 10 – 90 % (v/v) |
| | Isopropanol | 40 – 60 % (v/v) | No nucleation | 0 – 100 % (v/v) |
| | Isoamyl alcohol | 20 – 80 % (v/v) | No nucleation | No nucleation |

Table 2-3: Experimental solubility determined of paracetamol in the selected solvent at 22 °C (average lab temperature at which this anti-solvent effect study is conducted)

| | Solvent | Solubility (g API/g solvent) (at 22 °C) |
|--------------------------------|-------------------|--|
| Crystallisation Solvent | Ethanol | 0.1867 |
| | Isopropanol | 0.1141 |
| | Isoamyl Alcohol | 0.0526 |
| Wash Solvent | Acetonitrile | 0.0240 |
| | Isopropyl Acetate | 0.0059 |
| | N-heptane | 0.0003 |

Table 2- 4: ΔC achieved for the solvent combinations used. Blue cells represent scenarios where nucleation and crystallisation was observed. Orange cell represent scenarios where local supersaturation resulted in nucleation and then dissolution of crystals as bulk saturation is reached.

| AC values | | Ratio of the wash solution sample | | | | | | | | |
|-----------------------------|--|--|--------------|--------------|--------------|--------------|--------------|--------------|--------------|--------------|
| | | 100:0 | 90:10 | 75:25 | 50:50 | 40:60 | 30:70 | 20:80 | 10:90 | 0:100 |
| Solvent Combinations | Ethanol - Acetonitrile | 1.00 | 0.79 | 0.63 | 0.51 | 0.49 | 0.49 | 0.49 | 0.50 | 0.52 |
| | Ethanol - Isopropyl Acetate | 1.00 | 0.89 | 0.79 | 0.71 | 0.70 | 0.70 | 0.71 | 0.73 | 0.76 |
| | Ethanol - Heptane | 1.00 | 1.06 | 1.17 | 1.43 | 1.58 | 1.77 | 2.01 | 2.34 | 2.82 |
| | Isopropanol - Acetonitrile | 1.00 | 0.71 | 0.53 | 0.42 | 0.41 | 0.41 | 0.42 | 0.44 | 0.48 |
| | Isopropanol - Isopropyl Acetate | 1.00 | 0.90 | 0.81 | 0.72 | 0.71 | 0.70 | 0.70 | 0.71 | 0.73 |
| | Isopropanol - Heptane | 1.00 | 1.08 | 1.24 | 1.63 | 1.86 | 2.17 | 2.60 | 3.23 | 4.26 |
| | Isoamyl Alcohol - Acetonitrile | 1.00 | 0.65 | 0.46 | 0.36 | 0.36 | 0.36 | 0.37 | 0.39 | 0.43 |
| | Isoamyl Alcohol - Isopropyl Acetate | 1.00 | 0.85 | 0.46 | 0.36 | 0.63 | 0.63 | 0.64 | 0.67 | 0.71 |
| | Isoamyl Alcohol - Heptane | 1.00 | 1.09 | 1.25 | 1.63 | 1.83 | 2.08 | 2.38 | 2.77 | 3.28 |

The glass vial method used for anti-solvent effect screening was found to be effective for qualitative analysis of the wash solvent effect. The precipitation of crystals formed due to interaction between wash solution and the mother liquor is observable and this method can be used as a “quick” first approach to assess wash solvent compatibility.

However, quantitative analysis, to determine the amount and identity of solute precipitating out of the solution required a different methodology. The complete separation of solid from the liquid solution in the glass vial is not a trivial procedure due to the small size of the vial, and due to the difficulties related to the separation of the liquid and solid part of the sample. This methodology, therefore, does not allow a precise quantification of the species precipitated because the data generated using HPLC gave inconclusive evidence on the amount of impurities precipitating out, as the solid analysis results were affected by residual liquid solvent still present at the bottom of the vials (see Appendix A - **Exploring the role of anti-solvent effects**

during washing in active pharmaceutical ingredient purity). To get a better quantitative result, an improved wash screening analysis was devised to overcome these separation issues. Hence the centrifuge vial method was developed.

2.3.2 Anti-solvent effect– Centrifuge vial method

Table 2- 5: Precipitation caused by different solvent combinations - centrifuge vial method. The crystallisation solvent used is reported on the left side of the table whilst the wash solvent across the top of the table. The ratio of wash solution at which precipitation is first observed in these solvent system for paracetamol as a representative API is reported here. (The bold numbers correspond to the volume ratio of crystallisation solvent in the wash solution, while the italic number corresponds to the volume ratio of wash solvent in the wash solution.)

| | | <i>Wash solvent</i> | | |
|--------------------------------|------------------------|------------------------|---------------------|--------------------------|
| | | <i>n-heptane</i> | <i>Acetonitrile</i> | <i>Isopropyl acetate</i> |
| Crystallisation Solvent | Ethanol | 30 – 70 % (v/v) | No nucleation | No nucleation |
| | Isopropanol | 30 – 70 % (v/v) | No nucleation | No nucleation |
| | Isoamyl alcohol | 10 – 90 % (v/v) | No nucleation | No nucleation |

Table 2- 5 shows the anti-solvent effect observed using the centrifuge vial method. This is similar to the glass vial method described in Table 2-2. Due to the opaque character of the polypropylene centrifuge vials, nucleation and crystallisation phenomena were much harder to observe compared to using the clear glass vials.

Comparing the results shown in Table 2- 5 with those obtained using the glass vial method, (see Table 2-2), reveals some differences. Due to the opaque nature of the centrifuge vials, the nucleation observed due to local supersaturation effects for isopropyl acetate which were seen in glass vial method, could not be discerned in the centrifuge vial experiment. In all the cases of n-heptane as wash solvent, nucleation was observed for wash solution ratios with higher n-heptane concentration. This offset in observation of the anti-solvent effect can again be attributed to the opaque nature of the centrifuge vials giving difficulties in visualisation of precipitation of few, small crystals. Also, the slow crystallisation kinetics noticed in the 40:60

ethanol: n-heptane case in the glass vial experiments is not noticed in the centrifuge method as the solution is only left for 2 hours compared to 24 hours in the glass vial method.

However, the quantitative analysis achieved using the centrifuge vial method was found to be much more successful as almost complete separation of solid crystals from liquid solution was achieved. After stage 6 in Figure 2-3, HPLC is performed on both the separated solid and liquid samples. Quantitative results obtained from two different scenarios, ethanol – acetonitrile, and ethanol – n-heptane and are given below. The two scenarios presented illustrate the results which would be obtained for most cases – depending on whether precipitation is observed or not. The results for all the samples, for all solvent combinations, are available in Appendix A - Exploring the role of anti-solvent effects during washing in active pharmaceutical ingredient purity.

2.3.2.1 Centrifuge vial method – Quantitative Analysis: ethanol - acetonitrile (no nucleation)

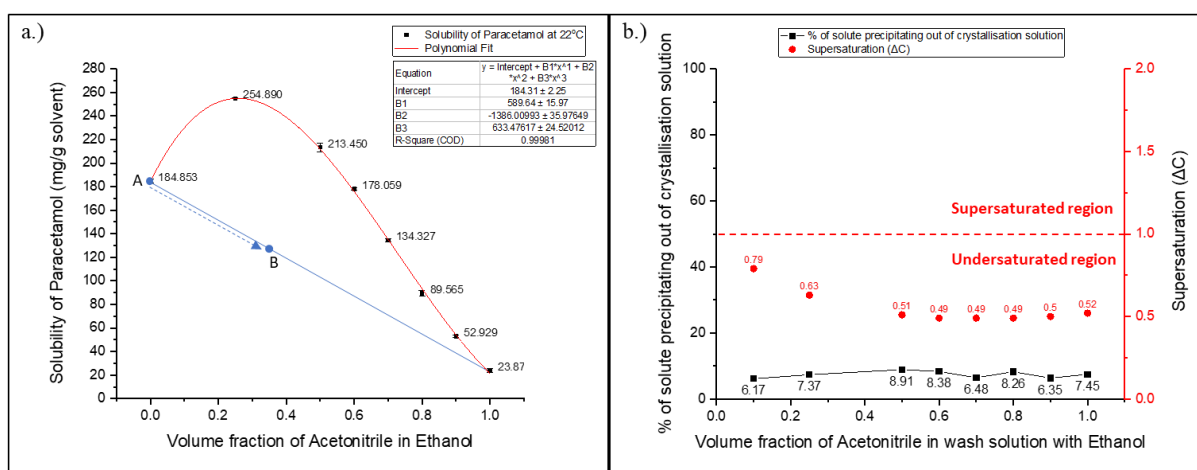


Figure 2-5: Quantitative analysis of the ethanol-acetonitrile case. a.) Solubility of paracetamol in ethanol-acetonitrile binary solvent mixture at 22 °C. b.) Percentage of solute precipitating out of solution for different wash solution compositions is shown in the Y axis on the left hand side of the graph, with the supersaturation achieved in the solution when different ratio of wash solution is added to the saturated crystallisation solvent shown on the Y axis on the right hand side of the graph.

Table 2-6: Ratio of wash solvent in the final solution mixture.

| | | | | | | | | |
|--|-------|-------|-------|-------|-------|-------|-------|-------|
| Ratio of wash solution used (v/v) (crystallisation: wash) | 90:10 | 75:25 | 50:50 | 40:60 | 30:70 | 20:80 | 10:90 | 0:100 |
| Volume fraction of wash solvent in final solution (end point of the final solution) | 0.07 | 0.175 | 0.35 | 0.42 | 0.49 | 0.56 | 0.63 | 0.7 |

As reported in the binary solvent mixture solubility data reported in Table 2-6 and in Figure 2-5, the ethanol and acetonitrile system does not show any anti-solvent effect. The blue line in Figure 2-5, graph a, represents the change in concentration of the API in the resultant solution mixture as the wash solution is added to the saturated crystallisation solvent. Point A in the graph is the starting API concentration of the saturated ethanoic solution. As the wash solution is added to the saturated crystallisation solvent, the concentration of API in the solution will change and move down following the path of the blue line. The calculated end point of the overall solution is dependent on the wash solution that is used, given in Table 2-6. Hence, the end point of the API concentration in the new system (mother liquor and wash solvent) depends on the composition and quantity of wash solution being used (in this study the total volume ratio of the system is fixed at 700 μ l wash solution to 300 μ l mother liquor). For example, if an experiment with wash solution comprising equal volumes of the wash solvent and the crystallisation solvent is used, then looking at Table 2-6, the final composition of the overall solution (containing saturated crystallisation solution and wash solution) would be 35 % by volume acetonitrile in ethanol. The value of paracetamol concentration at 35 % by volume wash solvent can then be determined from the blue line in graph a, of Figure 2-5, which would correspond to around 127 mg paracetamol / g solvent, point B.

The difference between the diluting line and the solubility curve dictates whether precipitation could take place. For the case of ethanol and acetonitrile (Figure 2-5), since the diluting line is below the solubility curve, the actual concentration of paracetamol in system is below the

solubility limit. Therefore, the solution would be undersaturated and no precipitation would occur.

In Figure 2-5b, the red dots represent the corresponding supersaturation across the solvent composition investigated, showing no precipitation of the API or the impurity as the system is in the undersaturated region. Table 2-7 shows the solubility data of the API and the selected impurities in the pure solvents used in this study. Since the solubility of the impurities, metacetamol and acetanilide, in pure solvent is similar or greater than that of paracetamol, and only 2 % by mass of impurity is present in each crystallisation solution, any impurity present in the precipitated material would be due to incorporation in API crystals rather than independent crystallisation of the impurities as separate crystalline species.

Table 2-7: Experimental solubility determined of Metacetamol and Acetanilide in the selected solvent at 25 °C.

| | Solvent | Solubility (g paracetamol/g solvent) (at 25 °C) | Solubility (g metacetamol/g solvent) (at 25 °C) | Solubility (g acetanilide/g solvent) (at 25 °C) |
|--------------------------------|-------------------|--|--|--|
| Crystallisation Solvent | Ethanol | 0.2057 | 0.2944 | 0.3322 |
| | Isopropanol | 0.1243 | 0.1948 | 0.1957 |
| | Isoamyl Alcohol | 0.0549 | 0.1049 | 0.1656 |
| Wash Solvent | Acetonitrile | 0.0294 | 0.0776 | 0.2060 |
| | Isopropyl Acetate | 0.0076 | 0.0246 | 0.0896 |
| | N-heptane | 0.0003 | 0.0003 | 0.0004 |

Even though there is no precipitation observed in the ethanol-acetonitrile case, the measured percentage precipitation value remains constant at around 7 ± 1 % as indicated by the black squares in graph b of Figure 2-5. This consistent amount of precipitation along the varying wash solution composition used can be explained by the presence of crystallised material formed from solution left on the porous media of the centrifuge vial basket. This crystallisation is therefore occurring during the solvent evaporation.

Since no precipitation takes place in ethanol-acetonitrile solvent combination, this does not automatically make acetonitrile a good candidate as the wash solvent for paracetamol in ethanol crystallisation solvent. Selecting a wash solvent with a modest solubility of paracetamol API can reduce the isolation yield by dissolution of the particles forming the API cake. Figure 2-5, graph a, shows that the operating dilution line is below the solubility curve and so the acetonitrile wash solution would tend to dissolve some of the paracetamol crystals present in the filter cake. Also, and probably of greater importance, the residual acetonitrile wash solution left in the deliquored cake would be likely to result in particle agglomeration during the drying process. Evaporation of the residual wash solution in the API cake would cause crystallisation of the dissolved solute on the crystal surfaces forming crystal bridges in the API cake (as seen in Figure 2-1).

2.3.2.2 Centrifuge vial method – Quantitative Analysis: ethanol - n-heptane

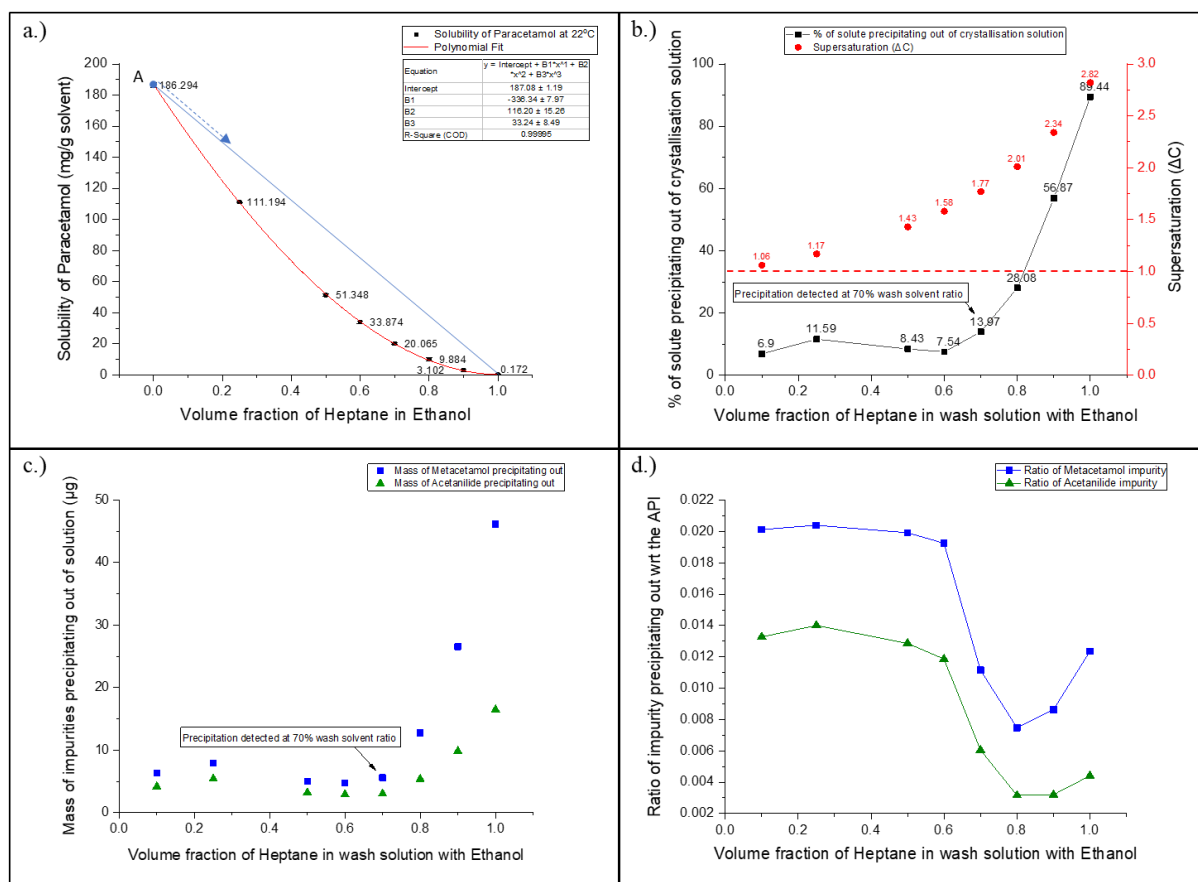


Figure 2-6: Quantitative analysis of the ethanol - n-heptane case. a.) Solubility of paracetamol in ethanol - n-heptane binary solvent mixture at 22 °

b.) Percentage of solute precipitating out of solution for different wash solution compositions is shown in the graph together with the supersaturation achieved in the solution when different ratio of wash solution is added to the saturated crystallisation solvent. c.) Mass of impurities precipitating out when using different ratios of wash solution. d.) Ratio of impurities precipitating out with respect to the paracetamol (API) precipitating out for each of the different ratios of wash solutions used.

As reported in Figure 2-4 and validated by the paracetamol solubility data determined for the ethanol - n-heptane binary solvent mixture (Figure 2-6, graph a), precipitation was detected. The figure shows paracetamol supersaturation was generated as wash solution is added to the saturated crystallisation solution. The end point composition of the solution on the operating dilution line would be dependent on the ratio of wash solution added (Table 2-6). Since the API concentration in the system would be higher than the solubility of the API in the solution (blue dilution line above the solubility curve), supersaturation would be generated, and precipitation would be likely to be observed.

Graph b in Figure 2-6 shows the percentage of solute precipitating out of solution (black line with square points) and the supersaturation level reached (red dots) for the different ratios of wash solution used. Precipitation of the solute was detected after a wash solution of 60% n-heptane and 40% ethanol by volume is used. Before that, the percentage of solute shown as precipitating out of the system is due to the retention of solution in the membrane similar to the effect observed in the ethanol - acetonitrile case, section 2.3.2.1 **Centrifuge vial method – Quantitative Analysis: ethanol - acetonitrile (no nucleation)**. Any increase in n-heptane above 60 % in the wash solution shows a significant increase in the amount of solute precipitating out of solution with around 89 % of the dissolved solute precipitating out of the solution when using pure n-heptane as the wash solvent. This increase in the amount of precipitation taking place is consistent with the increase in the supersaturation value as the amount of n-heptane increases in the system, as seen on the Y axis on the right hand side of graph b.

HPLC of the precipitated crystals was used to determine the composition of the crystals and to quantify the amount of impurities precipitating out of the solution. Graph c in Figure 2-6 shows the amount of impurities, both metacetamol and acetanilide, that were precipitated in the case of ethanol-n-heptane solvent system. There is a gradual increase in the amount of impurity precipitating out of the system, after 0.7 heptane volume fraction at which point precipitation is first detected. Knowing the initial concentration of API and impurities dissolved in the crystallisation solution (Table 2- 8Table 2- 8), over 10% of the metacetamol and around 5% of the acetanilide impurities were precipitated out of the solution when the wash solution used was pure n-heptane.

Table 2- 8: Mass of API and impurities in the 120 µl ethanoic solution

| | |
|-------------------------|---------|
| Mass of Paracetamol (g) | 0.01769 |
| Mass of Metacetamol (g) | 0.00031 |

| | |
|-------------------------|---------|
| Mass of Acetanilide (g) | 0.00035 |
|-------------------------|---------|

Graph d in Figure 2-6 shows the ratio of impurity precipitating out compared to the API in the solution, where the ratio is given in Equation 5 as:

$$\text{Ratio of impurity present} = \frac{\text{mass of impurity}}{\text{mass of API}} \quad \text{Equation 5}$$

As the impurities are uniformly dispersed throughout the solution, the ratio of impurity from 0.1 to 0.6 volume fraction of n-heptane in ethanol are relatively constant, graph d, Figure 2-6. This is because there is no precipitation observed in these samples, the impurities are only present because of the retention of solution in the porous membrane.

After a wash volume fraction of 0.6 n-heptane is exceeded, the precipitation of solute increases, there is a decrease in ratio of impurity precipitating out. Since the amount of impurities in the system is only 2% by mass, at the start of the precipitation process this ratio change is caused by the paracetamol API that is present in the system precipitating out. When the volume fraction of n-heptane in the wash solution reaches 0.8, there is an increase in the ratio of impurity precipitating out with respect to the API. Because the impurity concentrations in the mother liquor are so low, it is unlikely that the impurities are crystallizing as separate crystals. Rather that they are being incorporated in the crystals of paracetamol. When the volume fraction of n-heptane reaches 0.8, around 50% of the paracetamol solute is precipitated out of solution and the supersaturation level is around 2, under these conditions the paracetamol crystal precipitation is rapid and the impurities are easy incorporated into the API crystals. This affect is also seen in the other two solvent mixture cases where precipitation is observed; isopropanol - n-heptane and isoamyl alcohol - n-heptane (see Appendix A - **Exploring the role of anti-solvent effects during washing in active pharmaceutical ingredient purity**).

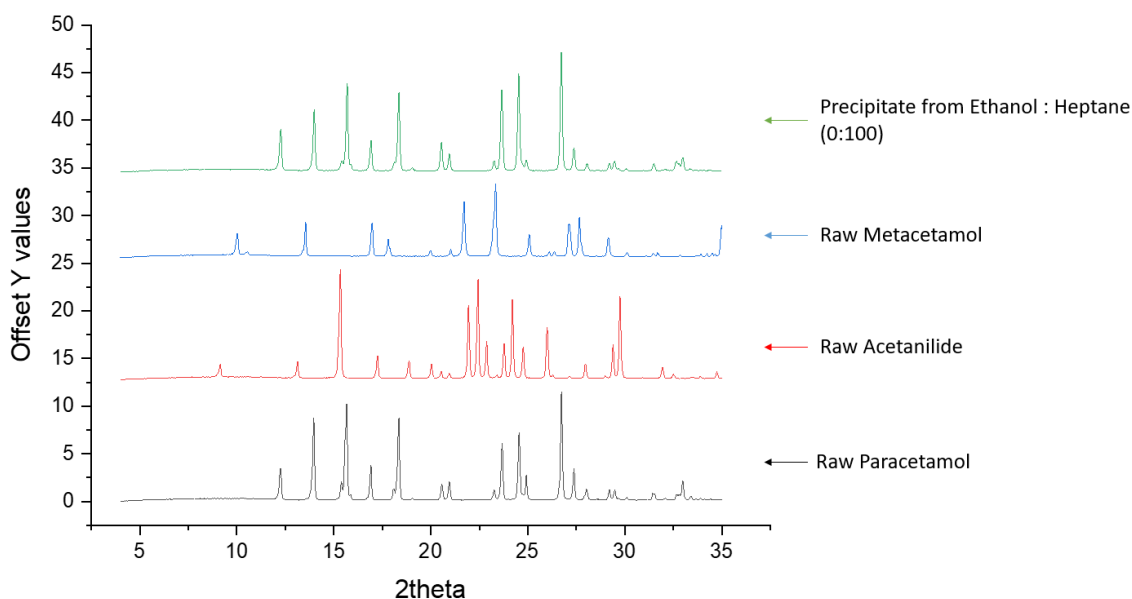


Figure 2-7: XRPD results for raw paracetamol, metacetamol and acetanilide together with the precipitate sample obtained from ethanol – n-heptane sample.

XRPD analysis was performed on the precipitate obtained from the ethanol - n-heptane experiments to analyse the structure of the crystalline material. The diffraction data in Figure 2-7 generated from pure paracetamol, metacetamol and acetanilide provide reference XRPDs. From the sample of precipitated material shown in Figure 2-7, only paracetamol crystals of form 1 are seen to be present, there are no peaks corresponding to metacetamol or acetanilide. DSC analysis was also performed on the raw materials and the precipitate sample obtained from all 3 solvent systems where precipitation was detected (Appendix A - **Exploring the role of anti-solvent effects during washing in active pharmaceutical ingredient purity**). DSC analysis was performed to investigate the effect of presence of impurities in the precipitate samples. The amount of impurities in the precipitate samples were found to be smaller than would be needed to be detected because the measured melting temperature of the samples correspond to the melting temperature of pure paracetamol and no other thermal effect related to the impurity species was observed.

The lack of peaks at 2θ values corresponding to impurities in the XRPD and absence of significant melting point reduction in the DSC result is presumed to be due to the small amount

of impurities present in the precipitate sample compared to the API, as indicated by the HPLC assays. This low concentration of impurities falls below the detection limit of the two techniques, XRPD and DSC, and hence could not be observed.^{22,23}

Use of pure n-heptane as wash solvent in the cases examined would not be an ideal washing strategy due to precipitation of both paracetamol and its impurities of synthesis in the system. Precipitation can be minimised or possibly eliminated by using a two or more-part washing strategy. In the example case, the first wash can be carried out using a 50:50 ethanol: n-heptane wash solution. This would allow for most of the saturated ethanoic solution in the API cake to be displaced by the wash solution without causing precipitation. To further improve purity and aid with the drying process, a second wash can then be carried out using pure n-heptane to wash out the 50:50 wash solution from the API crystal cake. This washing strategy minimises the risk of precipitation in the first wash by using a wash solution with higher solubility limit. Then, a second wash with pure n-heptane mitigates the effect of high supersaturation in the system as the pure wash solvent is not coming in contact with the supersaturated mother liquor in the API cake. Also, the residual n-heptane in the final deliquored API cake, is relatively easily evaporated and because of the low solubility of the API, compared to the 50:50 ethanol: n-heptane wash solution would ensure quicker drying and should also prevent crystalline bridges forming during wash solvent evaporation, minimising agglomeration.

2.4 Conclusion

The quality of the crystalline product which is primarily dominated and controlled in the crystallisation process is widely influenced by the downstream isolation processes. For overall isolation process optimization, it is important to understand and mitigate the adverse effect caused during the washing process. Lack of knowledge and understanding of the washing process can have a dramatic impact on the final crystal product quality achieved at the end of

the drying process. Designing an optimum washing regime is crucial to avoid API product batches that are out of specification.

This study investigates wash solvent selection and introduces a simple and material sparing methodology to help better design washing regimes for API isolation to prevent risk of impurity precipitation during washing. The glass vial anti-solvent methodology which was developed was found to be very effective as a qualitative evaluation based on visual detection of precipitation occurring during washing. Effects such as local nucleation can be identified using this method to provide an insight into the kind of process that can be taking place at the washing front inside a saturated API cake during washing.

The centrifuge vial anti-solvent methodology which was developed was found to be very efficient at quantitatively determining the amount of precipitation that can take place during a washing process. The composition of the precipitated crystals can be then determined using HPLC technique.

In this work paracetamol was used as the model compound. The solubility of the API was experimentally determined at different crystallisation and wash solvent ratios. The two anti-solvent evaluation methodologies developed in this study are straightforward to conduct and were able to provide a good indication of the effects that would occur within a paracetamol API cake during washing. The glass vial method readily indicates if precipitation is likely to occur due to the solvent interaction in a washing process. If so, then the centrifuge vial method can be used to determine the extent and composition of the precipitation taking place.

Both methods developed are quick and easy to perform and allow for prompt wash solvent evaluation. The qualitative results obtained in the 1 mL glass vial method were successfully replicated in 100 mL volumes. The small sample size required for this technique prevents any solvent wastage and is in line with environmental sustainability. The centrifuge vial method

could be further improved by using clear, larger 1 mL vials rather than the opaque 500 µl vials used. However, sourcing such vials with membrane basket compatible with the solvents used in this study proved difficult. Furthermore, using centrifuge vials which would be more solvent airtight would have allowed for mimicking of glass vial method, where the solvent system could be allowed to equilibrate over 24 hours. However, 20 minutes solvent contact time together with vortex mixing is found to be sufficient and the three replicates of each experiment obtained similar result with very good repeatability.

From the results, acetonitrile wash solvent did not cause any anti-solvent effect in the case of paracetamol crystal washing. Use of heptane wash solvent on the other hand caused anti-solvent effect in the case of all 3 crystallisation solvents used in this study. However, these finding alone does not make acetonitrile a good candidate for wash solvent or heptane a poor wash solvent. Developing the right washing strategy and hence choosing the appropriate wash solvent strategy depends on the aim/objective of the washing procedure within the API isolation processes. If removal of impurity is the main focus, then a wash solvent with high solubility can be used (such as acetonitrile in the case of paracetamol), but the yield would be adversely affected and there is a significant risk of agglomeration on drying. However, if complete removal of mother liquor together with minimal effect on the crystal product is the aim, then a multi-step washing strategy should be devised as exemplified in the ethanol - n-heptane solvent mixture example reported in this study. This would allow for removal of mother liquor with a significantly decreased chance of precipitation occurring and hopefully a corresponding expectation of a reduction in agglomerate formation during drying.

Future work would involve applying the anti-solvent wash selection methodology to other, more complex API products to assist with the wash regime design and scrutinise the versatility of the methodology developed on wider API products.

2.5 Abbreviations

International Council for Harmonisation of Technical Requirement for Pharmaceuticals for Human use (ICH); active pharmaceutical ingredient (API); scanning electron microscopy (SEM); paracetamol (PCM); high pressure liquid chromatography (HPLC); X-ray powder diffraction (XRPD); differential scanning calorimeter (DSC); concentration driving force for crystallisation (ΔC)

References

1. Genck, W. Make the most of anti-solvent crystallisation. *Chem. Process.* **2010**. [cited 2020/05/05] <https://www.chemicalprocessing.com/articles/2010/210/>
2. Desiraju, G. R.; Vittal, J. J.; Ramanan, A. *Crystal engineering: a textbook*. Chapter 4. World Scientific Publishing. **2011**.
3. Yazdanpanah, N.; Nagy, Z. K.; Price, C. J.; Barton, A.; Coleman, S. J. *The handbook of continuous crystallisation*. Chapter 13. RSC. **2020**.
4. Ottoboni, S.; Shahid, M.; Steven, C.; Coleman, S.; Meehan, E.; Barton, A.; Firth, P.; Sutherland, R.; Price, C. J. Developing a batch isolation procedure and running it in an automated semi continuous unit: AWL CFD25 case study. *Org. Process Res. Dev.* **2020**. 24. 4. 520-539.
5. Pietsch, W. B. The strength of agglomerates bound by salt bridges. *The Canadian J. Chem. Eng.* **1969**. 47.
6. Terdenge, L. M.; Wohlgemuth, K. Impact of agglomeration on crystalline product quality within the crystallisation process chain. *Cryst. Res. Technol.* **2016**.
7. Birch, M.; Marziano, I. Understanding and avoidance of agglomeration during drying processes: a case study. *Org. Process Res. Dev.* **2013**. 17. 1359–1366.
8. Heng, J. Y. Y.; Bismarck, A.; Lee, A. F.; Wilson, K.; Williams, D. R. Anisotropic surface energetics and wettability of macroscopic form I paracetamol crystals. *Langmuir.* **2006**.
9. Ellis, F. *Paracetamol – a curriculum resource*. Royal Society of Chemistry. **2002**. ISBN 0-85404-375-6.
10. Prasad, K. V. R.; Ristic, R. I.; Sheen, D. B.; Sherwood, J. N. Crystallisation of paracetamol from solution in the presence of impurity. *Int. J. Pharm.* 215. **2001**. 29-44.
11. Hulse, W. L.; Grimsey, I. M.; Matas, M. D. The impact of low-level inorganic impurities on key physicochemical properties of paracetamol. *Int. J. Pharm.* 349. **2008**. 61-65.

12. Martino, P. D.; Conflant, P.; Drache, M.; Huvenne, P.; Guyot-Hermann, A. M. Preparation and physical characterization of forms II and III of paracetamol. *J. Therm. Anal.* Vol 48. **1997**. 447-458.
13. Hendriksen, B. A.; Grant, D. J. The effect of structurally related substances on the nucleation kinetics of paracetamol (acetaminophen). *J. Cryst. Growth*. **1995**. 252.
14. Kossik, J. Small Scale Continuous Cake Filtration using the Disposable Rotary Drum Filter. *Filtr.* **2003**. 26-27.
15. Granberg, R. A.; Rasmuson, A. C. Solubility of Paracetamol in Pure Solvents. *J. Chem. Eng. Data*. **1999**. 44. 1391 – 1395.
16. Murugesan, S.; Sharma, P.K.; Tabora, J. E. Design of Filtration and Drying Operations., p315-346 in *Chemical Engineering in the Pharmaceutical Industry: R&D to Manufacturing*. Wiley New York. **2010**.
17. Kramer, H. J. M.; Van Rosmalen, G. M. Crystallisation. *Encyclopedia of Separation Science*. Academic Press. **2000**. 64-84.
18. Romero, S., Reillo, A., Escalera, B., Bustamante, P. The behaviour of paracetamol in mixtures of amphiprotic and amphiprotic-aprotic solvents. Relationships of solubility curves to specific and nonspecific interactions. *Chem Pharm Bull*. **1996**. 44. 1061-1064.
19. Prakongpan, S., Nagai, T. Solubility of acetaminophen in cosolvents. *Chem Pharm Bull*. **1984**. 32. 340-343.
20. Hojjati, H., Rohani, S. Measurement and Prediction of Solubility of Paracetamol in Water-Isopropanol Solution. Part 1. Measurement and Data Analysis. *Org Process Res Dev*. **2006**. 10. 1101-1109.
21. Subrahmanyam, C.V.S., Reddy, M.S., Rao, J.V., Rao, P.G. Irregular solution behaviour of paracetamol in binary solvents. *Int. Journal of Pharmaceutics*. **1992**. 78. 17-24.
22. Dutrow, B. L.; Clark, C. M. X-ray Powder Diffraction (XRD). *Geochemical Instrumentation and Analysis*. Carleton College. [cited 2020/05/10] https://serc.carleton.edu/research_education/geochemsheets/techniques/XRD.html
23. Durowoju, I. B.; Bhandal. K. S.; Hu, J.; Carpick, B.; Kirkitadze, M. Differential scanning calorimetry – a method for assessing the thermal stability and conformation of protein antigen. *J. Vis. Exp*. **2017**.
24. DDBST GmbH. [cited 2020/04/18] http://www.ddbst.com/en/EED/PCP/VIS_C11.php
25. CAMEO Chemicals. [cited 2020/05/01] <https://cameochemicals.noaa.gov/chemical/3659>
26. Wypych, G. A. *Databook of solvents*. ChemTec Publishing. 2014.
27. PubChem. [cited 2020/05/12] <https://pubchem.ncbi.nlm.nih.gov/compound/>
28. Accudynet. [cited 2020/05/12] https://www.accudynetest.com/visc_table.html

3. Employing constant rate filtration to assess active pharmaceutical ingredient (API) washing efficiency

[This chapter is published in Organic Process Research and Development;

Shahid, M.; Faure, C.; Ottoboni, S.; Lue, L.; Price, C. Employing constant rate of filtration to assess active pharmaceutical ingredient (API) washing efficiency. *Org. Process Res. Dev.* 2022. 26, 1, 97–110.]

3.1 Introduction

The pharmaceutical industry sets a high standard of purity which the final API must meet.¹ To achieve this, washing of the cake is a fundamental post-filtration treatment step. After filtration, residual mother liquor (crystallisation solvent containing un-reacted starting materials and unacceptable side-products) is retained, trapped inside the porous structure of the solid bed. If this mother liquor is not removed before the downstream drying process, the dissolved material will be deposited on the product crystal surfaces resulting in the presence of impurities in the final product.² Therefore, washing is a vital purification step, required to remove impurities from the filtered cake.

Washing of the cake is typically achieved using the same driving force (centrifugal, pressure, vacuum) as filtration and is carried out in the same process equipment used for filtration, so usually little or no additional equipment is required.³

Filtration can either be carried out using a constant pressure driving force or a constant rate filtration. Most laboratory filtration works to isolate the product by using constant pressure; normally using laboratory vacuum or overpressure from a compressed gas line.⁴ This is largely due to the readily available laboratory filtration equipment designed with this in mind.⁵

There are a number of advantages of using constant rate filtration in preference to constant pressure filtration. The homogeneous constant growth rate of the cake, using constant rate filtration, provides a better packing structure independent of cake thickness.^{6,7,8} Constant rate filtration allows the rate of liquid transport through the filter medium to be fixed whereas in constant pressure filtration the initial rate of flow through the filter medium is highest when the cake is thin but declines as the cake builds and the filter cake resistance increases. As a consequence, any fine particles present are less likely to be carried into the filter medium leading to filter medium blinding. Reports by many authors indicate that the measured cake

and medium resistances are influenced by the migration of fine particles accumulating in the lower layers of the cake close to and within the filter reducing the flow rate through them.⁹⁻¹⁵

A screening methodology was developed in a previous study, chapter 2, to qualitatively and quantitatively analyze the propensity for precipitation to occur during the washing of an API (paracetamol) with different solvents.^{16,17} This methodology allowed us to identify solvent combinations which would prevent/limit any precipitation or dissolution in the case of paracetamol. It was found that starting the washing with mixture consisting of both a well-chosen wash solvent and the crystallization solvent is best for avoiding precipitation during the initial stages of washing. This is followed by washing with the selected wash solvent in which the API has negligible solubility leading to a process where there is a reduced chance of agglomerates forming during drying. Although the methodology is exemplified with paracetamol, the approach is likely to be widely applicable.

This work took the selected wash solvents from the previous work,¹⁶ and used constant rate filtration to investigate wash performance for paracetamol as a representative API. Three different grades of paracetamol were used to allow investigation of the effect of particle size on washing performance. Constant rate filtration, and subsequently constant rate washing, was employed in this study to investigate whether the particle packing, and cake structure formed using this method allows for more uniform migration of the wash solvent through the API cake and therefore leads to improved washing performance. Furthermore, unlike in constant pressure filtration, the wash solvent flowrate through the saturated cake can be controlled in constant rate filtration. This enables the role of wash solvent contact time to be investigated using the very small quantities of material consistent with that typically available in early pharmaceutical development.

The ultimate aim of this work is to use constant rate filtration to design a washing process based on data and understanding with a focus on identifying a washing strategy which is effective

and reproducible in obtaining washed material with the required purity, yield and particle size distribution whilst minimizing waste generation.

3.2 Material and Method

3.2.1 Raw Materials

Paracetamol (PCM) was selected as a representative test compound with three different size distributions (micronised, crystalline and granular) being used. Micronised grade material (batch 042213E407; Mallinckrodt Inc., Staines-upon-Thames, UK.) settles very slowly from suspension and has a large wetted surface area to wash. Granular material (batch 161713J561; Mallinckrodt Inc.) on the other hand settles rapidly and has a wide particle size distribution. The intermediate grade (batch 637514D001; Mallinckrodt Inc.) is more typical of the size distribution of a pharmaceutical crystalline material. Particle size distribution (PSD) determined for all 3 PCM grades investigated is given in Table 3-1.

Table 3-1: Particle size distribution of different PCM grades investigated within this study

| Paracetamol Grades | Particle size distribution | | |
|--------------------|----------------------------|----------------------|----------------------|
| | D ₁₀ (µm) | D ₅₀ (µm) | D ₉₀ (µm) |
| Micronised | 6.52 | 27.6 | 198.2 |
| Crystalline | 12.48 | 43.9 | 101.3 |
| Granular | 246.8 | 361.4 | 517.8 |

Patent Blue V sodium salt (LOT: BCBP1872V; Sigma-Aldrich) was used as an impurity in the study to help evaluate wash performance and cake purity. The dye aids visualization of the filtration and washing process as well as being readily quantified spectroscopically.

To investigate washing efficiency of a “real process” slurry, three different crystallisation solvents, commonly used in industry, were used; ethanol (absolute, purity ≥ 99.8%, Sigma-Aldrich), isopropanol (purity ≥ 99.5%, Sigma-Aldrich) and 3-methylbutan-1-ol (also known as

isoamyl alcohol) (purity $\geq 99\%$, Sigma-Aldrich). Three wash solvents used in this study were; acetonitrile (purity $\geq 99.9\%$, Sigma-Aldrich), n-heptane (purity 99.9% , Sigma-Aldrich) and n-dodecane (purity 99% , Alfa Aesar). Acetonitrile was chosen due to the relatively high solubility of the API compared to that in both n-heptane and n-dodecane. n-Dodecane is immiscible in all 3 crystallisation solvents, hence is useful for investigating washing displacement mechanisms. Also in some experiments using n-heptane or n-dodecane, a wash solution consisting of a mixture of the crystallisation and the wash solvent was used as a first wash before using the pure wash solvent as a second wash (the composition ratios of the solvent mixtures were taken from results of previous work).¹⁶ This enabled examination of the approach for minimisation of “anti-solvent” effects taking place during washing. For acetonitrile, no “anti-solvent” effect was identified during previous studies and hence only pure acetonitrile was used as a first wash in all experiments containing acetonitrile.

For post experimental analysis, 2,2,4-trimethylpentane (isooctane) (purity 99.9% (GC), Merck) is used as a wet dispersant for particle size analysis of the input paracetamol grades as well as the final washed cake. Deuterated dimethyl sulfoxide (DMSO- d_6) (extent of deuteration, 99.8% , for NMR spectroscopy, VWR) was used for NMR analysis of the washed cake to quantify the amount of mother liquor present in the final API product.

3.2.2 Suspension Preparation

PCM particle suspension was prepared by adding the API in two stages: the first portion was to form a saturated solution at lab temperature ($22\text{ }^\circ\text{C}$). A known mass of Patent Blue V dye was then added to the saturated solution (below the solubility limit of each crystallization solvent), before a second portion of PCM was added to the saturated solution to form a crystal suspension with 15% by mass, solid loading. In this way minimal change to the PSD of the raw material was ensured.

The solubility of PCM and Patent Blue V dye in all the solvents used throughout this work was taken from literature where available,¹⁸ and also determined experimentally by gravimetric analysis. A Hailea HC-100A chiller was used to maintain the temperature at 22 °C (the average temperature of the lab where the anti-solvent screening experiments were conducted). Excess Paracetamol/Patent Blue V dye was added to 20mL, clear glass vials together with the solvent and a magnetic stirrer bar. The vials were sealed and left on a multi-position stirrer plate inside the water bath for around 48 hours to equilibrate. Samples of the solutions were then taken from the slurry in the vials using a syringe and filtered using a PES syringe filter (Fisher brand, Cat No. 15206869, 0.2µm, sterile), and added to a separate glass vial which was weighed and then left to dry. Table 3-2 shows the determined solubility in each solvent investigated, which is then used to prepare the PCM slurry with blue dye impurity.

Table 3-2: Solubility measurements determined experimentally at 22oC (lab temperature)

| Solvent | PCM Solubility (mg/g solvent) | Blue Dye Solubility (mg/g solvent) |
|-----------------|--|---|
| Ethanol | 186.8 | 1.027 |
| Isopropanol | 114.1 | 0.701 |
| Isoamyl Alcohol | 52.6 | 0.736 |
| Acetonitrile | 24.03 | 0.418 |
| n-heptane | 0.267 | 0.000 |
| n-Dodecane | 0.072 | 0.000 |

3.2.3 Experimental Setup & Design

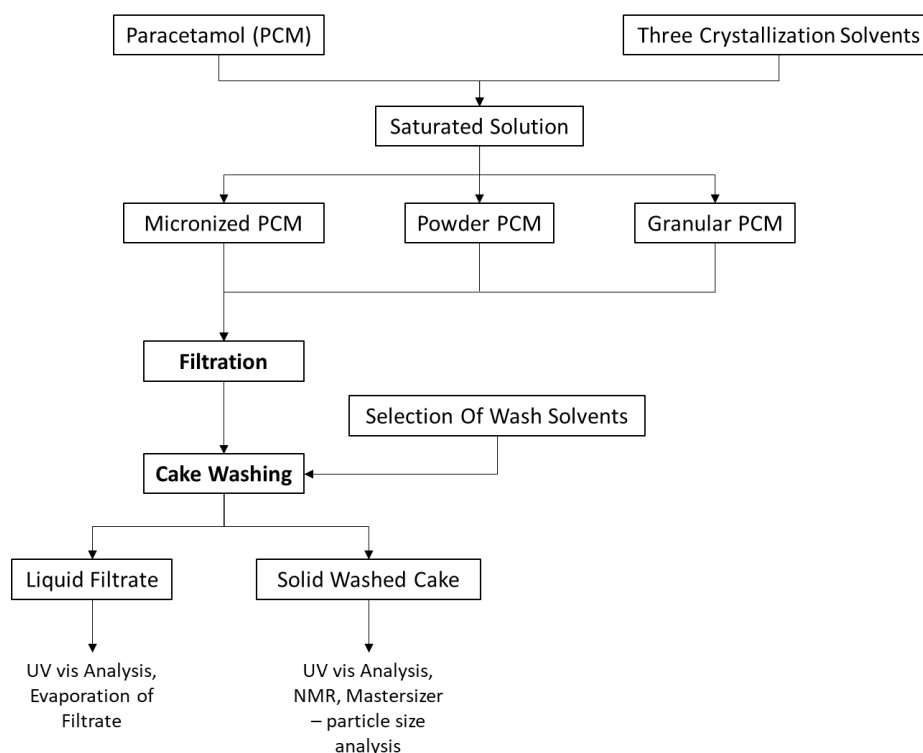


Figure 3-1: Experimental procedure

In order to investigate washing performance and the propensity of different grades of paracetamol to agglomerate under the different process conditions, the experimental procedure was divided into a series of consecutive steps as can be seen in Figure 3-1.

A multivariate design of experiment (DoE) approach was used to investigate the combined effects of the key parameters on final quality of the washed API cake. MODDE (Umetrics, Sweden) was the software used for the DOE analysis. For this work, a D-Optimal screening approach was used in order to minimize the number of experiments whilst maximizing the insight gained, this resulting in 22 experiments with 3 center point experiments to determine reproducibility of the experimental procedure (see Appendix B - **Employing constant rate filtration to assess active pharmaceutical ingredient (API) washing efficiency**).

The D-Optimal approach used in this work is appropriate because the experimental variables investigated comprised of a combination of quantitative and qualitative factors.¹⁹ Table 3-3

contains the list of variables and responses used within this study. A number of potential factors were kept constant and were not included in the DOE: the API used (Paracetamol), impurity used (Patent Blue V dye), volume of slurry (50mL), slurry solid loading (15% w/w), pore size of filter media used (nominal pore size of 20 μ m), the temperature of the suspension and wash solvent during filtration and washing (lab temperature \approx 20 °C).

Coefficient plots are used in section 3.3 **Results and Discussion** section to report the correlation between factors and responses. Coefficient plots provide graphical representation of the significance of the model terms in explaining each experimentally determined response. A significant term is one with a large distance from $y = 0$ as well as having an uncertainty level that DoEs not extend across the $y = 0$ value. The error bar represents the 95% confidence interval related to the coefficient. Some of the regression coefficient plots presented in section 3.3 **Results and Discussion** reports on the Y axis (responses) employ the expression “extended”. If a term in the model comprises a qualitative factor, C, with x levels, there will be $x - 1$ expanded terms associated with that term for the regular option, whereas in the expanded option all of the levels are correlated with the selected response. For example, considering the API grade as a qualitative factor, there are three levels; micronised, crystalline, and special granular. In the regular option for presenting the qualitative coefficients, MODDE plots report crystalline, and special granular, while with the expanded option MODDE plots all of the three levels.^{19,20}

Combination of qualitative and quantitative factors was used in this DoE design did not allow for the prediction of optimal design space. However, the use of qualitative factors was necessary to screen for essential washing parameters. Therefore, the results from the coefficient plot were used together with the experimental observations to qualitatively define optimal washing design space for paracetamol API with the blue dye impurity.

Table 3-3: Table of factors, responses and analytical techniques used to quantify the responses in the DoE

| Variables | |
|---------------------------------|--|
| Factors (abbreviation) | Range and units |
| Solid API grade (Par) | micronised, crystalline, granular |
| Crystallisation solvent (Cry) | ethanol, isopropanol, isoamyl alcohol |
| Wash solvent (Was) | n-dodecane, n-heptane, acetonitrile, mix dodecane, mix n-heptane |
| Filtration & washing rate (Fil) | 10 – 100rpm (1.3 – 11.7mL/min, respectively) |
| Volume of wash solvent (Vol) | 1 void volume ¹ , 2 void volume, 3 void volume |
| Number of washes (Num) | 1, 2, 3 |
| Responses | |
| Responses (abbreviation) | Analytical method used to quantify response |
| Mother liquor Remaining (MLR) | ¹ H NMR for residual solvent composition |
| Impurity removal (IR) | UV-vis Spectrophotometer |
| API lost to washing (APIL) | Mass balance |

¹Void volume refers to the wash volume quantity that corresponds to cake pore volume. It can be calculated using the Equation 6.

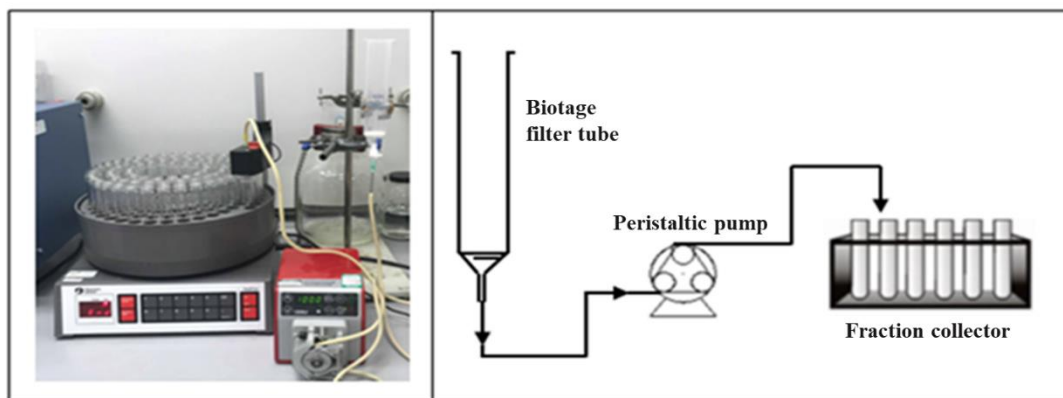


Figure 3-2: Experimental setup for constant rate filtration including process flow diagram of the setup used

Figure 3-2 shows the experimental setup used in the lab as well as a process flow diagram of the setup. For filtration and washing, a Biotage ISOLUTE (Biotage AB, Uppsala, Sweden) 70mL single-fritted polypropylene reservoir with 20 μ m pore size was used, this was connected to a PTFE valve and a flexible tube (Watson-Marlow, Marprene tubing, 302.0016.016#14, 1.6mm Bore x 1.6mm wall, volume hold up 2mL/m). The tube was connected to a peristaltic pump (Watson-Marlow, 120 pump drive, 40DM3 pump head) which controlled the flow of solvent. A fraction collector (RediFrac, Code No. 18-1003-64, GE Healthcare Bio-Sciences AB, Sweden) was placed at the end of the liquid discharge tube to segregate and collect the different fractions of filtrate, which were latter analysed using UV-vis spectrophotometry to obtain a high resolution time resolved washing profile. The volume of the individual fractions collected for each experiment was kept consistent at around 3.2mL by adjusting the filtrate collection time depending on the pumping rate, see Table 3-3.

Before the start of each experiment, the filter tube and filtrate collection vials were weighed. A complete mass balance was kept through-out the experiment. A 50mL sample of crystal suspension was transferred to the filter tube, making sure complete removal of slurry was achieved while transferring from the sample bottle to the biotage filter tube. The peristaltic pump was then turned on at the required pumping rate immediately before opening the valve

and allowing the filtrate to flow through the filter medium into the collection vials. On reaching dryland (the point when the filter cake surface is first exposed) the pump was halted, the PTFE valve closed and the filter tube with the valve was weighed, and the filter cake thickness measured. The required volume of wash solvent was then measured and carefully added to the filter tube by slowly running wash solvent down the wall of the tube, making sure not to disturb the filter cake surface. The wash volume corresponds to the cake pore volume, Equation 6:^{21,22}

$$V_{void} = V_{cake} - V_{solid} = \frac{\pi d^2 h}{4} - \frac{m_s}{\rho_s} \quad \text{Equation 6}$$

Where d is the cake diameter (m), h is the cake height (m), m_s is the mass of the API in the filter cake (kg) and ρ_s is the crystallographic particle density of the API (kg/m³). The role of wash volume is investigated in this study by adjusting both the wash quantity relative to cake void volume and the number of washes used, see Table 3-3.

The wash solvent passes through the cake and the medium at the same pumping rate as the filtration stage of the experiment. This procedure is repeated for each washing step if more than one was required. The final wash is followed by cake deliquoring which is stopped as soon as the bubble point is detected (the point at which a break in the steady flow of filtrate is observed). The filter tube mass and the filter cake thickness are then measured, and the vial numbers noted at the points where filtration and washing stops.

3.2.4 Liquid Filtrate Off-line Post Analysis

At the end of the experiment, the vials containing the filtrate are weighed. The filtrate sample is then analysed with UV-vis spectroscopy to quantify the Patent Blue V dye. This allows the high resolution time resolved wash profile of the experiment to be obtained. The impurity removal performance is calculated by determining the number collected vials of filtrate taken to remove the blue dye and for the blue dye concentration to level off at its minimum value. An example wash profile obtained from experiment 1 is presented in Figure 3-3. From the wash

profile it is apparent that the blue dye concentration remains constant for a period of time after the filtration reaches dryland and the wash solvent is transferred to the filter cake. The concentration starts to decrease at filtrate sample number 17. This is the point where the first of the wash solvent starts to emerge from the filter cake and is collected in the filtrate vial. The concentration declines and levels off at a final concentration at or close to 0 by filtrate sample number 22. Therefore, the impurity removal response input to the DoE software MODDE for experiment 1 is 6 as it took 6 filtrate samples for the blue dye concentration to approach zero.

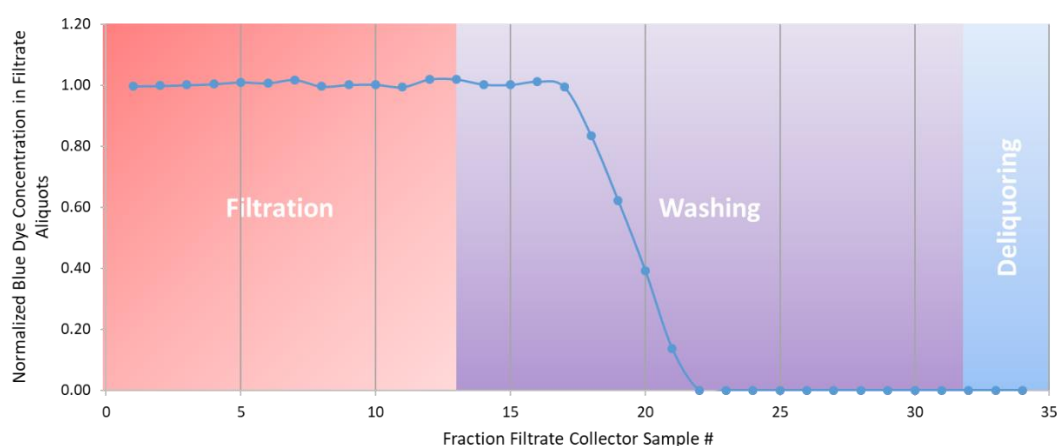


Figure 3-3: Evolution of blue dye impurity concentration in filtrate – EXP 1

Following the UV-vis analysis, the remaining filtrate in the vials were reweighed and the vials were left to dry out fully for gravimetric analysis. Determining the amount of API dissolved in each collected filtrate aliquot, together with knowledge of the quantity of API dissolved in the mother liquor solution at the start of experiment, allows the mass of API lost during the washing process to be calculated. This allows the API corresponding profile of API loss to washing to be determined, as shown in Figure 3-4. The data is also included as a DoE response for each experimental run, Table 3-3.

3.2.5 Solid API Cake Off-line Post Analysis

At the end of the experiment, the mass of filter tube with the washed API cake is measured before deliquored API cake is removed from the biotage filter tube. A small fraction of the

cake is taken and added to around 20mL of water. Any blue dye impurity still present in the API cake at the end of the washing process dissolves in the water. This was analysed using UV-vis spectroscopy, similar to the method used for liquid filtrate samples.

The particle size distribution of the raw PCM grades, as well as that of the damp washed cakes obtained at the end of each experiment was analysed using a wet dispersion laser diffraction technique. Further information on particle size distribution is provided in Chapter 4, section 4.2.

To quantify the amount of residual solvent(s) relative to solute, present within the washed cake, a few milligrams of the damp filtered cake was taken and dissolved in 0.75mL of DMSO-d₆, for ¹H-NMR analysis. An AVII+600 NMR Spectrometer BRUKER Advance 2+ (Bruker, UK) is used to collect proton NMR spectra. A T1/T2 relaxation time evaluation is performed for all solvent combinations (process parameters: frequency axis F1 equals to 32, pulse program t1ir, 4 scans, 2 replicas of T1/T2 analysis to evaluate T1 relaxation). Each sample was analysed in duplicate. This approach allowed the percentage of mother liquor still present in the washed cake (with respect to the quantity of the wash solvent) and hence the mother liquor remaining response to be determined, Table 3-3.

The remaining damp filter cake is weighed and left to dry in the fume hood, to determine the residual solvent content in the cake by loss on drying and the mass of API obtained at the end of the isolation process.

3.3 Results and Discussion

Using the constant rate filtration/washing experimental setup shown in Figure 3-2 allows sequential collection of aliquots of wash filtrate using a fraction collector, this high resolution sample collection would be challenging to achieve in a laboratory environment using a constant pressure vacuum filtration.⁵ The method used allowed detailed analysis of the evolving liquid

filtrate composition rather than just the purity of the isolated solid API, which is the part traditionally analysed during isolation process development.

Figure 3-4a shows a close-up of a few dried filtrate vials with precipitated PCM present inside with blue dye impurity in some of the vials. Figure 3-4b shows the sequence of filtrate samples collected during experiment 15. The solution in the vials shows a gradual decrease in color intensity arising from the blue dye impurity removal, with latter vials only showing API removal as all of the blue dye impurity is removed at the start of washing. Figure 3-5 graphically illustrates the blue dye impurity concentration in the filtrates shown in Figure 3-4b. In addition, the figure shows the loss of API occurring during washing in experiment 15. The x-axis of the graph represents the filtrate sample number in this experiment. The right hand y-axis of the graph corresponds to the normalized blue dye concentration calculated using $c^* = \frac{c}{c_0}$ Equation 1 and represented as grey dots in the graphs. The blue dye concentration seems to be decreasing after filtration stage, once all the mother liquor is removed, and reaches to zero at filtrate fraction sample 20 as all of the blue dye impurity is removed from the cake. This shows that no further washing of the API cake is required as all of the blue dye is removed and hence washing could be stopped at that point without any further usage of wash solvent. Analyzing the liquid wash filtrate hence allows us to determine the end point of washing, and so could help reduce any wastage of solvent.

The left-hand y-axis and the blue dots in Figure 3-5 corresponds to the cumulative API (paracetamol) lost in solution in the filtrate during the filtration and washing steps in experiment 15. Experiment 15 was carried out using acetonitrile wash solvent, in which paracetamol has the highest solubility of the three wash solvents used (Table 3-2). Examining the blue dotted line there is no difference in the gradient of the line between the filtration and washing step. Comparing this to experiment 1, Figure 3-6, we can clearly see difference in the

gradient of the blue dotted line as the mother liquor fronts end and the wash solvent flows through the API filtered cake and begins to be collected. This is due to n-heptane being used as wash solvent in experiment 1, in which the API has very low solubility (Table 3-2). Also the crystallisation solvent in experiment 15, Figure 3-5, is isoamyl alcohol, in which paracetamol has significantly lower solubility than ethanol crystallisation solvent used in experiment 1, Figure 3-6, (Table 3-2). Using this constant rate technique for wash process analysis allows us to relate product loss to the combination of solubility in the primary solvent, solubility in the mixture of primary solvent and wash solvent and finally solubility in the wash solvent, hence allows us to minimize loss of API. In seeking to improve wash efficiency by examining Figure 3-5 & Figure 3-6 is important to note that the API losses associated with displacing mother liquor cannot be reduced by modifying the washing regime, this is inherently tied to the crystallization process. The opportunity arises from minimizing the API loss associated with dissolution in the mixture of mother liquor and wash solvent and then subsequently in wash solvent.



Figure 3-4: a.) Close-up of a few dried filtrate vials showing presence of precipitated material. b.) Collected filtrate vials from experiment 15 showing gradual blue dye impurity removal from the system

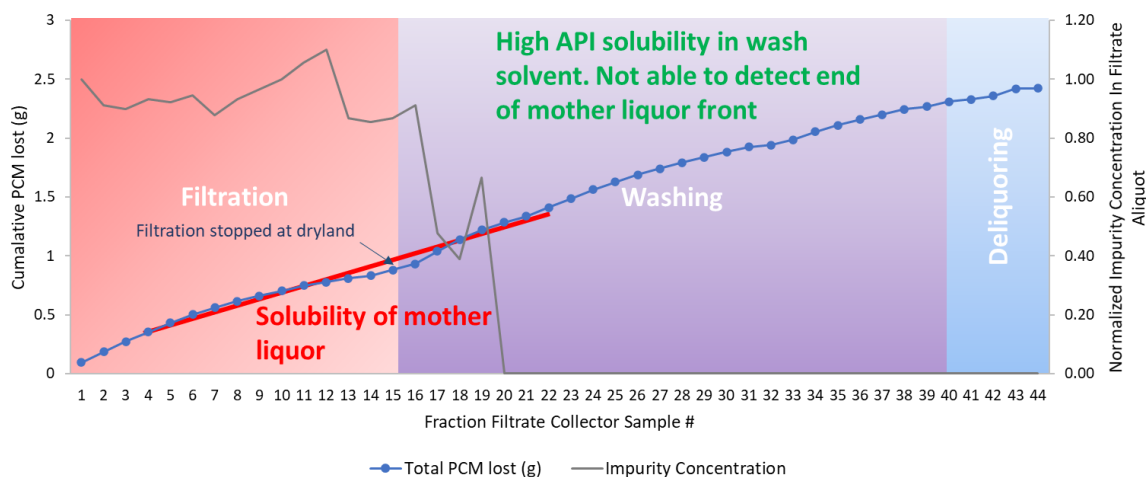


Figure 3-5: Experiment 15 – paracetamol grade – crystalline, crystallisation solvent: isoamyl alcohol, wash solvent – acetonitrile, filtration & washing rate – 100 rpm, volume of wash solvent – 3 cake void volume, number of washes – 3, mass of PCM API lost during wash = 1.48 g

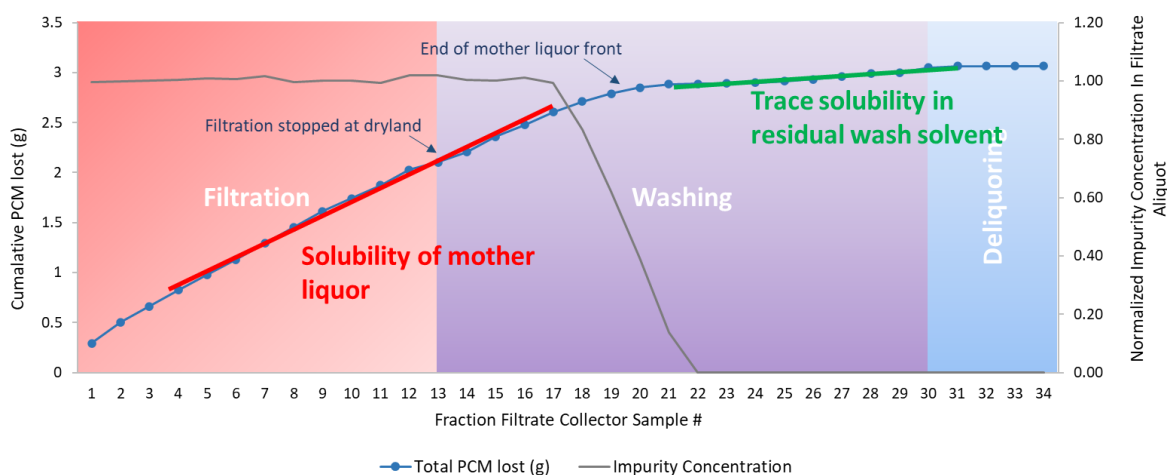


Figure 3-6: Experiment 1 – paracetamol grade – crystalline, crystallization solvent – ethanol, wash solvent – n-heptane, filtration & washing rate – 10 rpm, volume of wash solvent – 1 cake void volume, number of washes – 3, mass of PCM API lost during wash = 0.1 g

3.3.1 API loss

Figure 3-7 shows how the selected factors affect the API loss during the washing process. The coefficient plot (Figure 3-7) shows a good reproducibility value of 0.97 and a good fit between data and model, and hence the model has a good capability to predict responses. The plot demonstrates that API loss during washing is affected by factors such as API grade, crystallization solvent, wash solvent, filtration rate and the number of washes.

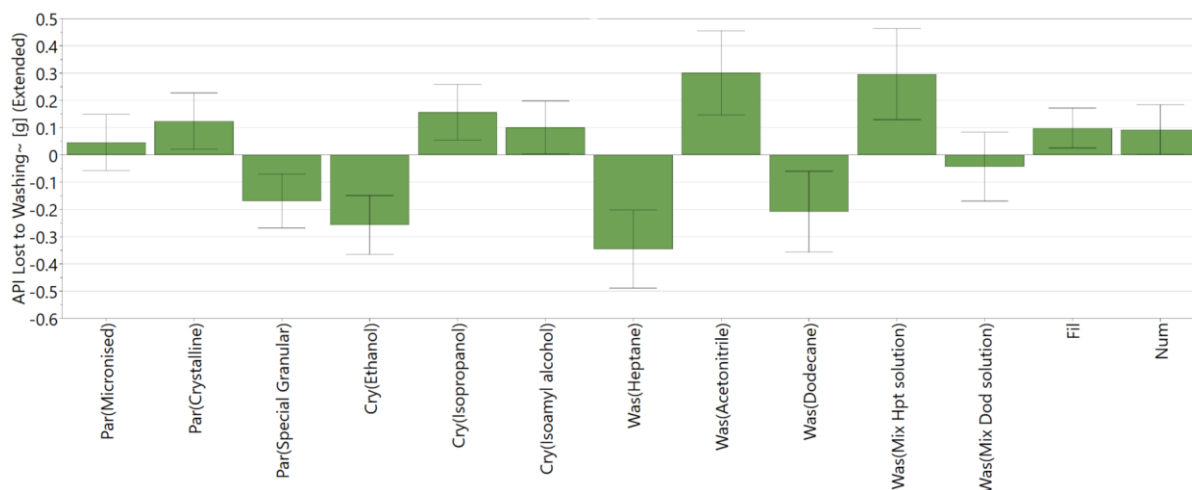


Figure 3-7: DoE variables that effect API loss during the wash process, $R^2 = 0.93$, $Q^2 = 0.61$, reproducibility = 0.97

The main factor affecting the API loss during washing is the identity of the wash solvent. Using a wash solvent with high API solubility such as acetonitrile results in a significant amount of API loss during the washing process, as shown by positive increase in paracetamol loss in Figure 3-7. The amount of API lost during washing using an n-heptane-crystallization wash solution mixture and n-dodecane-crystallization wash solution mixture is also found to be higher than when using pure n-heptane and n-dodecane wash solvent. The binary solvent mixtures have higher solubility than pure wash solvents and so the addition of these mixtures as first wash would result in higher API loss during the washing process.¹⁶

One of the problems encountered in the initial experimental procedure was the slow rate of filtrate evaporation in experiments containing n-dodecane as wash solvent. The tall 10.5mL vials with narrow base (67mm x 15mm) that are designed to use with the fraction collector combined with the high boiling point of n-dodecane prevented all of the n-dodecane from evaporating in some of the filtrate samples even after leaving them in a vacuum oven at high temperature for over one week. This resulted in not being possible to obtain the full mass balance to determine the API lost in the filtrate for experiments containing n-dodecane. However, by comparison with experiments where only n-heptane was used as the wash solvent, there was negligible API loss in the filtrate during the final phase of the washing process, where

the wash solvent is displaced, see Figure 3- 8 a and b for experiment 8 and 13 respectively. Considering paracetamol have similar negligible solubility in n-dodecane, (see Table 3-2), it was judged to be reasonable to assume similarly that there would be no measurable loss of API in the final filtrate samples collected during washing when using pure n-dodecane as wash solvent.

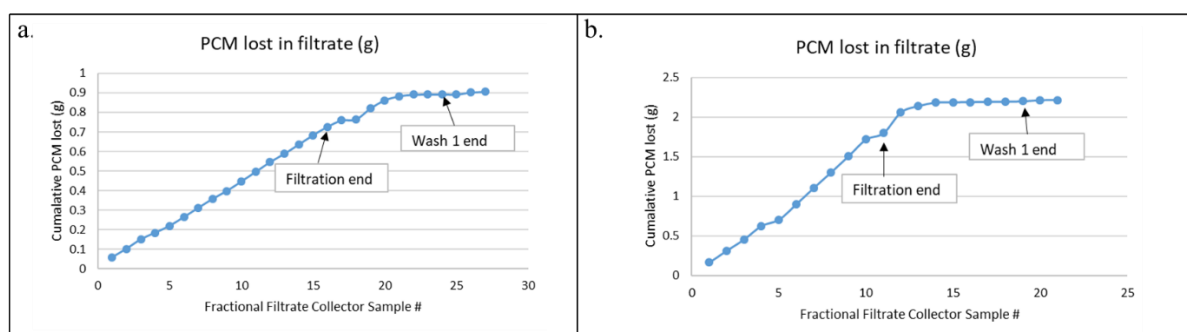


Figure 3- 8: a.) Graph showing cumulative API loss in filtrate samples throughout experiment 8, mass of PCM API lost during wash = 0. b.) Graph showing cumulative API loss in filtrate samples throughout the experiment 13, mass of PCM API lost during wash = 0

API grade was another factor affecting API loss during washing. The API grades with small particles, i.e. micronized and crystalline paracetamol have a larger surface area that allows for a greater amount API to dissolve during washing. Micronized API with broad particle size result in higher cake tortuosity resulting in longer wash solvent flow path through the API cake and so greater chance for API dissolution due to greater available surface area.^{2,9} Both filtration/washing rate and the number of washes carried out had an effect on the API loss during washing. The range of wash solvent flowrates investigated in the DoE was 1.3mL/min to 11.7mL/min, this made a substantial difference in the duration of contact time; around 20-25 minutes, at the low flow rate (depending on wash quantity) compared to the 2-3 minutes the wash solvent spent in contact with the cake at the high wash flowrate. This increased duration of contact time allows for a closer approach to thermodynamic equilibrium to be achieved (potentially allowing the API to approach the saturation solubility level), resulting in more API dissolving in and being removed with the wash solvent.²⁴ This can be observed when

comparing results obtained from experiment 2 (Figure B-7a, Appendix B - **Employing constant rate filtration to assess active pharmaceutical ingredient (API) washing efficiency**) with experiment 9 (Figure B-14a, Appendix B - **Employing constant rate filtration to assess active pharmaceutical ingredient (API) washing efficiency**). For both these experiments acetonitrile is used as a wash solvent, however much more API is lost during washing in experiment 9 where 10rpm filtration/washing rate is used, compared to very little API loss observed during washing in experiment 2, at 100rpm filtration/washing rate. Also, increasing the amount of wash solvent used with a higher number of washes again results in larger amount of API being dissolved, without necessarily changing the extent of impurity removal.

3.3.2 Purity

Figure 3-9 shows the factors affecting the removal of mother liquor/crystallization solvent from the filtered API cake during the wash process. The coefficient plot (Figure 3-9) shows a good reproducibility value and indicates a good fit between the model and the data for mother liquor removal, however does not demonstrate that the model has a good capability to predict responses based on the low Q^2 value of 0.27 compared with 0.61 for prediction of API losses. Figure 3-10 shows the main factors affecting the removal of the blue dye impurity during the washing process. The coefficient plot (Figure 3-10) shows good fit between the data and model and the model's capability to predict responses. The low reproducibility of the model, 0.44 is due to the variation in the results obtained from the three DoE centre point experiments. Due to the low prediction & fitting of these DOE models, the data from the experimental runs together with the images of the washed cakes taken in Figure 3-11 were used to understand the results obtained from DoE model.

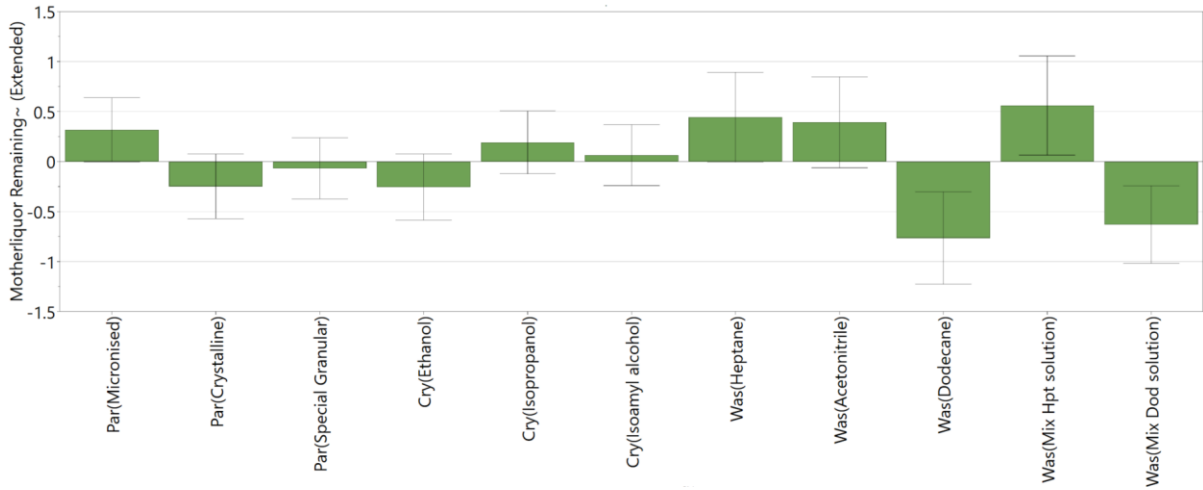


Figure 3-9: DoE variables that affect mother liquor removal during the wash process, $R^2 = 0.77$, $Q^2 = 0.27$, reproducibility = 0.80

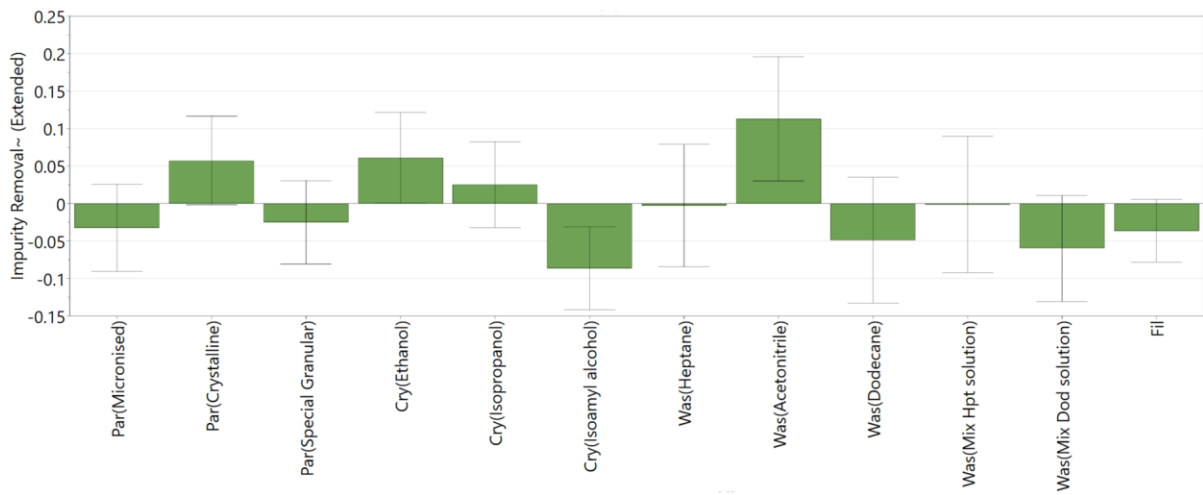


Figure 3-10: DoE variables that affect blue dye impurity removal during washing, $R^2 = 0.79$, $Q^2 = 0.35$, reproducibility = 0.44

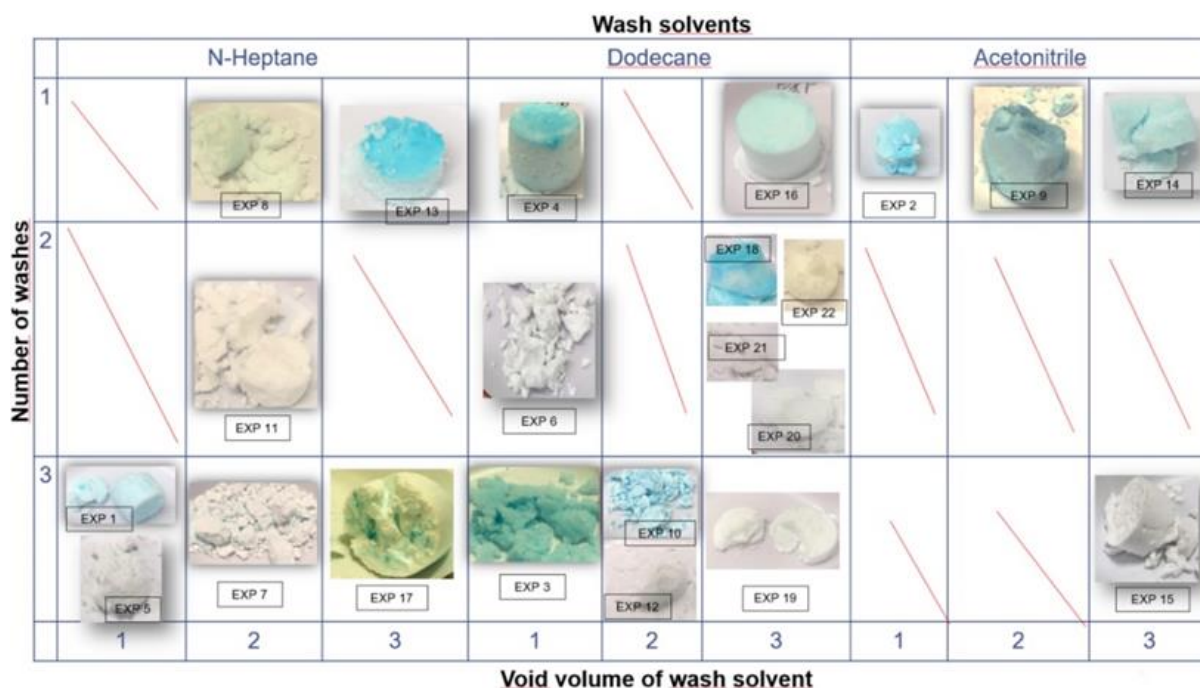


Figure 3-11: Images of all the API washed cakes taken at the end of experiment and sorted in terms of wash solvent, number of washes and void volumes of wash solvent used

The paracetamol grade, the identity of the crystallization and wash solvent and the filtration rate are the main factors affecting the removal of mother liquor and blue dye impurity during the washing process (Figure 3-9 and Figure 3-10). The increased amount of mother liquor present in the micronized paracetamol grade following washing is consistent with the porosity and tortuosity of the cake. Higher cake tortuosity increases the propensity to trap impure mother liquor in the cake during filtration and so decreases the capability of washing process to remove the impure mother liquor.^{9,25} Crystalline and granular API grade with larger crystal size result in larger interstices in the filtered cake, allowing the wash solvent to more easily flow through and penetrate through the whole API particle bed and hence displace the mother liquor and impurity which is present.^{9,26} This can be seen in Figure 3-11, which contain images of the washed and dried API cake from all the experiments. The washed API cake which can be seen to be completely washed with no blue dye impurity visually present are from experiments; 5, 6, 7, 8, 11, 12, 15, 19, 20, 21 & 22. The only experiments where granular paracetamol API was used and not found to have completely removed the blue dye were experiment 3, 13 & 14. This

was either due to the low amount of wash used in the experiment (as is the case for experiment 13 & 14) or due to the type of wash solvent used (as is the case for experiment 3, dodecane wash solvent) as explained later. Also, for crystalline PCM, the only experiment where blue dye was not completely removed in the API cake are experiments where only 1 wash was performed (experiments 1, 4, 9 & 16) and hence not enough wash solvent used. Comparing this to micronised PCM, even for experiment 17 where 3 washes were carried out each using 3 void volumes, the highest amount of wash solution used in the DoE, there was still blue dye present in the cake. Looking at the washed API cake image for experiment 17, in Figure 3-11, blue dye presence in the micronised API cake showcases low porosity of the cake where the wash liquor was not able to disperse and the trapped mother liquor and blue dye impurity causing the marble effect in the washed API cake.

Blue dye impurity removal analysis for DoE response is carried out by analyzing how quickly the blue dye is removed from the API cake as explained in section 3.2.4 **Liquid Filtrate Off-line Post Analysis** and also by checking that no blue dye impurity is present inside the washed API cake at the end, as explained in section 3.2.5 **Solid API Cake Off-line Post Analysis**. Using this analysis n-dodecane is generally found to be the best wash solvent for removal of the blue dye impurity, Figure 3-10. However, when using pure n-dodecane as wash solvent, on some occasions some of the blue dye impurity and the mother liquor was seen to rise to the top of filter tube as a layer resting above the added n-dodecane wash as soon as the wash solvent was added. This can be seen in Figure 3-12a, images taken from experiment 3, where there is small amount of blue dye which can be seen on the top of the n-dodecane wash solvent (experiment 3 is carried out with ethanol as crystallization solvent and n-dodecane as wash solvent, with one wash using 3 cake volumes at 100 rpm). This could be due to n-dodecane being immiscible in the ethanol crystallization solvent and a portion of the mother liquor being disturbed from the surface of the wet filter cake during the wash addition and remaining suspended on the top

of the layer of n-dodecane wash solvent. Because there was only 1 wash applied in experiment 3, this blue dye was deposited in the form of a layer at the top of the cake, Figure 3-12b. When a sample of the washed cake from experiment 3 was suspended in the solution to analyse by UV-vis spectroscopy, there was no blue dye present inside the washed cake and hence no blue dye was detected, the concentration being below the detection limit and the cake was deemed to be effectively impurity free, which was not the case. Similar phenomena was also observed for experiment 4, as can be seen from the dried washed API cake image in Figure 3-11. This phenomenon was not observed when a mixture of n-dodecane and crystallization solvent is used as first wash solution. (Full list of experiment with the different parameters used is provided in Appendix B - **Employing constant rate filtration to assess active pharmaceutical ingredient (API) washing efficiency**, Figure B-3).

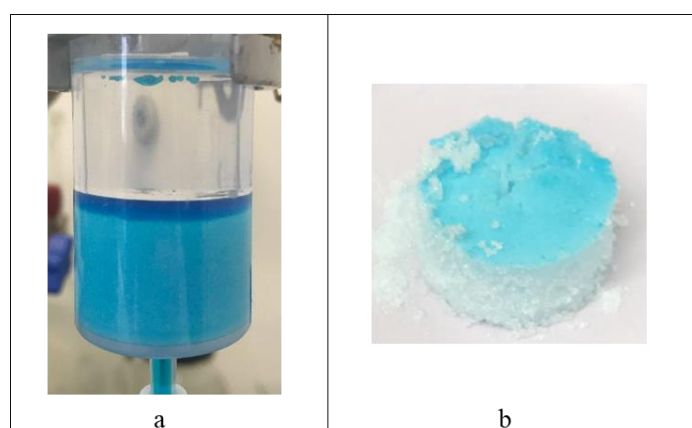


Figure 3-12: a.) Biotage filter tube from experiment 3 after n-dodecane wash solvent addition. b.) Paracetamol API cake obtained at the end of experiment 3 with a layer of the blue dye at the top of the washed cake.

In the design space investigated experimentally in the DoE, acetonitrile was found to be the worst wash solvent to use in terms of removal of residual mother liquor solution and the blue dye impurity (Figure 3-9 and Figure 3-10). Several factors are believed to contribute to this; acetonitrile has a big viscosity difference compared to the crystallization solvents used which results in poor displacement washing, (Table B-1 in Appendix B - **Employing constant rate filtration to assess active pharmaceutical ingredient (API) washing efficiency** provides viscosity

data for all the solvents used in study). The high solubility of blue dye impurity in the acetonitrile relative to the other wash solvents, (Table 3-2), may play a part through back diffusion of the dye present in mother liquor filling the voids in the API cake and so could contribute to the requirement of a higher volume of wash solvent for complete washing. For the 4 experiments conducted using acetonitrile wash solvent, 3 of those were performed with only 1 wash step, experiment 2, 9 and 14. From all of the experiment undertaken in the DOE study, experiments 2, 9 and 14 were also the only ones found to have blue dye still present in the collected wash filtrate till the end of the experiment, the wash profile curve for these experiments did not reach 0 for the concentration of blue dye (see Figure B-7, Figure B-14 and Figure B-19 in Appendix B - **Employing constant rate filtration to assess active pharmaceutical ingredient (API) washing efficiency**). Experiment 9 & 14 had higher level of blue dye present in the wash filtrate aliquots at the end as the lower pumping rate of 10 rpm (1.3 mL/min) was used in both cases. This low flowrate of solvent through the cake combined with the relatively high solubility of the blue dye in acetonitrile suggests there is greater risk of contamination of the wash solvent with the dye due to dispersion and back mixing. This resulted in less efficient washing. This in combination with a small wash volume as required in the DoE led to inadequate washing in both experiments, consequently some of the blue dye impurity was still present within the API cake, Figure 3-11, and the wash filtrate at the end of the washing process.¹⁸ Furthermore, the solubility of the API is around one order of magnitude higher in acetonitrile compared to other wash solvents (Table 3-2) which results in increased API loss during washing with acetonitrile.

There also seems to be a correlation on the type of mother liquor solution used and the blue dye impurity removal. From Figure 3-10, Isoamyl alcohol is found to be best mother liquor at removal of blue dye impurity from the DoE results. This is also the case from Figure 3-11, where 8 out of 9 experiments conducted using Isoamyl alcohol has found to have no blue dye

impurity visually present in the final washed API cake (experiments 5, 6, 7, 8, 15, 20, 21, 22). As stated in previous research, the viscosity of the crystallization solvent has an effect on the washing process.²⁶ (see Table B-1 in Appendix B - **Employing constant rate filtration to assess active pharmaceutical ingredient (API) washing efficiency** for viscosity data of solvents used in study). This work has shown that higher viscosity mother liquor solution, such as isoamyl alcohol results in better removal of impurity from the system.

As mentioned previously, the filtration rate is important during washing as it plays a role in minimizing back mixing of impurity or mother liquor with the wash solvent. The pumping rate of 10 rpm was too slow and found to result in back diffusion of blue dye impurity. This was evident as only 3 out of 10 experiments performed using pumping rate of 10 rpm (experiment 5, 7 & 12) had a completely washed cake without any blue dye impurity visually present, Figure 3-11. Experiments where 100 rpm pumping rate was used performed a little better with 5 out of the 9 experiment washed cakes were found to be clean with no blue dye impurity visually present (experiments 6, 8, 11, 15 & 19). The high pumping rate aided with better displacement wash of the mother liquor present within the filtered API cake however failed to fully remove blue dye impurity in experiment where immiscible wash solvent such as dodecane was used or when micronized paracetamol was used, as at high flowrate the wash solvent would fail to fully disperse in the washed cake and leave through the path of least resistance leaving area in the washed cake with impurity still present. The use of a pumping rate of 55rpm with granular PCM grade in the DoE midpoint experiments (experiments 20, 21 and 22) was found to be the best flow rate for removing both the coloured impurity and the crystallization solvent. This is evident from the ¹H-NMR results of the samples taken from the washed cakes that show the DoE midpoint experiments have least amount of mother liquor present at the end of washing (see Appendix B - **Employing constant rate filtration to assess active pharmaceutical ingredient (API) washing efficiency**). Also, from Figure 3-11, all the washed cakes from the midpoint

experiments were found to be clean without any blue dye impurity present. This is believed to be mainly due to the time allowed for the wash solvent to flow through the cake to achieve complete removal of impurity and mother liquor without causing any back mixing.

3.4 Conclusion

Washing API crystals is an important part of the isolation process to deliver a crystalline product of the desired; purity, particle size distribution and yield. The constant rate filtration/washing methodology developed in this study is easily implemented using readily available laboratory equipment and allows detailed investigation of filtrate fractions from the washing process. Analysis of the filtrate has been shown to be useful in determining the endpoint of washing, the amount of API lost during the washing process and the likely extent of agglomeration occurring during washing to be evaluated. Knowing these properties allows development of more sustainable washing processes with less solvent waste and improved product quality.

The ideal case for achieving good washing was found to be when the starting point was crystalline PCM wet cake was fully saturated in ethanol. Even though n-dodecane was found to be the best wash solvent in terms performing displacement washing, the immiscibility of the wash solvent with the crystallization solvent was found to jeopardize the removal of the blue dye impurity. In addition, the high boiling point of n-dodecane makes it difficult to remove during the drying process. Using lower flowrates resulted in dispersion of crystallization solvent, while using larger amounts of wash solvent was found to be inefficient, due to increased API loss and wash solvent being consumed after the point at which all the impurity has been removed. Whilst these results are specific to the paracetamol samples studied, for another API the same principles would be applied to develop a washing regime tailored to the specific API but along the same lines as described above.

The constant rate washing methodology developed using the blue dye impurity has been found to be very effective in analyzing washing processes and designing a washing strategy. A future investigation will involve using API with structurally related impurities and design a constant rate filtration strategy to demonstrate how this approach could be implemented on an industrial scale to washing processes.

3.5 Abbreviations

Active pharmaceutical ingredient (API); paracetamol (PCM); particle size distribution (PSD); proton nuclear magnetic resonance (^1H NMR); design of experiment (DoE)

References

1. Ruslim, F.; Hoffner, B.; Nirschl, H.; Stahl, W. Evaluation of pathways for washing soluble solids. *Chem. Eng. Res. Des.* **2009**, 87, 1075–1084.
2. Kuo, M. T.; Barrett, E. C. Continuous filter cake washing performance. *AIChE J.* **1970**, 16, 633–638.
3. Svarovsky, L. *Solid-Liquid Separation*. 4th ed. Oxford, UK. Butterworth-Heinemann. **2000**.
4. Holdich R.G. *Fundamentals of Particle Technology*. Midland Information Technology & Publishing. U.K. **2002**. ISBN: 0954388100.
5. Tarleton, S.; Wakeman, R. *Solid/liquid Separation: equipment selection and process design*. 1st Edition. Elsevier Science. **2006**. ISBN: 9781856174213.
6. Greil, P.; Gruber, U.; Travitzky, N.; Kulig, M. Pressure filtration of silicon nitride suspensions with constant filtration rate. *Mater. Sci. Eng.* **1992**, 151, 247–254.
7. Tien, C. *Introduction to Cake Filtration: Analyses, Experiments and Applications*; Elsevier: Amsterdam, The Netherlands. **2006**.
8. Rushton, A.; Ward, A.S.; Holdich, R.G. *Solid-Liquid Filtration and Separation Technology*; Wiley-VCH: Weinheim, Germany. **2000**.
9. Wakeman, R.J. The influence of particle properties on filtration. *Sep. Purif. Technol.* **2007**, 58, 234–241.
10. Wakeman, R.J.; Tarleton, E.S. *Solid: Principles of Industrial Filtration*; Elsevier: Bodmin, UK. **2005**.
11. Wakeman, R.J.; Wu, P. Neural Network Modelling of Vibration Filtration. *Filtration.* **2003**, 3, 237–244.

12. Wakeman, R.J.; Sabri, M.N.; Tarleton, E.S. Factors affecting the formation and properties of wet compacts. *Powder Technol.* **1991**, *65*, 283–292.
13. Yim, S.S.; Kwon, Y.-D.; Kim, H.-I. Effects of pore size, suspension concentration, and pre-sedimentation on the measurement of filter medium resistance in cake filtration. *Korean J. Chem. Eng.* **2001**, *18*, 741–749.
14. Kotlyarov, G.G. Investigations of the relations between the filtration constant of low-concentration suspensions and filtration pressure and solid-phase concentration. *Chem. Pet. Eng.* **1976**, *12*, 416–418.
15. Carman, P.C. Fundamental principles of industrial filtration. *Trans. Inst. Chem. Eng.* **1938**, *16*, 168–188.
16. Shahid, M.; Sanxaridou, G.; Ottoboni, S.; Lue, L.; Price, C. Exploring the role of anti-solvent effect during washing on active pharmaceutical ingredient purity. *Org. Process Res. Dev.* **2021**, *25*, 4, 969–981.
17. Ottoboni, S.; Wareham, B.; Robertson, M.; Brown, C.J.; Johnston, B.; Price, C. A novel integrated workflow for isolation solvent selection using prediction and modelling. *Org. Process. Res. Dev.* **2021**, *25*, 5, 1143–1159.
18. Hendriksen, B.A.; Grant, D.J.W. The effect of structurally related substances on the nucleation kinetics of paracetamol (acetaminophen). *J. Cryst Growth.* **1995**, *156*, 252.
19. Eriksson, L.; Johansson, E.; Kettaneh-Wold, n.; Wikström, C.; Wold, S. Design of Experiments – Principles and Applications. Umetrics Academy. ISBN-10: 91-973730-4-4. January **2008**.
20. Ottoboni, S.; Shahid, M.; Steven, C.; Coleman, S.; Meehan, E.; Barton, A.; Firth, P.; Sutherland, R.; Price, C. Developing a batch isolation procedure and running it in an automated semicontinuous unit: AWL CFD25 case study. *Org. Process Res. Dev.* **2020**, *24*, 520-539.
21. Murugesan, S.; Sharma, P.K.; Tabora, J.E. Design of Filtration and Drying Operations in Chemical Engineering in the Pharmaceutical Industry: R&D to Manufacturing. Wiley New York. **2010**.
22. Bai, R.; Tien, C. Further work on cake filtration analysis. *Chem. Eng. Sci.* **2005**, *301*.
23. Ottoboni, S.; Price, C.; Steven, C.; Meehan, E.; Barton, A.; Firth, P.; Mitchell, P.; Tahir, F. Development of a novel continuous filtration unit for pharmaceutical process development and manufacturing. *J. Pharm. Sci.* **2018**, *108*, 372.
24. Sou, T.; Bergström, C.A.S. Automated assays for thermodynamic (equilibrium) solubility determination. *Drug Discovery Today: Technologies.* Vol 27. **2018**.
25. Ruslim, F.; Nirschl, H.; Stahl, W.; Carvin, P. Optimization of the wash liquor flow rate to improve washing of pre-deliquored filter cakes. *Chem. Eng. Sci.* **2007**, *62*, 3951–3961.
26. Dullien, F. A. L. Porous Media Fluid Transport and Pore Structure. 2nd ed. Academic Press Inc. 1992.

27. Papageorgiou, C. D.; Langston, M.; Hicks, F.; AM Ende, D.; Martin, E.; Rothstein, S.; Salan, J.; Muir, R. Development of Screening Methodology for the Assessment of the Agglomeration Potential of APIs. *Org. Process Res. Dev.* **2016**, *20*, 1500–1508.
28. DDBST GmbH. [cited 2021/03/18] http://www.ddbst.com/en/EED/PCP/VIS_C11.php
29. CAMEO Chemicals. [cited 2021/03/01] <https://cameochemicals.noaa.gov/chemical/3659>
30. Wypych, G. A. Databook of solvents. ChemTec Publishing. 2014.
31. PubChem. [cited 2020/03/12] <https://pubchem.ncbi.nlm.nih.gov/compound/>
32. Accudynet. [cited 2020/03/12] https://www.accudynetest.com/visc_table.html

4. Investigating particle size distribution of agglomerates formed during washing process

4.1 Introduction

Particle size analysis is an important aspect of manufacture of particulate products in the pharmaceuticals and fine chemical industries. Previous work has shown agglomerate formation during filtration and washing process adversely affecting the particle size and shape.^{1,2} Various in-line and off-line measurement techniques have been developed and used in industry to monitor particle size distributions both of dry powders and particles in suspension with the aim of enabling control of particle size and shape during the crystallisation step and at the end of the drying step.^{3,4,5} However barely any work can be found in literature investigating particle size analysis during or at the end of filtration and washing process.

For crystallisation process both in-line and off-line measurement techniques are used, whereas mostly off-line measurement techniques are used for assessing material obtained at the end of the drying process.

Most off-line measurement techniques for particle size and shape measurement are based on sieve analysis, laser diffraction or imaging. These techniques are well established in batch processing for product characterisation and quality control. These off-line techniques require sampling which needs to be representative of the bulk material and special attention needs to be paid to sample handling to prevent alteration to particle size. Examples of off-line particle measurements instruments include Malvern Mastersizer 3000, Sympatec GmbH Qicpic and Morpholgi G3.^{6,7,8}

In-line measurement techniques used in-situ during crystallisation process, allow for real time monitoring and offer the possibility of control of particle size and shape. These techniques are used for estimation of size and shape information of particle dispersed in a slurry without the need for any sampling. The most common in-line particle measurement techniques include; particle chord length (CL) measurements, microscopic imaging and spectroscopy. Examples

of in-line instruments include focused beam reflectance measurement (FBRM), three dimensional optical reflectance (3D-ORM), particle vision and measurement (PVM) and EasyViewer with iC vision.^{9,10}

Chord length distribution describes the size, shape and spatial arrangement of particle being investigated. In-line measurement techniques, such as FBRM, uses a laser beam to pass light through suspension of particles, when a particle is illuminated in the instruments rotating beam light is then reflected back while the particle is in the beam. The duration of of the reflection from the particles is then converted to determine the chord length of the particle using linear laser velocity. The chord length measured is a function of measurement location and dependant upon the orientation of the particles presented to the probe. This chord length is hence not an exact measure of actual particle size and there have been many efforts made to use mathematical models to convert from chord length distribution to more accurate particle size distributions.

Square weighted and unweighted chord length distribution (CLDs) are used to analyse the distribution of bigger size and smaller sized particles, respectively, in a slurry suspension that spans different size ranges. Square weighted and unweighted CLDs are obtained by multiplying number of particle in each size bin by the square of the respective bin size. The CLDs can be normalized by dividing each of the resulting terms in the bin by sum of resulting terms in each bin spanning the entire domain. The normalized square weighted CLD tracks the distribution among the bigger sized particles and the lower particles are ignored, and vice versa.¹¹

Traditionally particle size measurements are usually only taken during or at the end of crystallisation and the drying process. Particle size analysis is not normally carried out during or at the end of the filtration or washing stages of manufacture despite the potential for these processes to modify particle attributes. Therefore, it is hard to determine whether these two

processes are involved in changing particle attributes and to what extent each is responsible for altering the particle size distribution and shape of crystal product.

Sample handling is one of the biggest issues for particle size measurement of material obtained at the end of the washing process. The API material obtained at the end of washing is a wet filtered cake, which then needs to be re-suspended in a solvent to allow for particle size measurement. Drying of any washed API crystal material for particle size analysis could result in further agglomeration caused by the drying process. Hence, wet cell analysis is the most desirable particle size analysis method for washed API material.

The two main wet cell analysis techniques used within this study to measure particle size distribution, were laser diffraction and chord length distribution measurement, obtained using the focused beam reflectance measurement technique. Static light scattering techniques such as laser diffraction mostly give a volume weighted distribution. In such distributions the contribution of each particle in the distribution relates to the volume of that particle (equivalent to mass if the density is uniform), i.e. the relative contribution is proportional to (size).¹³ Chord length distribution is based on the chord length of the particles, where particle size is determined by the distance between any two edges of a particle's 2-D projection. Chord length measurement is acquired by the duration of the signals reflected by particles passing in front of a laser illumination beam.^{4,14}

Previous work (chapters 2& 3) has shown that anti-solvent affect is a genuine phenomenon that takes place during the washing process and could result in formation of agglomerates which can alter particle size and shape at the end of drying process.¹² However measuring particle size only at the end of the drying process makes it difficult to distinguish between any agglomerate formation occurring due to phenomena taking place during washing and how much is due to the drying process resulting in agglomeration. A part of this chapter, section 4.2

PSD analysis of washed API material from Chapter 3, looks at employing an offline laser diffraction technique to measure particle size of washed material obtained at the end of the washing experiments in chapter 3 to quantify any changes in particle size distribution. Only laser diffraction technique is used for the washed material in chapter 3 due to lack of other particle size techniques available in the lab at the time of work performed in chapter 3.

Further work in this chapter, section 4.3 **Material and Method** onwards then looks at employing various lab-based particle size measurement techniques on separate washed paracetamol API material to determine the particle size of API material obtained at the end of the washing process. The aim of the work is to assess the capability of the currently available laboratory particle size analysis techniques to detect any changes occurring during the two processes of filtration and washing.

4.2 PSD analysis of washed API material from Chapter 3

Conducting particle size analysis of the washed API product before it is dried enables differentiation between agglomeration caused by the washing process and those agglomerates that are formed and are further strengthened by drying. Particle size distribution of the raw PCM grades, as well as that of the damp washed cakes obtained at the end of each experiment performed in chapter 3 was analysed using a wet dispersion laser diffraction technique (Mastersizer 3000 laser diffraction particle size analyser with hydro dispersion unit, Malvern Panalytical, UK).

The method parameters used for this study were as follows: measurement duration 10 seconds, number of measurements 5, obscuration limit 5–20%, stabilization time 30 seconds, beam length 2.5mm. To form the wet dispersions, samples of the raw material and the wet filter cakes obtained at the end washing experiments were suspended in isooctane due to negligible solubility of PCM in this solvent. The suspensions for analysis were prepared at the end of each

experiment. The washed cake was vertically sliced along the axis of the cake to take around a quarter of the cake (making sure not to disturb the whole cake or break any agglomerates) and was carefully dispersed in 50mL of isooctane. PSD analysis was then performed to measure any change in particle size caused due to agglomerate formation during the washing process. The wet dispersion particle size analysis approach was selected in preference to dry dispersion to avoid the problem of washed API cake drying out and so forming agglomerates during drying. This way, agglomeration caused due to anti-solvent effects during the washing process could be analysed without the effects of drying confounding the analysis.

Evaluation of particle size distribution is determined by the change in particle size response using Equation 7. This response is used as response factor in the DOE model to understand any relationship between the change in particle size distribution during washing of material caused due to the factors investigated in the study in chapter 3, Table 4-1.

$$\text{change in } D_x(\%) = \left(\frac{D_x \text{ of the washed cake} - D_x \text{ of the raw paracetamol API}}{D_x \text{ of the raw API}} \right) \times 100 \%$$

(where $x = 10, 50$ or 90) – Equation 7

Table 4-1: Response used for particle size distribution to quantify in the DoE

Responses

| Responses (abbreviation) | Analytical method used to quantify response |
|--------------------------|---|
| change in D_{10} (D10) | Particle size analyzer, Mastersizer 3000 |
| change in D_{50} (D50) | Particle size analyzer, Mastersizer 3000 |
| change in D_{90} (D90) | Particle size analyzer, Mastersizer 3000 |

Figure 4-1, Figure 4-2 and Figure 4-3 shows the main factors affecting the particle size distribution D_{10} , D_{50} and D_{90} during the washing process. All three coefficient plots (Figure 4-1, Figure 4-2 and Figure 4-3) show good reproducibility values. Coefficient plots for D_{10} and D_{50} (Figure 4-1 and Figure 4-2 respectively) show good fit between the data and the model

demonstrating the model’s capability to predict responses. The coefficient plot for D_{90} (Figure 4-3) shows good fit between the model and the data, however the low reproducibility value indicates that the model has limited usefulness in predicting responses.

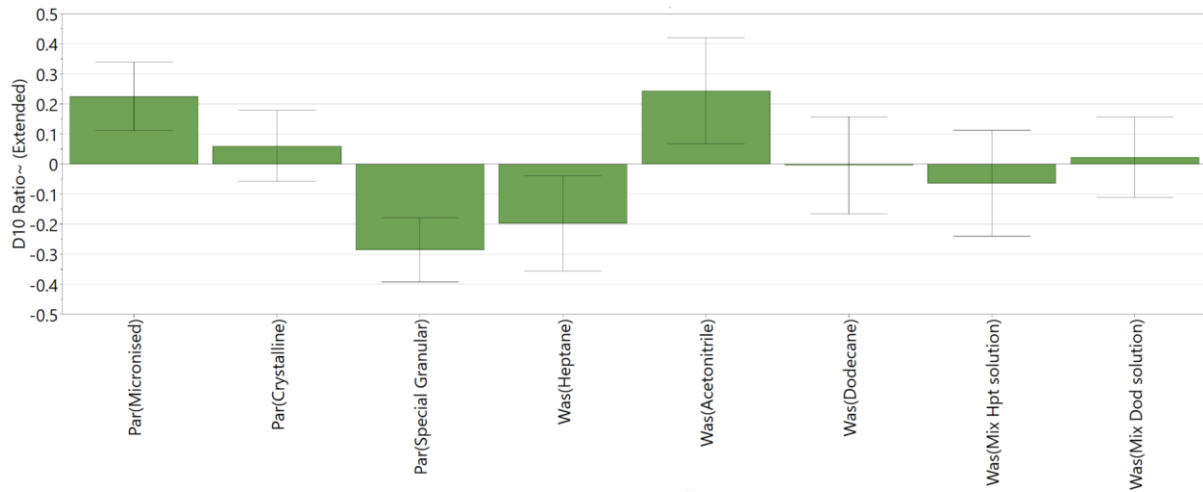


Figure 4-1: DoE variables that affect particle size distribution (D_{10}) of washed cake - change in D_{10} , $R^2 = 0.80$, $Q^2 = 0.52$, reproducibility = 0.97

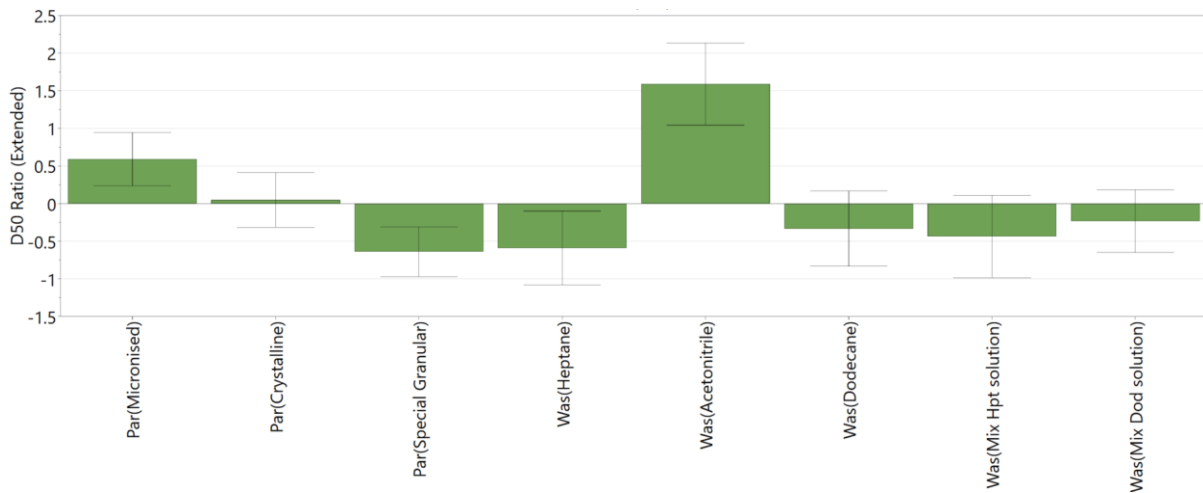


Figure 4-2: DoE variables that affect particle size distribution (D_{50}) of washed cake - change in D_{50} , $R^2 = 0.82$, $Q^2 = 0.58$, reproducibility = 0.97

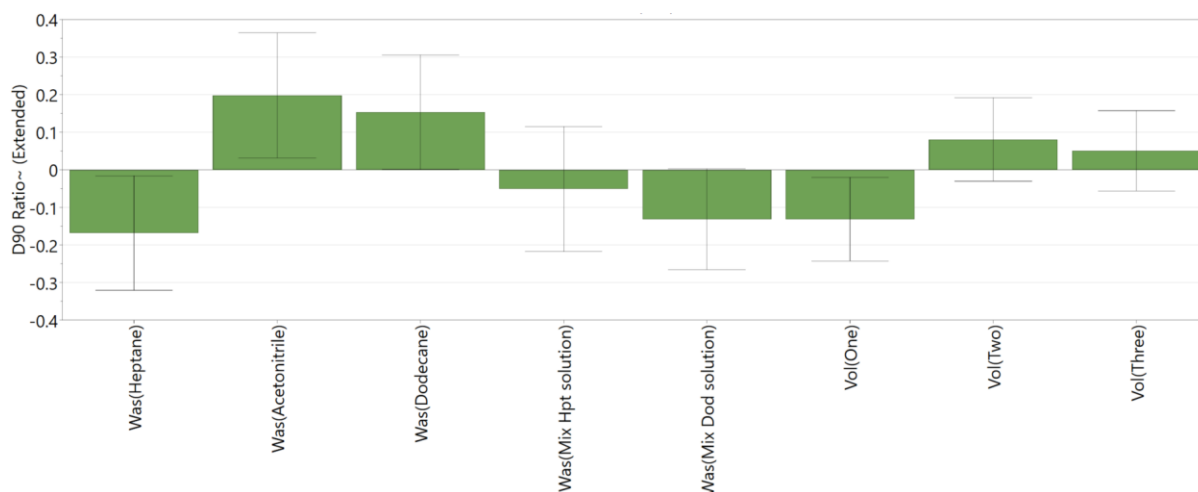


Figure 4-3: DoE variables that affect particle size distribution (D_{90}) of washed cake - change in D_{90} , $R^2 = 0.60$, $Q^2 = 0.05$, reproducibility = 0.81

Figure 4-1, Figure 4-2 and Figure 4-3 shows the main factors affecting the particle size distribution D_{10} , D_{50} and D_{90} during the washing process. All three coefficient plots (Figure 4-1, Figure 4-2 and Figure 4-3) show good reproducibility values. Coefficient plots for D_{10} and D_{50} (Figure 4-1 and Figure 4-2 respectively) show good fit between the data and the model demonstrating the model's capability to predict responses. The coefficient plot for D_{90} (Figure 4-3) shows good fit between the model and the data, however the low reproducibility value indicates that the model has limited usefulness in predicting responses.

The main factors linked to PSD change during the washing process are the paracetamol API grade and the wash solvent identity. Processing micronised paracetamol, results in increase in the PSD during washing, this is probably due to the wide PSD of the raw material, a contributing factor may be the finer particles being located in the small voids within the cake acting as bridge formation agents, correlated to the high surface area present.^{15,16} Granular paracetamol tended to maintain the initial PSD after the washing process.

Acetonitrile was found to be worst wash solvent in terms of causing agglomeration leading to an increasing PSD, this is consistent with the findings that acetonitrile is the worst wash solvent in this study in terms of removal of mother liquor and impurities due to back mixing and solvent viscosity differences, see Table B-1. Using acetonitrile as the wash solvent would result in a

final washed cake with the saturated solvent in the porous cake with API dissolved with it. Hence the presence of saturated mother liquor solution or solvent with API dissolved in it at the end of washing process could result in the API being deposited during the drying stage and causing severe agglomeration. The wet dispersion particle size analysis employed isooctane as dispersant, in which the API has negligible solubility. The presence of saturated acetonitrile as a solvent residue in the washed cake could potentially result in an anti-solvent effect during analysis. As the wet cake sample is dispersed the acetonitrile interaction with isooctane would lead to the deposition of API adversely affecting the PSD analysis of the sample.

Use of wash solvent in which the API has low solubility, such as n-heptane and n-dodecane, carries the risk of precipitation of API during the washing, due to anti-solvent effect occurring as the wash solvent interacts with the saturated mother liquor occupying the voids in the cake potentially a cause of agglomeration.¹² Figure 4-4 gives an example of how using a mixture of wash solvent and crystallization solvent as the initial wash solution reduces this anti-solvent effect and hence lowers the extent of agglomeration during washing. Figure 4-4 shows the PSD obtained for the three different PCM grades used within this study as well as the PSD of some of the washed cake samples from some of the experiments. Table 4- 2 contains the factors and washing regime used in all the experiments presented in Figure 4-4.

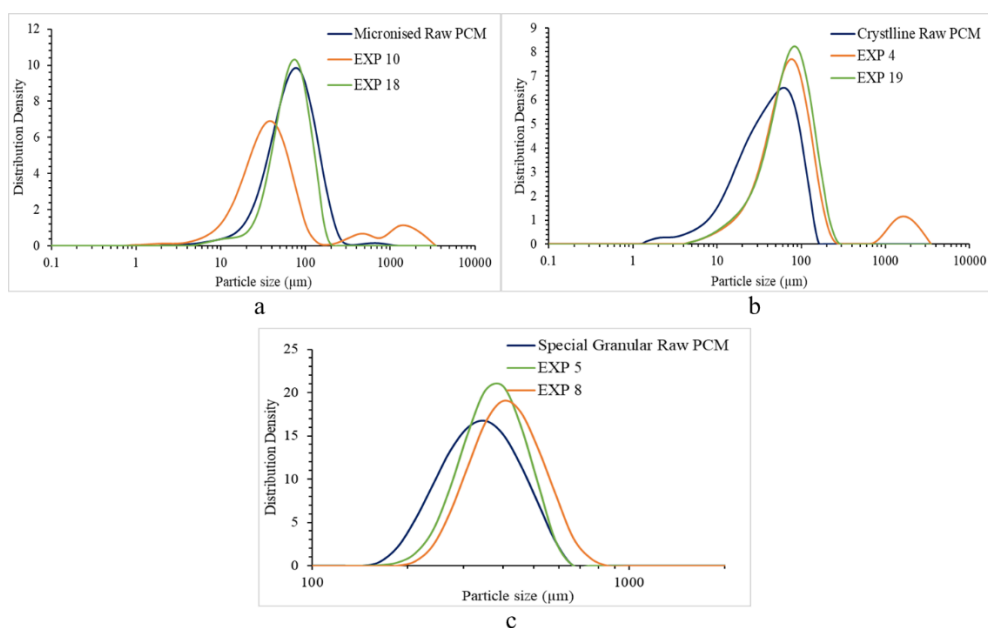


Figure 4-4: a.) PSD of raw micronised PCM and of final washed cakes from EXP 10 (D_{10} : 15.2 μm , D_{50} : 43.8 μm , D_{90} : 638.3 μm) & EXP 18 (D_{10} : 35.1 μm , D_{50} : 72.9 μm , D_{90} : 128.2 μm). b.) PSD of raw crystalline PCM and of final washed cakes from EXP 4 (D_{10} : 27.8 μm , D_{50} : 76.5 μm , D_{90} : 201.0 μm) & 19 (D_{10} : 26.8 μm , D_{50} : 76.7 μm , D_{90} : 154.4 μm). c.) PSD of raw granular PCM and of final washed cakes from EXP 5 (D_{10} : 292.4 μm , D_{50} : 397.4 μm , D_{90} : 531.8 μm) & EXP 8 (D_{10} : 312.8 μm , D_{50} : 437.0 μm , D_{90} : 606.4 μm)

Table 4- 2: Factors used for experiments presented in Figure 4-4

| | Micronised | | Crystalline | | Granular | |
|--------------------------------------|------------|---|-------------|---|---|-----------------|
| | EXP 10 | EXP 18 | EXP 4 | EXP 19 | EXP 5 | EXP 8 |
| Crystallisation solvent | Ethanol | Ethanol | Isopropanol | Isopropanol | Isoamyl Alcohol | Isoamyl Alcohol |
| Wash solvent | Dodecane | Mix of dodecane & crystallization solvent then dodecane | Dodecane | Mix of dodecane & crystallization solvent then dodecane | Mix of n-heptane & crystallization solvent then n-heptane | N-heptane |
| Filtration rate in rpm (in mL/min) | 100 (11.7) | 10 (1.3) | 10 (1.3) | 100 (11.7) | 10 (1.3) | 100 (11.7) |
| Volume of wash solvent (void volume) | 2 | 3 | 1 | 3 | 1 | 2 |
| No. of washes | 3 | 2 | 1 | 3 | 3 | 1 |

In Figure 4-4a, micronised PCM and ethanol is used in all the experiments. In Figure 4-4b, crystalline PCM and isopropanol is used in all the experiment and in Figure 4-4c, granular PCM and isoamyl alcohol is used in all the experiments. All the experiments showed an

increase in the PSD of the washed crystal particles, from the initial raw material. A D_{10} , D_{50} and D_{90} comparison of the raw crystal particles with the washed cake showed an increase of between 1.9 and 24 times the D_{10} , D_{50} and D_{90} of the original material when washed with pure wash solvent. An increase in D_{10} is believed to be mainly due to the anti-solvent effect within the cake structure, causing precipitation when wash solvent in which the API and impurity have the lowest solubility, comes in contact with the supersaturated crystallisation solvent present within the cake structure, causing an increase in supersaturation. This results in either further precipitation within the cake bed or crystal bridges being formed, causing agglomeration which is evident with increase in both D_{50} and D_{90} .¹²

Employing a more sophisticated wash strategy, in the case of all 3 crystallization solvents, where the first wash is carried out using a mixture of crystallization and wash solvent, followed by further washing using pure wash solvent, as employed in experiments in 5, 18 & 19 (Figure 4-4) produces much less agglomeration and precipitation caused due to anti-solvent effect. The D_{10} , D_{50} and D_{90} in this case has only increased between 1.1 and 2.6 times the D_{10} , D_{50} and D_{90} of the raw material.

This work demonstrates that agglomerate formation during isolation starts at the washing stage where inappropriate solvent choices combined with a poorly designed washing strategy can lead to the formation of agglomerates driven by the retention of crystallization solvent in the wet filter cake. This then results in further strengthening and formation of bigger agglomerates during drying, necessitating additional steps such as milling which increases production time and cost. The use of laser diffraction for particle size analysis of the damp washed cake was found to be satisfactory in identifying agglomerate formation during washing for the small sample size investigated. However further work is required to optimize the method for particle size analysis of washed cakes and hence has been further investigated in this chapter.

4.3 Material and Method

4.3.1 Raw Materials

Paracetamol (PCM) is the model API compound used, similar to chapters 2 & 3. For further investigating the change in particle size during the filtration and washing stages, three different API particle sizes were analysed; micronised, crystalline and granular (PSD of these three input raw materials is provided in Table 3-1). This allowed exploration and examination of the difficulties related to measuring the particle size of different grades of filtered and washed API filter cake whilst wet. The particle size distribution of raw PCM for all three grades was analysed before the experiments using both dry and wet cell analysis methods.

To investigate the particle size and shape of filtered and washed API material, a “real process” slurry was prepared using ethanol (absolute, purity $\geq 99.8\%$, Sigma-Aldrich). n-Heptane (purity 99.9%, Sigma Aldrich) was used as a wash solvent.

Paracetamol saturated ethanol solution and isooctane (purity 99.9% (GC), Merck) were used as dispersants for wet cell particle size analysis, preventing any particle dissolution due to the negligible solubility of PCM in isooctane and the already saturated state of the ethanol. Using these two different dispersants allowed for investigation of the effect of different dispersing solvents on particle size analysis. For API filter cake obtained at the end of filtration stage, saturated ethanol was used as dispersant in order to match the liquid phase in which API cake was wet. Using isooctane as dispersant for the filtered API cake could result in anti-solvent effect as the PCM saturated ethanol would be mixed with isooctane in which PCM has negligible solubility. Similarly, isooctane was used as dispersant for material obtained at the end of the washing process. Washing was carried out using heptane and so the washed API cake would be completely wet in heptane. Re-suspending heptane rich washed API cake in saturated ethanol could also result in anti-solvent effect. In this way the preferred dispersant

for the ethanol wet filter cake, saturated ethanol, and the preferred dispersant for the heptane washed filter cake, isooctane are evaluated and contrasted with the corresponding non-preferred diluent where anti-solvent effects were likely to be encountered.

4.3.2 Sample Preparation

Saturated ethanoic solution is prepared by adding the correct quantity of paracetamol API to a known quantity of ethanol solvent to form saturated solution at lab temperature (22°C). This saturated solution was then used both, as a dispersant for wet cell analysis as well for preparing PCM crystal slurries for filtration and washing experiments. To prepare a crystal slurry, a second portion of PCM was added to the saturated solution to achieve a solids loading of 15% by mass. Solubility data for PCM in ethanol, for preparing saturated solution, is given in Table 2-3 of Chapter 2.

4.3.3 Experimental Procedure

For investigating the variation in particle size caused during filtration and washing stages, the paracetamol crystal slurry produced was filtered and then washed using a Biotage ISOLUTE (Biotage AB, Uppsala, Sweden) 70mL single-fritted polypropylene reservoir with 20µm pore size. Both filtration and washing was carried out using the constant rate set-up described in Section 3.2.3 **Experimental Setup & Design**, Chapter 3, of this thesis.

15 % ethanoic PCM slurry was taken and filtration is performed with a pump setting of 55 rpm (7.1 mL/min filtrate flowrate), to obtain a filtered API cake. Filtration was performed to both breakthrough and dryland, to analyse for any difference in particle size obtained from these different filtration stopping points. To extract the filter cake from the filter tube, the Biotage tube is cut horizontally making sure not to disturb the filtered cake. Half of the filtered cake is then taken and re-suspended in a bottle with around 150 mL of saturated ethanol. This re-suspended slurry is then used for particle size analyses of the filtered API cake. Figure 4-5

shows the whole API cake obtained from the Biotage tube after filtration and also vertically sliced cake with the other half added to the dispersant.

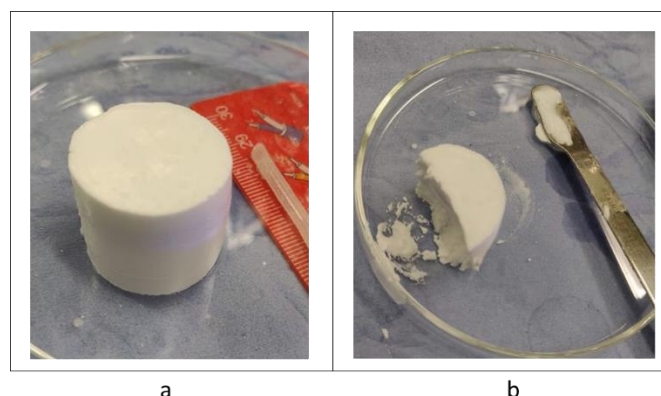


Figure 4-5: a. Filtered API cake obtained from a Biotage tube after filtration. b. Vertically sliced API cake, with the other half re-suspended in dispersant

For washing, the approach reported in Chapters 2 & 3 were used to obtain washed API cake from two different scenarios; a good washing case, and a bad washing case. For the good case of washing, the 15% ethanoic PCM slurry was filtered to dryland and then the first wash was performed using a 40:60 (by volume) ethanol : n-heptane mixture of 2 cake volumes, to prevent anti-solvent effects. Then the cake was then washed twice using 2 cakes volumes of n-heptane. For the good case, both filtration and washing was performed at 55 rpm pumping rate, which was found to be the best filtrate flowrate reported in chapter 2.

For the bad case of washing, filtration and washing was performed at 10 rpm pumping rate (1.3 mL/min filtrate flowrate) which was found to be the worst flowrate in chapter 2. After filtering to dryland, the API cake was washed twice with 2 cake volumes of n-heptane.

The washed PCM API cake at the end of both washing cases was partially deliquored, before the biotage tube was cut to obtain the cake, similarly to the filtered API cake shown above. Half of the washed API cake was then cut vertically and re-suspended in a bottle with around 150 mL of isooctane solvent, ready for particle size analysis.

4.3.4 Laser diffraction particle size analysis

Laser diffraction is widely used industrial particle size analysis technique for measuring wide range of particle types and sizes ranging from usually 1 to 3000 μm .¹⁵ Laser diffraction works by measuring the scattered light pattern generated by dispersed individual particles that are illuminated by a laser beam and the size distribution is generated based on the assumption that all particles are spherical.⁵ This process usually requires diluting the sample and so is mostly used as an off-line measurement technique.⁴

For the different grades of raw PCM, particle size analysis was carried out using both the dry and wet methods using laser diffraction. Laser diffraction particle size analysis was carried out using a Mastersizer 3000 (Malvern Panalytical, UK). For dry analysis the Aero S dry cell dispersion unit (Malvern Panalytical, UK) was used. For wet analysis the Hydro MV cell (Malvern Panalytical, UK) was used, with particles dispersed in saturated ethanoic solution or isooctane as suspension medium. The method parameters used for this study were as follows: measurement duration 10 seconds, number of measurements 5, obscuration limit 5–20%, stabilization time 30 seconds, beam length 2.5mm. The mixing of the wet cell was set at 300 rpm, which from previous best practice at CMAC, was found to be sufficient for keeping the particles suspended in the dispersion liquor while preventing breakage of large particle or agglomerates.

4.3.5 Focused Beam Reflectance Measurement (FBRM) analysis

For chord length measurement, the wet cake obtained after filtration and washing experiments was added to a 150 mL reaction vessel (R.B. Radleys & Co Ltd) and re-suspended in the dispersant with the stirrer set at 300 rpm to ensure the particles are well suspended in the dispersant. The chord length measurement was performed using FBRM G400 system (Mettler-Toledo, UK), where the probe is placed at a predefined position in the vessel. This instrument

expresses multiple chord length measurements as a distribution containing 100 geometrically spaced bins.

Several methods have been developed in the literature to extract particle size information from chord length distribution (CLD). However, the ill-posed nature of inversion presents significant challenge in obtaining a reliable solution. Even with accurate experimental data, the same chord length distribution can potentially corresponds to multiple combinations of particle shape and size distribution.^{4,18,19}

With the aim of the study to look for any changes in API particles caused due to filtration and washing process, chord length distribution was obtained at the end of both filtration and washing stages. These chord length distributions obtained were then compared to check if any key differences could be identified in the trends obtained and correlated back with the particle size distribution data obtained from laser diffraction technique.

4.4 Results and Discussion

4.4.1 Sample handling

Two issues were encountered during the experimental runs related to sample handling which could affect the final PSD result obtained. To mitigate these affects, precautions were taken during sample handling to minimise deviations caused during sample preparation and analysis.



Figure 4-6: Filtered and washed crystalline PCM API cake which is not deliquored properly

At the end of the washing process, the API cake is deliquored to ensure most of the solvent is removed from the washed cake, making the wet API cake easier to handle when taking out of the biotage tube. Failing to deliquor the cake would result in the washed wet cake pouring out of the biotage filter tube while trying to cut the cake. An example of this is given in Figure 4-6 where the wet cake freely poured out when cutting the tube and was caught in the petri dish kept at the bottom of the tube to capture any spillage avoiding wasting the sample. Hence deliquoring the washed cake was performed at the end of each run where the peristaltic pump was kept on after the solvent has passed through the API cake to allow air to freely pass through the API cake and filter media. The deliquoring continued until the first air bubble was seen at the end of the biotage filter tube and then the pump was stopped. The opaque biotage filter tube makes it a little difficult to detect when the first air bubble has passed through, and so special attention had to be paid at this stage of each sample run to ensure the pump is stopped in good time. Neglecting to stop the pump would result in the API starting to dry and so could result in agglomerate formation due to mechanisms associated with drying taking charge. Therefore, it had to be ensured that deliquoring was performed with most of the solvent removed but stopped in good time, as soon as air bubbles were detected at the end of the filter tube, to prevent drying process from taking effect.

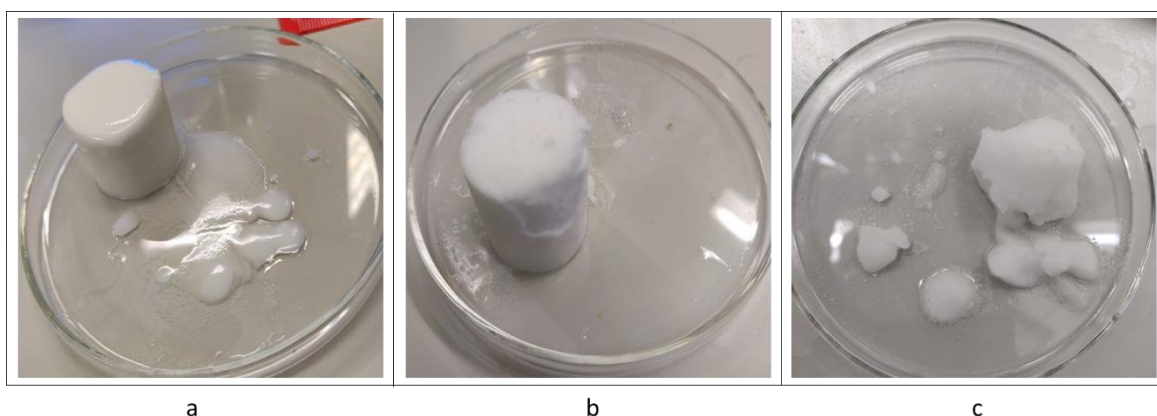


Figure 4-7: Examples of API cakes obtained at the end of washing process. a.) Micronised PCM API cake. b.) Crystalline PCM API cake. c.) Granular PCM API cake

Micronised and crystalline PCM washed cakes were easy to obtain from the biotage filter tube as the API cakes maintained the shape of the filter, as can be seen from Figure 4-7, and so cutting and obtaining the cake was easy. For granular PCM the particles would disperse as they did not tend to agglomerate significantly (as expected) and so the cake mostly came out of the tube freely with a higher chance of spillage during the cutting of the filter. Therefore, the practical solution to this was to make sure that a glass dish was placed underneath the filter tube during cutting with precautions taken to ensure no spillage or loss of material.

Once all the washed cake was obtained from the biotage tube it was quickly divided and resuspended in the dispersing solvent. This was done to prevent drying of the washed cake in lab, which could result in inaccurate PSD results.

4.4.2 Laser diffraction analysis results

Raw paracetamol API material was analysed using both the dry and wet cell methods using the Mastersizer laser diffraction instrument with the aim to analyse the effect of the different dispersing methods on the particle size distribution results obtained. Dry cell analysis was performed with the particles accelerated using compressed air and pulled through the measurement zone using a vacuum at different pressure settings. For wet cell analysis, isooctane solvent was used as dispersant due to paracetamol negligible solubility in the solvent. The result obtained from both dry and wet cell analysis for all 3 paracetamol API grades are shown in Figure 4-8.

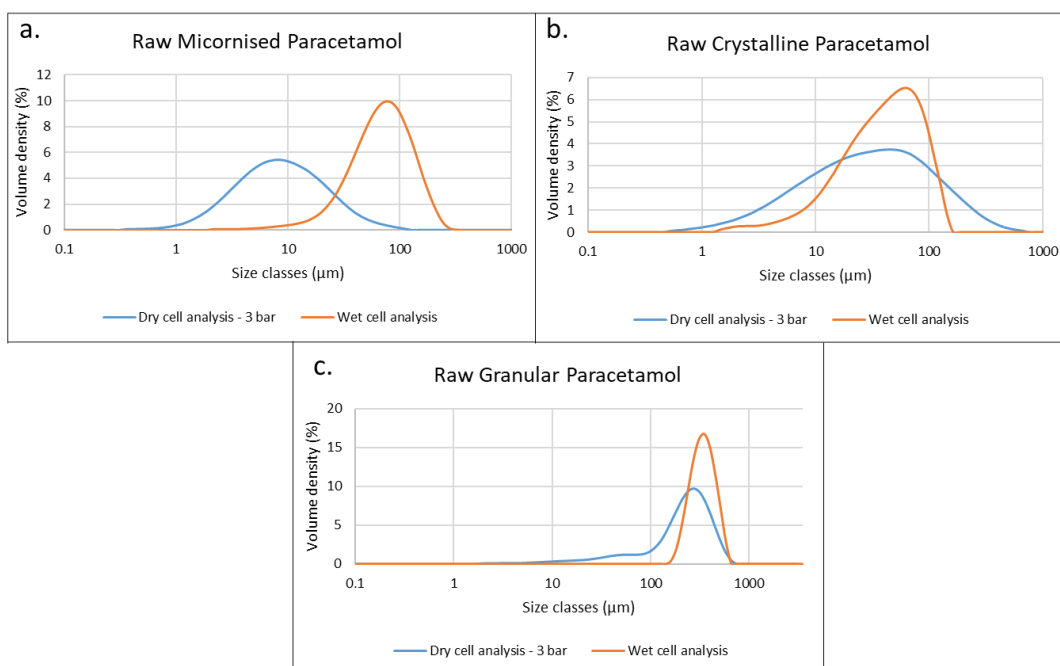


Figure 4-8: Particle size distribution of PCM API obtained from both dry and wet cell analysis. a.) Micronised PCM PSD obtained; Dry Cell Analysis - D10: 3 μm, D50: 9 μm, D90: 29 μm; Wet Cell Analysis - D10: 30 μm, D50: 75 μm, D90: 152 μm. b.) Crystalline PCM PSD obtained; Dry Cell Analysis - D10: 5 μm, D50: 32 μm, D90: 150 μm; Wet Cell Analysis - D10: 12 μm, D50: 44 μm, D90: 101 μm. c.) Granular PCM PSD obtained; Dry Cell Analysis - D10: 53 μm, D50: 249 μm, D90: 450 μm; Wet Cell Analysis - D10: 247 μm, D50: 361 μm, D90: 518 μm.

For each experiment carried out in the Mastersizer, the API cake suspended in dispersant was analysed 5 times in Mastersizer with the average of the runs represented in this results & discussion section. For micronised PCM, Figure 4-8a, a significant increase in the particle size distribution was observed when analysing using the wet cell method compared to dry method. Initially this was thought to be due to isooctane being unsuitable for PCM API dispersion. The measurement was repeated with the raw micronised PCM dispersed in saturated ethanol, as well as isooctane with lecithin added as a dispersant, and also the isooctane suspension of micronized PCM was sonicated before analysis. However, none of those approaches resulted in the PSD measurements using the wet cell analysis becoming comparable to the dry cell analysis. The results for these additional measurements can be seen in the Appendix D - **Investigating particle size distribution of agglomerates formed during washing process**, Figure D-1 to Figure D-6.

This resulted in one of the biggest issues encountered during this whole study, which is the inadequate dispersion of the micronised material using wet analysis methods to allow as representative a measurement as possible. This is a significant problem because the API cake material obtained at the end of filtration and washing process from the Biotage filter tube is a wet/damp API cake which needs to be resuspended in slurry and so the only way to obtain its PSD is to use a wet particle size analysis method.

Results obtained for raw crystalline and granular PCM API, Figure 4-8b and Figure 4-8c respectively, show a much more similar result for the dry and the wet particle size analysis methods. One thing to note is that for both crystalline and granular PCM grade D10 values obtained from the wet cell method is much higher than the one obtained from the dry method. This could be due to the small API particles present in both grades agglomerating together, similar to what was observed for micronised case, so resulting in much higher D10 values.

PCM API slurry was prepared and then filtered and washed as explained in the section 4.3.3 **Experimental Procedure**. Figure 4-9, Figure 4-10 and Figure 4-11 show the PSD results obtained from the API cakes obtained at the end filtration and washing process for all 3 PCM grades. Filtration was performed to both breakthrough and dryland cases to investigate any effect on the PSD caused. For washing, filtration was performed to dryland and then the wash solution was added to the top of the API cake to carry out washing for both good and bad washing case.

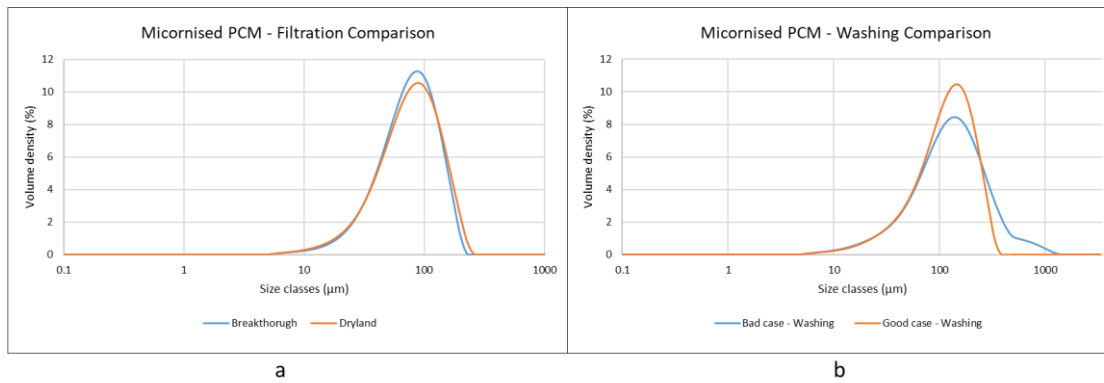


Figure 4-9: a.) PSD obtained for the two filtration runs for micronised PCM; Breakthrough - D10: 33 μm , D50: 77 μm , D90: 140 μm ; Dryland - D10: 32 μm , D50: 78 μm , D90: 150 μm . a.) PSD obtained for the two wash runs for micronised PCM; Bad case - D10: 42 μm , D50: 128 μm , D90: 316 μm ; Good case- D10: 42 μm , D50: 119 μm , D90: 226 μm .

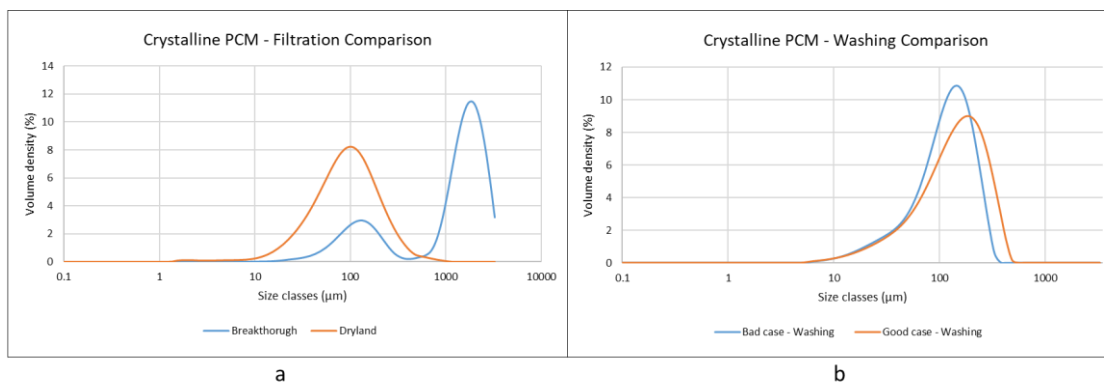


Figure 4-10: a.) PSD obtained for the two filtration runs for crystalline PCM; Breakthrough - D10: 101 μm , D50: 1470 μm , D90: 2610 μm ; Dryland - D10: 31 μm , D50: 93 μm , D90: 232 μm . a.) PSD obtained for the two wash runs for crystalline PCM; Bad case - D10: 39 μm , D50: 119 μm , D90: 221 μm ; Good case- D10: 42 μm , D50: 142 μm , D90: 294 μm .

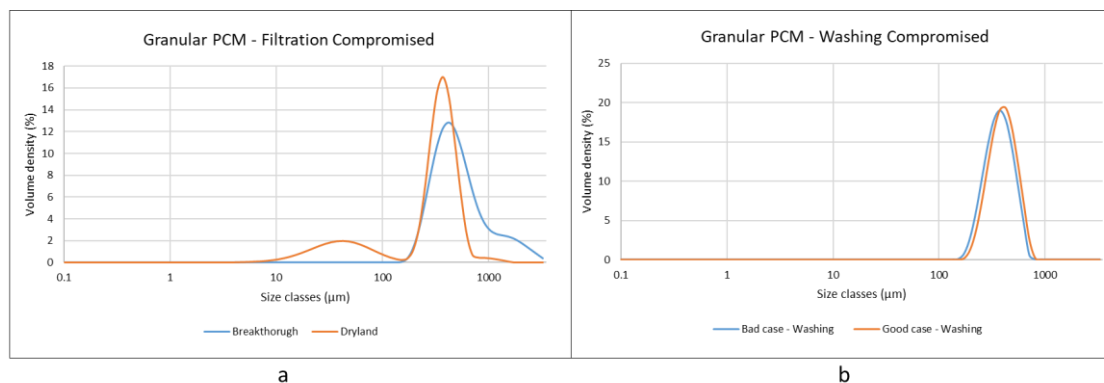


Figure 4-11: a.) PSD obtained for the two filtration runs for granular PCM; Breakthrough - D10: 280 μm , D50: 481 μm , D90: 1292 μm ; Dryland - D10: 202 μm , D50: 289 μm , D90: 512 μm . a.) PSD obtained for the two wash runs for granular PCM; Bad case - D10: 246 μm , D50: 367 μm , D90: 535 μm ; Good case- D10: 269 μm , D50: 397 μm , D90: 573 μm .

Looking at the filtration runs performed for micronised PCM Figure 4-9a, there is not much difference observed between the PSD obtained between filtration performed by breakthrough

and dryland. One of the issues of analysing filtered cake obtained from filtration stopped at dryland, is that the API cake is still completely saturated in the slurry solution. To be able to cut the biotage filter tube and obtain the cake without spillage, the cake had to be deliquored. This then causes the dryland filtration to effectively be filtration at breakthrough. In future studies, rather than analysing API cake at the end of filtration to evaluate for any differences in breakthrough and dryland, it might be worth carrying out the filtration to the desired mode followed by washing and then obtaining cake for analyses. This would allow for better investigation of the PSD obtained of the isolated washed API depending on whether the filtration is carried out to breakthrough or dryland mode. As the API cake from both modes of filtration will be obtained after deliquoring, at the end of washing, but the effect of wash solvent interaction with the filtered cake could be quite different depending on it being fully or partially saturated in the mother liquor and so could affect particle size distribution of the washed API obtained.

The results obtained for breakthrough filtration for crystalline PCM, Figure 4-10a, indicate something unexpected happened the particle size value obtained was much higher than expected. It is not clear whether this was due to sample handling or any other reason. For all the 5 particle size measurements carried out in Mastersizer for the API cake showed similar results with the average shown in Figure 4-10a. Further investigation would have been desirable by repeating this run, however, this was not possible at the time due to time constraints on the PhD project caused by COVID lockdown. As the main aim of this work is to investigate possibilities of analysing PSD of washed API cake using current lab particle size analysis techniques, and the best comparison of the washed cake particle would be with the API obtained from dryland filtration, hence repeating the breakthrough experiment with the time constraint was deemed non-essential experimentation.

Looking at the washing runs performed for all 3 PCM grades (Figure 4-9b, Figure 4-10b and Figure 4-11b), there was not a large difference between the PSDs obtained for washed cake produced from the “good” and “bad” washing procedures, especially for the crystalline and granular cases. For the micronised case, Figure 4-9b, there is an increase in the D_{90} value for the bad case of washing compared to good case. This result is as expected from previous studies, since using pure heptane as wash solvent for ethanoic PCM filter cake would be expected to result in the formation of agglomerates and so would lead to a higher D_{90} value, as observed. Micronised material is most prone to becoming agglomerated due to the higher tendency for micronised material to clump together.¹⁷ For the granular API on the other hand, hardly any difference in PSD was observed for the two different washing regimes. This again corresponds to what has been observed previously, with bigger particles resulting in bigger pores in the API cake and less wetted surface area so less retention of solvent in the filtered API cake. Hence less chance of interaction between the saturated crystallisation solvent and the wash solvent in the API cake to cause any anti-solvent effect and so formation of agglomerates. Another aspect which one can speculate/consider is that whilst the quantity of material forming crystal-crystal bridges might be similar for different crystal sizes, the force exerted on the bridge by the larger crystals may make them more vulnerable to breakage.

In Figure 4-12, Figure 4-13 and Figure 4-14 the evolution of PCM API material’s PSD obtained from wet cell analysis using laser diffraction is presented. The graphs show PSD going from raw API in liquid dispersant to filtration at dryland and then washing using both the “good” and “bad” washing cases for the 3 API grades.

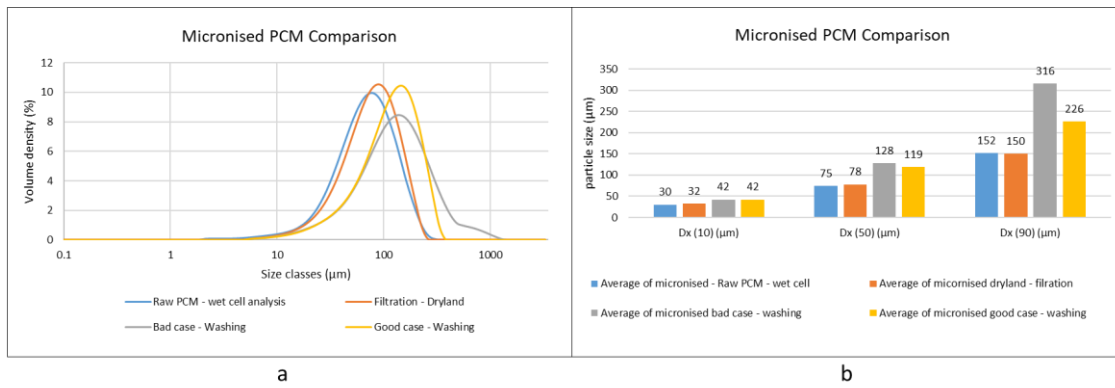


Figure 4-12: a.) PSD obtain for micronised PCM during different isolation stages. b.) Percentile particle size values obtained for the distributions shown in a.

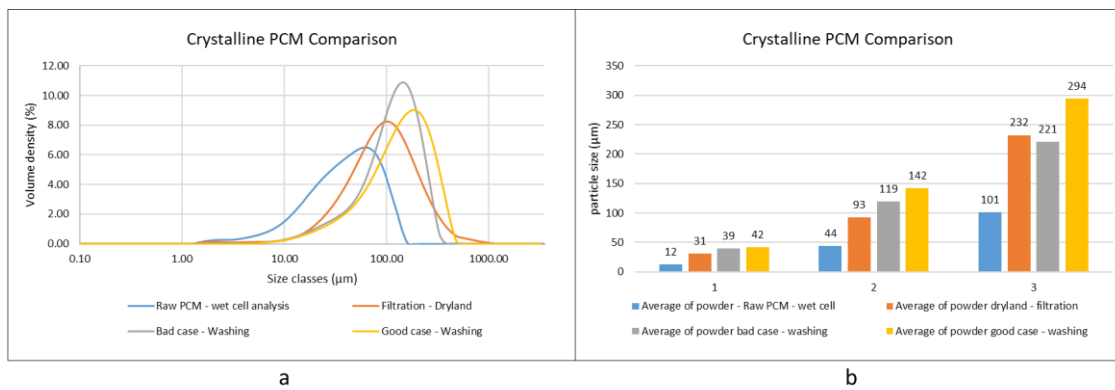


Figure 4-13: a.) PSD obtain for crystalline PCM during different isolation stages. b.) Percentile particle size values obtained for the distributions shown in a.

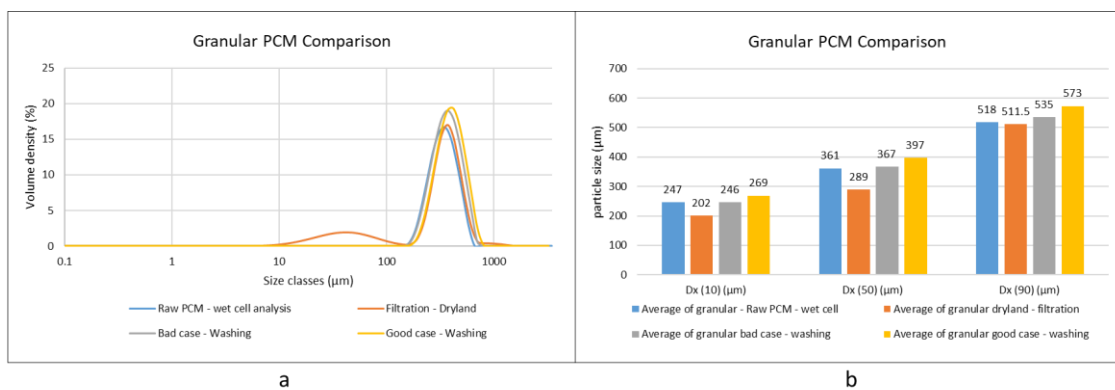


Figure 4-14: a.) PSD obtain for granular PCM during different isolation stages. b.) Percentile particle size values obtained for the distributions shown in a.

For micronised API, Figure 4-12, the results obtained are in line with expectations. The PSD from raw PCM and API cake obtained at the end of dryland filtration were very similar. The result from the two washing modes are as expected with the PSD obtained from the “good washing” experiment being closer to the raw API material result and so exhibiting a lower extent of agglomeration than the “bad washing” case. However, the “good washing”

experiment still shows higher D_{50} and D_{90} values than the one obtained for filtration to dryland. These higher D_{50} and D_{90} values could correspond to the formation of agglomerates during the washing process. The multiple stage wash solution used in the case of “good washing” helps to reduce agglomerate formation, but it doesn’t completely prevent agglomeration during the washing process. It could be the case that no matter how good the washing is when the particle size distribution of the raw API is very small, such as for the micronised PCM, there will always be some agglomerate formation.

For crystalline API, the results obtained are quite differing from the ones obtained from micronized API. There is a big increase in PSD obtained from raw PCM API to the filtered API material. Also, the PSD obtained from the “good” and “bad” washing procedures are the opposite to what is expected, with higher D_{50} and D_{90} values obtained for good case of washing.

Not much change in PSD was observed between different washing process for granular API, Figure 4-14. This is similar to what was observed in previous studies as the large API particles have less of a tendency to agglomerate during isolation. The large pores in the granular API cake structure allows for quicker removal of the mother liquor solution and hence less chance of interaction between the washing solvent and mother liquor solution. Also, large pore size reduces the number of API sites in contact and so reduces the amount of crystal bridges that can form to cause agglomerate formation.²⁰

Overall, from the results obtained it’s hard to determine whether the laser diffraction technique is effective for analysing wet API cake at the end of the washing process. Some of the results obtained match expectation with what has been observed/predicted in previous studies but there are issues encountered due to sample handling and the off-line nature of the analysis technique.

One of the issues encountered during Mastersizer analysis is that the result obtained were not the truest representation of the API cake sample. This is due to issues resulting from large

agglomerate (> 1 mm) settling in bottom of the Duran bottle. A 10 mL pipette was used to take the dispersed API cake sample from the Duran bottle and add to the Mastersizer Hydro MV cell for analysis. Even though the end tip of the pipette was cut to allow for larger particles to be transferred it can be seen that very large particle as shown in Figure 4-15b & Figure 4-15c would not be able to transfer and so would not be accounted for in the particle size analysis.

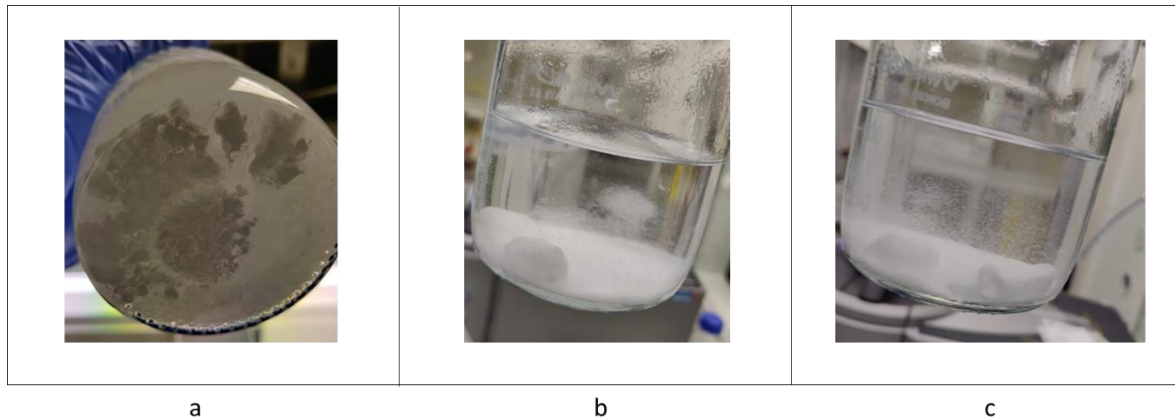


Figure 4-15: Images obtained of dispersed filtered/washed API cake samples for mastersizer analysis. a.) Image of dispersed sample in a duran bottle taken from bottom showing the large agglomerates present in the sample. b & c.) Images of API mastersizer samples allowed to settle showing the large agglomerates present within.

4.4.3 Focused Beam Reflectance Measurement (FBRM) analysis results

An FBRM probe was inserted in a vessel to collect data on the wet cake dispersed as described in section 4.3.5 **Focused Beam Reflectance Measurement (FBRM) analysis**. The FBRM probe was used with iC FBRM software provided by Mettler Toledo. This combination of instrument and software records in-line particle size data of the particles suspended in the vessel and provide the data in the format shown in Figure 4-16. Figure 4-16a show the particle statistics as a graph providing the particle size and number trends of the sample at different time points during analysis. By clicking on the trend viewer at different time points, it is possible to view the chord length distribution of the sample at that moment in time. This trend viewer provides a particularly useful application for processes where an FBRM probe is used in-line to indicate how particle size and count react to varying process parameters. For the purposes of this study,

the FBRM probe is used to analyse the particle size distribution of a sample, which shouldn't vary. This can be seen for Figure 4-16a, where the API cake particle statistics trends settle at a particular point very quickly. Chord length distribution (CLD) is then taken at five different time points as shown by the yellow line in Figure 4-16a, and the average of those five distributions is used as the chord length distribution of that sample for comparison in this study. Figure 4-16b shows the average chord length distribution of the micronised PCM sample analysed in Figure 4-16a.

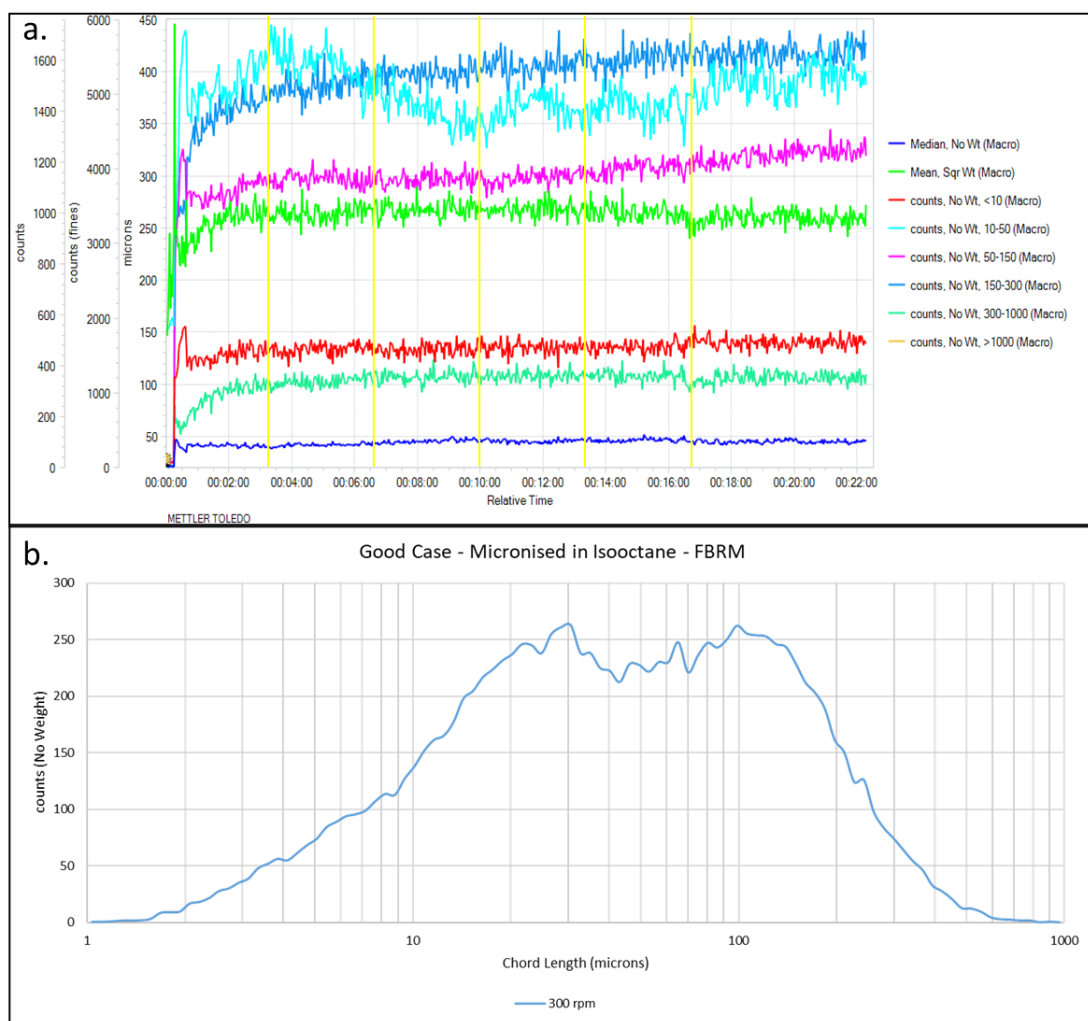


Figure 4-16: a.) Example of particle size trend obtained from Mettler Toledo FBRM iC software for micronised PCM obtained at the end of good case of washing. b.) Average chord length distribution obtained for micronised PCM (good washing case) using FBRM.

Figure 4-17 contains the chord length distributions obtained for micronised PCM at different isolation stages, similar to PSD shown in Figure 4-12a. Figure 4-17a shows the unweighted

CLD which allows for enhanced resolution of fine particle changes while Figure 4-17b contains square-weighted CLDs which allows for enhanced resolution of coarse particle changes.

Looking at Figure 4-17a, unweighted CLDs for micronised PCM, there is an increase in counts of fine particles for the bad case of washing compared to the raw micronised PCM. This is as expected for bad case of washing where introduction of pure heptane wash to the filtered API cake containing saturated ethanoic solution would result in an antisolvent effect and so cause an increase in the number of fine particles due to precipitation of PCM crystals. For a case of good washing there are fewer fine particles seen in the unweighted distribution, however from the square-weighted distribution there is a shift to the left side corresponding to higher amount of agglomerate formation when compared with raw micronised PCM, Figure 4-17b. This is similar to the result obtained using mastersizer, Figure 4-12a, where micronised material is seen to result in agglomerate formation even in the case of good washing.

Figure 4-18 shows images obtained using the PVM probe which was inserted in the EasyMax™ vessel while the particle size analysis was performed using an FBRM probe. Further information related to the PVM technique is provided in section 5.3.4 **Liquid Filtrate Post Offline Analysis**. The images from the PVM are not of a good quality as it was challenging for the camera system in the probe to focus on all the particles present in its optical plane. This resulted in images where some particles are in focus while others are out of focus and the lack of clear particle boundaries made any PSD analysis using the image analysis function impossible. Hence, in this work, the PVM images are used as a qualitative descriptor to extract any relevant information that could support the results obtained from the CLD analysis obtained using the FBRM.

From the images provided in Figure 4-18a, the raw micronised PCM API particles are more dispersed than in the images seen for both the bad and the good washing cases, Figure 4-18c

and Figure 4-18d respectively. For both the bad washing case, Figure 4-18c, and the good washing case, Figure 4-18d, the particles appear to be more aggregated than is the case for raw and filtered micronised cases. One of the reasons for this aggregation could be due to the agglomeration caused during the washing process. However, it is also important to note that for the raw and the filtered PCM cases, saturated ethanol was used as a dispersant, whereas for API cake obtained for both good and bad case of washing, isooctane solvent is used as a dispersant. This was to prevent precipitation occurring in the vessel if heptane (used for washing) and saturated ethanol come in contact during analysis. However, PCM would disperse better in saturated ethanol due to better wettability compared to isooctane and so this could also be a reason for the particle aggregation seen for both good and bad cases of washing in images from PVM.

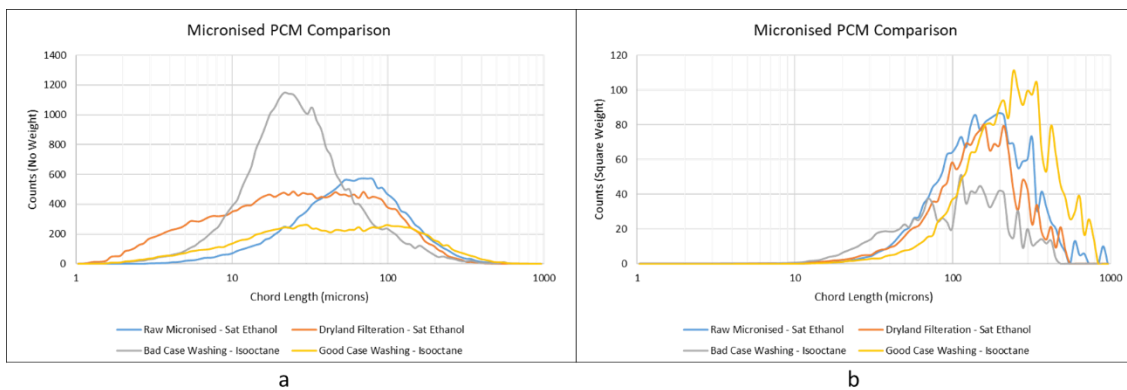


Figure 4-17: a.) Unweighted CLD obtained for micronised PCM during different isolation stages. b.) Square-weighted CLD obtained for micronised PCM during different isolation stages.

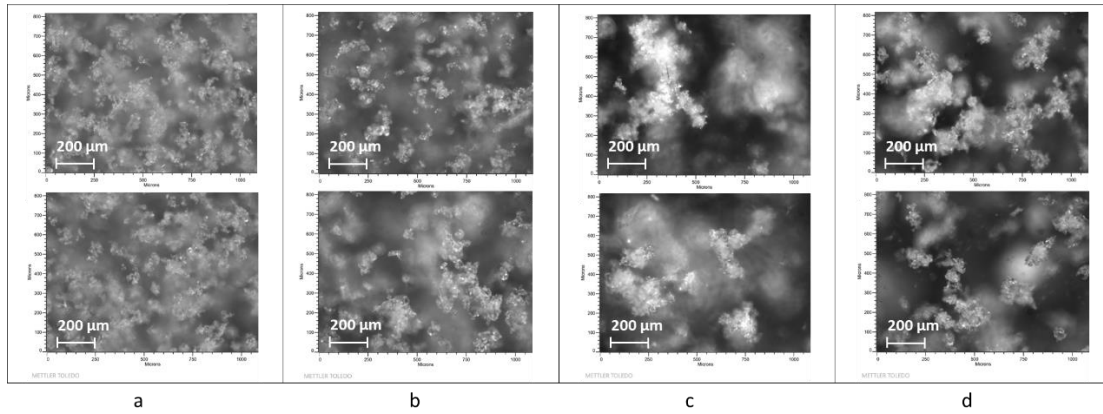


Figure 4-18: Images obtained from PVM probe during the different micronised analysis runs, with FBRM results attached in Figure 4-17. a.) Images of raw micronised PCM dispersed in saturated ethanol. b.) Images of micronised PCM filtered to dryland and then dispersed in saturated ethanol. c.) Images of micronised PCM washed using bad case scenario and then dispersed in isooctane. d.) Images of micronised PCM washed using good case scenario and then dispersed in isooctane.

Both unweighted and square weighted chord length distributions are presented in Figure 4-19 and Figure 4-21 for crystalline and granular PCM grade respectively. The PVM images obtained for the analysis of crystalline and granular PCM API cakes are presented in Figure 4-20 and Figure 4-22 respectively.

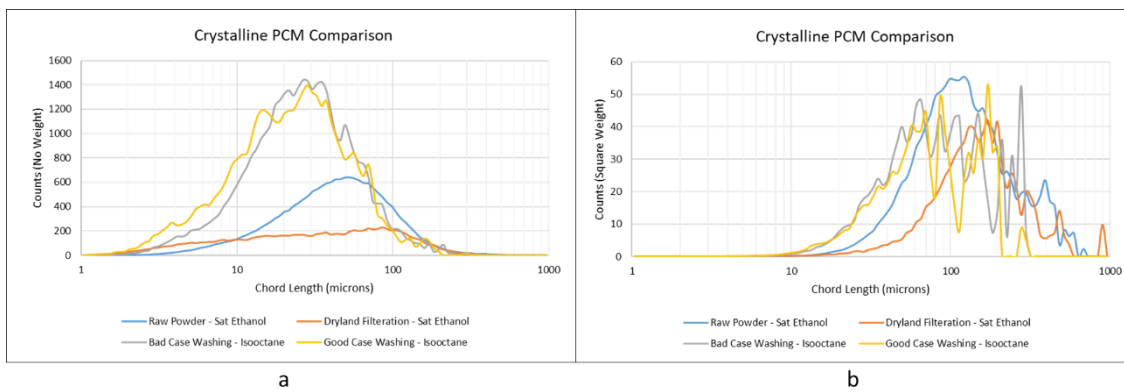


Figure 4-19: a.) Unweighted CLD obtained for crystalline PCM during different isolation stages. b.) Square-weighted CLD obtained for crystalline PCM during different isolation stages.

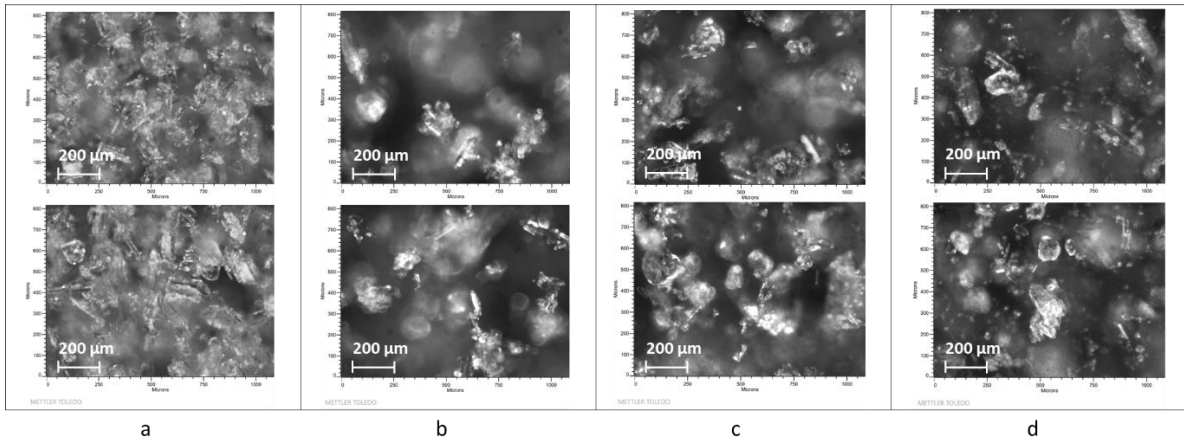


Figure 4-20: Images obtained from PVM probe during the different crystalline analysis runs, with FBRM results attached in Figure 4-19. a.) Images of raw crystalline PCM dispersed in saturated ethanol. b.) Images of crystalline PCM filtered to dryland and then dispersed in saturated ethanol. c.) Images of crystalline PCM washed using bad case scenario and then dispersed in isooctane. d.) Images of crystalline PCM washed using good case scenario and then dispersed in isooctane.

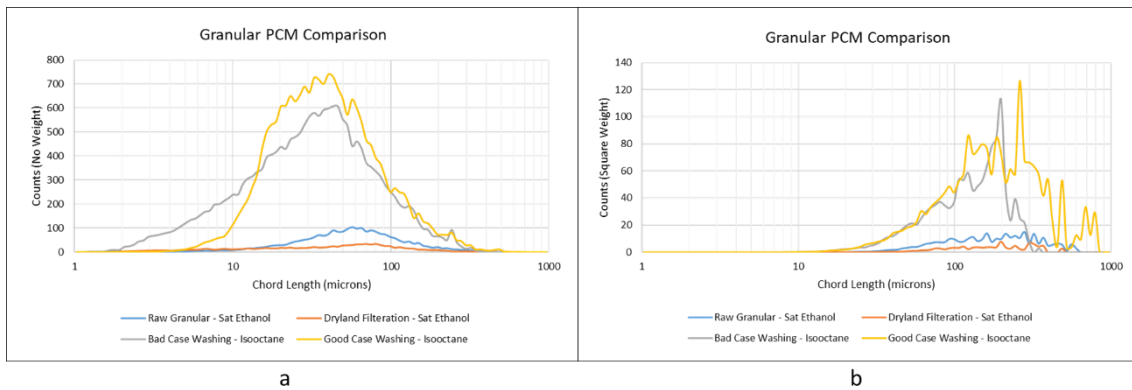


Figure 4-21: a.) Unweighted CLD obtained for granular PCM during different isolation stages. b.) Square-weighted CLD obtained for granular PCM during different isolation stages.

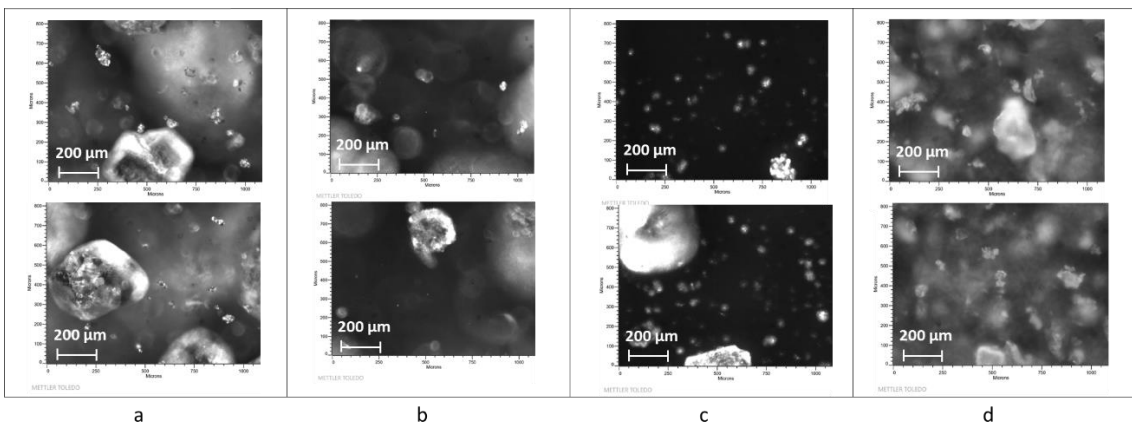


Figure 4-22: Images obtained from PVM probe during the different crystalline analysis runs, with FBRM results attached in Figure 4-21. a.) Images of raw granular PCM dispersed in saturated ethanol. b.) Images of granular PCM filtered to dryland and then dispersed in saturated ethanol. c.) Images of granular PCM washed using bad case scenario and then dispersed in isooctane. d.) Images of granular PCM washed using good case scenario and then dispersed in isooctane.

The chord length distribution results obtained from both crystalline and granular PCM, Figure 4-19 and Figure 4-21 respectively, show the same effect where there is an increase in the fine particles present in the API cake for the good and the bad washing cases when compared with the raw PCM. This could be due to precipitation taking place either during washing of the API cake in the biotage filter tube or in the Radley's vessel during particle analysis as any left-over saturated ethanol in the washed API cake interacts with the isooctane solvent causing supersaturation. This second theory seems probable as one of the issues encountered during analysis of both crystalline and granular material was particles adhering to the side walls of the vessel and on the FBRM and PVM probes, as shown in images in Figure 4-23. This made any particle analysis of the API cake difficult as the chord length distribution of the sample started to vary after around 4 to 5 minutes of the probe's in the vessel. (Trends obtained for all the different API cakes are attached in the Appendix D - **Investigating particle size distribution of agglomerates formed during washing process**, Figure D-7 to Figure D-18.) This fouling on the vessel wall and the probe was not observed in the micronised API case.



Figure 4-23: Images showing PCM API stuck to the wall of the vessel and the probe at the end of analysis.

4.4.4 Other particle analysis techniques tested

Apart from Mastersizer – laser diffraction and FBRM, other lab-based particle analysis measurement techniques were also evaluated during this study. However, none of these

techniques were not found to be useful for analysis of wet agglomerated cake obtained at the end of filtration and washing. The reasons for this are presented below and indicate the challenging nature of this objective to both determine the extent of agglomeration and the size distribution of the agglomerates.

Static microscopic-imaging analysis was performed using Morpholgi G3 (Malvern Panalytical, UK). The equipment consisted of a 2 mL wet dispersion cell together with a high-resolution digital camera to analyse particle size and shape. For this measurement technique, filtered / washed API cake had to be re-suspended in a dispersant similar to procedure explained in section 4.3.4 **Laser diffraction particle size analysis**. The re-suspended material had to be pumped into the Morpholgi G3's wet cell using a syringe. The force exerted by the syringe to push API particles into the cell caused most of the agglomerates to break and so this technique was deemed not to be suitable for analysis of agglomerates formed at the end of filtration & washing process.

As discussed in section 4.4.3 **Focused Beam Reflectance Measurement (FBRM) analysis results** particle vision microscope (PVM) (Mettler-Toledo, UK) was found to be inefficient for analysis of wet API cake obtained after filtration and washing process. The PVM probe is mostly used in-line to investigate a particle suspension, similar to the FBRM probe, with the equipment capturing the projection of free-flowing particles in the optical plane of the instrument. The issue with this method is the accuracy of particle analysis, a function of its optical measurement volume, which depends on its optical setting. To get a full story of the particles in the API cake, half of the API cake was cut vertically, as shown in Figure 5-1, and added to the 150 mL vessel to ensure particles from different regions of the filter wall as well as all the depth of the cake are analysed. However, this resulted in the system being oversaturated with too many particles in the system for PVM analysis as in-focused particles

images and analysis were affected by particle in the background and so severely compromising the accuracy of results from this technique. However, PVM images were found to be somewhat useful for visual analysis to go with the data analysis carried out for FBRM in section 4.4.3

Focused Beam Reflectance Measurement (FBRM) analysis results.

EasyViewer (Mettler-Toledo, UK) is another in-line particle size analysis tool similar to PVM, based on high-resolution microscopic images and image analysis. This PAT tool, even though not available in CMAC laboratory at the time of this PhD project, was being showcased for a day and so the opportunity was taken to analyse the three different PCM APIs using this tool. PCM API slurry was prepared in saturated ethanol (similar particle concentration as the slurry used for filtration and washing) and was analysed using EasyViewer tool. The slurry had to be analysed without being filtered and washed due to the time constraint, as the equipment was only available in the lab for one day for showcase purposes.

All of the results obtained from the easy viewer are presented in Appendix D - **Investigating particle size distribution of agglomerates formed during washing process**, Figure D-19 to Figure D-22. The result from micronised API is presented in Figure 4-24 . Micronised PCM ethanoic slurry was added to a 150 mL EasyMax vessel with an in-line EasyViewer probe. After some time, once consistent PSD reading was achieved , then heptane solvent was added to the ethanoic slurry in the vessel to analyse the effect of heptane addition in the slurry. The result for this including images obtained are shown in Figure 4-24 & Figure 4-25. Addition of heptane in the system caused the particles to aggregate together, as heptane acts as a hydrophobic solvent due to the low solubility of PCM in heptane. If a similar effect is experienced in a filtered API cake during the washing after introduction of heptane the wash solvent, then the particles in the filter cake are more likely to aggregate. This would reduce the effectiveness of washing of the API cake which then in turn result in greater agglomeration which is consistent

with what was experienced. A similar effect is also observed for the crystalline slurry system as seen in Figure D-19 and Figure D-21.

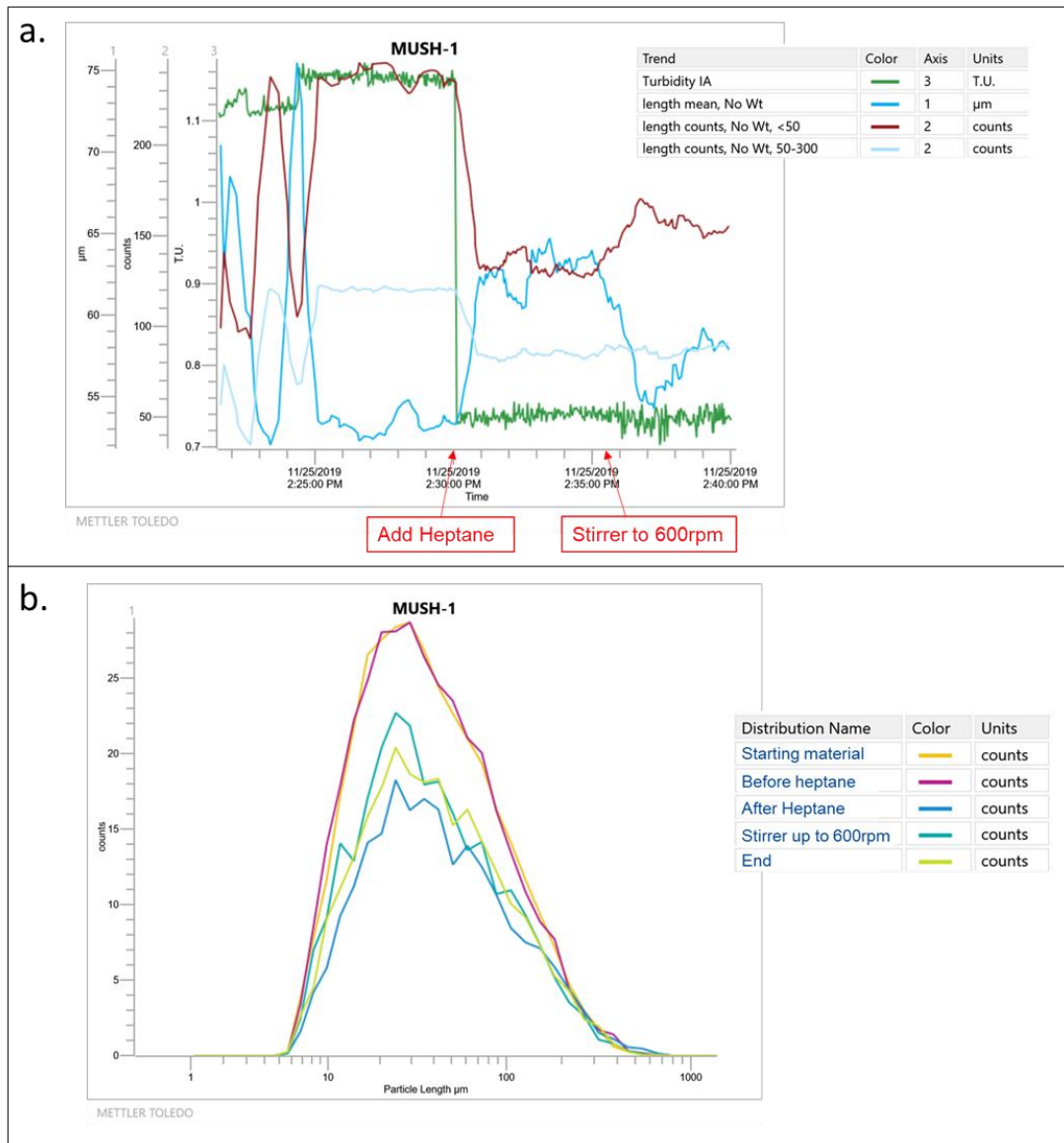


Figure 4-24: Graphs obtained from a micronised PCM measurement carried out using an EasyViewer provided by Mettler Toledo. a.) Trend for turbidity and chord length obtained during the micronised PSD analysis run. b.) Chord length distribution obtained for micronised PCM during the different stages of the run.

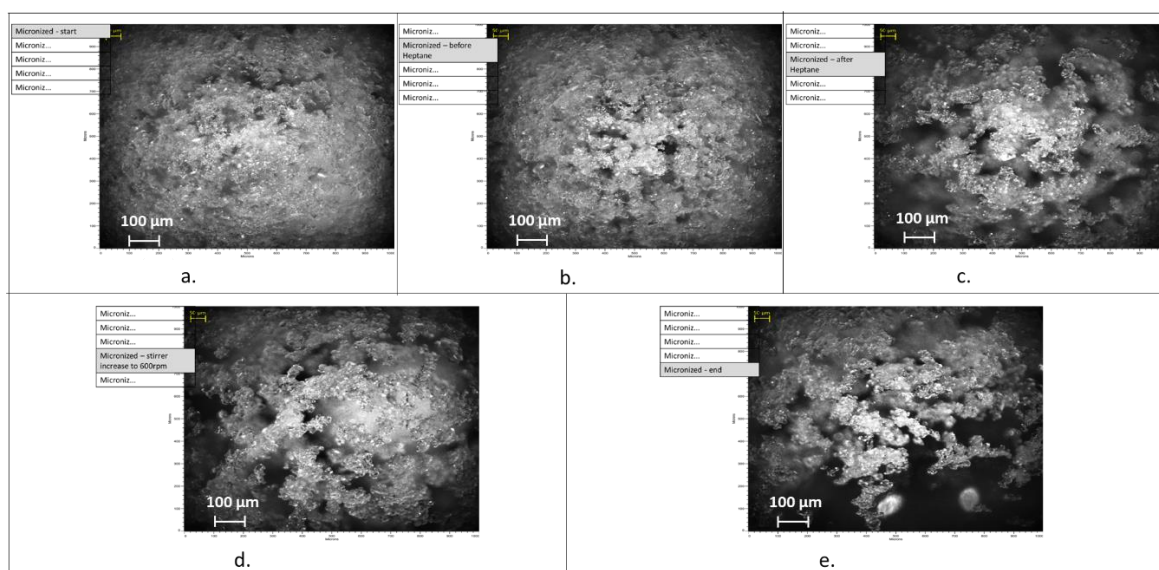


Figure 4-25: Images obtained from an EasyViewer for micronised PCM at different stages of the run with results shown in Figure 4-24. a.) Image of micronised PCM particles at the start of analysis dispersed in saturated ethanol. b.) Image of micronised PCM particles at the start of analysis dispersed in saturated ethanol before heptane addition. c.) Image of micronised PCM particles after heptane addition to the slurry mixture, causing aggregation. d.) Image of micronised PCM particles after heptane addition with an increase in stirrer speed to 600 rpm. e.) Images of micronised PCM particles at the end with the increase in stirring causing the aggregate to break up a little.

The image resolution obtained from EasyViewer and the automated analyses performed by ic vision software were found to be effective and a quick method of analysis compared to other optical imaging particle size analysis technique used within this study. However further full investigation of particle analysis of API material obtained from filtration and washing process is required, similar to work carried out with FBRM probe, section 4.4.3 **Focused Beam Reflectance Measurement (FBRM) analysis results**, to provide insight as to whether this analysis technique could be useful for evaluating PSD of wet filtered/washed API cake.

4.5 Conclusion

Particle analysis of API material obtained during various isolation stages is important to allow for better understanding of particle changes caused during isolation. This would allow for greater optimisation of these key isolation processes. In this study, filtered API cake obtained after the washing process was analysed using various particle size analysis techniques. The wet

filtered cake was taken from the filter tube and analysed off-line after being dispersed in a solvent.

From the various particle analysis techniques investigated in this work, focused beam reflectance measurement, using Malvern Panalytical's Mastersizer 3000, and chord length distribution, using Mettler Toledo's FBRM probe, were the two main particle analysis techniques employed for analysis of the washed API cake. These techniques were found to be most practical in off-line analysis of a wet cake obtained after the washing process. Even though Mastersizer was found to be adequate within the initial study using small set of sample material from study conducted in chapter 3, further work using larger number of varied samples revealed some of the issues encountered.

One of the biggest problems encountered throughout this study is the analysis of wet API was sampling and sample preparation of damp / wet filtered API cake obtained at the end of the washing process. Care must be taken while dispersing the washed cake to prevent any breakage of agglomerated present while ensuring it is done rapidly enough to prevent the solvent present in cake from drying and causing particle changes. The identity of the dispersing solvent also needs to be considered carefully to prevent either prevent any dissolution of the API cake or the dispersing solvent interacting with the wash solvent or any saturated mother liquor present in the API cake and causing precipitation or agglomeration.

This study has illustrated the challenge of characterising API particles obtained from a multi-component system at the end of the washing process. Further work is required to develop a definitive approach to be able to use an off-line particle measurement technique for analysis of a wet API cake.

4.6 Abbreviation

Paracetamol (PCM); Active Pharmaceutical Ingredient (API); Particle Size Distribution (PSD); Focused Beam Reflectance Measurement (FBRM); Chord Length Distribution (CLD); Particle Vision Microscope (PVM)

References

1. Liu, L.X.; Marziano, I.; Bentham, A.C.; Litser, J.D.; White, E.T.; Howes, T. Effect of particle properties on the flowability of ibuprofen crystallines. *Int. J. Pharm.* **2008**.
2. Morrison, H.G.; Tao, W.; Trieu, W.; Walker, S.D.; Cui, S.; Huggins, S.; Nagapudi, K. Correlation of drug substance particle size distribution with other bulk properties to predict critical quality attributes. *Org. Process. Res. Dev.* **19**. **2015**.
3. Agimelen, O.S.; Jawor-Baczynska, A.; McGinty, J.; Dziewierz, J.; Tachtatzis, C.; Cleary, A.; Haley, I.; Michie, C.; Andonovic, I.; Sefcik, J.; Mulholland, A.J. Integration of in situ imaging and chord length distribution measurements for estimation of particle size and shape. *Chemical Engineer Sci.* **144**. **2016**.
4. Ferreira, C.; Cardona, J.; Agimelen, O.; Tachtatzis, C.; Andonovic, I.; Sefcik, J.; Chen, Y.C. Quantification of particle size and concentration using in-line techniques and multivariate analysis. *Crystalline Technology*. **376**. **2020**.
5. Silva, A.F.T.; Burggraefe, A.; Denon, Q.; Meeren, P.V.; Sandler, N.; Kerkhof, T.V.D.; Hellings, M.; Vervaet, C.; Remon, J.P.; Lopes, J.A.; Beer, T.D. Particle sizing measurements in pharmaceutical applications: comparison of in-process methods versus off-line methods. *Eur J Pharm Biopharm.* **2013**.
6. ISO 13320:2009. Particle Size Analysis—Laser Diffraction Methods. Part 1: General Principles. **2009**.
7. Sympatec GMBH Qicpic. Analysis of particle size and particle shape in laboratory and process from 1 μm to 34,000 μm . <https://www.chemurope.com/en/products/61666/particle-analysis-size-shape-sympatec-qicpic.html>. [seen on 28/08/2021]
8. Malvern Panalytical, Morphologi G3. <https://www.malvernpanalytical.com/en/support/product-support/morphologi-range/morphologi-g3>. [seen on 28/08/2021]
9. Barrett, P.; Gelnnon, B. Characterizing the metastable zone width and solubility curve using lasentec FBRM and PVM. *Chem. Eng. Res. Des.* **80**. **2002**.
10. Henrich, J.U. Application of laser-backscattering instruments for in situ monitoring of crystallization processes—a review. *Chem. Eng. Technol.* **35**. **2012**.

11. Pandit, A.V.; Ranade, V.V. Chord length distribution of particle size distribution. *AiChE Journal*. **2016**.
12. Shahid, M.; Sanxaridou, G.; Ottoboni, S.; Lue, L.; Price, C. Exploring the role of anti-solvent effect during washing on active pharmaceutical ingredient purity. *Org. Process Res. Dev.* **2021**.
13. Malvern Instruments Worldwide. A basic guide to particle characterization. **2015**.
14. Kumar, V.; Taylor M.K.; Mehrotra, A.; Stagner, W.C. Real-time particle size analysis using focused beam reflectance measurement as a process analytical technology tool for a continuous granulation–drying–milling process. *AAPS Pharm. Sci. Tech.* 14. **2013**.
15. Ottoboni, S.; Price, C.; Steven, C.; Meehan, E.; Barton, A.; Firth, P.; Mitchell, P.; Tahir, F. Development of a novel continuous filtration unit for pharmaceutical process development and manufacturing. *J. Pharm. Sci.* **2018**, 108, 372.
16. Papageorgiou, C. D.; Langston, M.; Hicks, F.; AM Ende, D.; Martin, E.; Rothstein, S.; Salan, J.; Muir, R. Development of Screening Methodology for the Assessment of the Agglomeration Potential of APIs. *Org. Process Res. Dev.* **2016**, 20, 1500–1508.
17. ISO 13320:2009. Particle Size Analysis—Laser Diffraction Methods. Part 1: General Principles. **2009**.
18. Agimelen, O.S.; Hamilton, P.; Haley, I.; Nordon, A.; Vasile, M.; Sefcik, J.; Mulholland, A.J. Estimation of particle size distribution and aspect ratio of non-spherical particles from chord length distribution *Chem. Eng. Sci.* 123. **2015**.
19. Yu, W.; Erickson, K. Chord length characterization using focused beam reflectance measurement probe - methodologies and pitfalls. *Crystalline Technol.* 185. **2008**.
20. Ottoboni, S.; Simurda, M.; Wilson, S.; Irvine, A.; Ramsay, F.; Price, C.J. Understanding effect of filtration and washing on dried product: Paracetamol case study. *Powder Technology*. Volume 366. April **2020**.

5. Optimising removal of impurity on an industrial active pharmaceutical ingredient (API) using constant rate washing methodology

5.1 Introduction

Filter cake washing is a common process in solid-liquid separation, particularly in pharmaceutical industry, with the aim of removing impurities from the wet filter cake until the product has reached a required level of purity.^{1,2} The work performed in the three previous chapters of this thesis, chapters 2, 3 & 4, have demonstrated the importance of a well-designed washing process for isolation of API crystals. One of the aims of this PhD project is to use the learning developed throughout to produce a workflow which provides an optimum strategy for designing of washing processes in pharmaceutical isolation of APIs. This chapter introduces the wash process workflow developed and uses an industrial API drug substance to evaluate the methodology.

In chapter 3, a constant rate washing process was developed using paracetamol model API with patent blue dye as impurity to investigate and optimise the washing process. This method is different from the constant pressure approach usually employed in laboratory research and industrial practice as it allows for detailed analysis of both the liquid filtrate aliquots and the solid API cake obtained at the end of washing experiment. Analysing both evolving filtrate composition and API cake, allows for a more complete picture of the washing process to be built. The data and the understanding obtained from the constant rate method is found to be beneficial in designing an efficient wash process that is effective and reproducible in obtaining washed API with the required purity, yield, and particle size distribution.³

The work described in this chapter reports the deployment of the constant rate washing process to an industrial compound to investigate the applicability and the versatility of this methodology in designing a washing strategy and optimising washing process performance of a pharmaceutical product. This work was carried out in collaboration with AstraZeneca (AZ). The API used is a marketed drug product and due to confidentiality is referred to as AZ Compound 1 (AZC1) for the purposes of this work. The impurity considered in this study, is

related to drug substance and is referred to as Impurity Compound 1 (IC1). To meet the stringent final drug product quality requirements, the level of IC1 impurity in the final product must be less than 8 ppm. Currently the industrial washing process is performed at 0°C in a centrifuge. To understand the role of washing in ensuring the IC1 impurity concentration levels in the API product are met a parametric study of the variables influencing washing effectiveness was carried out to optimise impurity removal.

This study allowed investigation of the efficiency of the wash process workflow and the constant rate methodology in designing a washing strategy by using a challenging API drug substance.

5.2 Wash process workflow

Figure 5-1 showcases the wash workflow developed. There are four main stages in the workflow: identifying the wash process aim, wash solvent screening, lab-scale wash process development (DOE), scale-up of the wash process and validation (DOE).

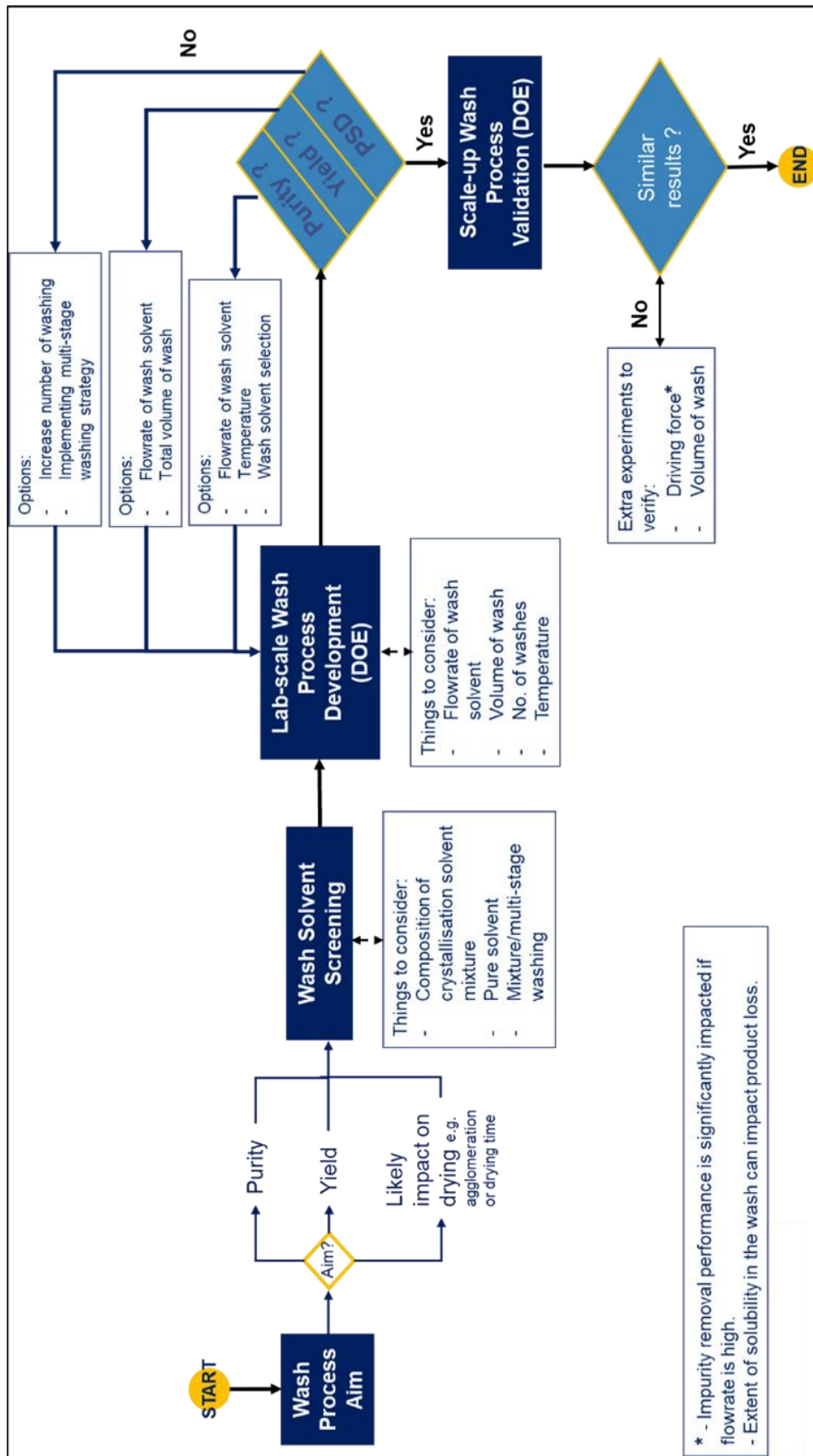


Figure 5-1: Washing isolation workflow developed

At the start of designing a washing process, it is vital to have a clear aim of the washing objective(s) as this plays a big part in choosing the best possible wash solvent to achieve the required outcome. The likely aims of the washing process are listed in Figure 5-1:

- Improve the purity of the filtered cake by removing impurity containing mother liquor solution present in the API filtered cake. Also potentially using wash solvent to dissolve any crystallised impurity present within the API cake.
- Maintain a high yield of the API product, especially if the final drug product is expensive. Making sure not to dissolve very much API during washing while displacing the mother liquor solution with a wash solvent.
- Improve performance of the downstream drying process; to decrease drying process time, and / or to prevent agglomerate formation during the drying process caused by crystal deposition from saturated mother liquor present in the API cake.

The main aim of the washing process guides the wash solvent selection process. In the second stage of the workflow, the operator starts screening for the possible wash solvent candidates. The solubility of the API and the impurities in the candidate wash solvents and the miscibility of the wash solvent candidates with the mother liquor are some of the properties of potential wash solvents which need to be considered. Anti-solvent screening of the wash solvent candidates should be performed to eliminate candidates where there is significant API and impurity precipitation during the washing process, (ideally there would be none) see Chapter 2. If the aim of the washing process is to improve purity level by optimising residual mother liquor removal, then a wash solvent with similar polarity should be chosen to allow for complete wetting and good contact with the of crystals forming the API cake. In the ideal case, a wash solvent that has low API solubility, but high impurity solubility would be best for removal of impurities while maintaining yield. However, it's often difficult and may not be possible to find such solvent for systems with API related impurities. If no solvents meeting

the required specification, then washing could be carried out using a mixture of an anti-solvent and the crystallisation solvent (potentially common in case of anti-solvent crystallisation), see Chapter 2, or pure crystallisation solvent could be used as wash solvent with washing carried out at a lower temperature than the isolation point to prevent high yield loss.

Thermodynamic properties of the wash solvent, such as boiling point and enthalpy of vaporisation are important if choosing a wash solvent with the aim of reducing drying time. However, using a wash solvent in which the API has a high or even moderate solubility can result in crystal bridge formation linking the product particles as the dissolved API in the wash solvent would precipitate out during solvent evaporation process and because liquid tends to collect at points of contact between the product crystals in the cake this would lead to agglomeration during the drying process.

The industrial compound used in this study already had a wash solution in place which had gone through the NDA (new drug application) filing and had been approved by FDA. To prevent having to go to the regulatory authority and due to the short time available for this remote industrial placement, it was decided to omit this step of the workflow from this project.

Following wash solvent screening, stage 3 of the workflow looks at using a design of experiment (DOE) approach to develop a washing process for the API at lab scale. Washing experiments are carried where; identity of wash solvent (selected from a shortlist identified at the wash solvent screening stage), contact time (related to the driving force causing the solvent to flow through the API filter cake), volume of wash solvent (related to cake volume and voidage), number of washes, and the temperature of the washing process are the list of variables to be investigated. Washing should be carried out using the constant rate methodology developed and described in thesis chapters 3, where analysis of both the washed API cake and the collected filtrate provide the necessary wash process performance information. The particle

size distribution of the washed API cake should also be analysed after washing, see thesis chapter 4, to investigate any agglomerate formation, crystal breakage or dissolution caused during the washing process. The washed API cake sample should be dried using a vacuum oven and analysed to verify the final purity at the end of the washing process.

The results obtained from the DOE experiments are then related back to the aim of the washing process to define the optimal parameters to achieve the desired wash process outcome. Once the optimised parameters are identified, 3 further repeated washing experiments should be carried out with the selected parameters to validate the DOE results and ensure the desired wash process outcome is achieved consistently.

The final part of the workflow looks at using the parameters obtained from the design of washing process at lab scale and scaling this up to the manufacture scale. This is one of the areas of workflow which has not been actively researched in this PhD project due to time constraints and Covid-19 preventing access to the larger scale equipment available in the project partner organisation AstraZeneca, as the placement was performed remotely at CMAC. Two of the main parameters to consider during scaling up of the process are the amount of wash solvent used and the driving force applied. One of the easier methods of scaling up washing process would be to use a semi-continuous method, such as that used in the AWL continuous carousel filter unit. With the size of each filter aliquot similar to the Biotage filter tube used in this work, the transfer of parameters from small lab scale to larger scale continuous operation would be much simpler. However, if a more conventional agitated filter dryer is used for washing at manufacturing scale, then using a constant rate approach during lab scale experiment should allow the operator to match the wash solvent contact time anticipated at large scale in the laboratory investigation such that the process can be investigated to optimise for yield improvement and wash solvent quantity reduction to achieve sustainability goals.

Once similar results are obtained at the end of the scale-up experimental work compared to the lab scale then wash process design is completed.

5.3 Material and Method

5.3.1 Raw Materials

The AZC1 used in this study was provided by AZ. The particle size distribution of the input API was determined at the start of the study to be D₁₀: 3.15 µm, D₅₀: 8.52 µm, D₉₀: 26.5 µm. The particle size analysis was performed using a laser diffraction technique in a wet dispersion unit (Mastersizer 3000 laser diffraction particle size analyser with hydro dispersion unit, Malvern Panalytical, UK). The method used consists of; measurement duration, 10 seconds, number of measurements, 5, obscuration limit, 5–20%, stabilization time, 30 seconds, beam length, 2.5mm. For wet dispersions, the raw material is suspended in 2,2,4-trimethylpentane (isooctane) (purity 99.9% (GC), Merck) with dissolved lecithin solution to avoid particle size variation during the analysis (negligible solubility of AZC1 in isooctane). To obtain true particle size distribution of the API material, without any agglomerates present during the analysis, around 0.12 mg/mL of lecithin surfactant (powder from soybean, LOT: 8030-76-0, VWR Chemicals) was added to the isooctane dispersant. The API particles are found to settle very slowly and have a large wetted surface area due to the product's particle size, which was in fact similar to the micronized paracetamol used in previous study.⁴

The IC1 impurity present with the AZC1 API crystal slurry at the end of the crystallization process has been shown to exhibit clastogenicity based on in vitro and in vivo testing.⁵ Clastogenicity is the phenomena by which a mutagenic agent disrupts or breaks chromosomes, leading to sections of the chromosome being deleted, added, or rearranged. Therefore, to safeguard the wellbeing of patients it is essential to prevent exposure to IC1 in the API product.

This is accomplished by demonstrating that the IC1 impurity level is always below 8 ppm to comply with the product specification limit.

The API product provided by AZ contained around 7 ppm of the IC1 impurity. Therefore, to mimic the crystallized suspension obtained during manufacturing and to test the capability of the washing process in removal of the specific IC1 impurity, the API slurry in this study was spiked with a small amount of IC1 impurity.

Oil Red EGN dye (LOT: 234117-25G; Sigma-Aldrich) was also used as impurity in this work. The main aim of using this dye as impurity is to aid with visualization of the washing process, as well as to compare the effectiveness or removal with that of the API related impurity to help evaluate wash performance and cake purity.

To investigate the washing efficiency of the industrial process slurry, the crystallisation solvent and the wash solvent used in this study were the same as those used in the manufacturing process, which was approved by the relevant regulatory authority. To mimic the slurry at the end of crystallisation process, a solvent system consisting of ethyl acetate (purity > 99%, LOT: 141-78-6, VWR chemicals), isooctane (purity 99.9% (GC), Merck) and water (Millipore water) were used. The wash solution consisted of a mixture of ethyl acetate and isooctane.

5.3.2 Suspension Preparation

The AZC1 slurry for each experiment was prepared by adding the required mass of API in two parts: the amount of API required to form saturated solution at the target isolation temperature was first measured and added to 50 mL crystallization solution. The required amount of impurity was then measured and added to the saturated crystallization solution. The mixture was then left in the sonicating bath (at 30°C) until no particles could be observed by naked eye, to ensure complete dissolution of the API and the impurity. The clear solution was then left in a Hailea HC-100A circulator / chiller for one hour to adjust the temperature of the saturated

solution to the desired level for the experiment. Once the solution has reached the target temperature in the chiller, some of the API particles are seen to have precipitated out as the API at the start is added in small excess of the solubility limit to ensure a saturate solution is achieved. This suspension is then filtered using a biotage ISOLUTE (Biotage AB, Uppsala, Sweden) 70-mL single-fritted polypropylene reservoir with 5 μm pore size to ensure a particle free saturated solution of AZC1 API is obtained. To ensure the temperature of the saturated solution is maintained to the desired level during filtration, a cooling jacket for the Biotage filter tube was created as seen in Figure 5-2. This cooling jacket was assembled by rolling tube around a plastic cylinder, creating a pocket in which a biotage filter could easily slot into for the experimental run. The cooling medium is then flowed in the tube. This was found to do an adequate job of maintaining the temperature of the solvent present within the filter tube during the filtration and the washing steps. A second precisely measured portion of AZC1 API was then added to the saturated solution to form slurry with 7.5% solid loading, by volume, this being similar to the solid loading achieved at the end of crystallization process going onto the filtration step in industry. Adding API in these two steps ensures that there is minimal change to the particle size distribution of the raw material. If all the API were added to the solvent at the start of the experiment, each crystal would be subject to some dissolution and the particle size distribution would be modified hence altering the results of this filtration and washing study as PSD would not be similar to the material in the process at the end of crystallisation. The slurry formed at the end of this sequence is left stirring in chiller, using a magnetic stirrer, at 250 rpm for an hour to ensure a homogenous mixture at the required temperature is achieved before the start of filtration/washing experiment.



Figure 5-2: Cooling jacket used for biotage filter tube

For experiments spiked with IC1 impurity, around 0.5 mg of impurity is measured and added to the saturated solution. This equates to a concentration of around 1900 ppm of IC1 impurity in the slurry mixture. This addition of the IC1 impurity to the API solution allows the washing performance in terms of removal of the IC1 impurity at relatively high concentrations consistent with the industrial situation which occurs at the end of crystallization stage.

The solubility data required for creating saturated AZC1 API solution at the various temperatures investigated was provided by AstraZeneca, however this data is not been included in this thesis for confidentiality reasons.

Some experiments were conducted using the red dye impurity to aid visualization of the wash process. For experiments carried out using red dye impurity, 5 mg of the impurity is added to 50 mL of saturated API solution. The impurity amount was dictated by the UV spectrophotometer dynamic range and limit of detection, based on the calibration curve obtained, see Appendix C - **Optimising removal of impurity on an industrial active pharmaceutical ingredient (API) using constant rate washing methodology.**

The original experimental aim was to incorporate both the IC1 API impurity and the colored dye impurity in the same slurry such that the removal of both impurities could be assessed from

the same experiment using two different analytical techniques. However, the patent blue V sodium dye impurity used in paracetamol study (Chapter 3) was found to be immiscible in the solvent system used in this work. The Oil red EGN dye impurity was found to be miscible with the crystallization and the wash solution mixture however was immiscible with acetonitrile and water, used as HPLC mobile phase (used for analysis of IC1 impurity). Hence, it was decided to perform a DoE using the IC1 impurity, as this API related impurity was the main focus of this study. Then a small number of additional independent experiments were carried out using the red dye impurity.

5.3.3 Experimental Setup

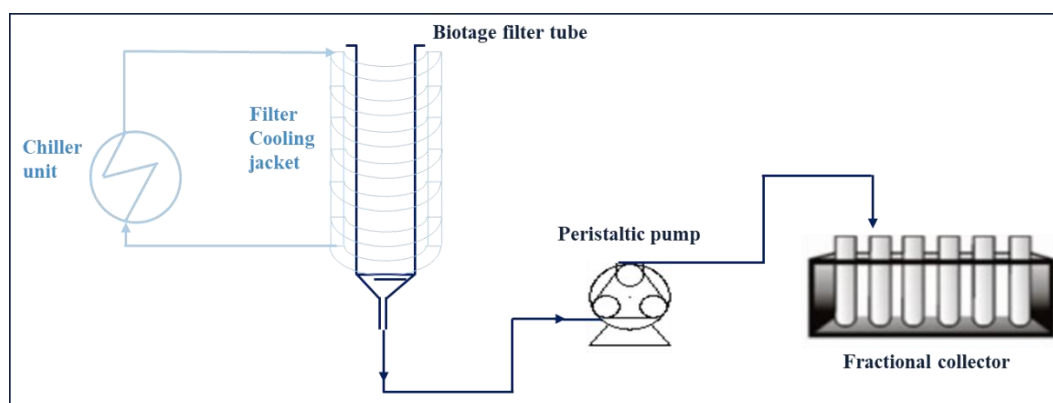


Figure 5-3: Process flow diagram of the filtration/washing experimental set-up

Figure 5-3 shows the process flow diagram of the experimental setup used for this work. For filtration and washing, a biotage ISOLUTE (Biotage AB, Uppsala, Sweden) 70-mL single-fritted polypropylene reservoir with 5 μm pore size was used. The biotage filter tube was placed inside a cooling jacket, Figure 5-2, to maintain the temperature of the slurry and solvent at the desired value during filtration and washing. The cooling jacket was connected to a Hailea HC-100A chiller unit for recirculation of the coolant through the cooling jacket. The outlet of the Biotage tube was connected to a peristaltic pump, which controlled the flow of solvent through a PTFE valve and a flexible tube (Watson-Marlow, Marprene® tubing, 302.0016.016#14, 1.6 mm Bore x 1.6 mm Wall). A fraction collector is placed at the end of the tube to collect the

different fractions of filtrate, which were latter analysed, as reported in section 5.3.4 **Liquid Filtrate Post Off-line Analysis**. The tubing connecting the biotage filter tube to the peristaltic pump and the fraction collector was kept as short as practicable and the hold-up volume was approximately 1.5 mL. The volume of fraction collected for aliquot in each experiment was kept consistent by varying the filtrate sample collection time depending on the pumping rate, Table 4-1. The pump is calibrated for each of the solvent system used in this study and the pump setting is analogous to the filtration rate and is used to represent the filtration rate in this chapter.

Before the start of each experiment, the filter tube and vials were weighed. A complete mass balance was kept throughout each experiment that was conducted. The slurry and the wash solution were kept in the chiller at the desired experimental temperature beforehand. At the start of experiment, the 50 mL sample slurry was taken from the chiller and was quickly and carefully transferred to the jacketed filter tube, making sure complete removal of slurry was achieved while transferring from sample bottle to the biotage filter tube without much deviation in temperature, Table 5-1. The objective of the jacket around the Biotage tube is to maintain the temperature at the required level that has been obtained in the chiller throughout the experiment. The valve at the end of biotage tube is opened and the peristaltic pump is then turned on at the required rpm, allowing the filtrate to flow through the medium into the vials. On reaching dryland, the point when the filter cake surface is first exposed, the pump is halted and the filtrate vial at which filtration stops is noted. The wash solution bottle is then taken from the chiller and 10 mL of unsaturated wash solution is measured out. This is then carefully added to the filter tube by slowly running wash solvent down the wall of the tube using a disposable pipette making sure not to disturb the filter cake surface.

The wash solvent is then filtered through the cake and the medium at the same pumping rate as the filtration stage until, dry land was reached and again halting the pump. This procedure is repeated for two more washing sequences, with a total of 30 mL of wash solution used in total in each of the DoE experiments, Table 5-2. The volume of wash solution used is kept consistent with the relative volumes used within the manufacturing process. The final wash step was followed by cake deliquoring during which the pump ran at the same rate until the bubble point is detected and a break in the steady flow of filtrate is observed at which point the pump was turned off. Bubble point during deliquoring step is when air is freely able to pass the API cake and filter media. This is observed during the experiment as the first air bubble is seen at the end of the biotage filter tube. The filter tube mass is then measured and the vial number noted at points where washing and deliquoring stops occurred.

5.3.4 Liquid Filtrate Post Off-line Analysis

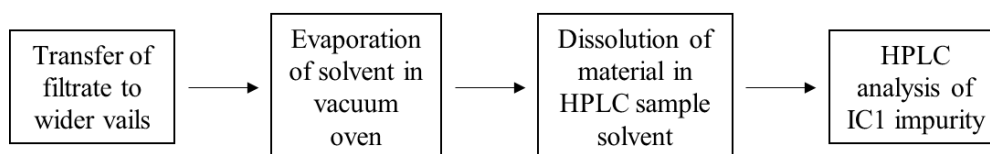


Figure 5-4: Post washing experiment analysis of the filtrate fraction samples (IC1 impurity)

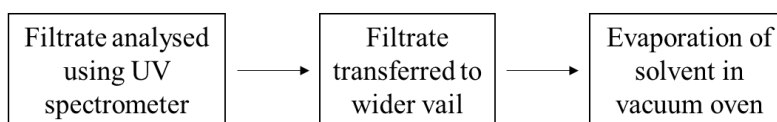


Figure 5-5: Post washing experiment analysis of the filtrate fraction samples (Red Dye impurity)

At the end of the washing experiment, the post filtration analysis carried out for each experiment was dependant on whether the experiment is carried out using IC1 API impurity or the red dye impurity. Figure 5-4 and Figure 5-5 shows the experimental steps used for filtrate analysis employed for the IC1 and the red dye impurity respectively.

For the experiment with the IC1 impurity, Figure 5-4, the vials containing the filtrate samples collected at the end of the experiment were weighed. The filtrate samples were then poured

from the long, narrow vials (17 mm diameter x 67 mm height, 10.5 mL volume capacity, Scilabware Ltd, UK) used in the fraction collector to pre-weighed shorter wider necked vials (24 mm diameter x 24 mm height, 5 mL volume capacity, Glaswarenfabrik, Karl Hecjt GmbH & Co KG, Germany) to aid evaporation of the solvent in the vacuum oven. The vials with filtrate were then placed in a vacuum oven at 45 °C with vacuum pressure of 10 Torr to completely evaporate of the solvent, leaving behind any dissolved API and impurity present in the filtrate. The temperature of the vacuum oven was not increased higher than 45 °C to prevent any degradation of the AZC1 API. The dried vials were then weighed to determine the amount of API lost during the washing process.

To determine the concentration of the IC1 impurity present in the filtrate vials and obtain a wash profile, high-performance liquid chromatography (HPLC) was conducted using an Agilent Technologies HP1100 unit. A 50:50 v/v mixture of acetonitrile : water is added to the dried filtrate vials to dissolve the API and the impurity. Acetonitrile and water are the sample solvent and the mobile phase for HPLC analysis method developed for determining the concentration of IC1 in samples. The reason for first evaporating the crystallisation and wash solution present in the filtrate before re-dissolution of solute in HPLC sample solution is due to the immiscibility of the two solutions, see section 5.4.1 **Experimental complications**.

For experiment with red dye impurity, Figure 5-5, the vials containing the filtrate are weighed at the end of the experiment. The filtrate sample is then analysed using UV-vis spectroscopy (ALS SP700 UV Spectrophotometer, Automated Lab Systems Ltd.) to quantify the Red Dye. The dye concentration was chosen to allow direct analysis without further dilution allowing the wash profile of the experiment to be obtained easily and accurately. After UV-vis analysis, the remaining filtrate in the vials is transferred to the smaller wider vials and then left to dry in

the vacuum oven at 45°C to determine API dissolved in each filtrate aliquot. Vials are weighed after each stage to ensure complete mass balance is kept throughout the experiment.

5.3.5 Solid API Cake Post Off-line Analysis

At the end of the experiment, the biotage filter tube containing the deliquored API cake is taken out of the cooling jacket and the mass of filter tube with the washed API cake is measured. The damp cake is carefully taken out of the filter tube, weighed and a small section is sliced and added to 60 mL of isooctane and lecithin dispersant solution (5g lecithin / 1 L isooctane) for particle size analysis using mastersizer. The wet dispersion method used for this analysis is similar to the method used for raw API material analysis, see section 5.3.1 **Raw Materials**. The reason for performing PSD analysis at this stage is to detect any agglomerate formation or change in PSD at the end of the washing process prior to drying the cake.

The remaining damp cake is then again weighed and left to dry in the vacuum oven, to determine the residual solvent content in the cake and complete the mass balance to understand the mass of API obtained at the end of the isolation process. This is determined by using the percentage of residual solvent present in dried cake to back calculate the mass of API present in the full damped cake.

The dried AZC1 API cake is gently milled using mortar and pestle to ensure a homogenous mixture of the washed dried API powder is obtained. Three samples each of 150 mg of the washed API powder are taken from each experiment and dissolved in the HPLC sample solvent for analysis of IC1 impurity concentration in the final washed cake.

5.3.6 Design of Experiment (DoE)

AZC1 is a marketed drug product therefore the manufacturing process and the process variable ranges are already approved by the regulatory authorities. Therefore, there is not a lot of freedom available to adjust the various variables affecting the washing process without having

to go through the procedure of getting approval from the relevant regulatory authority. For this reason, only two variables, the filtration/washing flowrate and the temperature at which the washing is carried out were varied in this experimental work, Table 5-1. Parameters such as the slurry loading, wash solution identity, volume of wash solution, number of washes were kept consistent with the values used in the manufacturing process.

A multivariate design of experiment (DOE) approach was used to investigate the combined effects of the selected parameters on removal of IC1 impurity and hence washing performance. MODDE (Umetrics, Sweden) was the software used for the DOE approach. For this work, since only two factors were investigated a full factorial screening DoE approach was used. As can be seen from Table 5-2, the experimental design created compromised all the possible combinations of the factor levels. Also, the design consisted of 7 factorial experiments, including the 3 midpoint experiments and so could be performed within the limited time frame of this industrial project.

Table 5-1: Table of factors, responses and analytical techniques used to quantify the responses in the DOE

| Variables | |
|---|---|
| Factors (abbreviation) | Range and units |
| Filtration & Washing rate (Fil) | Pump setting 10 – 100 rpm (1.3 – 11.7 mL/min, respectively) |
| Temperature (Tem) | 0 °C, 11 °C, 22 °C |
| Responses | |
| Responses (abbreviation) | Analytical method used to quantify response |
| IC1 concentration in washed cake (IC1c) | HPLC |
| % Decrease in IC1 (DIC1) | HPLC |
| API lost to washing (APIL) | Mass balance |
| % change in D ₁₀ (D10) | Particle size analyzer, Mastersizer 3000 |

% change in D₅₀ (D50)

Particle size analyzer, Mastersizer 3000

% change in D₉₀ (D90)

Particle size analyzer, Mastersizer 3000

Table 5-2: Experiments carried out with IC1 impurity

| Experiment Name | Run Order | Filtration Rate (rpm) | Temperature (°C) |
|-----------------|-----------|-----------------------|------------------|
| 1 | 6 | 10 | 0 |
| 2 | 1 | 100 | 0 |
| 3 | 5 | 10 | 22 |
| 4 | 4 | 100 | 22 |
| 5 | 7 | 55 | 11 |
| 6 | 2 | 55 | 11 |
| 7 | 3 | 55 | 11 |

Table 5-1 lists the responses used in this study. IC1 concentration in washed cake and the percentage decrease in IC1 impurity responses were determined by calculating the concentration of IC1 impurity added at the start of the experiment and using the HPLC method to analyse the IC1 concentration in the final washed cake. Tracking mass balance of the filtrate vials throughout the experiment, section 5.3.4 **Liquid Filtrate Post Off-line Analysis**, allowed the API loss during the washing process in each experimental run to be determined. Particle size analysis of the washed cake was performed at the end of each experiment as explained in section 5.3.5 **Solid API Cake Post Off-line Analysis**. The percentage change in particle size response for D₁₀, D₅₀ & D₉₀ is hence determined using the same Equation 7 as used in chapter 4 for particle size analysis:

$$\text{change in } D_x(\%) = \left(\frac{D_x \text{ of the washed cake} - D_x \text{ of the raw paracetamol API}}{D_x \text{ of the raw API}} \right) \times 100 \%$$

(where x = 10, 50 or 90) – Equation 7

Table 5-3: Experiments carried out with Red Dye impurity

| Experiment Name | Filtration Rate (rpm) | Temperature (°C) | Wash Volume (mL) |
|-----------------|-----------------------|------------------|------------------|
| R1 | 10 | 0 | 15 |

| | | | |
|----|-----|----|----|
| R2 | 100 | 0 | 20 |
| R3 | 10 | 22 | 20 |
| R4 | 100 | 22 | 20 |

Table 5-3 shows the filtration/washing experiments that were carried out at the end of the study using red dye impurity. For red dye experiment even though they were not part of the DoE there was still enough time to carry out the 4 experiments with red dye which allowed for investigation of all the possible combination of factor levels in removal of the red dye impurity. The volume of wash for these experiments was increased from 10 mL in IC1 impurity investigation to 15 mL in R1 experiment and then to 20 mL for subsequent experiments to ensure a complete wash is obtained. This increase in wash volume was due to presence of red dye in the API cake at the end of the wash process in experiment R1, observed from the naked eye. Extra volume of wash solution ensured that the washing process was complete with optimal removal of the red dye impurity.

5.4 Results and Discussion

5.4.1 Experimental complications

Throughout this study, there were several problems encountered in implementing the constant rate washing strategy on the AZC1 process system to analyse and optimise the washing performance. One of the main problems was the lack of analytical method available for detecting the IC1 impurity in the wash filtrate. The HPLC method developed in AZ was only able to detect IC1 impurity in the dry API powder at the end of the drying process. The crystallisation and the wash solution, consisting of ethyl acetate and isooctane, was immiscible with the mobile phase required for the HPLC, consisting of acetonitrile and water. Therefore, the methodology had to be modified, from the methodology of detecting a dye using UV-vis spectrometer as in paracetamol study or when using red dye, (section 5.4.3 **Experimental result obtained – Red Dye impurity**), where the filtrate had to be dried in the vacuum oven to obtain

any solid API and impurity present in the filtrate. In the modified procedure the solid precipitate was dissolved in the HPLC sample solution, of acetonitrile and water, before being analysed for IC1 impurity concentration in the wash filtrate.

Evaporation of the solvent from the long vials used in the filtrate collector was another experimental issue encountered. In a trial experiment, performed before the start of the DoE experimental study, the vials with filtrate from the faction collector obtained at the end of the washing process were left in the vacuum oven to dry. Even after leaving the vials for over 7 days there was still small amounts of solvent present in some vials, which had not evaporated off. This is similar to the problem encountered with evaporation dodecane solvent in paracetamol study, chapter 3. To ensure complete evaporation of filtrate for DoE experiments, the filtrate samples were transferred onto smaller, wider vials, similar to the one used for gravimetric solubility study in chapter 2.¹⁶ This change in vials allowed for the solvent to evaporate off confirmed by establishing that the masses of vials taken after two consecutive days were found to be similar. However, this change in experimental methodology did result in a significant increase in experimental duration as all the 40 or so filtrate vials had to be weighed and then transferred onto smaller pre-weighed vials and then weighed again to obtain complete mass balance.

Figure 5-6 shows an image of a dried filtrate sample. Even though the vial looked dry by naked eye and the mass stayed consistent in vacuum oven over a period of 24 hr, there were still some immiscible solvent visible as a separate droplet found when the HPLC sample solvent was added to dissolve the API and the impurity. This could be caused by the API and impurity precipitating out as small agglomerates, or aggregating together as can be seen from Figure 5-6. There could be a small amount of solvent trapped within the aggregated material, which would then take a very long time to evaporate off. Because the amount of residual immiscible

solvent present was very small and due to the project time constraints, it was decided that the methodology could be used to perform DoE experiments. Any presence of solvent in the wider dried vials was taken into account when performing mass balance calculations to determine the API loss during washing; this is detailed in Table C- 1 in Appendix C - **Optimising removal of impurity on an industrial active pharmaceutical ingredient (API) using constant rate washing methodology**.

In future work problems due to evaporation of traces of residual solvent could be overcome by using a centrifuge vacuum evaporator (e.g. Genevac), which allows for more efficient solvent evaporation at lower pressure while maintaining temperature allowing thermal sensitive sample to be processed more efficiently.⁷ Due to the unavailability of such equipment, this was not possible for this study.

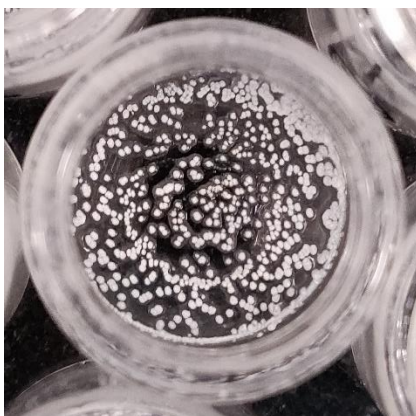


Figure 5-6: Dry filtrate sample vial take from the vacuum oven

Using a dye as a representative impurity, such as in the paracetamol study (chapter 3) or the red dye in this study, (section 5.4.3 **Experimental result obtained – Red Dye impurity**), measuring the wash profile using the UV-vis spectrometer was found to be a practical and precise method to determine dye content in filtrate samples (Figure 5-13). However, this was not found to be the case while using HPLC for wash profile analysis of the IC1 impurity. Figure 5-7 show the graph obtained for IC1 impurity concentration in the filtrate samples from

experiment 8. Experiment 8 was an extra experiment conducted after the DoE experimental work to investigate further the reason for the significant variance in IC1 concentration in the early filtrate samples. Experiment 8 was conducted with same parameter conditions as the DoE midpoint experiment, except that the volume of wash was increased from 10 mL to 20 mL to ensure a complete washing had been achieved. To ensure there were no issues due to variation in amount of filtrate in each sample, 1 mL of filtrate from each filtrate sample was pipetted into a clean wide neck vial and left to dry. The results for this test are included in the experiment 8 results graphs in Figure C-14 of Appendix C - **Optimising removal of impurity on an industrial active pharmaceutical ingredient (API) using constant rate washing methodology** demonstrates that the masses of filtrate added to each of the small filtrate vials was consistent.

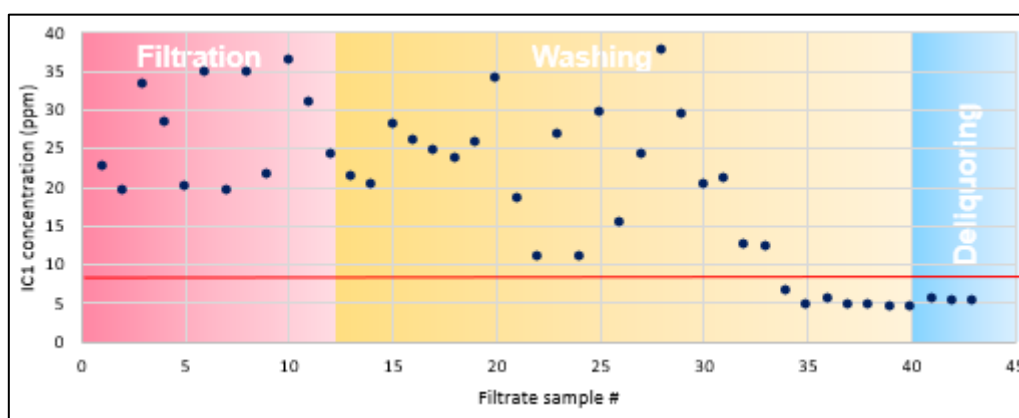


Figure 5-7: IC1 concentration in filtrate obtained from experiment 8. The red line shows the 8 ppm limit specification of the HPLC test

From Figure 5-7 it can be seen that the concentration of IC1 in the filtrate during filtration and early stages of washing is found to vary quite a lot. Approximately 1900 ppm of IC1 impurity was added to the AZC1 slurry at the start however, the HPLC method is only able to accurately detect around 20 to 35 ppm of IC1 impurity in the filtrate vials, Figure 5-7. This is due to a limitation of the HPLC method which was developed by AstraZeneca for detection of trace quantities of the IC1 impurity in the AZC1 compound. The HPLC method is designed to be capable of accurately quantifying the IC1 concentration at levels of 8 ppm or lower. For the

quantification of IC1 using this method, a limit test calibration solution is prepared at 8ppm, which is the specification limit for IC1 in AZC1. This impurity limit test solution was measured daily by HPLC and the within-day precision (coefficient of variation) was less than 4.0% for the HPLC method employed. The peak area obtained in the limit test solution is then used to quantify the IC1 concentration of the sample of interest. For samples with concentrations of IC1 above 8ppm, the HPLC method is not able to accurately quantify the IC1 concentration this is manifested as noise in the data. Therefore, IC1 concentration in filtrate sample vials obtained during filtration and most of washing is not accurate and does not give a wash profile as expected. However, we are able to clearly see the endpoint of washing from Figure 5-7 as the IC1 concentration in the filtrate sample becomes consistent toward the end at around 5 ppm.

In order to obtain a wash profile of any impurity to be investigated it is essential that the analytical method is able to quantify the concentration within the whole range from the start of filtration until the end of washing process. Because this was an industrial project, developing a new HPLC analysis methodology to extend the range of detection for this impurity was out of scope especially since the HPLC procedure is rather complex to differentiate the impurity reliably from other interfering species. This aspect should be considered in the design of other API washing investigations. One factor which could be considered in future experiment is to dilute the 1000 ppm sample to 10-30 ppm to get more accurate measurements but was not considered at the time of the experimental work.

5.4.2 DoE results obtained – IC1 impurity

Figure C-5 in Appendix C - **Optimising removal of impurity on an industrial active pharmaceutical ingredient (API) using constant rate washing methodology** contains all the responses obtained for the experiments carried out in the DoE study. Due to some variation

recorded in responses for the mid-point experiments and because some additional material and time being available at the end of the campaign, experiment 4 was repeated.

Figure 5-8 shows the impact of the factors investigated that affect API loss during the washing process in this study. The coefficient plot in Figure 5-8 shows a good level of reproducibility and a good fit between the data and the model, confirming the model's capability to predict responses. From the coefficient plot, temperature is found to be the major factor affecting the API loss during washing. Filtration rate of the wash solvent only seem to have a very small effect on the API loss when compared with temperature. This is also visible in Table 5- 4, which presents the API loss results for the 4 DoE experiments. The experiments carried out at 0°C have a much smaller loss of API during the washing process compared to the experiment carried out at 22°C. Comparing experiments with same filtration rate but differing temperature in Table 5- 4, such as experiment 1 & 3, the API loss is seen to increase from 116 mg at 0°C to 361 mg at 22°C. This is consistent with the solubility dependence of the API with respect to the temperature. The solubility of API increases around 3.5 fold in the wash solution as the temperature is increased from 0°C to 22°C.

Comparing experiments at the same temperature, experiment 1 with 2, and experiment 3 with 4, in Table 5- 4, a small effect on API loss due to filtration rate is visible and more notable at the lower temperature. This effect is similar to the one seen in the paracetamol study. The low wash solvent flowrate through the API cake results in greater contact time between the wash solvent and the particle. This increased amount of time allows solvent to reach nearer to the saturation solubility level.

Figure 5-8b, the contour plot for the API loss dependence on temperature and flow rate shows temperature is the main factor affecting the loss of API. The small gradient of the horizontal lines in the graph towards the left hand side indicates the small effect due to the filtration rate

and the change in slope of that gradient with temperature is due to the interaction present between the two factors investigated.

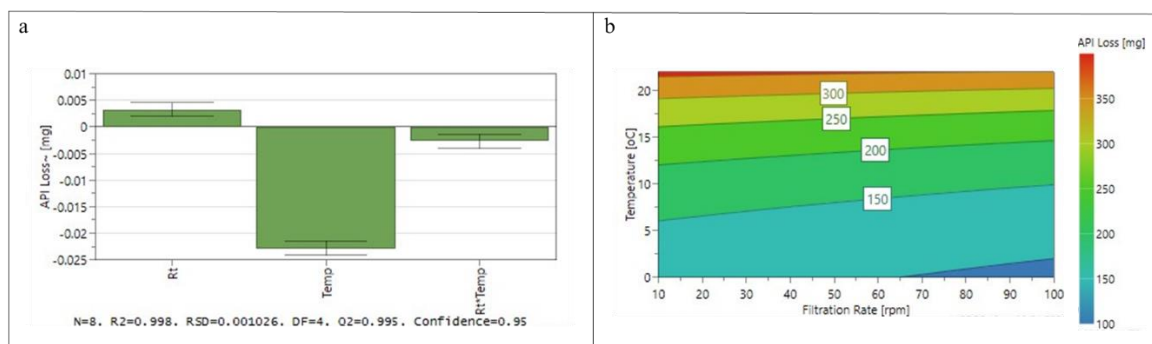


Figure 5-8: a.) Coefficient plot of DoE variables that effect API loss during the washing process, $R^2 = 0.998$, reproducibility = 0.996. b.) Contour plot obtained for the API loss

Table 5- 4: API loss responses obtained from DoE experiment

| Experiment Name | Filtration rate (rpm) | Temperature (°C) | API Loss (mg) | API Loss (%) |
|-----------------|-----------------------|------------------|---------------|--------------|
| 1 | 10 | 0 | 116 | 3.6 |
| 2 | 100 | 0 | 91 | 2.8 |
| 3 | 10 | 22 | 361 | 11.2 |
| 4 | 100 | 22 | 354 | 11 |
| 4 (repeat) | 100 | 22 | 340 | 10.6 |

Figure 5-9 and Figure 5-10 show the coefficient and contour plot for the factor investigated affecting the removal of IC1 impurity during washing. Figure 5-9 presents the final IC1 residual concentration response in the washed cake while Figure 5-10 shows the percentage change in IC1 concentration at the end of washing process. Both coefficient plots, Figure 5-9a and Figure 5-10a, show the main variable affecting the response, however the DoE model obtained is not capable of accurately predict this responses, this is visible in the low Q^2 value obtained for the models and the big difference between the R^2 and Q^2 values for the models. The contour plots, Figure 5-9b and Figure 5-10b, are included to allow visualisation of the direction of change in IC1 impurity level.

Temperature is only significant term found in the DoE models to influence IC1 impurity removal, as the error bar for the term does not cross the y-axis in the coefficient plots. Similar to the solubility of API, the solubility of the IC1 impurity in the wash solution is affected by the temperature. Carrying out washing at higher temperature would allow for greater amount of impurity to dissolve in the wash solution and exit the API cake.

Filtration flowrate did not seem to have any effect in removal of IC1 impurity according to the DoE model. However, as mentioned earlier the low R2 and Q2 value, the model obtained is not high enough to obtain reliable predictions. From the previous study of paracetamol, the API in chapter 3, we would expect the contact time and hence the filtration rate of the wash solvent to play a part in efficient removal of the impurity. The lack of any noticeable effect of the filtration rate term could be due to the major impact of temperature masking any difference which would be caused due to change in filtration rate.

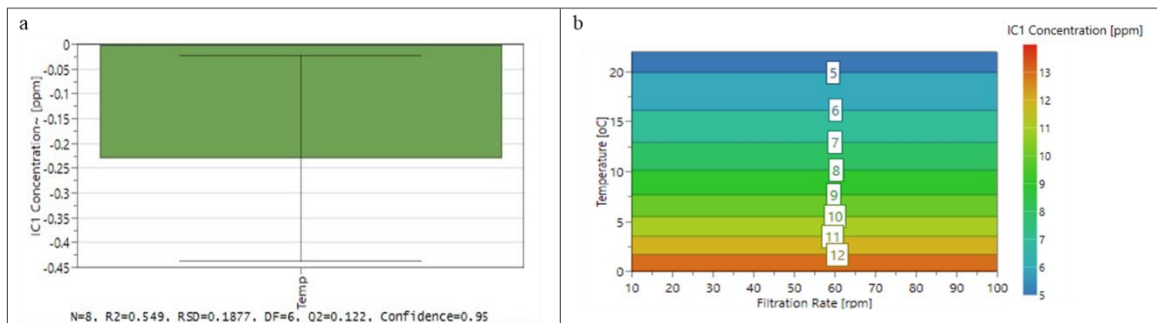


Figure 5-9: a.) Coefficient plot of DoE variable that effect the final washed cake IC1 concentration, R2 = 0.549, reproducibility = 0.546. b.) Contour plot obtained for the IC1 concentration

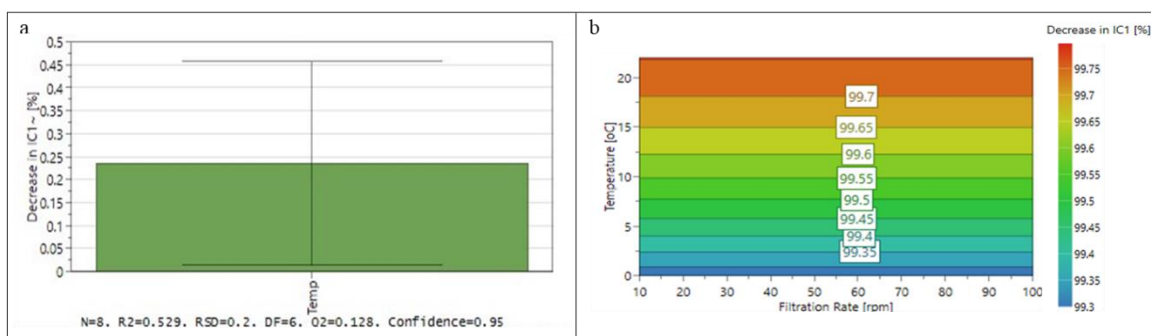


Figure 5-10: a.) Coefficient plot of DoE variable that effect the percentage decrease in IC1 concentration, $R^2 = 0.529$, reproducibility = 0.439. b.) Contour plot obtained for the percentage decrease in IC1 concentration

Figure 5-11 shows the coefficient plots obtained for the change in particle size distribution at the end of the washing process. For particle size distribution the DoE models did not show good reproducibility, nor there was good fit between the data and the model. The negative values obtained for Q2 for the D_{50} and D_{90} coefficient plot (Figure 5-11b and Figure 5-11c) reveals the poor model capability to predict responses.

The weak DoE models obtained from particle size distribution analysis suggests that there is some inherent variation in the experiment or the analysis of particle size distribution that is not taken into account. Particle size analysis is a complex procedure involving sampling, dispersion, and accurate use of instrument.⁸ For micronized material with particle size below 20 μm , particle size analysis comes with additional issues of particles adhering to one another due to electrostatic forces forming secondary particles, agglomerates and aggregates.⁹ The particle size analysis was made even more difficult in this study by analysing damp API cake which had been re-suspended in a dispersant for analysis.

The dispersion and the accurate use of instrument was established beforehand by designing a method for the Mastersizer laser diffraction equipment using raw AZC1 API material. Analysis of the as supplied API material was first carried out using a dry dispersion unit at different pressures to obtain a size measurement consistent with the formal AstraZeneca measurement

of the API particle size distribution. These measurement conditions were then used to design a method for the instrument's wet dispersion unit. The wet analysis method developed using the as supplied material which formed to input to these experiments was then used for analysis of the washed API samples.

Sampling of the washed cakes obtained at the end of experiments is possibly the point where there could be the greatest source of variance in the particle size analysis. Factors such as the amount of deliquoring time in each experiment and the amount of time taken between the end of the experiment and the cake sample being re-suspended in the dispersant could be anticipated to have an impact on the particle size analysis. Whilst efforts were made to control these sources of variation these factors cannot be controlled perfectly. Further investigation is required to improve the particle size analysis of damp washed API cakes to better understand the different factors involved, especially for micronized material.

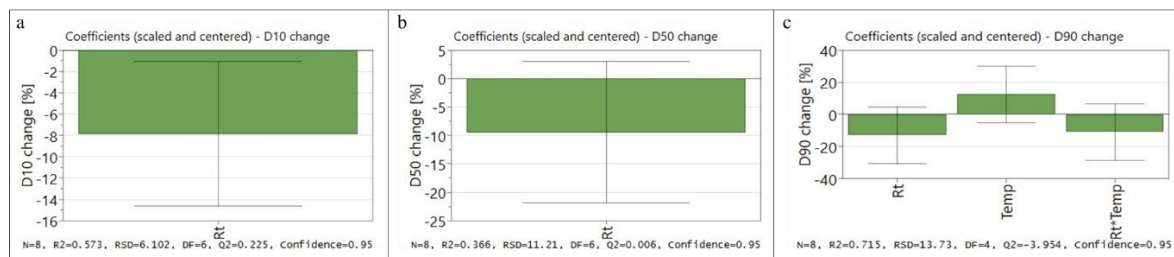


Figure 5-11: a.) Coefficient plot of DoE variables that effect the change in particle size, D10, $R^2 = 0.573$, reproducibility = 0.585. b.) Coefficient plot of DoE variable that effect the change in particle size, D50, $R^2 = 0.366$, reproducibility = 0.122. c.) Coefficient plot of DoE variable that effect the change in particle size, D90, $R^2 = 0.715$, reproducibility = 0.742.

Figure 5-12 shows the sweet spot plot obtained for the IC1 impurity removal from Modde using the models obtained for the API loss response and IC1 impurity concentration response. This graph shows the range of values of both variables which the washing process should be operated within to obtain the desired process outcome. One thing to note is that the IC1 impurity removal model is not completely sufficient for prediction so the sweet spot plot presented cannot be used for accurate prediction. However experimental work can be

conducted to help improve the model. Figure 5-12 gives a good representation of how the sweet spot could be used for a more accurate model for constant rate washing investigation.

For the sweet plot in Figure 5-12 the API loss criteria is set between 0 and 200 mg, while the IC1 concentration is set between the 3.45 ppm and 8 ppm. The lower IC1 concentration criteria was set at 3.45 ppm as that was the lowest concentration achieved in the DOE experiments and setting the criteria boundary to zero made the sweet spot very small, as its not practicle to achieve 100% removal. The green area in the graph, Figure 5-12, shows the sweet spot plot where both the coniditions set in the model are matched. Temperature is the major factor affecting the responses choosen (Figure 5-8, Figure 5-9 and Figure 5-10) and so the shape of sweet spot plot obtained is justified. Operating at temperature values above the sweet spot area can result in unnecessarily high yield loss during the washing process while operating at temperature level below the sweet spot area can result in an unacceptably high amount of the IC1 impurity retained in the final washed cake.

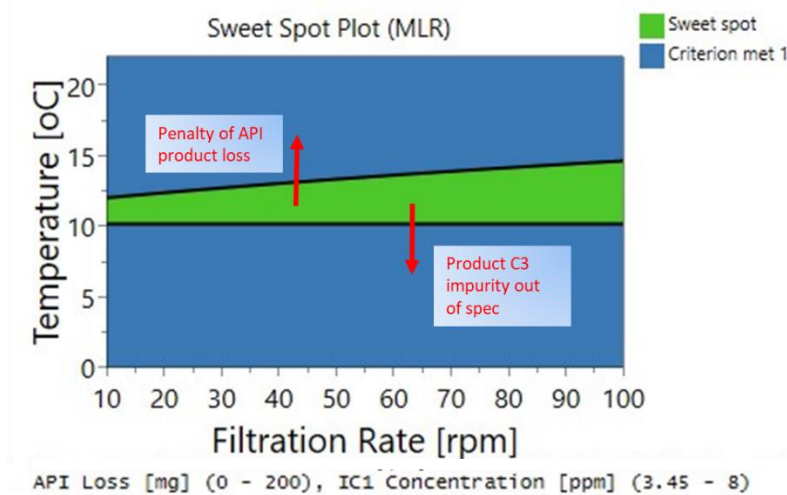


Figure 5-12: Sweet spot plot for reducing IC1 impurity using the DoE result obtained

The sweet spot plot shows the recommended range of conditions to operate within for the variables investigated. One cautionary note relating to the sweet spot recommendation is the potential effect of agglomeration that could be encountered at the end of drying when operating

the washing process at higher temperatures and low flowrate. Residual wash solution within the API cake would contain a higher amount of dissolved API, as longer residence time of wash the wash solvent gives longer time for API to reach solubility limits. This API would be deposited during the drying process and can cause formation of crystal bridges between the product crystals resulting in agglomeration.⁴ Therefore, it is also important to consider downstream effects on the API product from changing washing process parameters in a scaled-up industrial manufacturing process. Carrying out multiple washes introducing a final washing step using a solvent in which the API has very low solubility can assist in preventing agglomeration after the drying stage.¹⁶

5.4.3 Experimental result obtained – Red Dye impurity

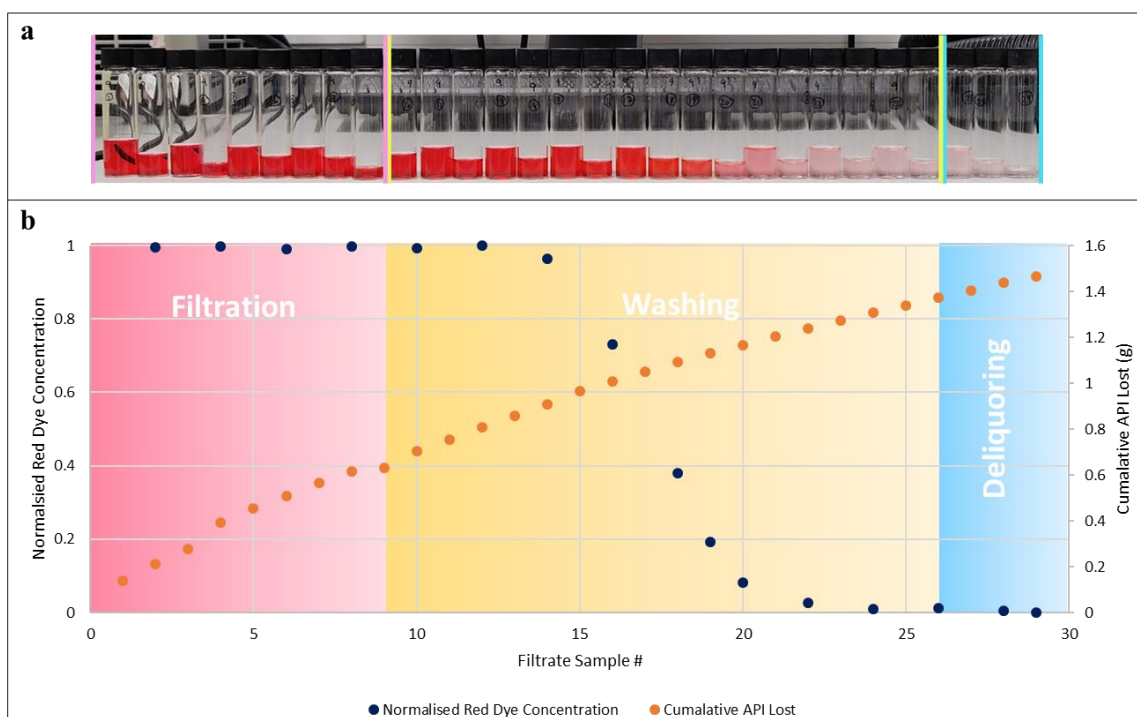


Figure 5-13: a.) Filtrate vial samples obtained for experiment R1. b.) Wash profile curve for red dye impurity concentration and the cumulative API lost graph obtained for experiment R1

An example of wash profile obtained from an experiment using red dye impurity is shown in Figure 5-13. Figure 5-13a shows the filtrate vials obtained from the fraction collector at the end of the filtration/washing experiment. The concentration of red dye impurity is similar at

the end of filtration to the start of the washing stage. Filtration is stopped at dryland and so the remaining mother liquor present in the filtered API cake is first displaced from the wash solvent front. There is a gradual decrease in red impurity concentration which can be seen in the filtrate vials obtained towards the middle and the end of the washing stage. The blue dots in the graph in Figure 5-13b displays the wash profile obtained using UV-vis spectrometer, with the decrease in red dye concentration aligned with visual aid provided from the filtrate samples.

For the dye impurity, the impurity removal is assessed by determining the sequence number of the collected wash filtrate required to remove the red dye and for the red dye concentration to level off at its minimum value, this is similar to the method employed for blue dye concentration in paracetamol study, chapter 3. For experiment R1 in Figure 5-13b, the red dye concentration starts decreasing at filtrate sample number 14 and reaches concentration of around 0 and levels off at filtrate sample number 28. Therefore, the impurity removal in experiment R1 takes around 15 filtrate samples. Since the volume of filtrate collected in each vials at different filtrate rate is similar, hence this is found to be valid method for analysis of impurity removal using wash profiles. The wash profile obtained for the other 3 experiments carried out using red dye is provided in Appendix C - **Optimising removal of impurity on an industrial active pharmaceutical ingredient (API) using constant rate washing methodology** with the final result obtained shown in Table 5-5. The only big difference found from comparison of the 4 wash profiles obtained, is the removal of red dye in experiment R3. In experiment R3 the low filtration rate together with the increased solubility of the impurity in the wash solution due to the high temperature would result in back-mixing effect.² Hence, higher amount of wash solvent would be required for complete removal of impurity. This is similar to the result obtained from previous work carried out with paracetamol in the earlier study.¹⁰

² Prolonged contact between the mother liquor and the pure wash solvent results in mixing of the two solvent with migration of the impurity into the pure solvent with consequent reduction of washing efficiency.

The red dots in the graph in Figure 5-13b, shows the cumulative API loss progressively throughout the filtration and washing stages. One thing to note is that presence of any isooctane in individual filtrate vial samples is not taken into account when determining the cumulative API loss graph in Figure 5-13b. The total API loss during the washing process, Table 5-5, takes any isooctane present in the whole system into account using the calculation given in the Table C- 1, Appendix C - **Optimising removal of impurity on an industrial active pharmaceutical ingredient (API) using constant rate washing methodology**. The API loss result in Table 5-5 corresponds to the result obtained from the IC1 impurity result in Figure 5-8. Temperature is the significant factor effecting API loss with the effect of filtration rate more visible in Table 5-5 due to higher amount of wash solution being used in the red dye experiments.

Table 5-5: API loss and impurity removal results obtained from the red dye impurity experiments

| Experiment Name | Filtration rate (rpm) | Temperature (°C) | Volume of wash (mL) | API Loss (mg) | API Loss (%) | No. of filtrate to remove impurity |
|------------------------|------------------------------|-------------------------|----------------------------|----------------------|---------------------|---|
| R1 | 10 | 0 | 15 | 187 | 5.8 | 15 |
| R2 | 100 | 0 | 20 | 140 | 4.4 | 15 |
| R3 | 10 | 22 | 20 | 714 | 22.2 | 21 |
| R4 | 100 | 22 | 20 | 430 | 13.4 | 14 |

Due to the Mastersizer particle size analysis equipment being faulty, it was not possible to measure the particle size distribution for the washed cake sample obtained from experiments R1 or R2. The results obtained for the R3 and R4 experiment together with the result obtained for the extra experiment 8 are given in Table 5- 6.

Table 5- 6: Change in particle size distribution at the end of the washing process for experiment with 20 mL wash volume. Negative percentage values in the table represent a decrease in the particle size after the washing process

| Experiment Name | % change in D10 | % change in D50 | % change in D90 |
|------------------------|------------------------|------------------------|------------------------|
| | | | |

| | | | |
|-------|-----|-----|------|
| R3 | 24 | 29 | 8 |
| R4 | - 6 | - 7 | - 13 |
| Exp 8 | 0 | 0 | - 3 |

All three experiments presented in Table 5- 6 were carried out with 20 mL of wash solution compared to 10 mL of wash used for the DoE IC1 experiments. When comparing the results obtained for these three experiments with the DoE experiments, given in Appendix C - **Optimising removal of impurity on an industrial active pharmaceutical ingredient (API) using constant rate washing methodology**, the API particle size is maintained when using higher volume of washes which is consistent with results obtained from previous work and literature.⁴ However, these are only three experiments and due to issues encountered with the results obtained for particle size analysis from the DoE, Figure 5-11, further investigation is required before any definite conclusions can be made.

5.5 Conclusion

A wash workflow is developed and introduced in this chapter, using the findings from previous PhD chapters with the aim of it being tested on an industrial compound. This work takes the constant rate washing methodology developed in previous Chapter 3 using a model compound, step 3 of wash workflow developed, and investigates the implementation of the methodology to assist in optimisation of washing process on an industrial compound. Other stages of the wash workflow could not be investigated in this project due to the lack of time available during this remote industrial project as COVID19 hampered any chances of this work being performed at AZ's site.

Even though there were several problems encountered in applying the constant rate methodology for the AZC1 API system, this study was successfully implemented to investigate the variables of interest using this method. Because the API investigated is a marketed medicine with a registered manufacturing process this restricted the variables which could be changed in

the washing process and this restriction made the implementation of the methodology slightly difficult. However, this work shows the versatility of this method and indicates that it could be applied to other industrial APIs, especially during the process development to investigate and design an effective washing strategy for API product crystals.

A parametric study was carried out to investigate the effect of temperature and filtration rate on removal of API related impurity during the washing process. Temperature was found to be the significant variable in removal of the impurity as well as the loss of API during the washing process. This is in consistent with the change in solubility linked to wash solvent temperature. This investigation of the impact of temperature on constant rate displacement washing in a lab setting has been found to be useful to validate and further develop the wash process workflow presented.

Similar to previous work, chapter 4, particle size distribution analysis of washed API cake was not found to be deliver conclusive results in the DoE. Current lab-based particle size analysis techniques are not suitable for analysing damp API cake material and further work is required to develop a methodology or a measuring to technique to adequately measure PSD of damp wet API cake obtained at the do the washing process.

5.6 Abbreviations

AstraZeneca (AZ); Active pharmaceutical ingredient (API); high-pressure liquid chromatography (HPLC); particle size distribution (PSD); design of experiment (DoE)

References

1. Estime, N.; Teychené, S.; Autret, J.M.; Biscans, B. Impact of downstream processing on crystal quality during the precipitation of a pharmaceutical product. *Powder Technology*. Volume 208. **2011**.
2. Ruslim, F.; Nirschl, H.; Stahl, W.; Carvin, P. Optimization of the wash liquor flow rate to improve washing of pre-deliquored filter cakes. *Chemical Engineering Science*. **2007**.

3. Shahid, M.; Faure, C.; Ottoboni, S.; Lue, L.; Price, C. Employing constant rate filtration to assess active pharmaceutical ingredients (APIs) washing efficiency. **Under Review**.
4. Ottoboni, S.; Simurda, M.; Wilson, S.; Irvine, A.; Ramsay, F.; Price, C. Understanding effect of filtration and washing on dried product: Paracetamol case study. *Powder Technology*. **2020**. 305-323.
5. U.S. Department of Health and Human Services. Food and Drug Administration. S2(R1) Genotoxicity testing and data interpretation for pharmaceuticals intended for human use. ICH. June **2012**.
6. Shahid, M.; Sanxaridou, G.; Ottoboni, S.; Lue, L.; Price, C. Exploring the role of anti-solvent effect during washing on active pharmaceutical ingredient purity. *Org. Process Res. Dev.* **2021**.
7. Ontko, J. A.; Jones, R. F. Centrifugal evaporation of organic solvents from series of solutions. *Journal of the American Oil Chemists Society*. **1965**. 462-464.
8. Meyers, R. A.; Lloyd, P. J. Pa. *Encyclopedia of Physical Science and Technology*. Chapter – Particle Size Analysis. Elsevier Science Ltd. **2001**.
9. De Villiers, M. M. Influence of cohesive properties of micronized drug powders on particle size analysis. *Journal of Pharmaceutical & Biomedical Analysis*. Volume 13. **1995**.
10. Ottoboni, S.; Price, C.; Steven, C.; Meehan, E.; Barton, A.; Firth, P.; Mitchell, P.; Tahir, F. Development of a novel continuous filtration unit for pharmaceutical process development and manufacturing. *J. Pharm. Sci.* **2018**, 108, 372.

Conclusion and Future Work

6.1 Conclusion

The washing process is a vital part of the isolation of crystalline API products. The work in this PhD project has highlighted some of the key mechanisms and phenomena that take place during the washing process and which can affect the process performance and product quality. The complex multi-component system present during the washing process has been thoroughly investigated with different studies performed to build a deeper understanding around this process and add to the scientific knowledge.

The first study conducted, chapter 2, in this thesis project investigates the interaction of the solution system in the complex multi-component system present during the washing process consisting of the saturated mother liquor solution and the wash solution, minus the API crystals. Solubility studies of binary solvent mixtures of crystallisation and wash solvents were performed. Some of the solution mixtures investigated formed solubility maxima at certain solvent composition and exhibited possible impact caused due to difference in solubility for the constantly evolving solution system present in API packed bed during the washing process. Two anti-solvent evaluation methodologies were developed to investigate wash solvent selection and to aid with better washing regime design for the API isolation to prevent risk of impurity precipitation. The glass vial methodology presented can readily indicate if precipitation is likely to occur due to solvent interaction during the wash process and provide an insight into the kind of process that might take place in the saturated API cake during washing. The centrifuge vial method developed can then be used to quantify the extent and composition of the precipitation taking place. These methodologies were used on an API and it was found that for complete removal of mother liquor during the washing process with minimal impact on crystal product, a multi-step washing strategy is advised. This would

significantly decrease chance of any precipitation occurring during washing due to antisolvent phenomena and reduce any agglomerate formation during the dry process.

The second study, chapter 3, investigates the constant rate filtration/washing methodology developed using readily available lab equipment to analyse filtrate obtained from the filtration and washing process. Analysis of filtrate using paracetamol API product with blue dye impurity showcased the usefulness of such data for optimising the washing process by understanding process performance, such as: wash process end point analysis based on impurity and mother liquor removal for the filtered API cake, determining the amount of API lost during the washing process and likely extent of agglomeration occurring during the drying process. Control and use of different flowrates using the constant rate methodology identified best wash solution flowrate through the API packed bed for effective removal of impurity. Use of low flowrates result in back diffusion and higher dispersion of mother liquor and impurity retention while too high flowrate causes wash solution to form channels within the packed API bed and so larger amount of wash solvent is required for complete removal which in turn results in greater API loss and inefficient use of solvent within the process.

Particle analysis of API crystals during the washing process is important to understand possible particle changes caused during washing due to interaction between wash solution, mother liquor solution and the crystal API packed bed. The filtered washed API cake obtained from the constant rate washing work in chapter 3 together with further filtration and wash studies performed, were used to investigate various particle size analytical technique to analyse washed API material, in chapter 4. Offline particle size analytical techniques such as focused beam reflectance measurement, using Malvern Panalytical's Mastersizer 3000, and chord length distribution, using Mettler Toledo's FBRM probe were used within this study. This work demonstrated the challenges involved in characterising API particles obtained at the end of the

washing process. Offline analysis involved sample preparation of washed damp API particle cake which was hard to handle and prevent any damage to the sample. The dispersing solvent used for sample analysis also needs to be carefully considered to prevent any interaction of the solvent with the solid sample. None of the techniques investigated were found to be reliable for washed API cake particle size measurement and further work is required to develop a definitive approach to be able to use an off-line particle measurement technique for analysis of a wet API cake.

Paracetamol has been widely used in this PhD project as the model API compound due to vast amount of data available. The anti-solvent study looking into the effect of solubility of binary solvent mixtures on the API crystal during the washing process, the constant rate methodology developed to better examine washing processes and the PSD work looking into particle characteristics of wash damped API cake are all investigated using Paracetamol API. The key findings from these studies are used to develop a wash process workflow which aims to help practitioners with designing a washing strategy which can aid with obtaining isolated API crystals with minimum agglomeration, product loss and solvent waste. This workflow is presented in chapter 5 of this thesis with some parts of the workflow applied on an industrial compound from AstraZeneca.

The constant rate methodology was successfully used to investigate the optimum washing parameters for the industrial compound that would prevent API loss during the washing process. This was the main part of the workflow investigated due to lack of time available during this remote industrial project as COVID19 hampered any chances of this work being performed at AZ's site. The parametric study investigated the effect of temperature and filtration rate on removal of API related impurity. An optimal washing process parameter was discovered and presented to the AstraZeneca project team. Use of the constant rate

methodology and the wash workflow during this study showcased the versatility of this being applied to industrial API projects to design an optimised wash process for the API drug substance. This constant rate approach and the associated workflow is now used routinely as part of the AZ crystallization and isolation process development workflow.

6.2 Future Work

This PhD project was able to demonstrate the importance of the washing process in the isolation of an API product and show case a practical approach to optimise washing performance. As mentioned previously, the lack of literature on API washing makes it even more vital to further investigate the washing process to ensure optimised washing can be designed into every API crystallization and isolation process.

The constant rate filtration methodology showcased in this PhD project in chapter 3 allows for easy data collection during the washing process. Due to the lack of washing process data for API drug substance in literature there has been very little to no work looking into investigation of axial dispersion models and coefficients for such systems. The data gathered in this work for different washing process scenarios using several crystallization and wash solvents in three different paracetamol crystal sizes can be used to develop wash process dispersion models to predict wash process performance for different APIs with similar crystal physical properties in different solvent systems. Such models can be used to aid with wash process design by predicting optimal process parameters before investigating/validating the model result in labs.

Constant pressure filtration is widely used in pharmaceutical industry for filtration and washing of batch processes. Work in this PhD project have shown constant rate filtration allows for better control during the filtration and washing process. With continuous manufacturing of pharmaceutical products being widely explored in industry, constant rate filtration can be applied to continuous and semi-batch processes for integration of inline analysis during

washing process with feedforward and feedback control present to ensure adequate process performance is achieved every time. Integration of such system in a continuous process might be easier to implement with peristaltic pump compared to vacuum/pressure systems employed for constant pressure filtration.

One of the main areas for further research and technology development highlighted during this PhD project is particle size distribution measurement of wet / damp API filter cake obtained at the end of the washing process. Obtaining a true representation of the particle attributes at the end of washing process is very beneficial to optimising the process to decrease the extent of agglomeration occurring during isolation. Several different laboratory particle size analysis techniques, have been tried during this PhD, as reported in chapter 4. None of these techniques were found to be extremely effective in obtaining reliable measurements of particle attributes due to the wet API cake having to be recovered, resuspended and analysed off-line. Further work is required in this field, looking at employing in-situ imaging techniques such as X-Ray Nano Computed Tomography to obtain API cake particle analysis during washing without having to resuspend the material. This should help eliminate some of the errors caused during sampling and resuspending of the washed API cake.

The API wash process workflow developed is one of the main practical outcomes of this PhD project which aims to help facilitate and simplify designing of a pharmaceutical API washing processes. This API washing workflow should be trialled with other industrial API crystals to assess the validity of the workflow with more complex API compounds. This workflow should ideally become a living document, able to be modified if required to ensure it encompasses any further developmental findings.

Sometimes agglomeration is beneficial for a crystal API product compared to single crystals (dependant on the final crystal morphology) in terms of flowability, filterability and

compaction properties. For these processes it could be worthwhile to investigate integration of the isolation processes such as crystallisation, filtration and washing processes to obtain the desired agglomerate at the end of the drying process. These processes could be designed in a way where the aim of filtration and washing process is to continue the crystallisation process and promote agglomeration, in the API cake, to a certain extent while ensuring to replace the impure mother liquor solution with a solvent that can aid during the drying process.

Developing the API washing workflow has provided a means of presenting and applying the conclusions of the work in a form which is readily disseminated.

Appendix A - Exploring the role of anti-solvent effects during washing in active pharmaceutical ingredient purity

Table A-1: Main properties of the solvents used in this work.²⁴⁻²⁸

| Solvent | Boiling point (°C) | Enthalpy of vaporization (kJ/mol) | Viscosity (cP) (Temperature °C) | Density (g/mL) (Temperature °C) | Surface tension (mN/m) (Temperature °C) |
|-------------------|--------------------|-----------------------------------|---------------------------------|---------------------------------|---|
| Ethanol | 78.4 | 38.58 | 1.26 (20) | 0.79 (20) | 21.99 (20) |
| Isopropanol | 82.2 | 39.85 | 2.1 (25) | 0.78 (25) | 21.4 (20) |
| Isoamyl alcohol | 132 | 55.2 | 3.74 (25) | 0.81 (15) | 24.77 (15) |
| Acetonitrile | 81.6 | 33.23 | 0.35 (20) | 0.78 (20) | 29.04 (20)_ |
| n-Heptane | 98.4 | 31.77 | 0.397 (25) | 0.68 (20) | 19.7 (20) |
| Isopropyl acetate | 88.5 | 37.2 | 0.52 (25) | 0.87 (20) | 22.3 (20) |

Table A-2: Calculated final ratio of wash solvent in solution mixtures at the end of wash solution addition.

| | | | | | | | | |
|--|-------|-------|-------|-------|-------|-------|-------|-------|
| Starting volume of crystallisation solvent (µl) | 300 | | | | | | | |
| Ratio of wash solution (crystallisation : wash) | 90:10 | 75:25 | 50:50 | 40:60 | 30:70 | 20:80 | 10:90 | 0:100 |
| Volume of crystallisation solvent in wash solution (µl) | 630 | 525 | 350 | 280 | 210 | 140 | 70 | 0 |
| Volume of wash solvent in wash solution (µl) | 70 | 175 | 350 | 420 | 490 | 560 | 630 | 700 |
| Final volume of crystallisation solvent in solution (µl) | 930 | 825 | 650 | 580 | 510 | 440 | 370 | 300 |
| Final volume of wash solvent in solution (µl) | 70 | 175 | 350 | 420 | 490 | 560 | 630 | 700 |
| Therefore volume fraction of wash solvent in final solution | 0.07 | 0.175 | 0.35 | 0.42 | 0.49 | 0.56 | 0.63 | 0.7 |

Table A-3: Initial experiment conducted of liquid holdup inside centrifuge vial using water. The rpm was set at 6000. The amount of time of centrifugation was varied. The cells with italic and bold numbering are the one where the vials were left in the centrifuge for an extra 2-3 minutes before

taking the sample out and measuring the mass. This extra time helped in draining much more of the solvent out of the filter and so resulted in much less solvent hold-up in those samples

| Vial | Weight of centrifuge filter tare (g) | Weight of centrifuge filter after 1 min centrifuging (g) | Mass of solvent holdup in the filter after 1 minute (g) | Weight of centrifuge filter after another 1 min centrifuging (g) | Mass of solvent holdup in the filter after 2 minute (g) |
|------|--------------------------------------|--|---|--|---|
| 1 | 0.40129 | 0.42540 | 0.02411 | 0.41587 | 0.01458 |
| 2 | 0.40213 | 0.41018 | 0.00805 | 0.40592 | 0.00379 |
| 3 | 0.40235 | 0.40870 | 0.00635 | 0.40563 | 0.00328 |
| 4 | 0.40125 | 0.43443 | 0.03318 | 0.4052 | 0.00395 |
| | | Average holdup | 0.01792 | | 0.0064 |

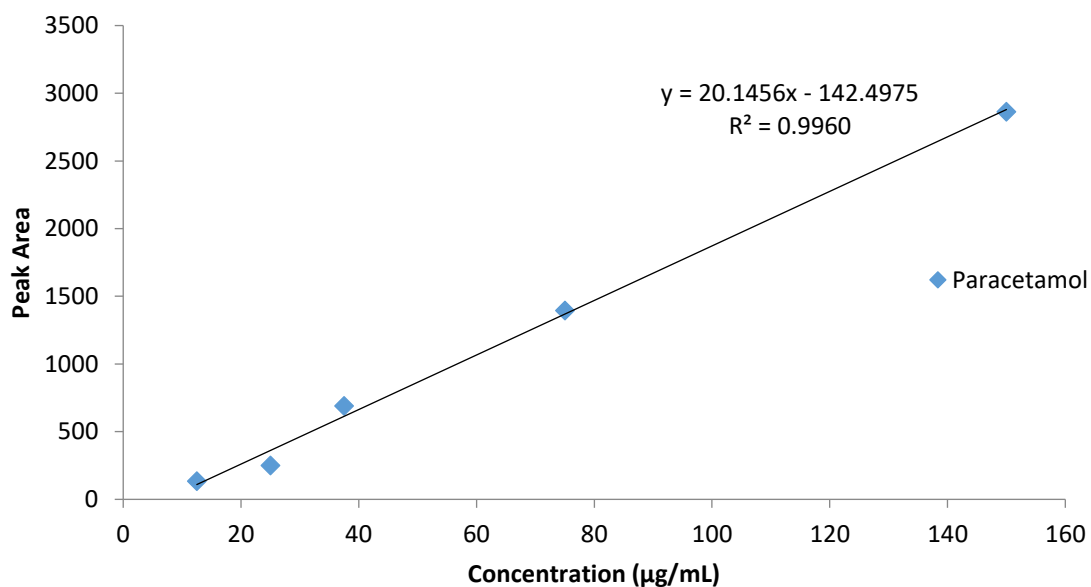


Figure A-1: HPLC calibration curve of paracetamol

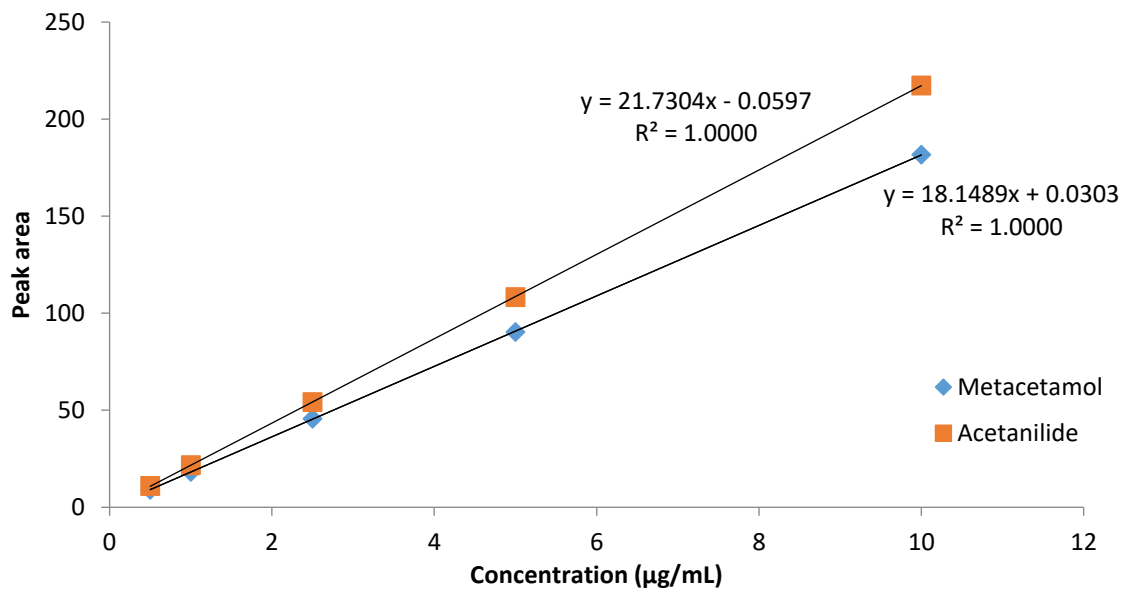


Figure A-2: HPLC calibration curve of metacetamol and acetanilide

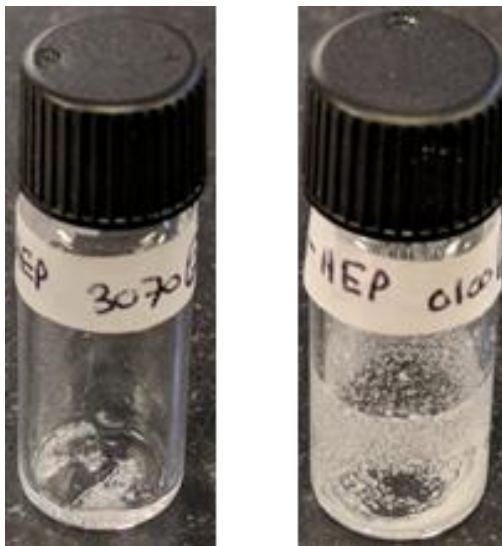


Figure A-3: Glass vial showing presence of liquid solution still present at the bottom of the vial with the solid precipitate (incomplete separation of solid and liquid sample).

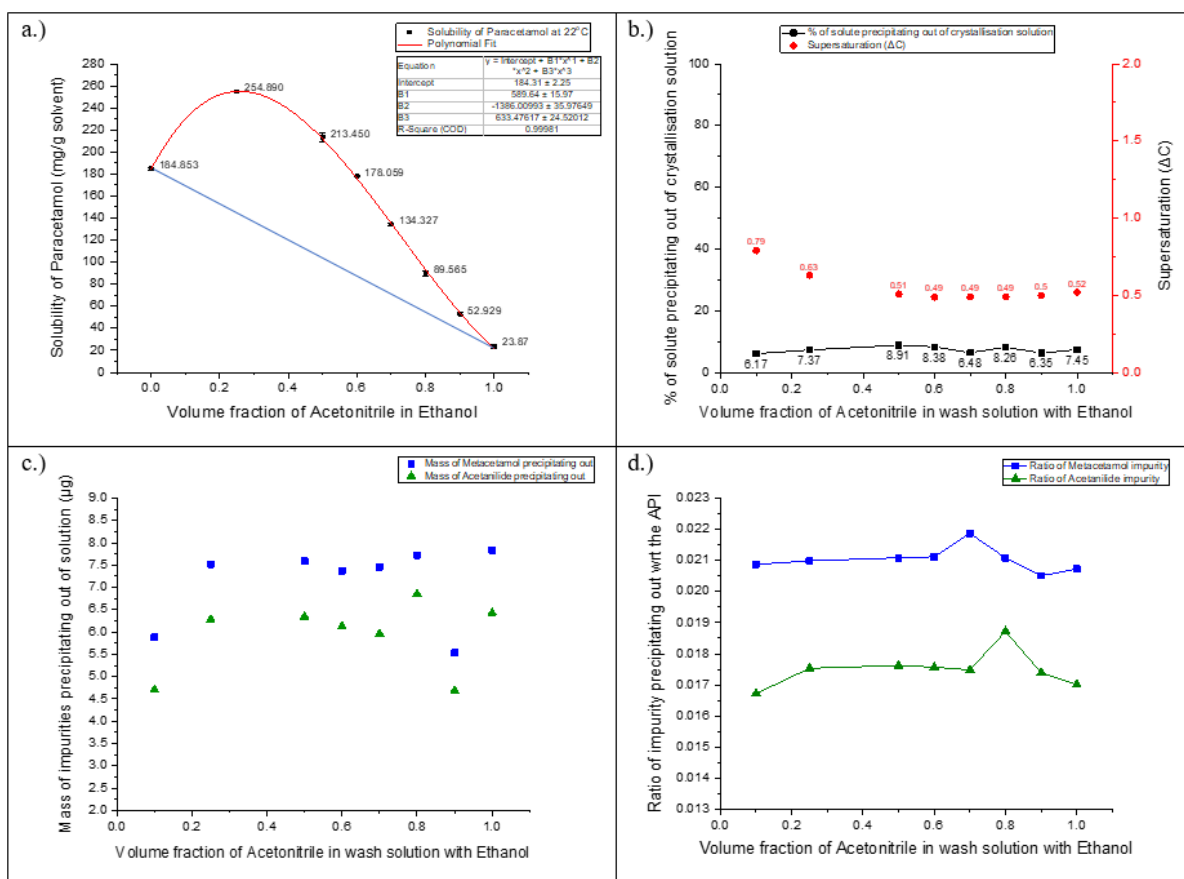


Figure A-4: Full quantitative analysis of ethanol-acetonitrile case. a.) Solubility of paracetamol in ethanol-acetonitrile binary solvent mixture at 22 oC. b.) Percentage of solute precipitating out of solution for different wash solution is shown in the graph together with the supersaturation achieved in the solution when different ratio of wash solution is added to the saturated crystallisation solvent. c.) Mass of impurities precipitating out when using different ratios of wash solution. d.) Ratio of impurities precipitating out with respect to the paracetamol (API) for each of the different ratios of wash solutions used.

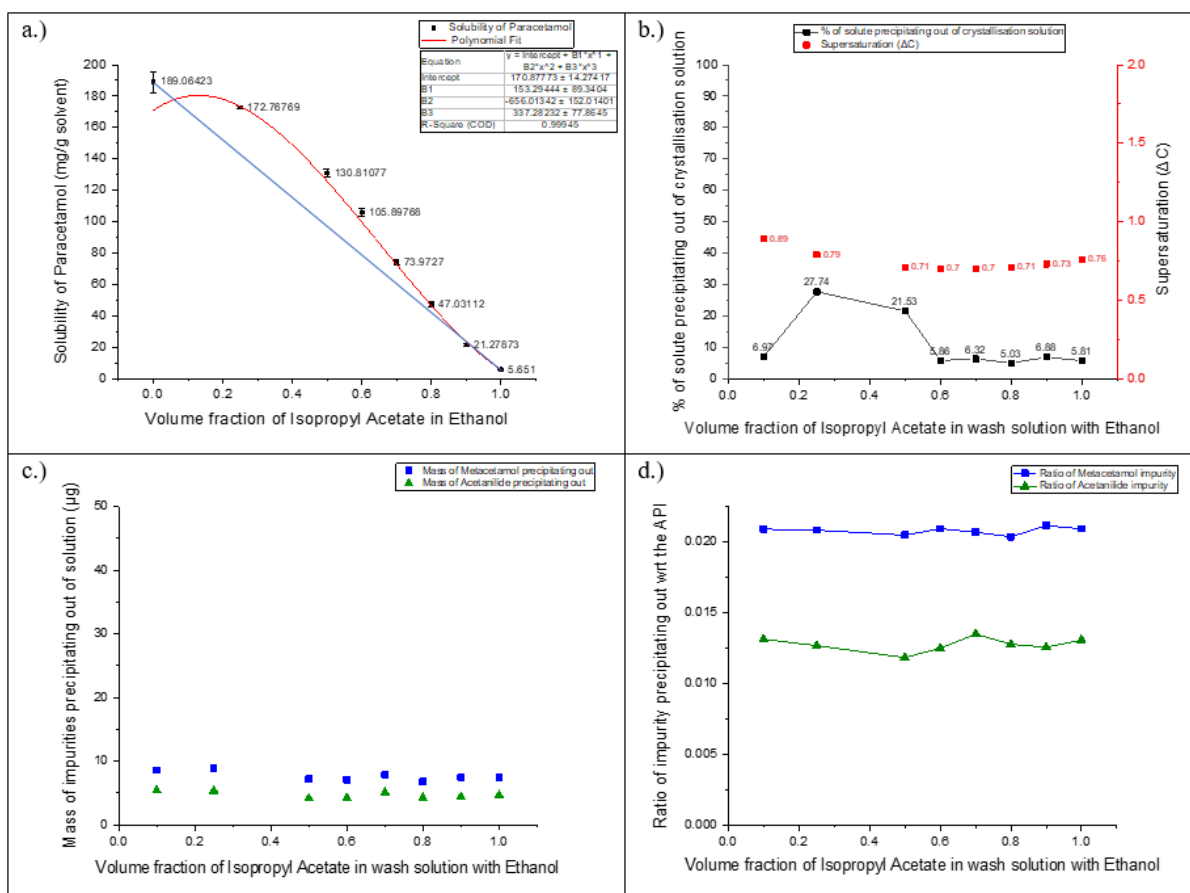


Figure A-5: Quantitative analysis of ethanol-isopropyl acetate case. a.) Solubility of paracetamol in ethanol-isopropyl acetate binary solvent mixture at 22 °C. b.) Percentage of solute precipitating out of solution for different wash solution is shown in the graph together with the supersaturation achieved in the solution when different ratio of wash solution is added to the saturated crystallisation solvent. c.) Mass of impurities precipitating out when using different ratios of wash solution. d.) Ratio of impurities precipitating out with respect to the paracetamol (API) for each of the different ratios of wash solutions used.

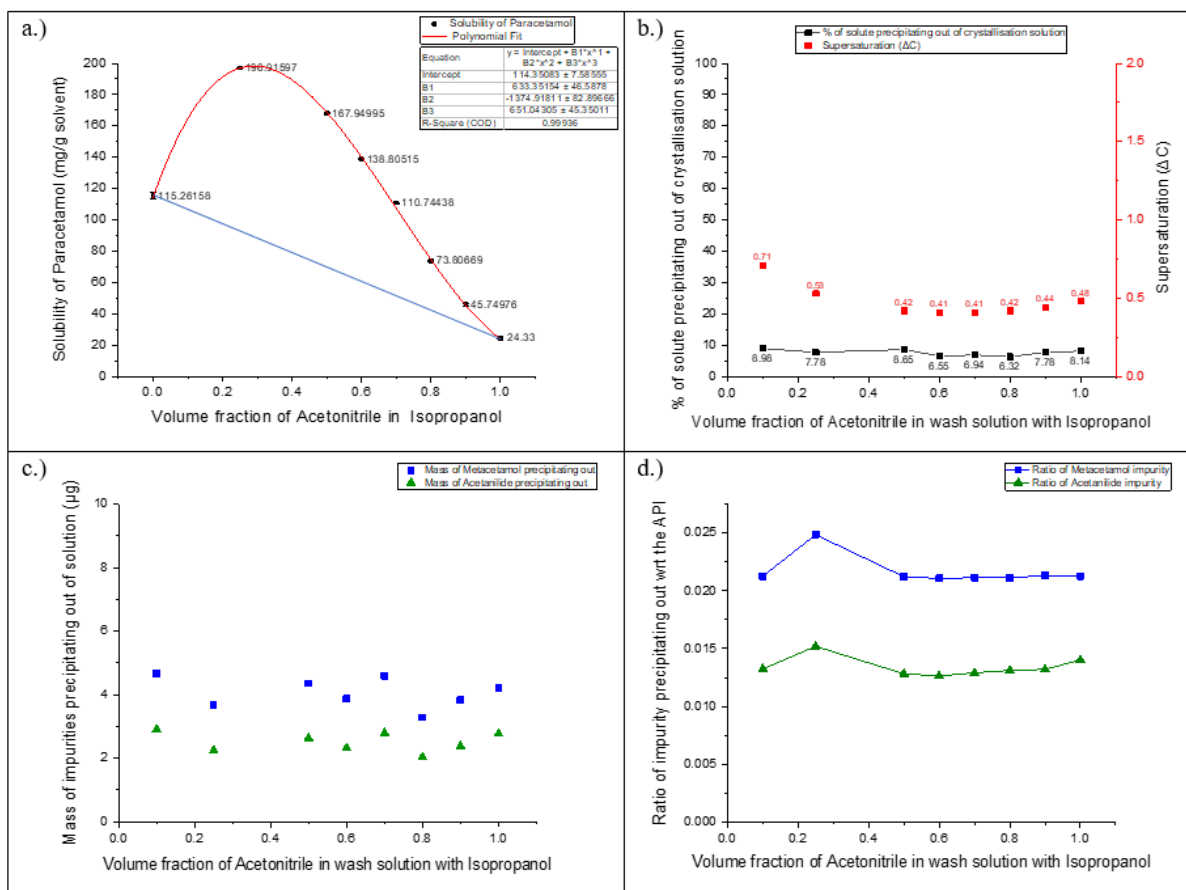


Figure A-6: Quantitative analysis of isopropanol-acetonitrile case. a.) Solubility of paracetamol in isopropanol-acetonitrile binary solvent mixture at 22 oC. b.) Percentage of solute precipitating out of solution for different wash solution is shown in the graph together with the supersaturation achieved in the solution when different ratio of wash solution is added to the saturated crystallisation solvent. c.) Mass of impurities precipitating out when using different ratios of wash solution. d.) Ratio of impurities precipitating out with respect to the paracetamol (API) for each of the different ratios of wash solutions used.

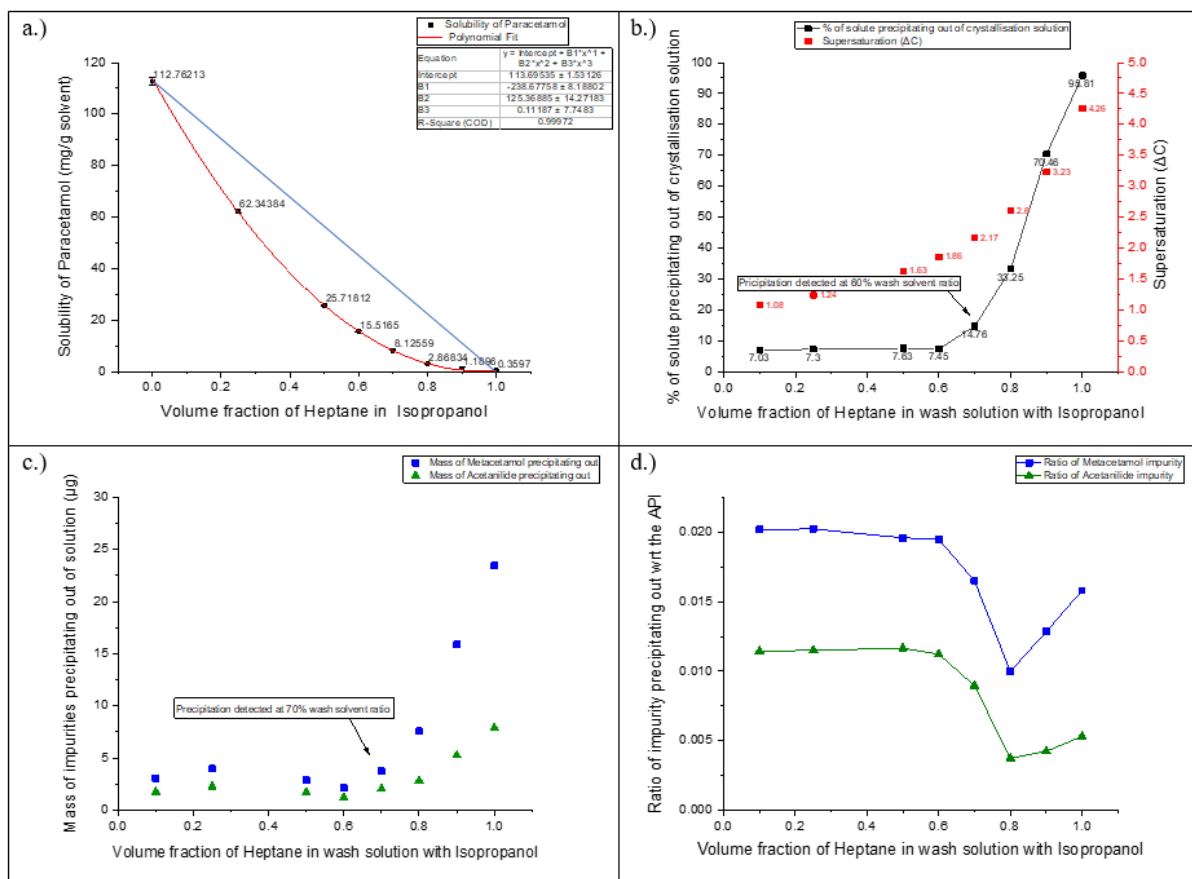


Figure A-7: Quantitative analysis of isopropanol-heptane case. a.) Solubility of paracetamol in isopropanol-heptane binary solvent mixture at 22 oC. b.) Percentage of solute precipitating out of solution for different wash solution is shown in the graph together with the supersaturation achieved in the solution when different ratio of wash solution is added to the saturated crystallisation solvent. c.) Mass of impurities precipitating out when using different ratios of wash solution. d.) Ratio of impurities precipitating out with respect to the paracetamol (API) for each of the different ratios of wash solutions used.

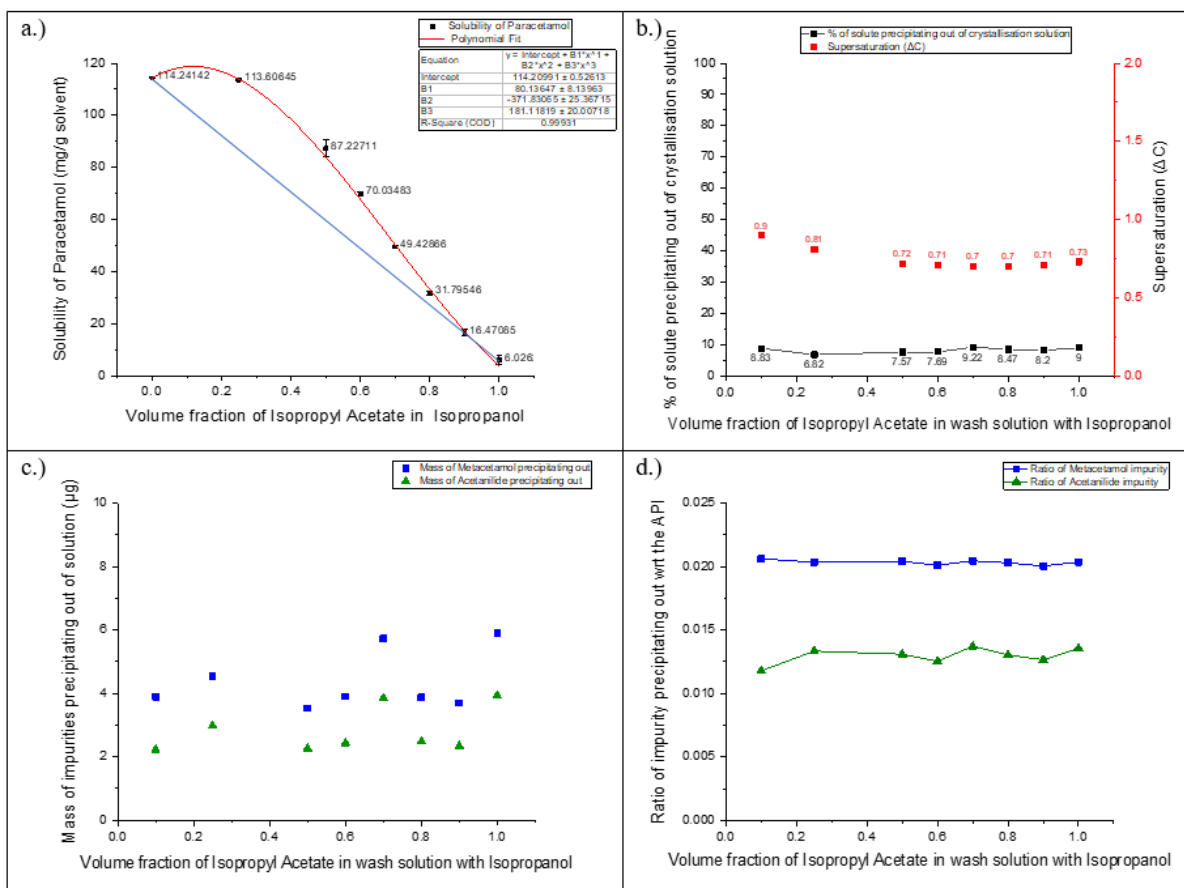


Figure A-8: Quantitative analysis of isopropanol-isopropyl acetate case. a.) Solubility of paracetamol in isopropanol-isopropyl acetate binary solvent mixture at 22 oC. b.) Percentage of solute precipitating out of solution for different wash solution is shown in the graph together with the supersaturation achieved in the solution when different ratio of wash solution is added to the saturated crystallisation solvent. c.) Mass of impurities precipitating out when using different ratios of wash solution. d.) Ratio of impurities precipitating out with respect to the paracetamol (API) for each of the different ratios of wash solutions used.

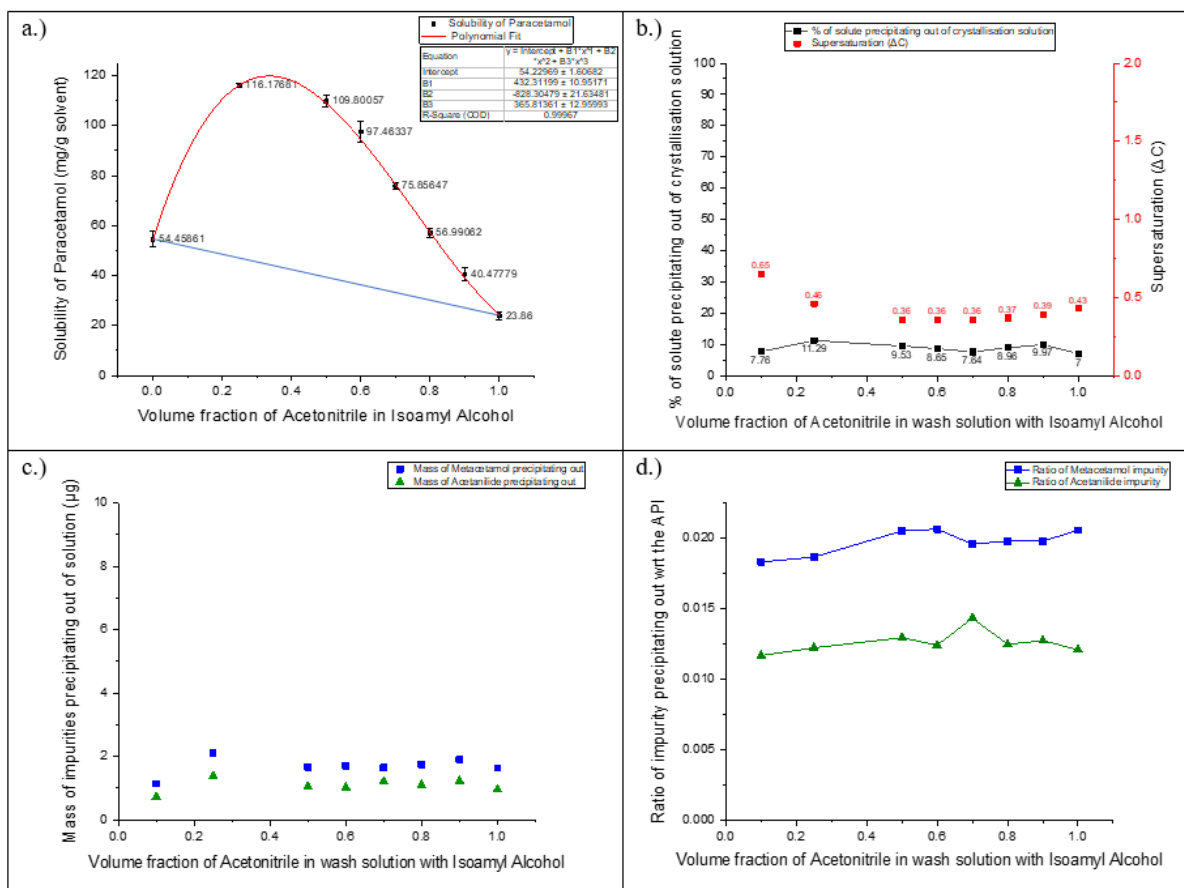


Figure A-9: Quantitative analysis of isoamyl alcohol-acetonitrile case. a.) Solubility of paracetamol in isoamyl alcohol-acetonitrile binary solvent mixture at 22 oC. b.) Percentage of solute precipitating out of solution for different wash solution is shown in the graph together with the supersaturation achieved in the solution when different ratio of wash solution is added to the saturated crystallisation solvent. c.) Mass of impurities precipitating out when using different ratios of wash solution. d.) Ratio of impurities precipitating out with respect to the paracetamol (API) for each of the different ratios of wash solutions used.

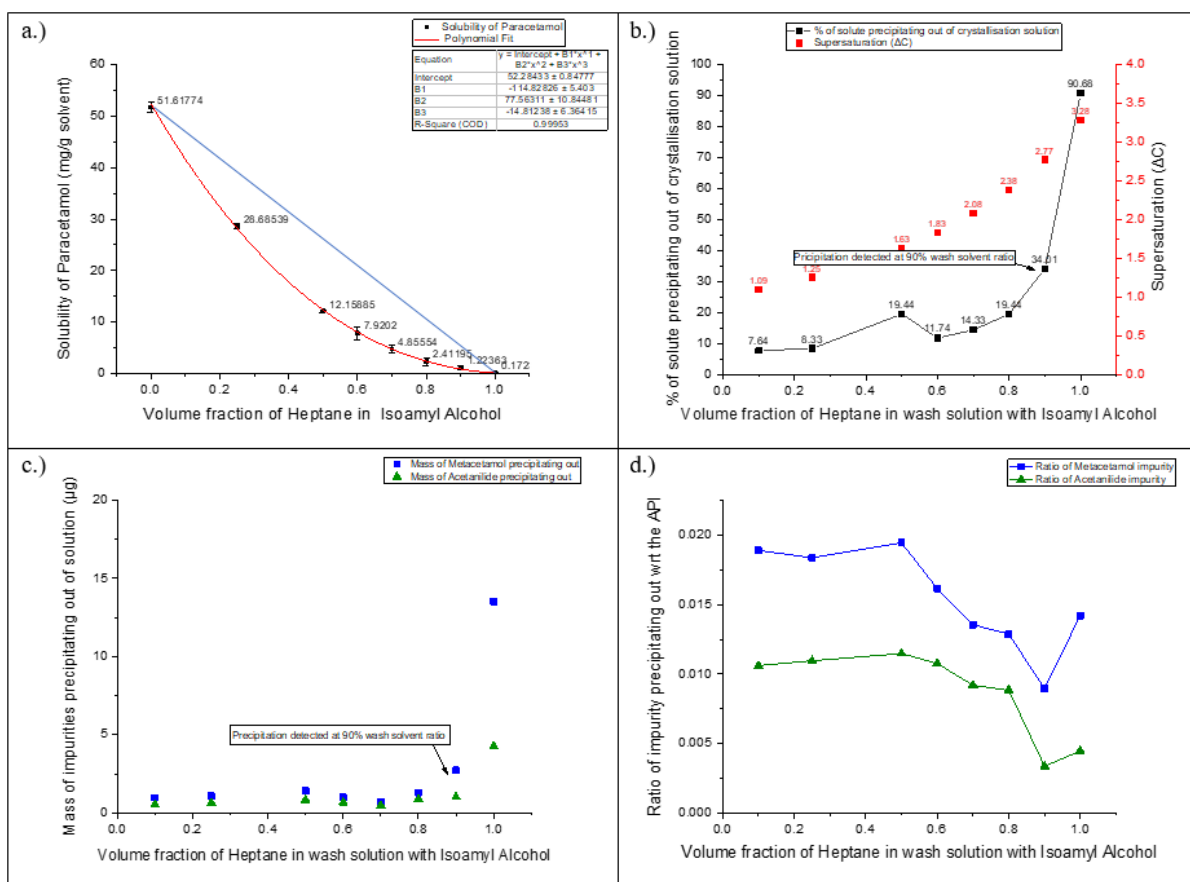


Figure A-10: Quantitative analysis of isoamyl alcohol-heptane case. a.) Solubility of paracetamol in isoamyl alcohol-heptane binary solvent mixture at 22 oC. b.) Percentage of solute precipitating out of solution for different wash solution is shown in the graph together with the supersaturation achieved in the solution when different ratio of wash solution is added to the saturated crystallisation solvent. c.) Mass of impurities precipitating out when using different ratios of wash solution. d.) Ratio of impurities precipitating out with respect to the paracetamol (API) for each of the different ratios of wash solutions used.

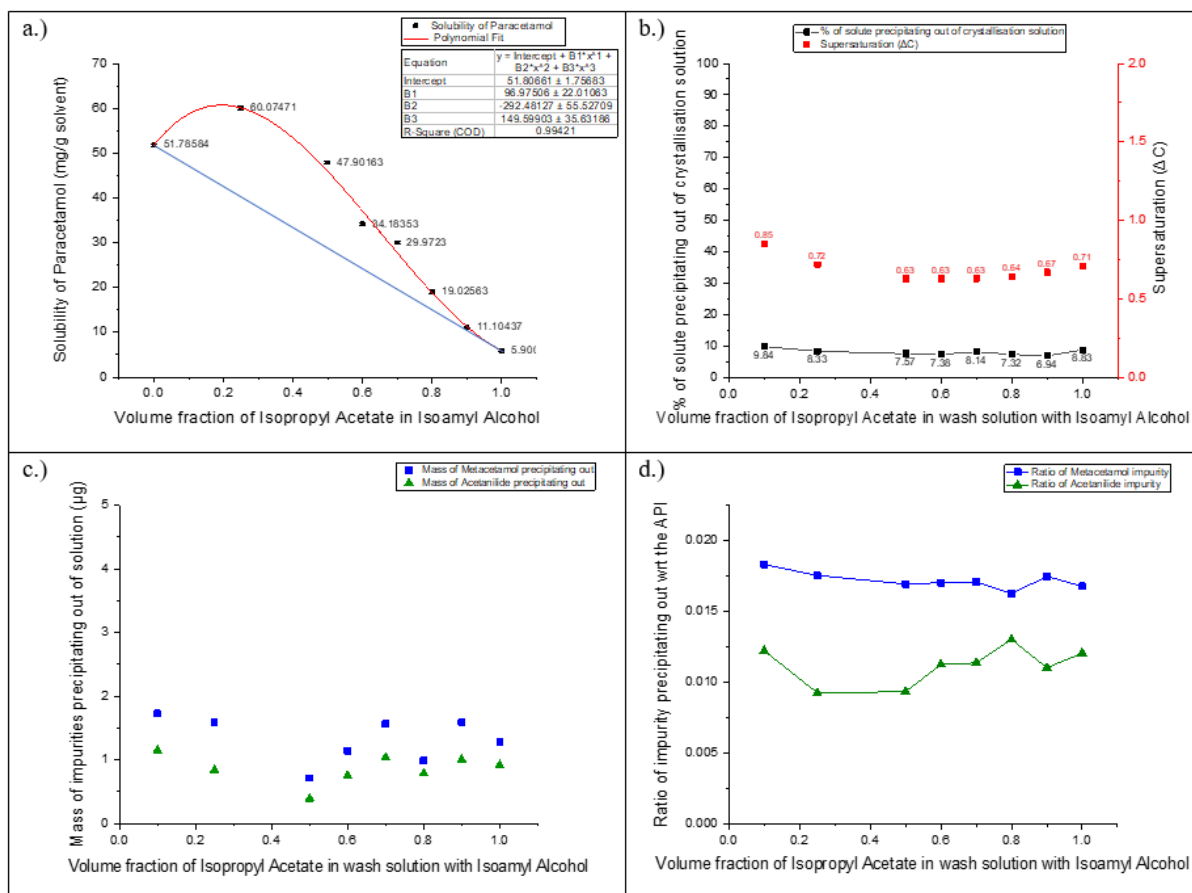


Figure A-11: Quantitative analysis of isoamyl alcohol-isopropyl acetate case. a.) Solubility of paracetamol in isoamyl alcohol-isopropyl acetate binary solvent mixture at 22 oC. b.) Percentage of solute precipitating out of solution for different wash solution is shown in the graph together with the supersaturation achieved in the solution when different ratio of wash solution is added to the saturated crystallisation solvent. c.) Mass of impurities precipitating out when using different ratios of wash solution. d.) Ratio of impurities precipitating out with respect to the paracetamol (API) for each of the different ratios of wash solutions used.

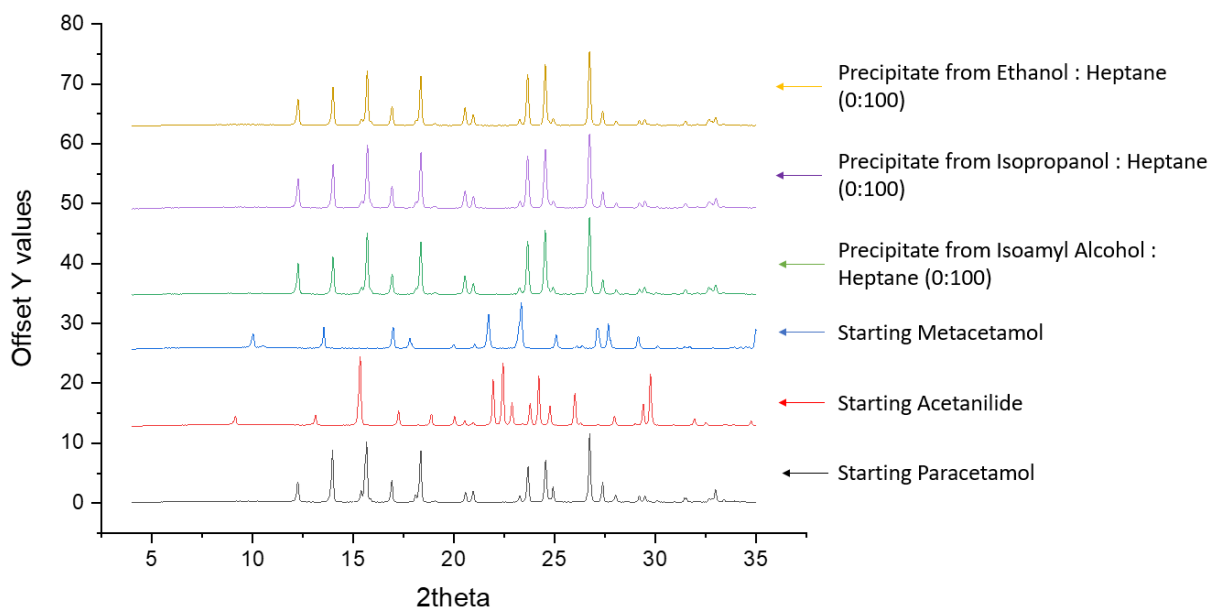


Figure A-12: XRPD results for raw API (paracetamol) and its impurities (metacetamol and acetanilide) together with the precipitate obtained from some sample wash solution results.

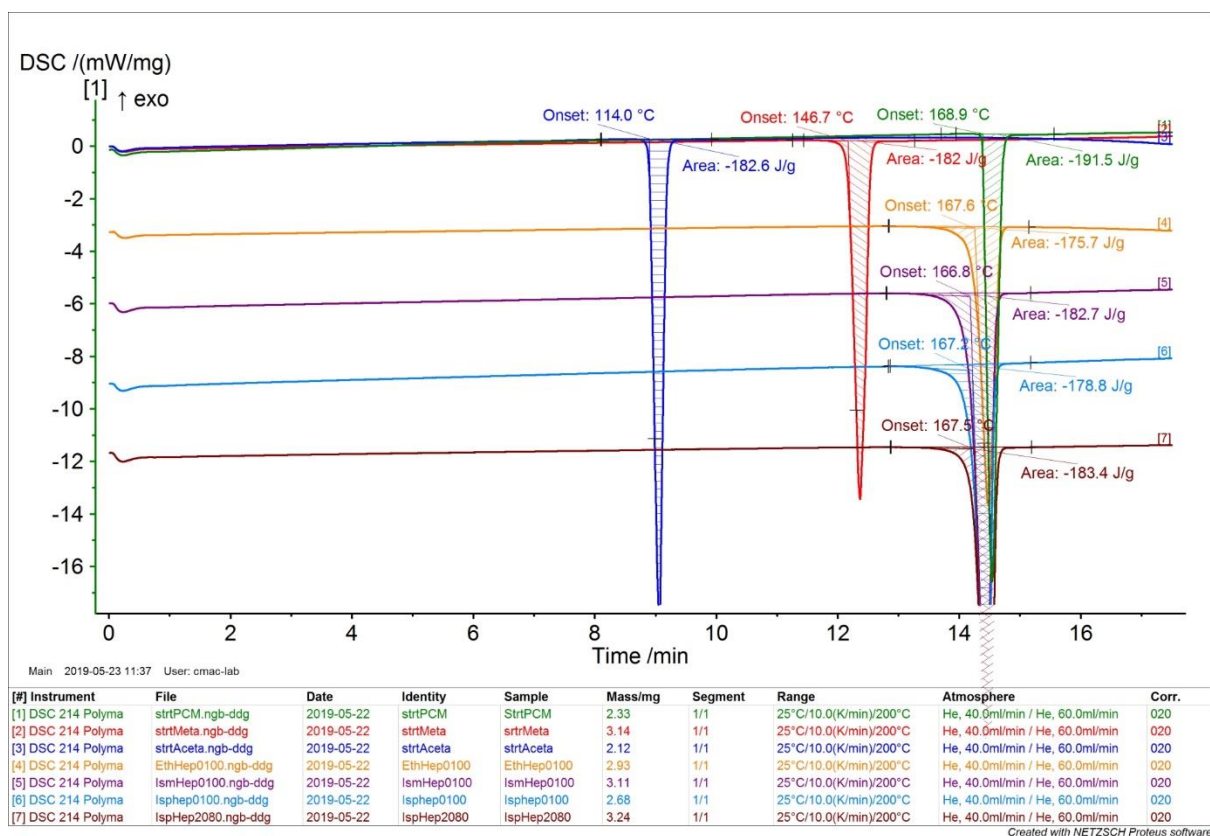


Figure A-13: DSC result obtained for raw API (paracetamol) and its impurities (metacetamol and acetanilide) together with the precipitate obtained from some sample wash solution results at 10 oC/min heating rate.

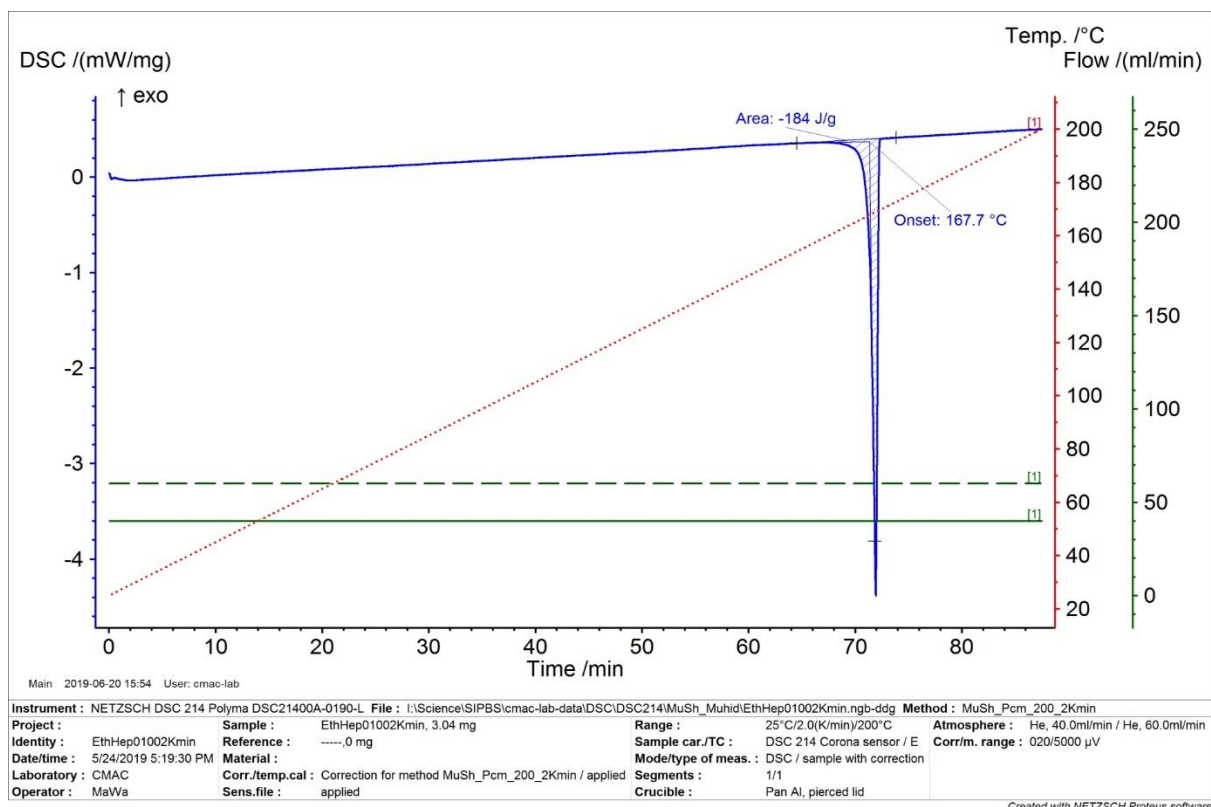


Figure A-14: DSC result obtained for precipitate obtained from ethanol-heptane system at 2 °C/min heating rate.

Appendix B - Employing constant rate filtration to assess active pharmaceutical ingredient (API) washing efficiency

Table B-1: Main properties of the solvents used in this work.²⁸⁻³²

| Solvent | Boiling point (°C) | Enthalpy of vaporization (kJ/mol) | Viscosity (cP) (Temperature °C) | Density (g/mL) (Temperature °C) | Surface tension (mN/m) (Temperature °C) |
|-----------------|--------------------|-----------------------------------|---------------------------------|---------------------------------|---|
| Ethanol | 78.4 | 38.58 | 1.26 (20) | 0.79 (20) | 21.99 (20) |
| Isopropanol | 82.2 | 39.85 | 2.1 (25) | 0.78 (25) | 21.4 (20) |
| Isoamyl alcohol | 132 | 55.2 | 3.74 (25) | 0.81 (15) | 24.77 (15) |
| Acetonitrile | 81.6 | 33.23 | 0.35 (20) | 0.78 (20) | 29.04 (20)_ |
| n-Heptane | 98.4 | 31.77 | 0.397 (25) | 0.68 (20) | 19.7 (20) |
| n-Dodecane | 216.3 | 61.52 | 1.5 (25) | 0.75 (20) | 25.35 (20) |

| Factors | | | | | | | |
|---------|---------------------------|--------------------------|-------|--------------|---|-----------|-----------|
| | Name | Abbr. | Units | Type | Settings | Transform | Precision |
| 1 | Paracetamol Grade | Par | | Qualitative | Micronised, Crystalline, Special Granular | | |
| 2 | Crystallisation solvent | Cry | | Qualitative | Ethanol, Isopropanol, Isoamyl alcohol | | |
| 3 | Wash Solvent | Was | | Qualitative | Heptane, Acetonitrile, Dodecane, Mix Hpt solution, Mix Dod solution | | |
| 4 | Filtration & Washing Rate | Fil | rpm | Quantitative | 10 to 100 | None | 2.25 |
| 5 | Volume of Wash Solvent | Vol | | Qualitative | One, Two, Three | | |
| 6 | Number of washes | Num | | Quantitative | 1 to 3 | None | 0.05 |
| | | Double-click here to add | | a new factor | | | |

Figure B-1: Factors of DoE

| Responses | | | | | | | | |
|-----------|------------------------|--------------------------|-------|-------------------|---------|-----|--------|-----|
| | Name | Abbr. | Units | Transform | Type | Min | Target | Max |
| 1 | Impurity Removal | IR | | Log: 10Log(Y) | Regular | | 1 | |
| 2 | Motherliquor Remaining | MLR | | Log: 10Log(Y) | Regular | | | |
| 3 | API Lost to Washing | APIL | g | Log: 10Log(Y+0.1) | Regular | | | |
| 4 | D10 Ratio | D10 | | Log: 10Log(Y) | Regular | | | |
| 5 | D50 Ratio | D50 | | None | Regular | | | |
| 6 | D90 Ratio | D90 | | Log: 10Log(Y) | Regular | | | |
| | | Double-click here to add | | a new response | | | | |

Figure B-2: Responses of DoE

| Worksheet | | | | | | | | | |
|-----------|----------|-----------|-----------|-------------------|-------------------------|------------------|---------------------------|------------------------|------------------|
| 1 | 2 | 3 | 4 | 5 | 6 | 7 | 8 | 9 | 10 |
| Exp No | Exp Name | Run Order | Incl/Excl | Paracetamol Grade | Crystallisation solvent | Wash Solvent | Filtration & Washing Rate | Volume of Wash Solvent | Number of washes |
| 1 | N1 | 17 | Incl | Crystalline | Ethanol | Heptane | | 1.0 One | 3 |
| 2 | N2 | 22 | Incl | Micronised | Isopropanol | Acetonitrile | | 1.0 One | 1 |
| 3 | N3 | 5 | Incl | Special Granular | Ethanol | Dodecane | | 1.0 One | 3 |
| 4 | N4 | 4 | Incl | Crystalline | Isopropanol | Dodecane | | 1.0 One | 1 |
| 5 | N5 | 14 | Incl | Special Granular | Isomyyl alcohol | Mix Hpt solution | | 1.0 One | 3 |
| 6 | N6 | 10 | Incl | Micronised | Isomyyl alcohol | Mix Dod solution | | 1.0 One | 2 |
| 7 | N7 | 13 | Incl | Micronised | Isomyyl alcohol | Heptane | | 1.0 Two | 3 |
| 8 | N8 | 15 | Incl | Special Granular | Isomyyl alcohol | Heptane | | 1.0 Two | 1 |
| 9 | N9 | 1 | Incl | Crystalline | Isopropanol | Acetonitrile | | 1.0 Two | 1 |
| 10 | N10 | 20 | Incl | Micronised | Ethanol | Dodecane | | 1.0 Two | 3 |
| 11 | N11 | 9 | Incl | Crystalline | Ethanol | Mix Hpt solution | | 1.0 Two | 2 |
| 12 | N12 | 7 | Incl | Special Granular | Isopropanol | Mix Dod solution | | 1.0 Two | 3 |
| 13 | N13 | 21 | Incl | Special Granular | Isopropanol | Heptane | | 1.0 Three | 1 |
| 14 | N14 | 3 | Incl | Special Granular | Ethanol | Acetonitrile | | 1.0 Three | 1 |
| 15 | N15 | 18 | Incl | Crystalline | Isomyyl alcohol | Acetonitrile | | 1.0 Three | 3 |
| 16 | N16 | 16 | Incl | Crystalline | Isomyyl alcohol | Dodecane | | 1.0 Three | 1 |
| 17 | N17 | 2 | Incl | Micronised | Isopropanol | Mix Hpt solution | | 1.0 Three | 3 |
| 18 | N18 | 8 | Incl | Micronised | Ethanol | Mix Dod solution | | 1.0 Three | 2 |
| 19 | N19 | 12 | Incl | Crystalline | Isopropanol | Mix Dod solution | | 1.0 Three | 3 |
| 20 | N20 | 6 | Incl | Special Granular | Isomyyl alcohol | Mix Dod solution | | 55 Three | 2 |
| 21 | N21 | 11 | Incl | Special Granular | Isomyyl alcohol | Mix Dod solution | | 55 Three | 2 |
| 22 | N22 | 19 | Incl | Special Granular | Isomyyl alcohol | Mix Dod solution | | 55 Three | 2 |

Figure B-3: DoE experimental worksheet with factors

| | 11 | 12 | 13 | 14 | 15 | 16 |
|--|------------------|------------------------|---------------------|-----------|-----------|-----------|
| | Impurity Removal | Motherliquor Remaining | API Lost to Washing | D10 Ratio | D50 Ratio | D90 Ratio |
| | 6 | 0.0317 | 0 | 2.11 | 1.758 | 0.743 |
| | 5 | 0.5148 | 0.66 | 7.71 | 4.456 | 1.102 |
| | 4 | 0.0147 | 0 | 1.31 | 1.207 | 1.168 |
| | 5 | 0.0135 | 0.07 | 2.22 | 1.74 | 1.984 |
| | 3 | 0.5488 | 0.17 | 1.18 | 1.1 | 1.027 |
| | 3 | 0.01 | 0.39 | 6.22 | 3.25 | 1.507 |
| | 3 | 0.5448 | 0 | 1.65 | 1.787 | 1.47 |
| | 4 | 0.2843 | 0 | 1.27 | 1.209 | 1.171 |
| | 7 | 0.1528 | 0.37 | 4.83 | 3.617 | 2.906 |
| | 3 | 0.0042 | 0 | 2.33 | 1.59 | 3.221 |
| | 5 | 0.0281 | 0.31 | 1.73 | 1.354 | 1.228 |
| | 4 | 0.0088 | 0.17 | 1.27 | 1.29 | 1.331 |
| | 3 | 0.0691 | 0 | 0.68 | 1.123 | 1.088 |
| | 7 | 0.021 | 0 | 2.12 | 3.348 | 4.361 |
| | 4 | 0.1135 | 1.48 | 9.72 | 29.436 | 24.205 |
| | 4 | 0.0019 | 0.08 | 5.85 | 3.055 | 2.204 |
| | 5 | 0.3657 | 0.95 | 4.61 | 2.888 | 1.983 |
| | 4 | 0.0603 | 0 | 5.939 | 2.647 | 0.647 |
| | 4 | 0.0207 | 0.29 | 2.15 | 1.745 | 1.524 |
| | 2 | 0.0049 | 0.1 | 1.29 | 1.38 | 1.539 |
| | 3 | 0.0072 | 0.05 | 1.29 | 1.223 | 1.187 |
| | 3 | 0.0214 | 0.07 | 1.05 | 1.038 | 1.03 |

Figure B-4: DoE experimental worksheet with responses






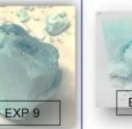




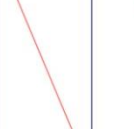
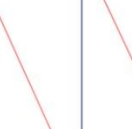

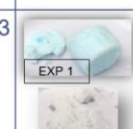







| | | Wash solvents | | | | | | | | |
|------------------|---|--|---|---|---|---|---|---|---|---|
| | | N-Heptane | | | Dodecane | | | Acetonitrile | | |
| Number of washes | 1 | |  |  |  | |  |  |  |  |
| | 2 | |  | |  | |     | | | |
| | 3 |   |  |  |  |   |  | | | |
| | | 1 | 2 | 3 | 1 | 2 | 3 | 1 | 2 | 3 |
| | | Void volume of wash solvent | | | | | | | | |

Figure B-5: Images of all the API washed cakes taken at the end of experiment and sorted in terms of wash solvent, number of washes and void volume of wash solvent

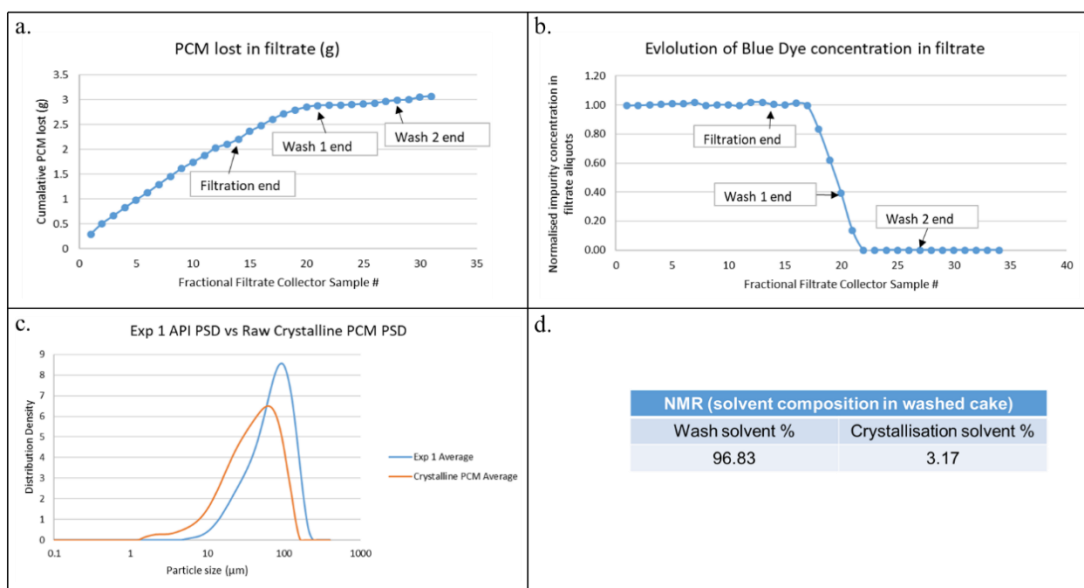


Figure B-6: Results obtained from experiment 1; crystallisation solvent: ethanol; wash solvent: *n*-heptane; API grade: crystalline; filtration rate (rpm): 10; volume of wash: 1 void volumes; number of washes: 3. a.) Graph showing cumulative API loss in filtrate samples throughout the experiment, mass of PCM API lost during wash = 1.48 g. b.) Normalised concentration of blue dye impurity in each filtrate sample obtained throughout the experiment. c.) Particle size distribution of the raw paracetamol API and the washed cake sample obtained at the end of the washing experiment, from the damp cake. d.) ¹H-NMR analysis results showing the residual crystallisation solvent content in the final washed cake.

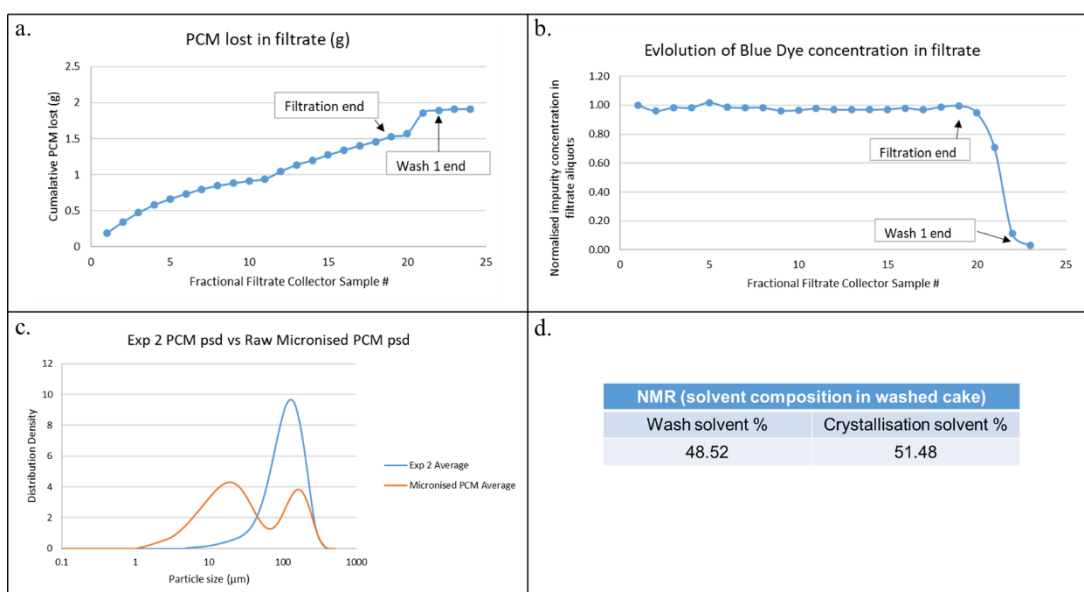


Figure B-7: Results obtained from experiment 2; crystallisation solvent: isopropanol; wash solvent: acetonitrile; API grade: micronised; filtration rate (rpm): 100; volume of wash: 1 void volumes; number of washes: 1. a.) Graph showing cumulative API loss in filtrate samples throughout the experiment, mass of PCM API lost during wash = 0.66 g. b.) Normalised concentration of blue dye impurity in each filtrate sample obtained throughout the experiment. c.) Particle size distribution of the raw paracetamol API and the washed cake sample obtained at the end of the washing experiment, from the damp cake. d.) ¹H-NMR analysis results showing the residual crystallisation solvent content in the final washed cake.

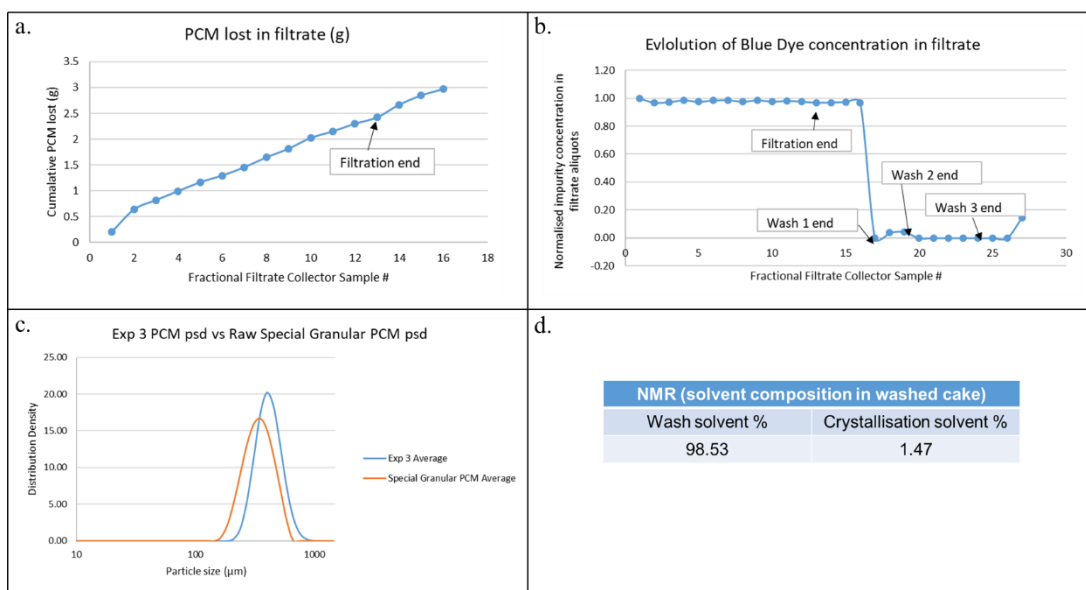


Figure B-8: Results obtained from experiment 3; crystallisation solvent: ethanol; wash solvent: n-dodecane; API grade: special granular; filtration rate (rpm): 100; volume of wash: 1 void volumes; number of washes: 3. a.) Graph showing cumulative API loss in filtrate samples throughout the experiment, mass of PCM API lost during wash = 0 g. b.) Normalised concentration of blue dye impurity in each filtrate sample obtained throughout the experiment. c.) Particle size distribution of the raw paracetamol API and the washed cake sample obtained at the end of the washing experiment, from the damp cake. d.) 1H-NMR analysis results showing the residual crystallisation solvent content in the final washed cake.

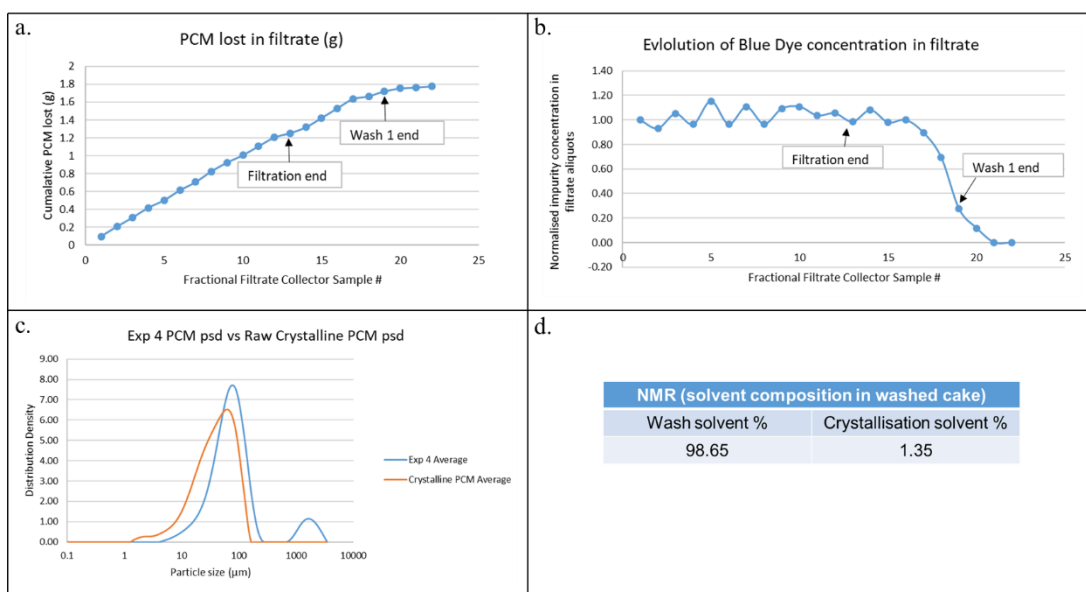


Figure B-9: Results obtained from experiment 4; crystallisation solvent: isopropanol; wash solvent: n-dodecane; API grade: crystalline; filtration rate (rpm): 10; volume of wash: 1 void volumes; number of washes: 1. a.) Graph showing cumulative API loss in filtrate samples throughout the experiment, mass of PCM API lost during wash = 0.07 g. b.) Normalised concentration of blue dye impurity in each filtrate sample obtained throughout the experiment. c.) Particle size distribution of the raw paracetamol API and the washed cake sample obtained at the end of the washing experiment, from the damp cake. d.) 1H-NMR analysis results showing the residual crystallisation solvent content in the final washed cake.

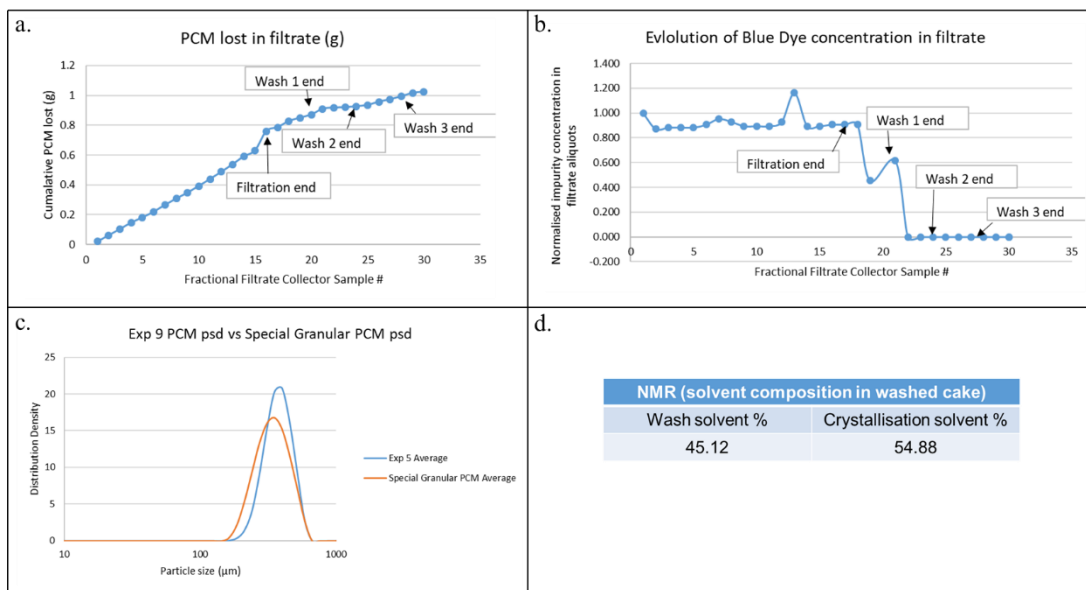


Figure B-10: Results obtained from experiment 5; crystallisation solvent: isoamyl alcohol; wash solvent: mix n-heptane solution; API grade: special granular; filtration rate (rpm): 10; volume of wash: 1 void volumes; number of washes: 3. a.) Graph showing cumulative API loss in filtrate samples throughout the experiment, mass of PCM API lost during wash = 0.17 g. b.) Normalised concentration of blue dye impurity in each filtrate sample obtained throughout the experiment. c.) Particle size distribution of the raw paracetamol API and the washed cake sample obtained at the end of the washing experiment, from the damp cake. d.) ¹H-NMR analysis results showing the residual crystallisation solvent content in the final washed cake.

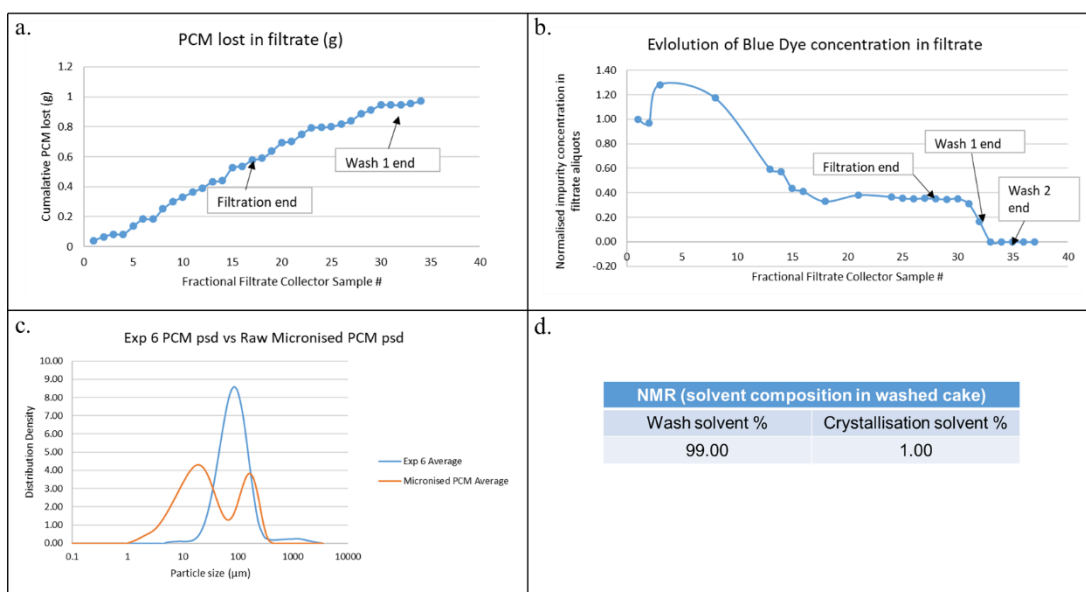


Figure B-11: Results obtained from experiment 6; crystallisation solvent: isoamyl alcohol; wash solvent: mix n-dodecane solution; API grade: micronised; filtration rate (rpm): 100; volume of wash: 1 void volumes; number of washes: 2. a.) Graph showing cumulative API loss in filtrate samples throughout the experiment mass of PCM API lost during wash = 0.39 g. b.) Normalised concentration of blue dye impurity in each filtrate sample obtained throughout the experiment. c.) Particle size distribution of the raw paracetamol API and the washed cake sample obtained at the end of the washing experiment, from the damp cake. d.) ¹H-NMR analysis results showing the residual crystallisation solvent content in the final washed cake.

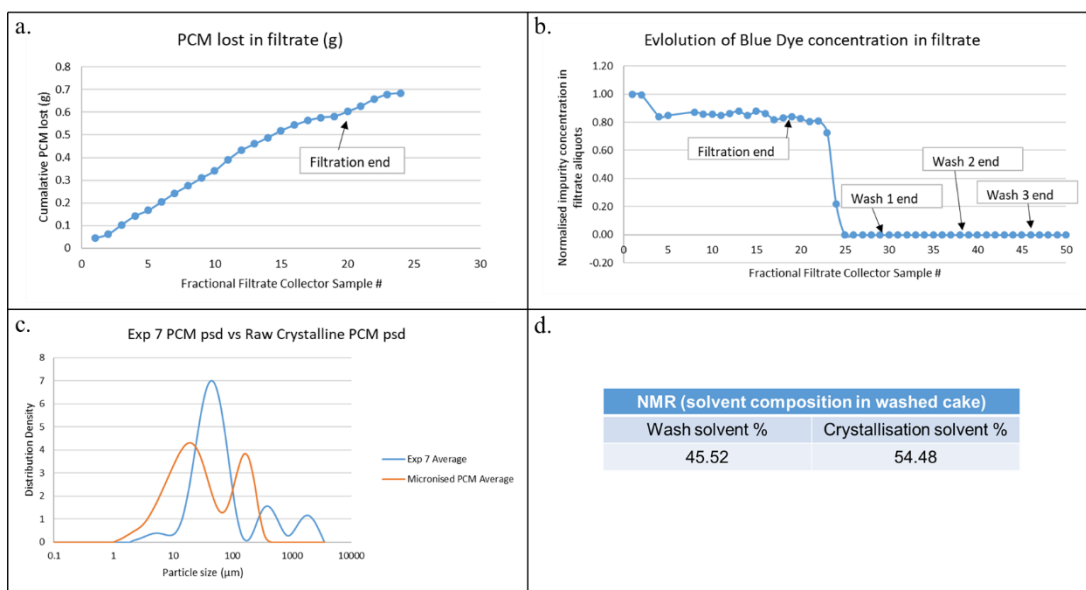


Figure B-12: Results obtained from experiment 7; crystallisation solvent: isoamyl alcohol; wash solvent: n-heptane; API grade: micronised; filtration rate (rpm): 10; volume of wash: 2 void volumes; number of washes: 3. a.) Graph showing cumulative API loss in filtrate samples throughout the experiment, mass of PCM API lost during wash = 0 g. b.) Normalised concentration of blue dye impurity in each filtrate sample obtained throughout the experiment. c.) Particle size distribution of the raw paracetamol API and the washed cake sample obtained at the end of the washing experiment, from the damp cake. d.) 1H-NMR analysis results showing the residual crystallisation solvent content in the final washed cake.

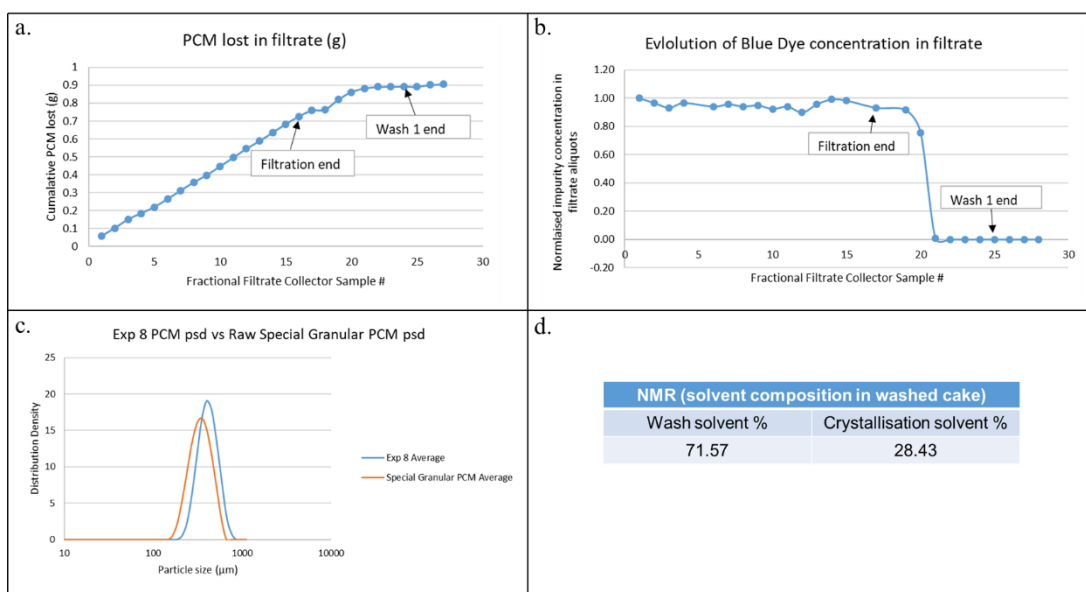


Figure B-13: Results obtained from experiment 8; crystallisation solvent: isoamyl alcohol; wash solvent: n-heptane; API grade: special granular; filtration rate (rpm): 100; volume of wash: 2 void volumes; number of washes: 1. a.) Graph showing cumulative API loss in filtrate samples throughout the experiment, mass of PCM API lost during wash = 0 g. b.) Normalised concentration of blue dye impurity in each filtrate sample obtained throughout the experiment. c.) Particle size distribution of the raw paracetamol API and the washed cake sample obtained at the end of the washing experiment, from the damp cake. d.) 1H-NMR analysis results showing the residual crystallisation solvent content in the final washed cake.

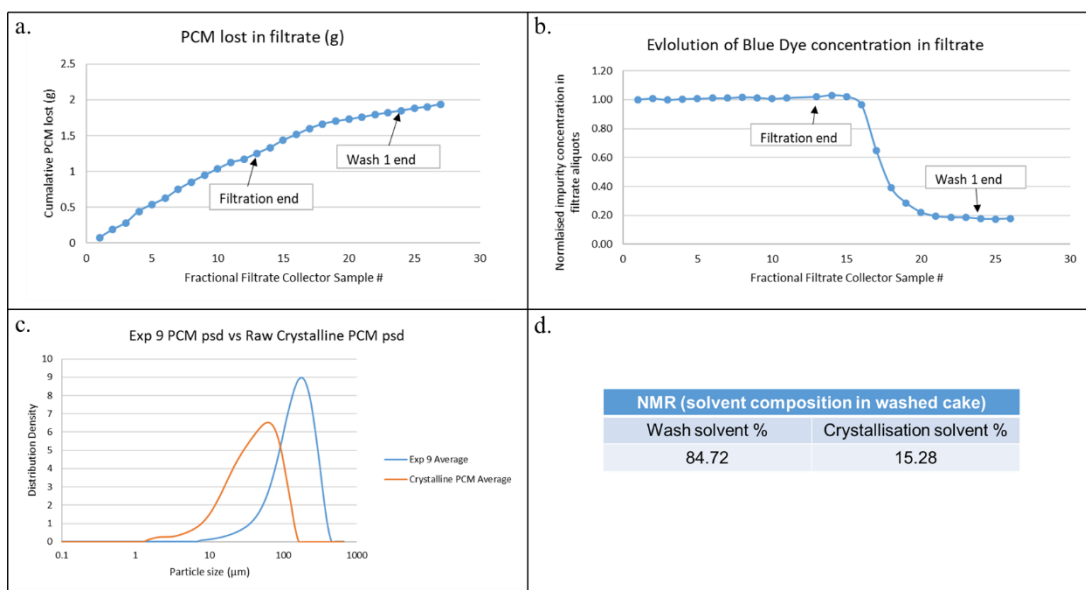


Figure B-14: Results obtained from experiment 9; crystallisation solvent: isopropanol; wash solvent: acetonitrile; API grade: crystalline; filtration rate (rpm): 10; volume of wash: 2 void volumes; number of washes: 1. a.) Graph showing cumulative API loss in filtrate samples throughout the experiment, mass of PCM API lost during wash = 0.37 g. b.) Normalised concentration of blue dye impurity in each filtrate sample obtained throughout the experiment. c.) Particle size distribution of the raw paracetamol API and the washed cake sample obtained at the end of the washing experiment, from the damp cake. d.) 1H-NMR analysis results showing the residual crystallisation solvent content in the final washed cake.

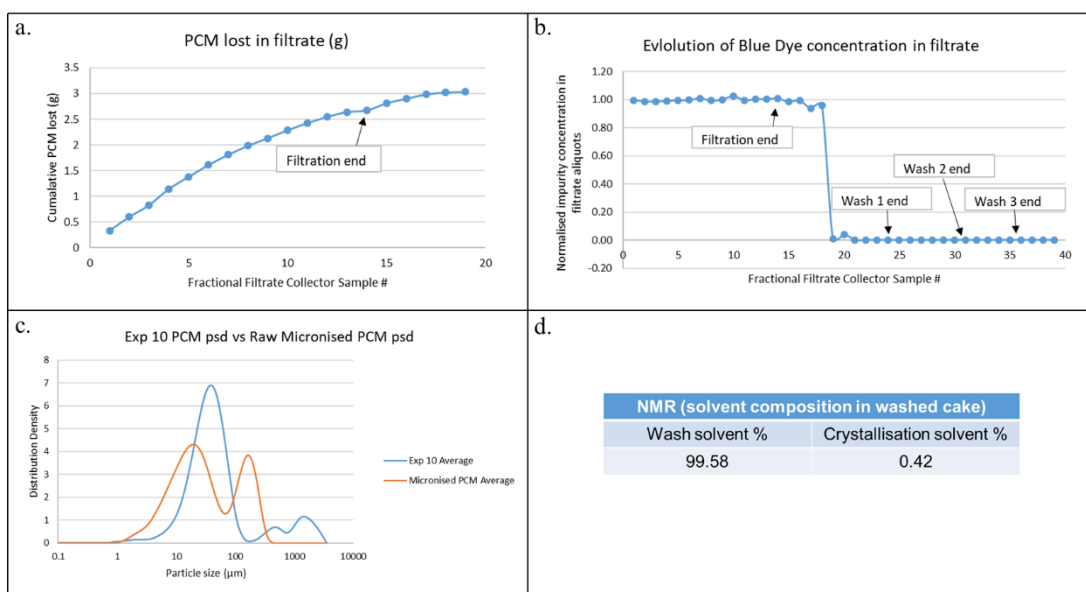


Figure B-15: Results obtained from experiment 10; crystallisation solvent: ethanol; wash solvent: n-dodecane; API grade: micronised; filtration rate (rpm): 100; volume of wash: 2 void volumes; number of washes: 3. a.) Graph showing cumulative API loss in filtrate samples throughout the experiment, mass of PCM API lost during wash = 0 g. b.) Normalised concentration of blue dye impurity in each filtrate sample obtained throughout the experiment. c.) Particle size distribution of the raw paracetamol API and the washed cake sample obtained at the end of the washing experiment, from the damp cake. d.) 1H-NMR analysis results showing the residual crystallisation solvent content in the final washed cake.

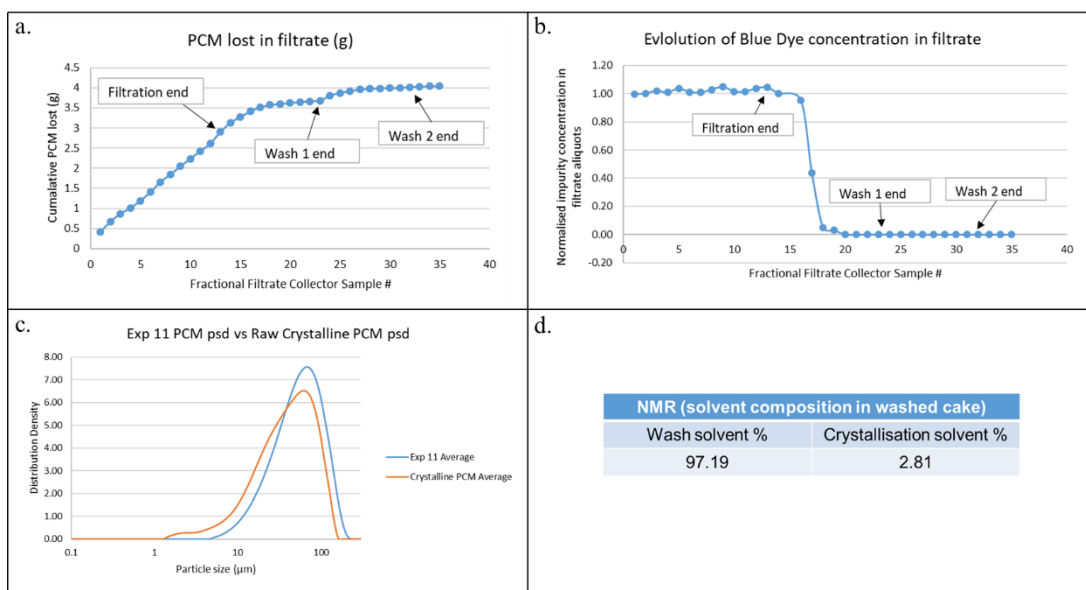


Figure B-16: Results obtained from experiment 11; crystallisation solvent: ethanol; wash solvent: mix *n*-heptane solution; API grade: crystalline; filtration rate (rpm): 100; volume of wash: 2 void volumes; number of washes: 2. a.) Graph showing cumulative API loss in filtrate samples throughout the experiment, mass of PCM API lost during wash = 0.31 g. b.) Normalised concentration of blue dye impurity in each filtrate sample obtained throughout the experiment. c.) Particle size distribution of the raw paracetamol API and the washed cake sample obtained at the end of the washing experiment, from the damp cake. d.) ¹H-NMR analysis results showing the residual crystallisation solvent content in the final washed cake.

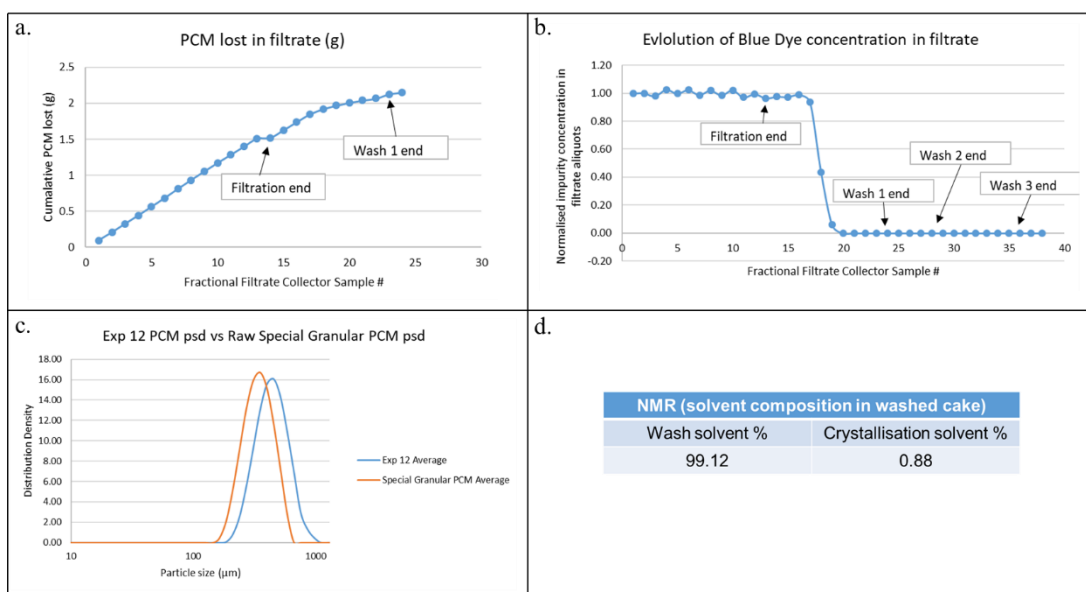


Figure B-17: Results obtained from experiment 12; crystallisation solvent: isopropanol; wash solvent: mix *n*-dodecane solution; API grade: special granular; filtration rate (rpm): 10; volume of wash: 2 void volumes; number of washes: 3. a.) Graph showing cumulative API loss in filtrate samples throughout the experiment, mass of PCM API lost during wash = 0.17 g. b.) Normalised concentration of blue dye impurity in each filtrate sample obtained throughout the experiment. c.) Particle size distribution of the raw paracetamol API and the washed cake sample obtained at the end of the washing experiment, from the damp cake. d.) ¹H-NMR analysis results showing the residual crystallisation solvent content in the final washed cake.

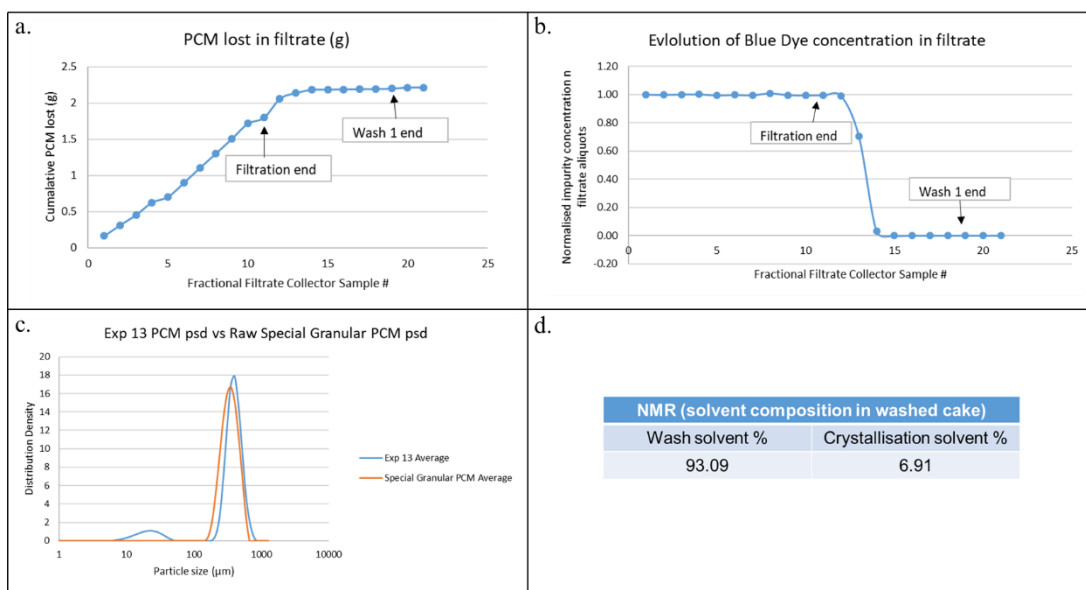


Figure B-18: Results obtained from experiment 13; crystallisation solvent: isopropanol; wash solvent: n-heptane; API grade: special granular; filtration rate (rpm): 10; volume of wash: 3 void volumes; number of washes: 1. a.) Graph showing cumulative API loss in filtrate samples throughout the experiment, mass of PCM API lost during wash = 0 g. b.) Normalised concentration of blue dye impurity in each filtrate sample obtained throughout the experiment. c.) Particle size distribution of the raw paracetamol API and the washed cake sample obtained at the end of the washing experiment, from the damp cake. d.) 1H-NMR analysis results showing the residual crystallisation solvent content in the final washed cake.

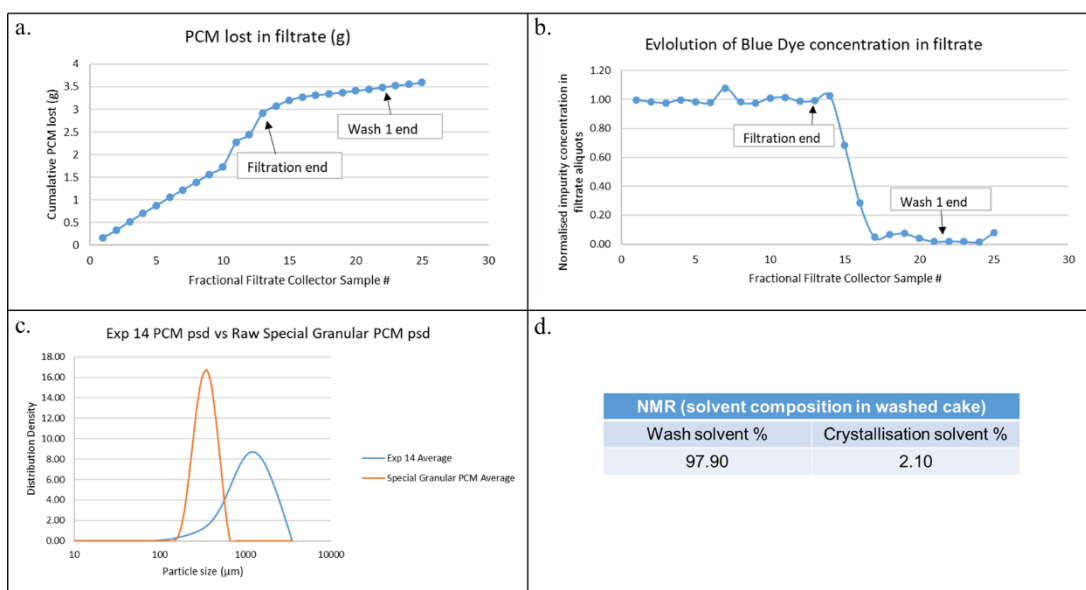


Figure B-19: Results obtained from experiment 14; crystallisation solvent: ethanol; wash solvent: acetonitrile; API grade: special granular; filtration rate (rpm): 10; volume of wash: 3 void volumes; number of washes: 1. a.) Graph showing cumulative API loss in filtrate samples throughout the experiment, mass of PCM API lost during wash = 0 g. b.) Normalised concentration of blue dye impurity in each filtrate sample obtained throughout the experiment. c.) Particle size distribution of the raw paracetamol API and the washed cake sample obtained at the end of the washing experiment, from the damp cake. d.) 1H-NMR analysis results showing the residual crystallisation solvent content in the final washed cake.

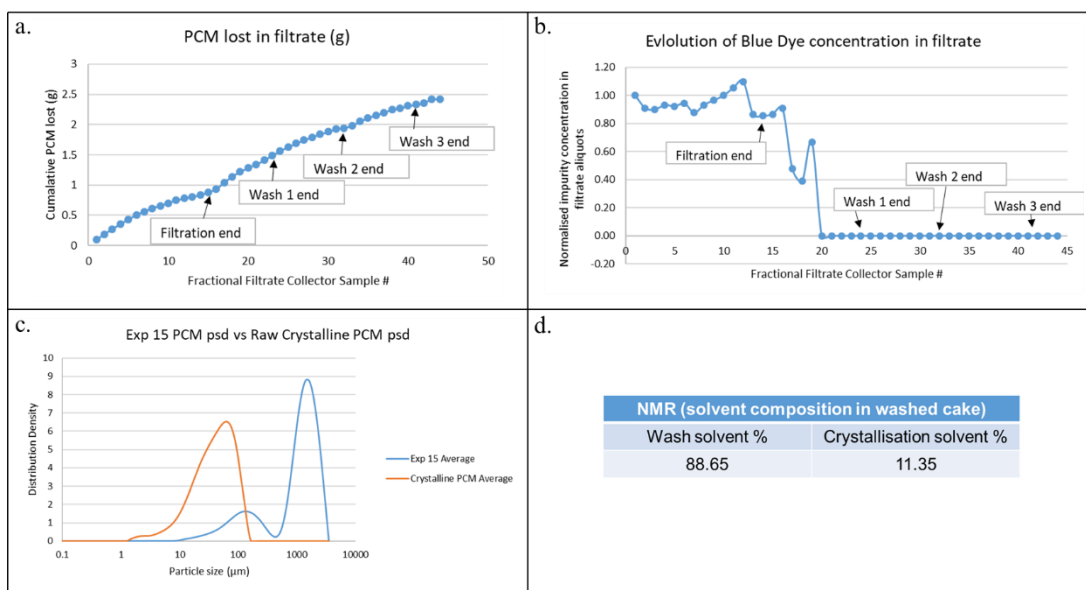


Figure B-20: Results obtained from experiment 15; crystallisation solvent: isoamyl alcohol; wash solvent: acetonitrile; API grade: crystalline; filtration rate (rpm): 100; volume of wash: 3 void volumes; number of washes: 3. a.) Graph showing cumulative API loss in filtrate samples throughout the experiment, mass of PCM API lost during wash = 1.48 g. b.) Normalised concentration of blue dye impurity in each filtrate sample obtained throughout the experiment. c.) Particle size distribution of the raw paracetamol API and the washed cake sample obtained at the end of the washing experiment, from the damp cake. d.) ¹H-NMR analysis results showing the residual crystallisation solvent content in the final washed cake.

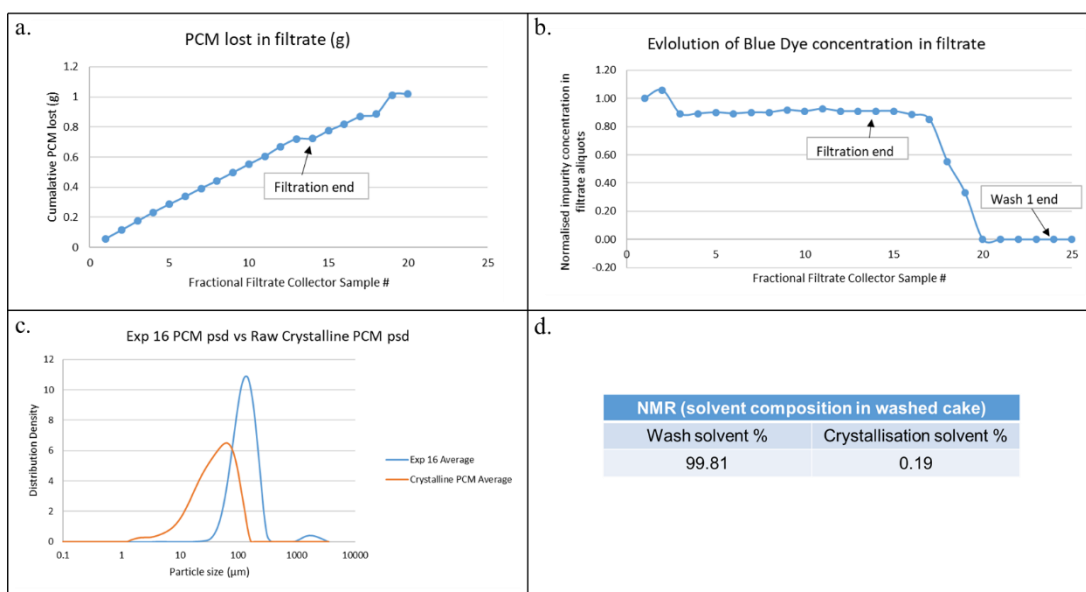


Figure B-21: Results obtained from experiment 16; crystallisation solvent: isoamyl alcohol; wash solvent: n-dodecane; API grade: crystalline; filtration rate (rpm): 10; volume of wash: 3 void volumes; number of washes: 1. a.) Graph showing cumulative API loss in filtrate samples throughout the experiment, mass of PCM API lost during wash = 0.08 g. b.) Normalised concentration of blue dye impurity in each filtrate sample obtained throughout the experiment. c.) Particle size distribution of the raw paracetamol API and the washed cake sample obtained at the end of the washing experiment, from the damp cake. d.) ¹H-NMR analysis results showing the residual crystallisation solvent content in the final washed cake.

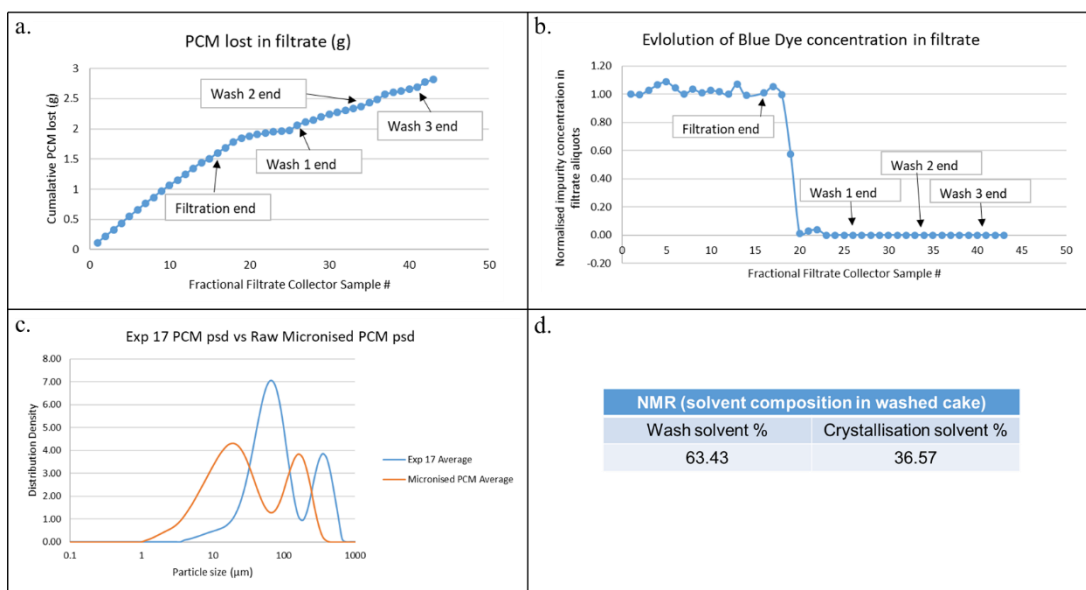


Figure B-22: Results obtained from experiment 17; crystallisation solvent: isopropanol; wash solvent: mix n-heptane solution; API grade: micronised; filtration rate (rpm): 10; volume of wash: 3 void volumes; number of washes: 3. a.) Graph showing cumulative API loss in filtrate samples throughout the experiment, mass of PCM API lost during wash = 0.95 g. b.) Normalised concentration of blue dye impurity in each filtrate sample obtained throughout the experiment. c.) Particle size distribution of the raw paracetamol API and the washed cake sample obtained at the end of the washing experiment, from the damp cake. d.) ¹H-NMR analysis results showing the residual crystallisation solvent content in the final washed cake.

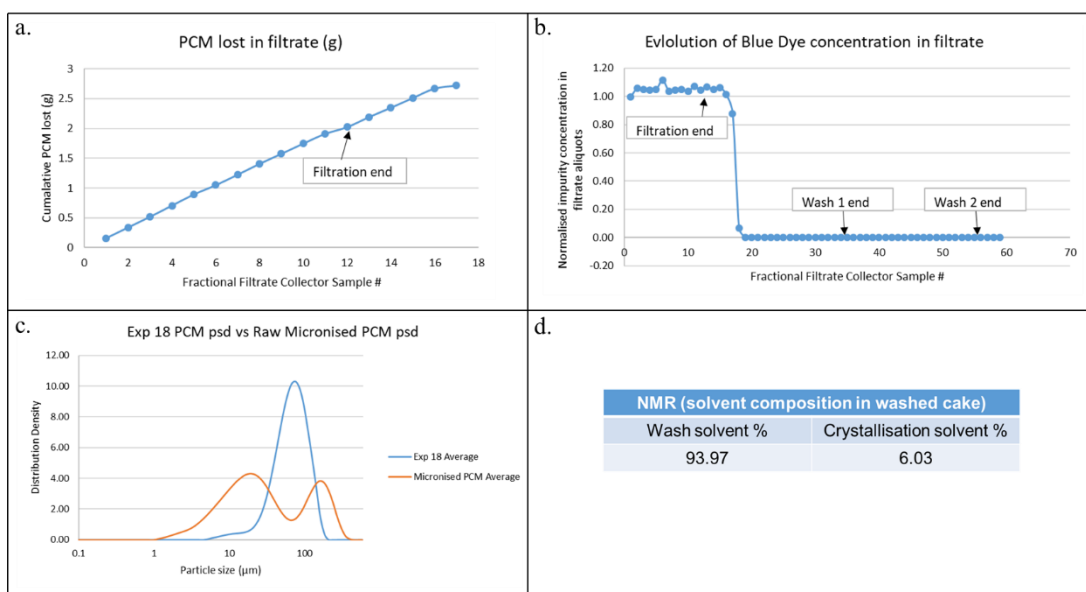


Figure B-23: Results obtained from experiment 18; crystallisation solvent: ethanol; wash solvent: mix n-dodecane solution; API grade: micronised; filtration rate (rpm): 10; volume of wash: 3 void volumes; number of washes: 2. a.) Graph showing cumulative API loss in filtrate samples throughout the experiment, mass of PCM API lost during wash = 0 g. b.) Normalised concentration of blue dye impurity in each filtrate sample obtained throughout the experiment. c.) Particle size distribution of the raw paracetamol API and the washed cake sample obtained at the end of the washing experiment, from the damp cake. d.) ¹H-NMR analysis results showing the residual crystallisation solvent content in the final washed cake.

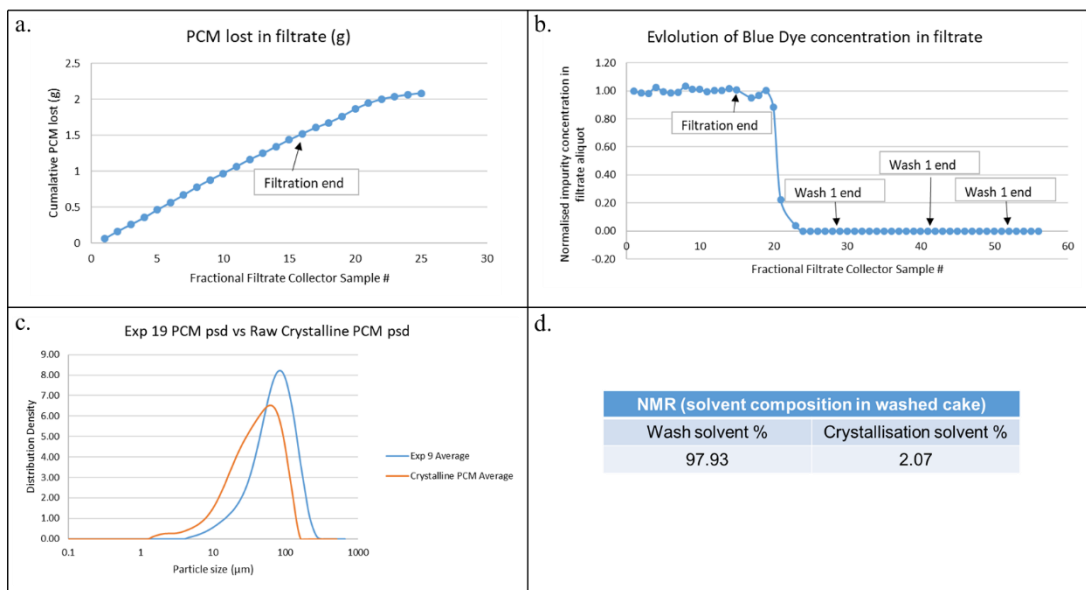


Figure B-24: Results obtained from experiment 19; crystallisation solvent: isopropanol; wash solvent: mix n-dodecane solution; API grade: crystalline; filtration rate (rpm): 100; volume of wash: 3 void volumes; number of washes: 3. a.) Graph showing cumulative API loss in filtrate samples throughout the experiment, mass of PCM API lost during wash = 0.29 g. b.) Normalised concentration of blue dye impurity in each filtrate sample obtained throughout the experiment. c.) Particle size distribution of the raw paracetamol API and the washed cake sample obtained at the end of the washing experiment, from the damp cake. d.) 1H-NMR analysis results showing the residual crystallisation solvent content in the final washed cake.

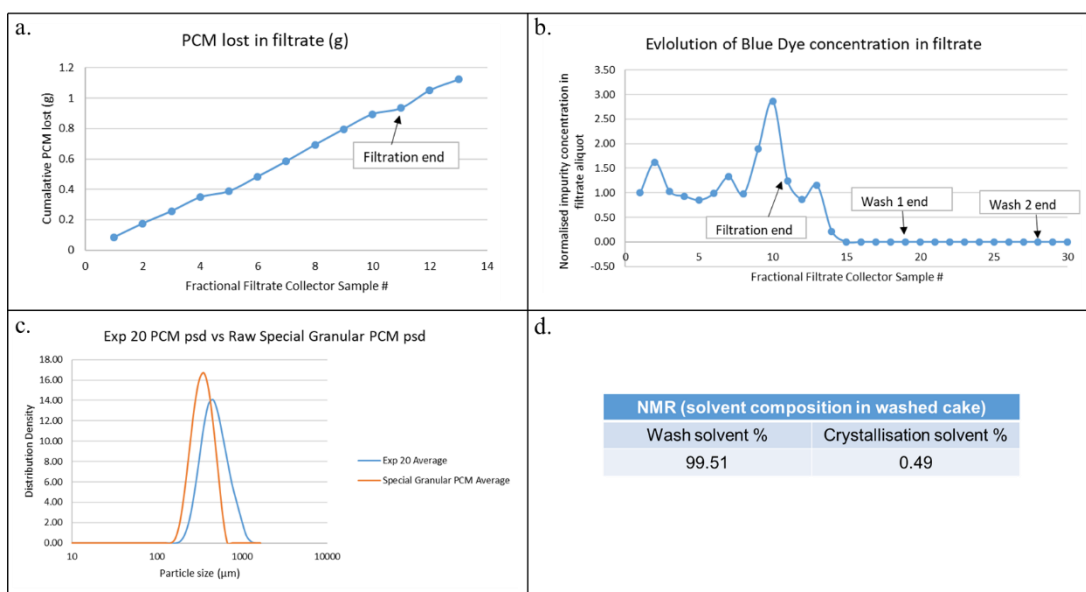


Figure B-25: Results obtained from experiment 20; crystallisation solvent: isoamyl alcohol; wash solvent: mix n-dodecane solution; API grade: special granular; filtration rate (rpm): 55; volume of wash: 3 void volumes; number of washes: 2. a.) Graph showing cumulative API loss in filtrate samples throughout the experiment, mass of PCM API lost during wash = 0.1 g. b.) Normalised concentration of blue dye impurity in each filtrate sample obtained throughout the experiment. c.) Particle size distribution of the raw paracetamol API and the washed cake sample obtained at the end of the washing experiment, from the damp cake. d.) 1H-NMR analysis results showing the residual crystallisation solvent content in the final washed cake.

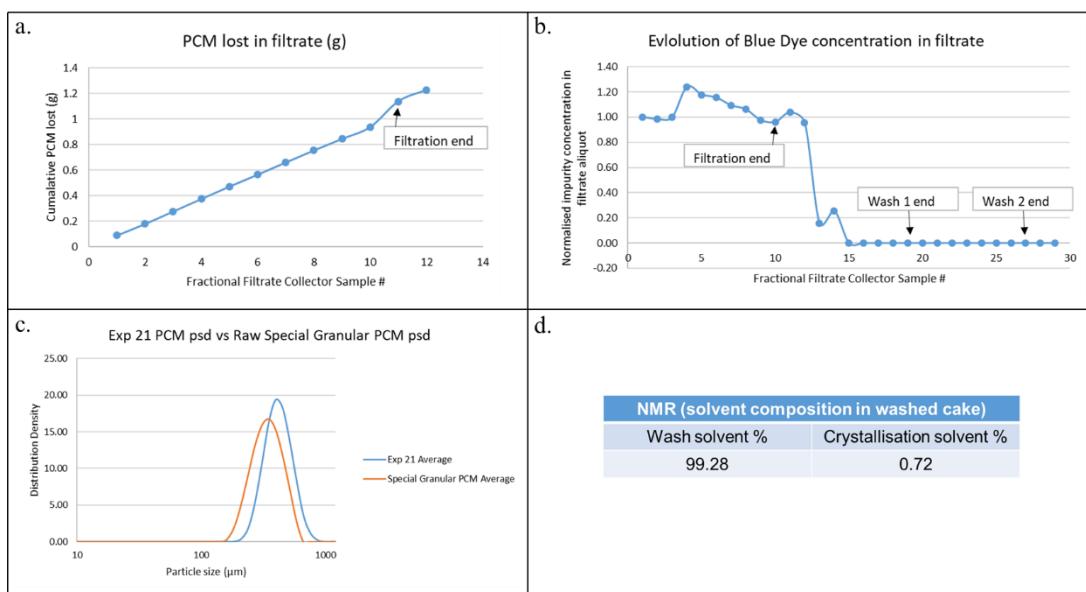


Figure B-26: Results obtained from experiment 21; crystallisation solvent: isoamyl alcohol; wash solvent: mix n-dodecane solution; API grade: special granular; filtration rate (rpm): 55; volume of wash: 3 void volumes; number of washes: 2. a.) Graph showing cumulative API loss in filtrate samples throughout the experiment, mass of PCM API lost during wash = 0.05 g. b.) Normalised concentration of blue dye impurity in each filtrate sample obtained throughout the experiment. c.) Particle size distribution of the raw paracetamol API and the washed cake sample obtained at the end of the washing experiment, from the damp cake. d.) 1H-NMR analysis results showing the residual crystallisation solvent content in the final washed cake.

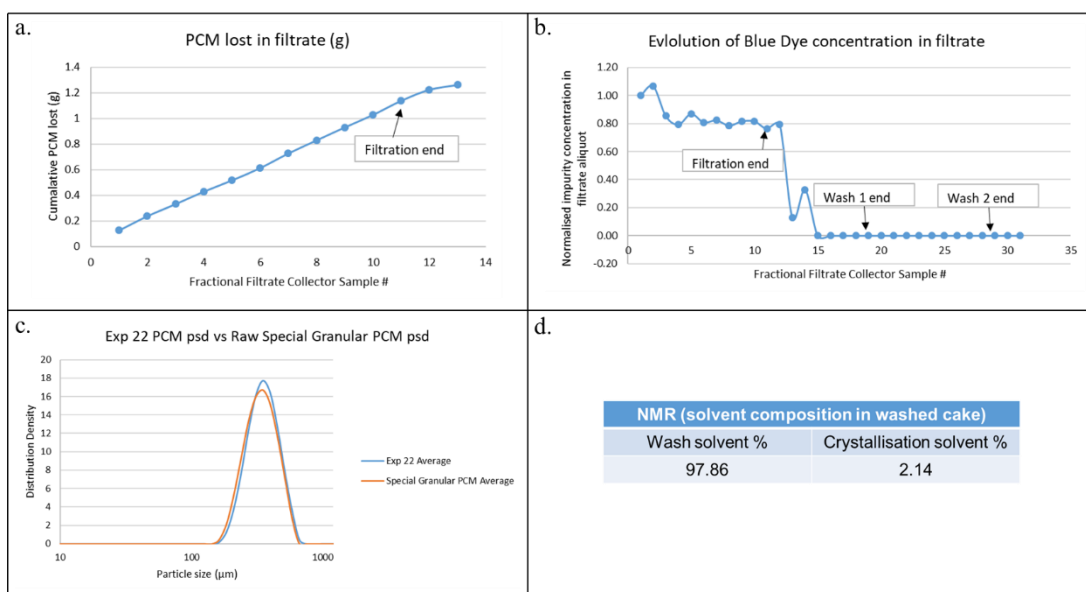


Figure B-27: Results obtained from experiment 22; crystallisation solvent: isoamyl alcohol; wash solvent: mix n-dodecane solution; API grade: special granular; filtration rate (rpm): 55; volume of wash: 3 void volumes; number of washes: 2. a.) Graph showing cumulative API loss in filtrate samples throughout the experiment, mass of PCM API lost during wash = 0.07 g. b.) Normalised concentration of blue dye impurity in each filtrate sample obtained throughout the experiment. c.) Particle size distribution of the raw paracetamol API and the washed cake sample obtained at the end of the washing experiment, from the damp cake. d.) 1H-NMR analysis results showing the residual crystallisation solvent content in the final washed cake.

Appendix C - Optimising removal of impurity on an industrial active pharmaceutical ingredient (API) using constant rate washing methodology

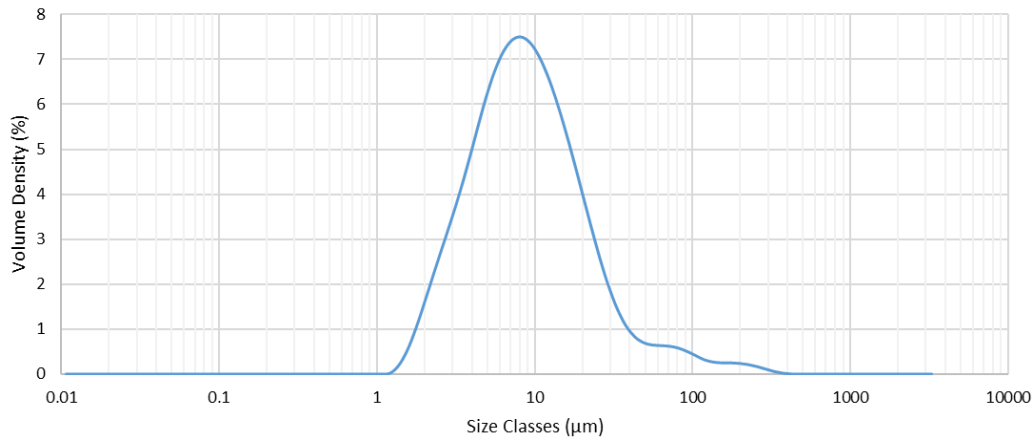


Figure C-1: Particle size distribution of raw AZC1 API, determined using mastersizer wet dispersion unit

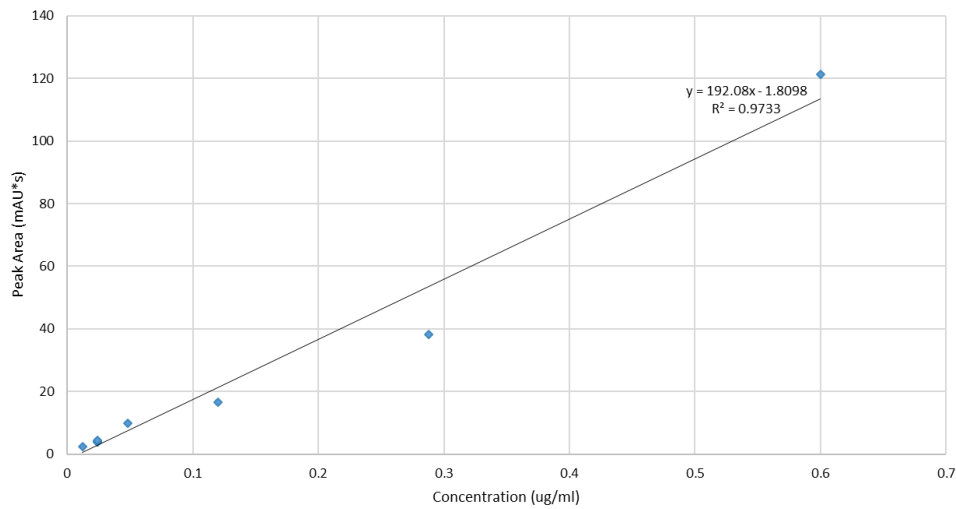


Figure C-2: HPLC calibration curve for ICI impurity

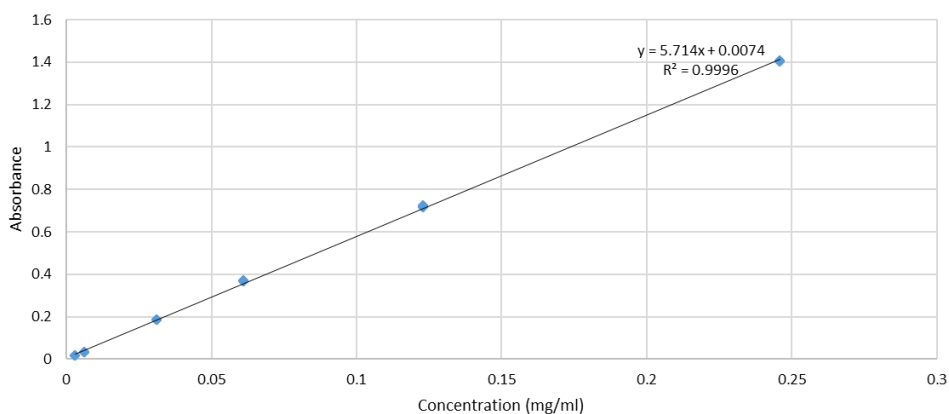


Figure C-3: UV-vis calibration curve for red dye in mother liquor solvent system

| Worksheet | | | | | | |
|-----------|--------|----------|-----------|-----------|-----------------|-------------|
| | 1 | 2 | 3 | 4 | 5 | 6 |
| | Exp No | Exp Name | Run Order | Incl/Excl | Filtration Rate | Temperature |
| 1 | 1 | N1 | 6 | Incl | 10 | 0 |
| 2 | 2 | N2 | 1 | Incl | 100 | 0 |
| 3 | 3 | N3 | 5 | Incl | 10 | 22 |
| 4 | 4 | N4 | 4 | Incl | 100 | 22 |
| 5 | 5 | N5 | 7 | Incl | 55 | 11 |
| 6 | 6 | N6 | 2 | Incl | 55 | 11 |
| 7 | 7 | N7 | 3 | Incl | 55 | 11 |

Figure C-4: Design of Experiment worksheet obtained

| Worksheet | | | | | | | | | | | | |
|-----------|--------|----------|-----------|-----------|-----------------|-------------|------------|------------|------------|----------|-------------------|-----------------|
| | 1 | 2 | 3 | 4 | 5 | 6 | 7 | 8 | 9 | 10 | 11 | 12 |
| | Exp No | Exp Name | Run Order | Incl/Excl | Filtration Rate | Temperature | D10 change | D50 change | D90 change | API Loss | IC1 Concentration | Decrease in IC1 |
| 1 | 1 | N1 | 6 | Incl | 10 | 0 | 40 | 56 | 37 | 116 | 7.04 | 99.6 |
| 2 | 2 | N2 | 1 | Incl | 100 | 0 | 13 | 24 | 33 | 91 | 18.42 | 99.03 |
| 3 | 3 | N3 | 5 | Incl | 10 | 22 | 30 | 56 | 84 | 361 | 4.59 | 99.76 |
| 4 | 4 | N4 | 4 | Incl | 100 | 22 | 20 | 38 | 29 | 354 | 4.47 | 99.73 |
| 5 | 5 | N5 | 7 | Incl | 55 | 11 | 26 | 43 | 29 | 171 | 7.13 | 99.6 |
| 6 | 6 | N6 | 2 | Incl | 55 | 11 | 27 | 51 | 43 | 182 | 15.9 | 99.04 |
| 7 | 7 | N7 | 3 | Incl | 55 | 11 | 15 | 23 | 20 | 172 | 6.87 | 99.62 |
| 8 | 8 | N8 | 8 | Excl | 55 | 11 | 0 | 0 | -3 | 249 | 6.43 | 99.67 |
| 9 | 9 | N9 | 9 | Incl | 100 | 22 | 23 | 46 | 36 | 340 | 3.45 | 99.83 |

Figure C-5: Final DoE worksheet with responses of all the experiments carried out. (Experiment 9 is just the repeat of experiment 4)

Table C- 1: Calculation to correct for API loss during washing process due to isooctane presence in filtrate, DoE, Experiment 1

| | |
|---|-----|
| Vail filtration stopped | 11 |
| Cumulative API mass loss at filtration (mg) | 870 |

| | |
|--|--------------------------------|
| API dissolved in saturated solution at 0 °C (mg) | 141 |
| Cumulative API mass loss at the end of experiment (mg) | 1584 |
| Mass loss during washing (mg) | = 1584 – 870 = 714 |
| Corrected mass loss to washing (mg) | = (141/870) * 714 = 116 |

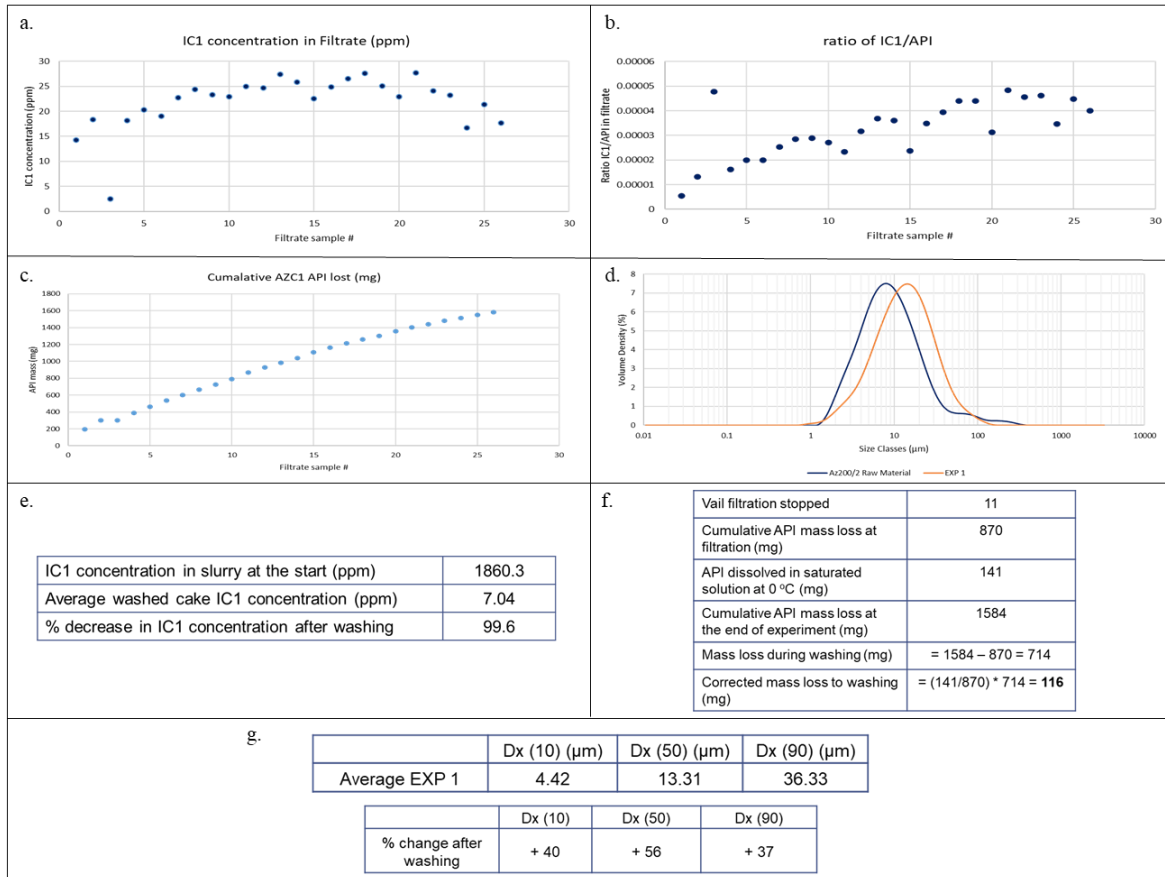


Figure C-6: DoE Experiment 1. a.) Graph showing the IC1 concentration in each filtrate vail collected. b.) Normalised concentration of IC1 impurity in each filtrate sample with respect to the API. c.) Cumulative API loss in filtrate samples throughout the experiment. d.) Particle size distribution of the raw AZC1 API material and the washed cake sample obtained at the end of the experiment. e.) Table showing the IC1 concentration in slurry at the start of experiment and the IC1 impurity concentration in the final washed cake. f.) Calculation to correct for API loss during washing process due to isooctane presence in the dry filtrate vails. g.) Particle size distribution comparison of the washed material obtained vs the raw material started with.

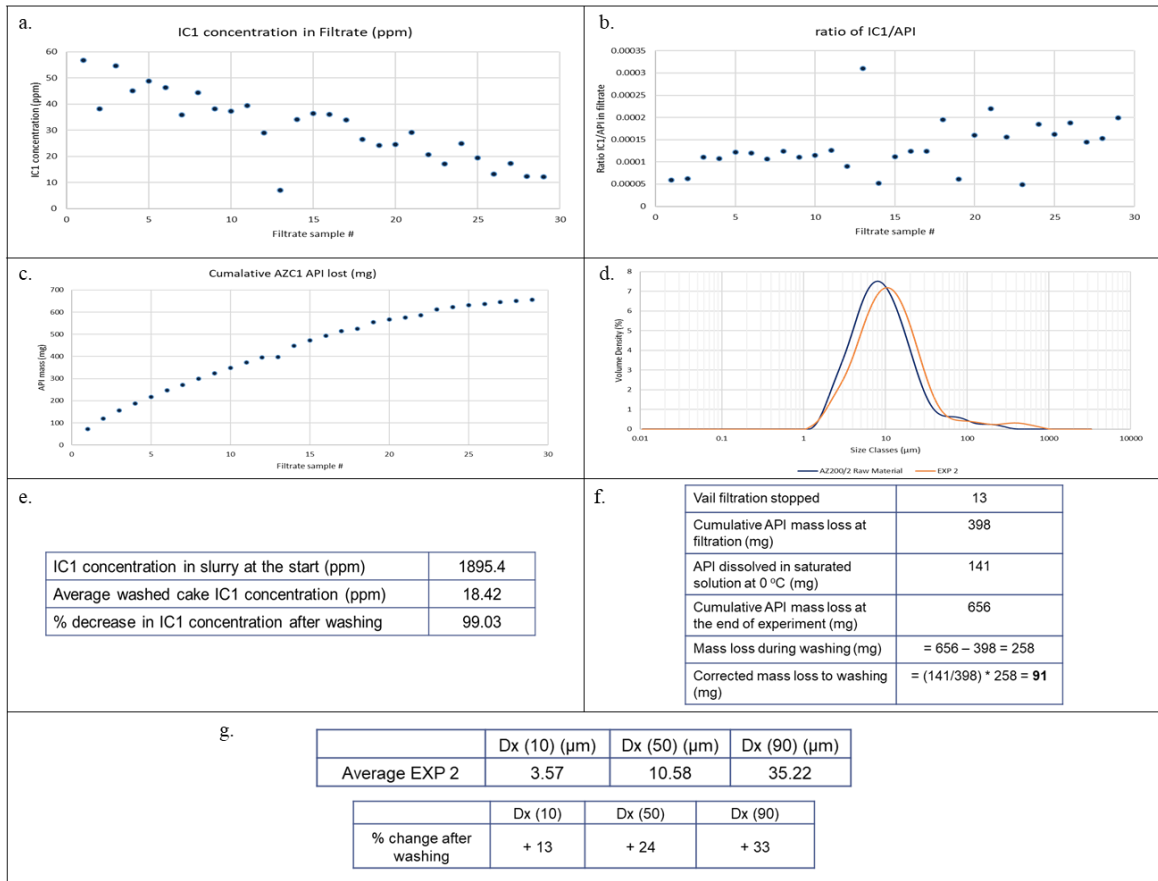


Figure C-7: DoE Experiment 2. a.) Graph showing the IC1 concentration in each filtrate vail collected. b.) Normalised concentration of IC1 impurity in each filtrate sample with respect to the API. c.) Cumulative API loss in filtrate samples throughout the experiment. d.) Particle size distribution of the raw AZC1 API material and the washed cake sample obtained at the end of the experiment. e.) Table showing the IC1 concentration in slurry at the start of experiment and the IC1 impurity concentration in the final washed cake. f.) Calculation to correct for API loss during washing process due to isooctane presence in the dry filtrate vails. g.) Particle size distribution comparison of the washed material obtained vs the raw material started with.

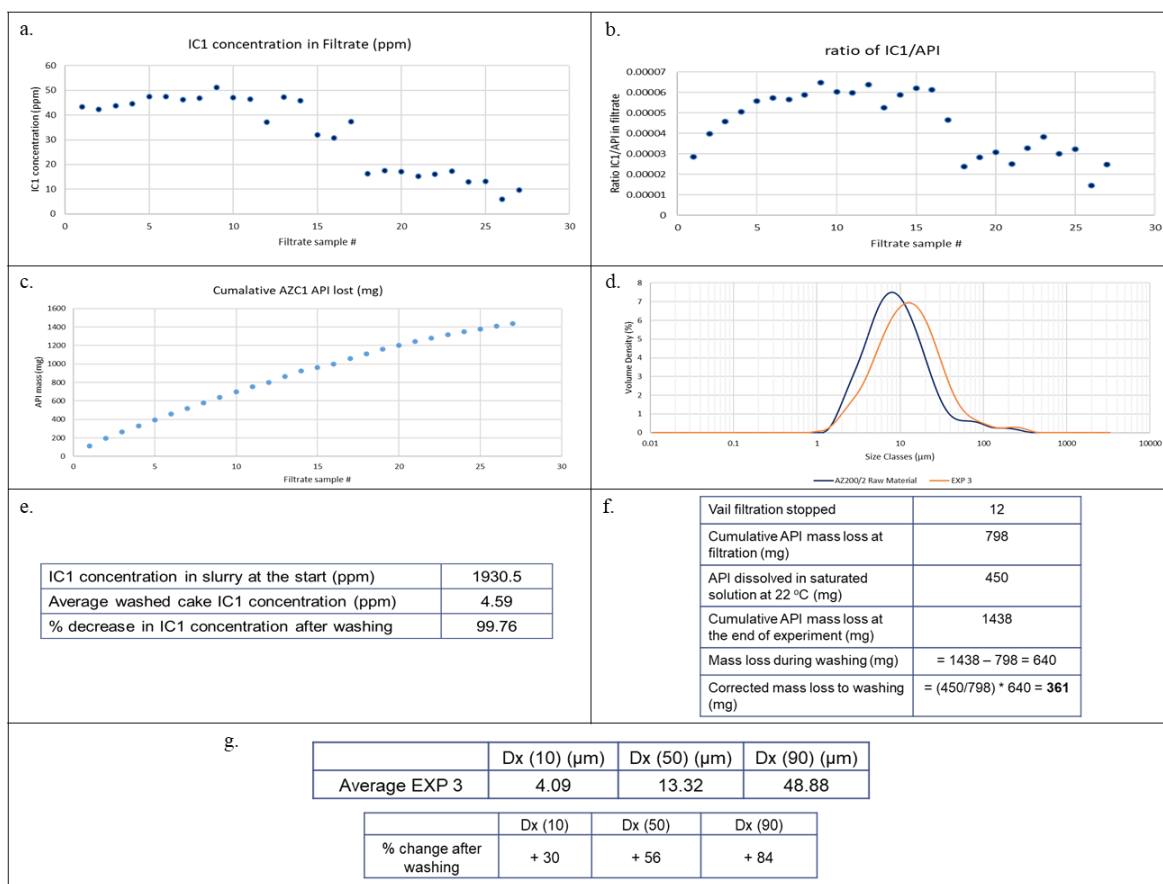


Figure C-8: DoE Experiment 3. a.) Graph showing the IC1 concentration in each filtrate vail collected. b.) Normalised concentration of IC1 impurity in each filtrate sample with respect to the API. c.) Cumulative API loss in filtrate samples throughout the experiment. d.) Particle size distribution of the raw AZC1 API material and the washed cake sample obtained at the end of the experiment. e.) Table showing the IC1 concentration in slurry at the start of experiment and the IC1 impurity concentration in the final washed cake. f.) Calculation to correct for API loss during washing process due to isooctane presence in the dry filtrate vails. g.) Particle size distribution comparison of the washed material obtained vs the raw material started with.

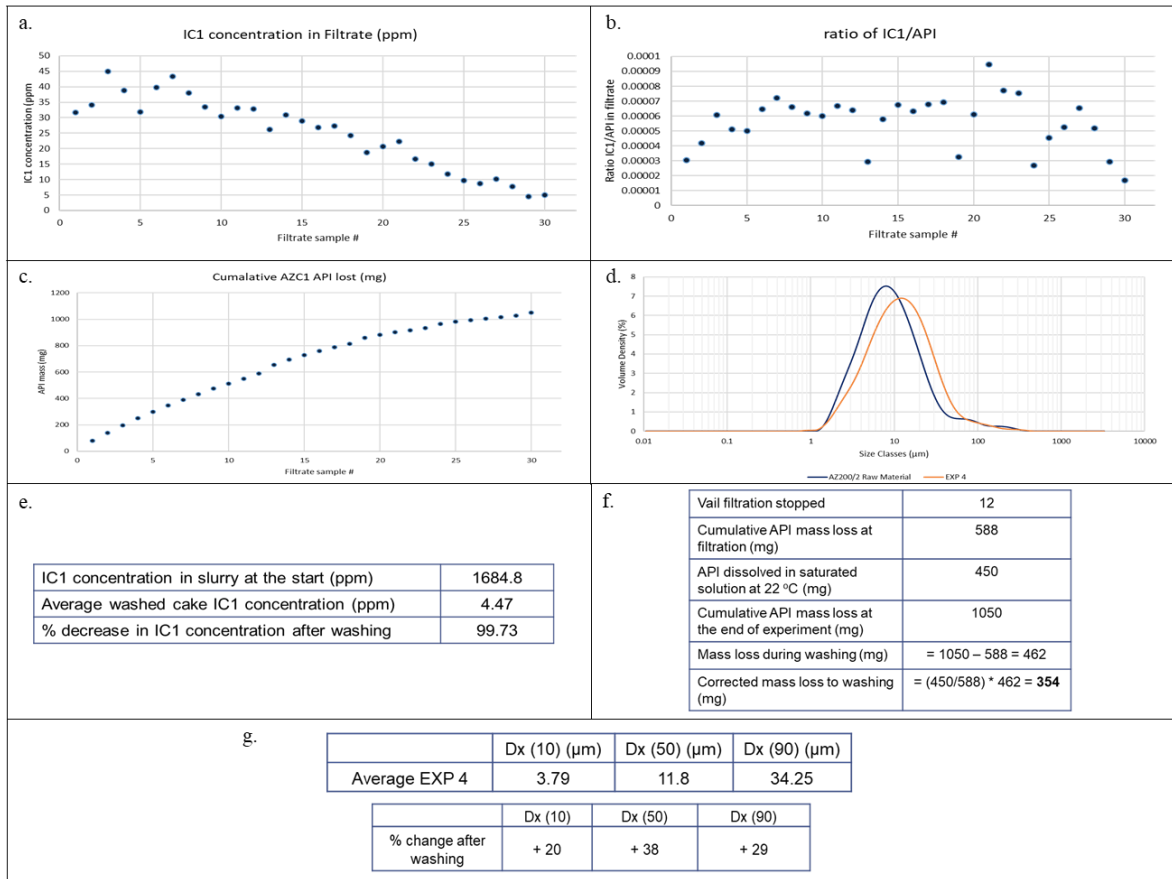


Figure C-9: DoE Experiment 4. a.) Graph showing the IC1 concentration in each filtrate vail collected. b.) Normalised concentration of IC1 impurity in each filtrate sample with respect to the API. c.) Cumulative API loss in filtrate samples throughout the experiment. d.) Particle size distribution of the raw AZC1 API material and the washed cake sample obtained at the end of the experiment. e.) Table showing the IC1 concentration in slurry at the start of experiment and the IC1 impurity concentration in the final washed cake. f.) Calculation to correct for API loss during washing process due to isooctane presence in the dry filtrate vails. g.) Particle size distribution comparison of the washed material obtained vs the raw material started with.

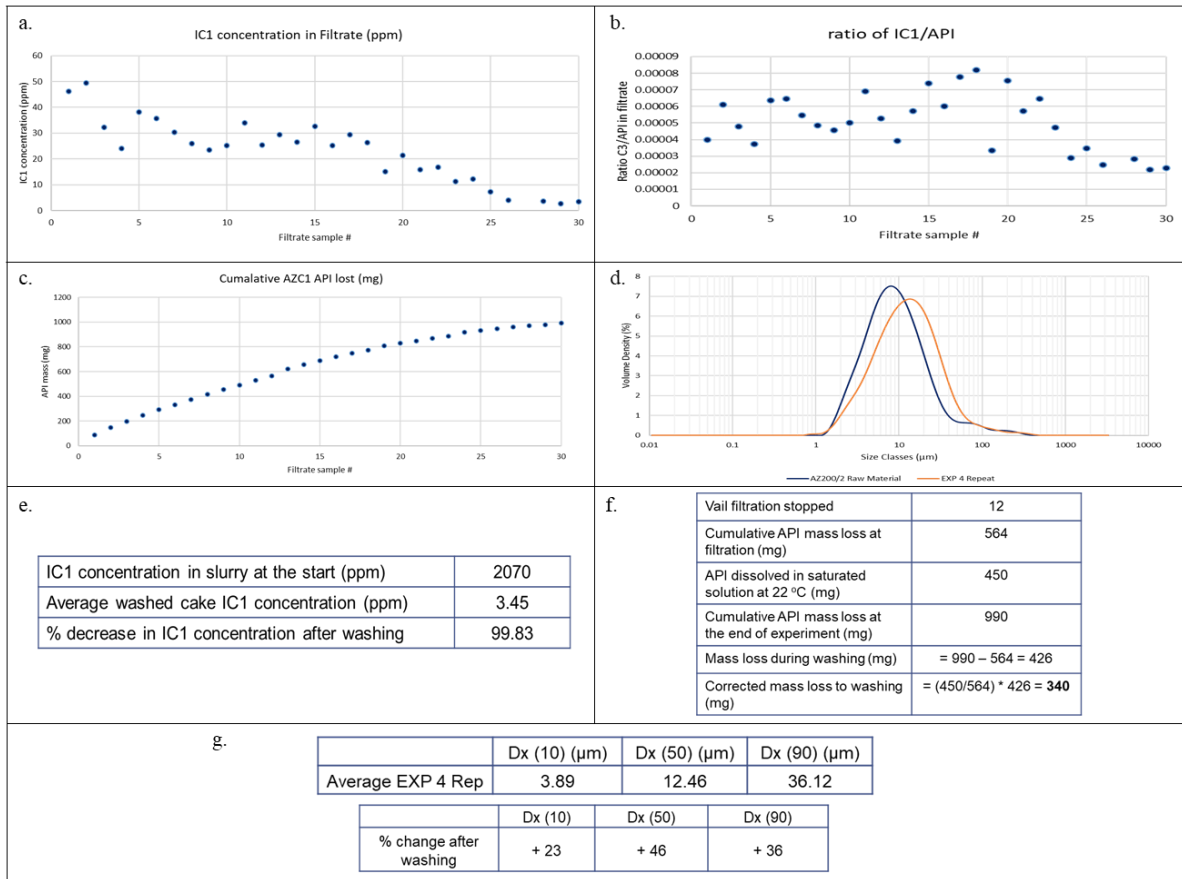


Figure C-10: DoE Experiment 4 Repeat. a.) Graph showing the IC1 concentration in each filtrate vail collected. b.) Normalised concentration of IC1 impurity in each filtrate sample with respect to the API. c.) Cumulative API loss in filtrate samples throughout the experiment. d.) Particle size distribution of the raw AZC1 API material and the washed cake sample obtained at the end of the experiment. e.) Table showing the IC1 concentration in slurry at the start of experiment and the IC1 impurity concentration in the final washed cake. f.) Calculation to correct for API loss during washing process due to isooctane presence in the dry filtrate vails. g.) Particle size distribution comparison of the washed material obtained vs the raw material started with.

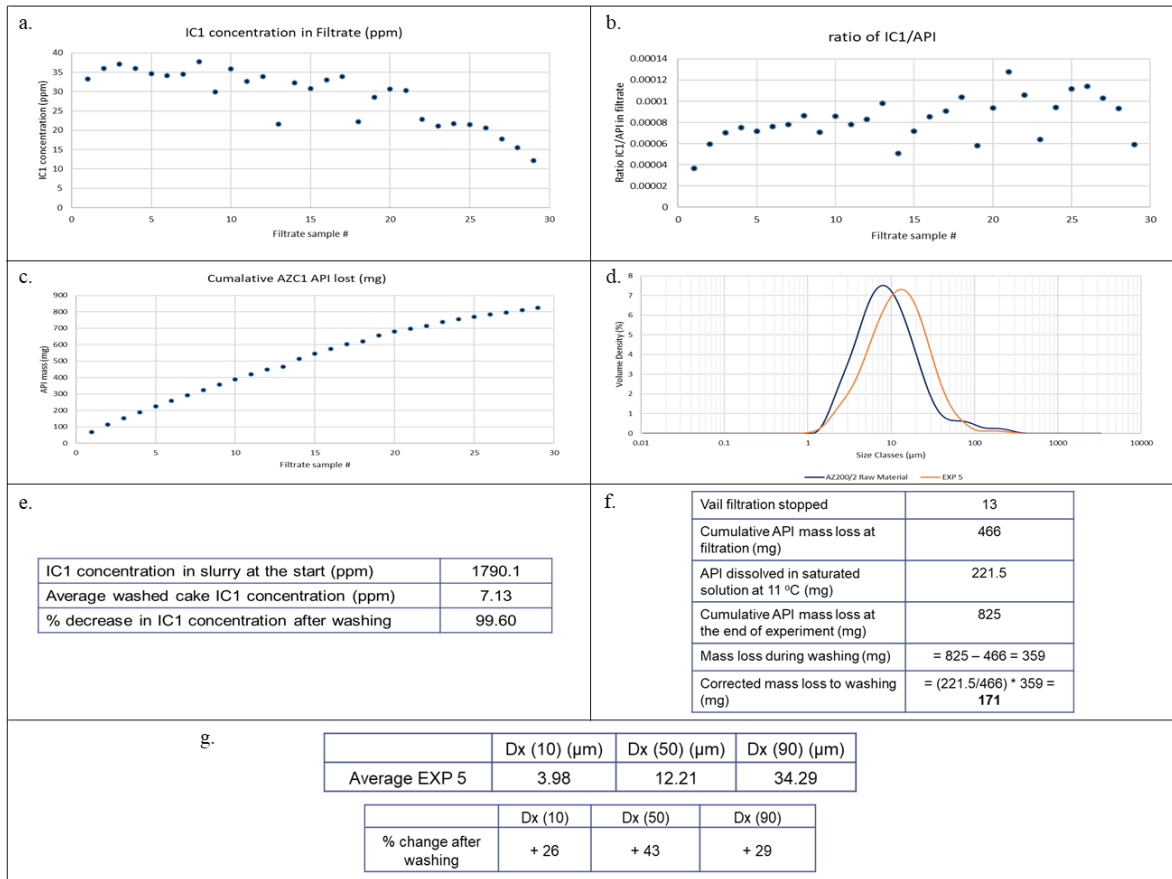


Figure C-11: DoE Experiment 5. a.) Graph showing the IC1 concentration in each filtrate vail collected. b.) Normalised concentration of IC1 impurity in each filtrate sample with respect to the API. c.) Cumulative API loss in filtrate samples throughout the experiment. d.) Particle size distribution of the raw AZC1 API material and the washed cake sample obtained at the end of the experiment. e.) Table showing the IC1 concentration in slurry at the start of experiment and the IC1 impurity concentration in the final washed cake. f.) Calculation to correct for API loss during washing process due to isooctane presence in the dry filtrate vails. g.) Particle size distribution comparison of the washed material obtained vs the raw material started with.

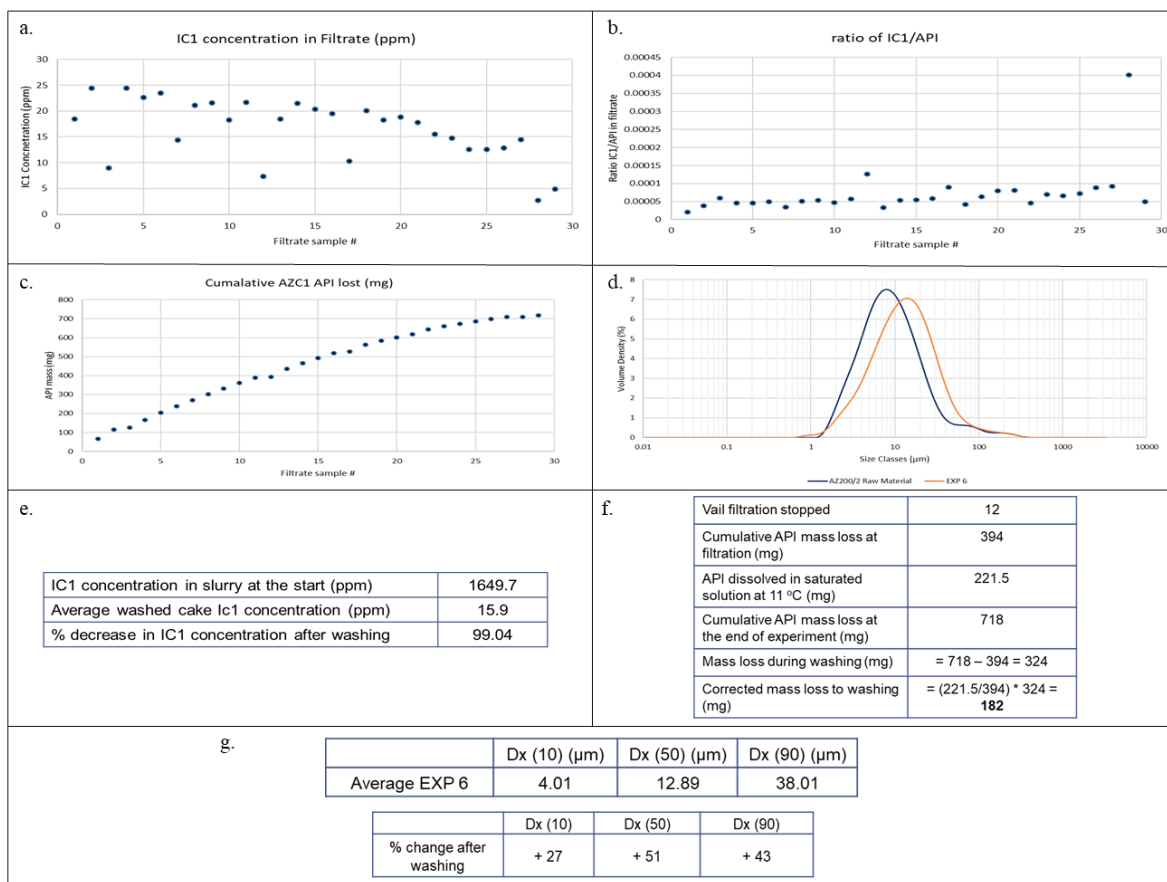


Figure C-12: DoE Experiment 6. a.) Graph showing the IC1 concentration in each filtrate vial collected. b.) Normalised concentration of IC1 impurity in each filtrate sample with respect to the API. c.) Cumulative API loss in filtrate samples throughout the experiment. d.) Particle size distribution of the raw AZC1 API material and the washed cake sample obtained at the end of the experiment. e.) Table showing the IC1 concentration in slurry at the start of experiment and the IC1 impurity concentration in the final washed cake. f.) Calculation to correct for API loss during washing process due to isooctane presence in the dry filtrate vails. g.) Particle size distribution comparison of the washed material obtained vs the raw material started with.

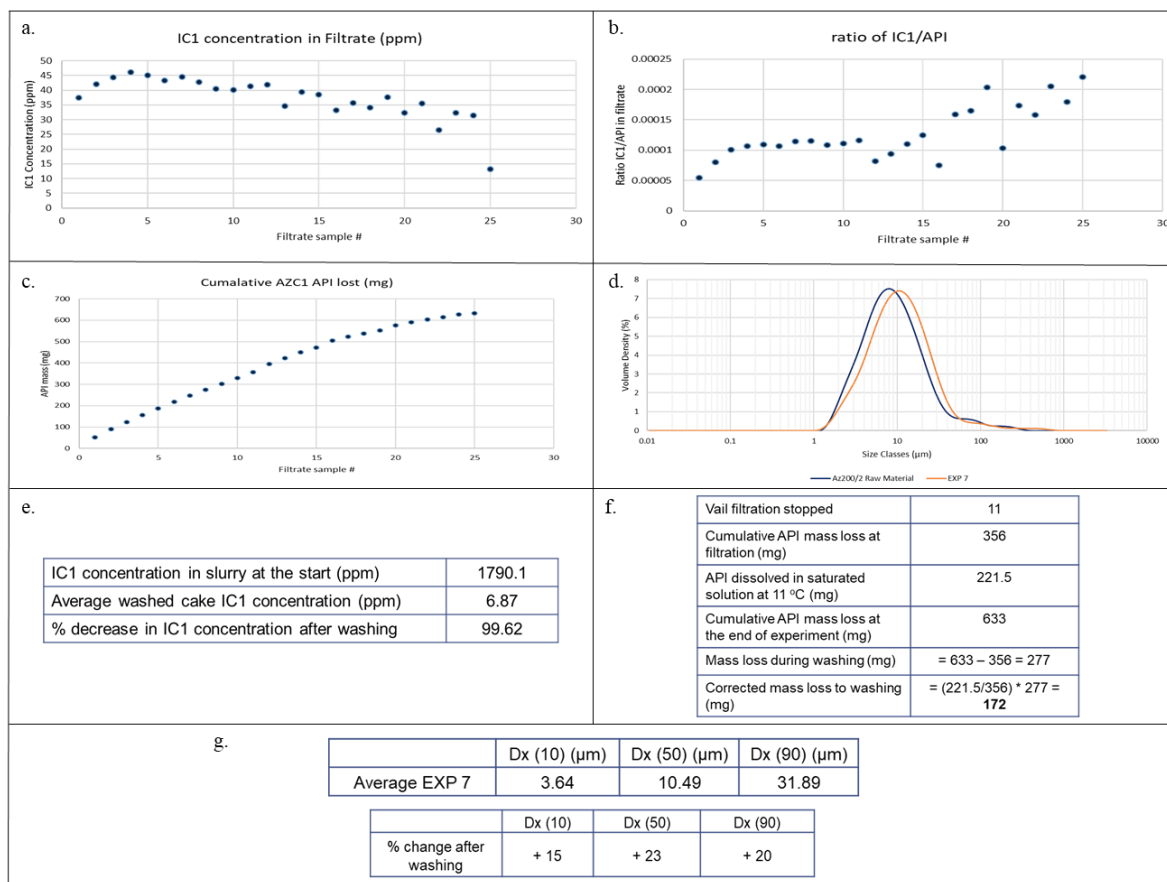


Figure C-13: DoE Experiment 7. a.) Graph showing the IC1 concentration in each filtrate vail collected. b.) Normalised concentration of IC1 impurity in each filtrate sample with respect to the API. c.) Cumulative API loss in filtrate samples throughout the experiment. d.) Particle size distribution of the raw AZC1 API material and the washed cake sample obtained at the end of the experiment. e.) Table showing the IC1 concentration in slurry at the start of experiment and the IC1 impurity concentration in the final washed cake. f.) Calculation to correct for API loss during washing process due to isooctane presence in the dry filtrate vails. g.) Particle size distribution comparison of the washed material obtained vs the raw material started with.

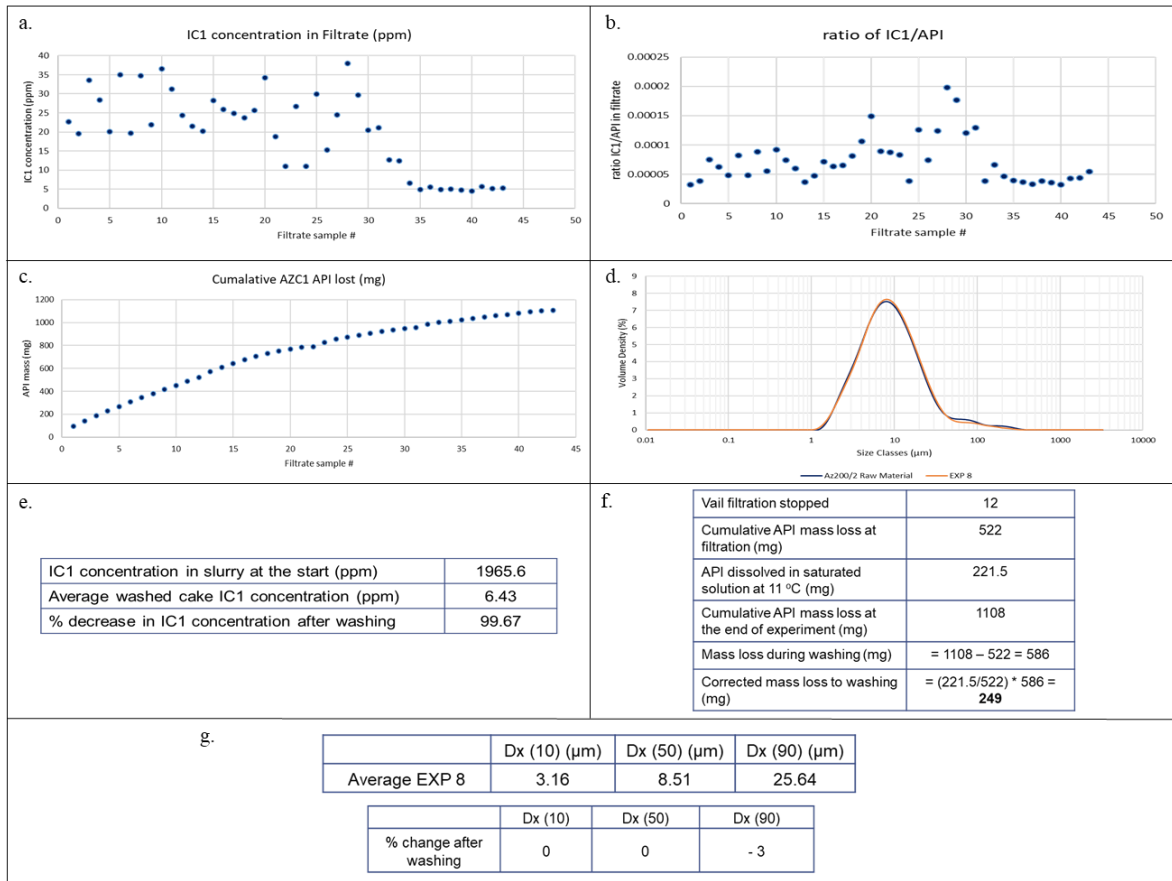


Figure C-14: Experiment 8. a.) Graph showing the IC1 concentration in each filtrate vial collected. b.) Normalised concentration of IC1 impurity in each filtrate sample with respect to the API. c.) Cumulative API loss in filtrate samples throughout the experiment. d.) Particle size distribution of the raw AZC1 API material and the washed cake sample obtained at the end of the experiment. e.) Table showing the IC1 concentration in slurry at the start of experiment and the IC1 impurity concentration in the final washed cake. f.) Calculation to correct for API loss during washing process due to isooctane presence in the dry filtrate vials. g.) Particle size distribution comparison of the washed material obtained vs the raw material started with.

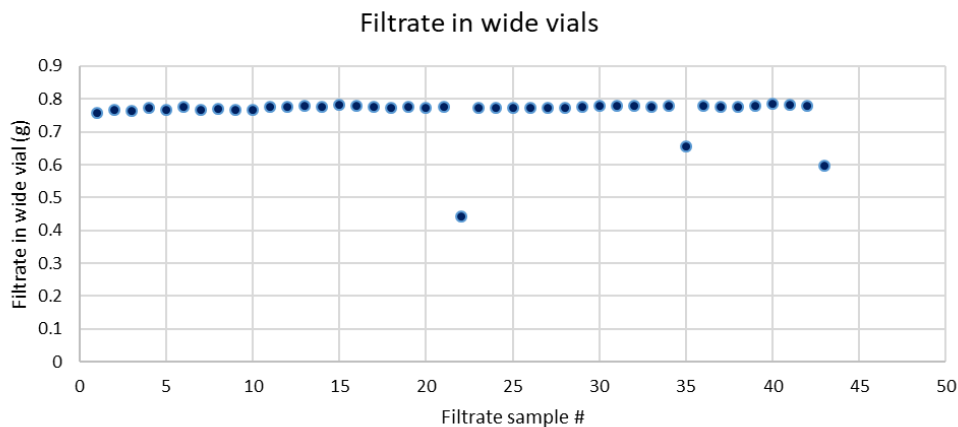


Figure C-15: Experiment 8, the mass of filtrate pipetted into each small vial to dry and then analyse using HPLC

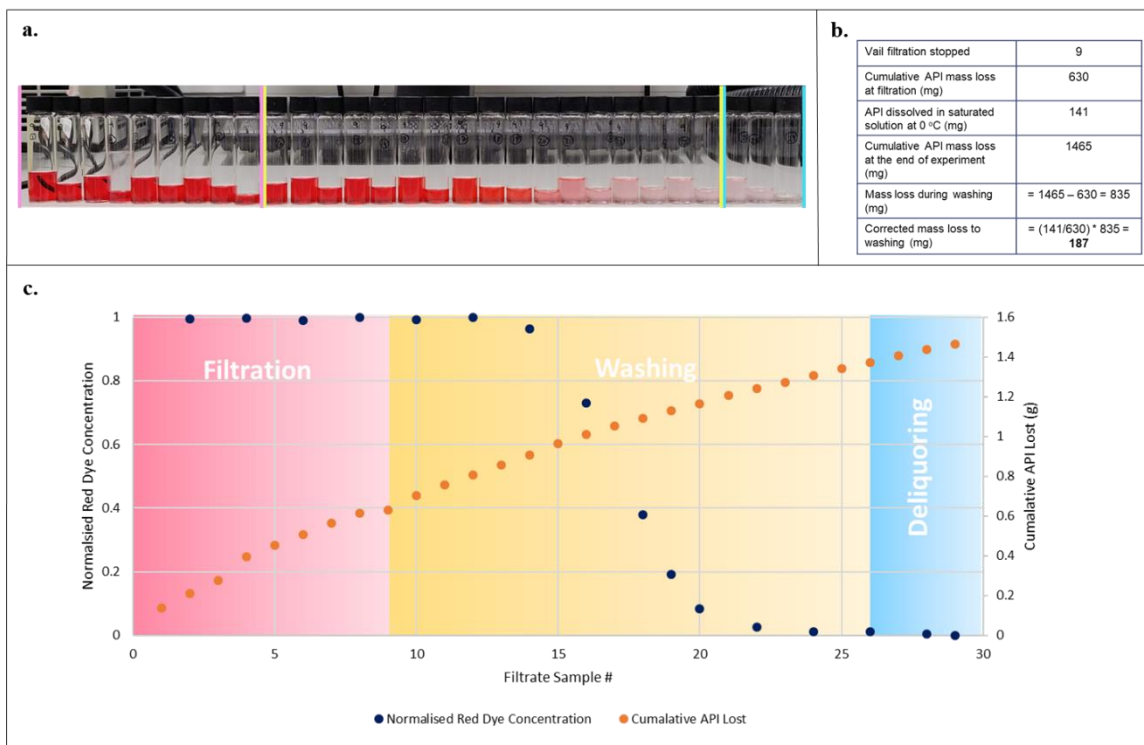


Figure C-16: Experiment R1. a.) Filtrate vails samples obtained, showing gradual decrease in red dye impurity concentration. b.) Calculation to correct for API loss during washing process due to isooctane presence in the dry filtrate vails. c.) Wash profile curve obtained for red dye impurity concentration and the cumulative API lost graph obtained for the experiment.

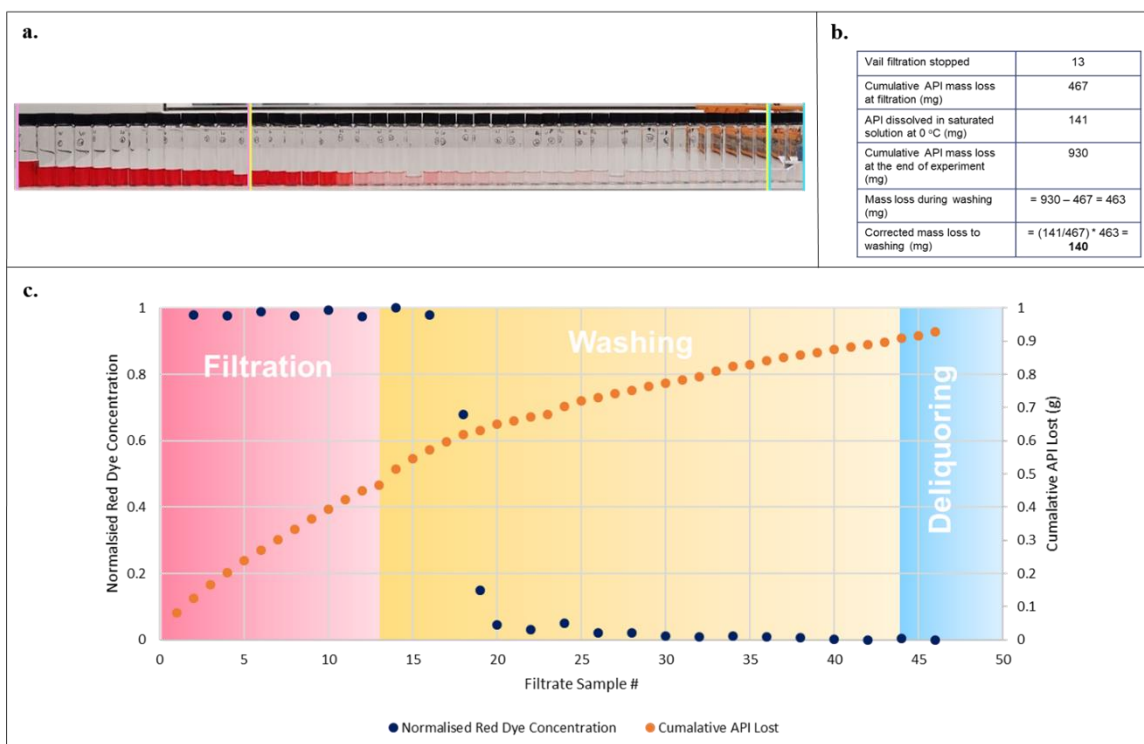


Figure C-17: Experiment R2. a.) Filtrate vails samples obtained, showing gradual decrease in red dye impurity concentration. b.) Calculation to correct for API loss during washing process due to isooctane presence in the dry filtrate vails. c.) Wash profile curve obtained for red dye impurity concentration and the cumulative API lost graph obtained for the experiment.

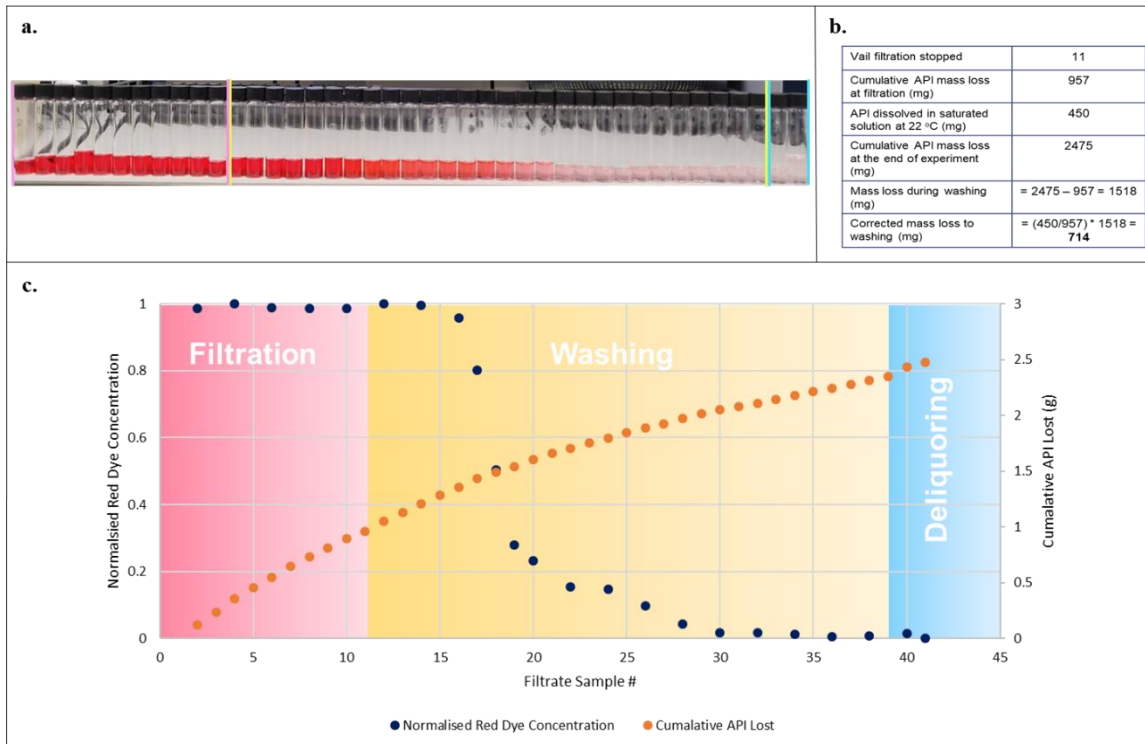


Figure C-18: Experiment R3. a.) Filtrate vails samples obtained, showing gradual decrease in red dye impurity concentration. b.) Calculation to correct for API loss during washing process due to isooctane presence in the dry filtrate vails. c.) Wash profile curve obtained for red dye impurity concentration and the cumulative API lost graph obtained for the experiment.

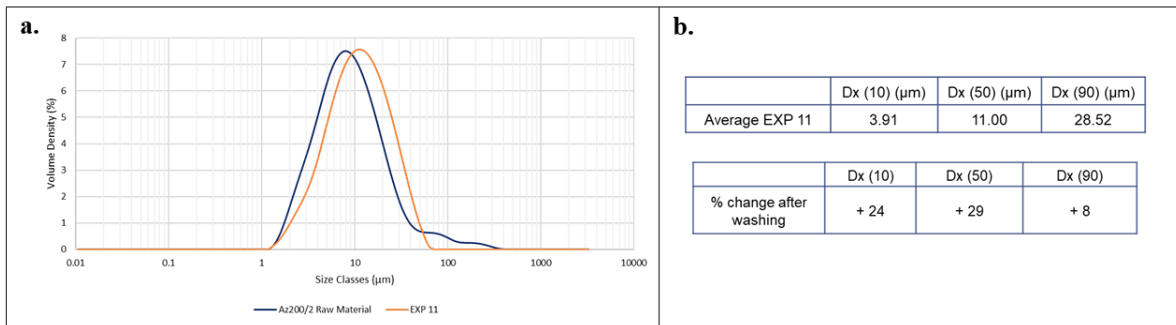


Figure C-19: Experiment R3. a.) Particle size distribution of the raw AZC1 API material and the washed cake sample obtained at the end of the experiment. b.) Particle size distribution comparison of the washed material obtained vs the raw material started with.

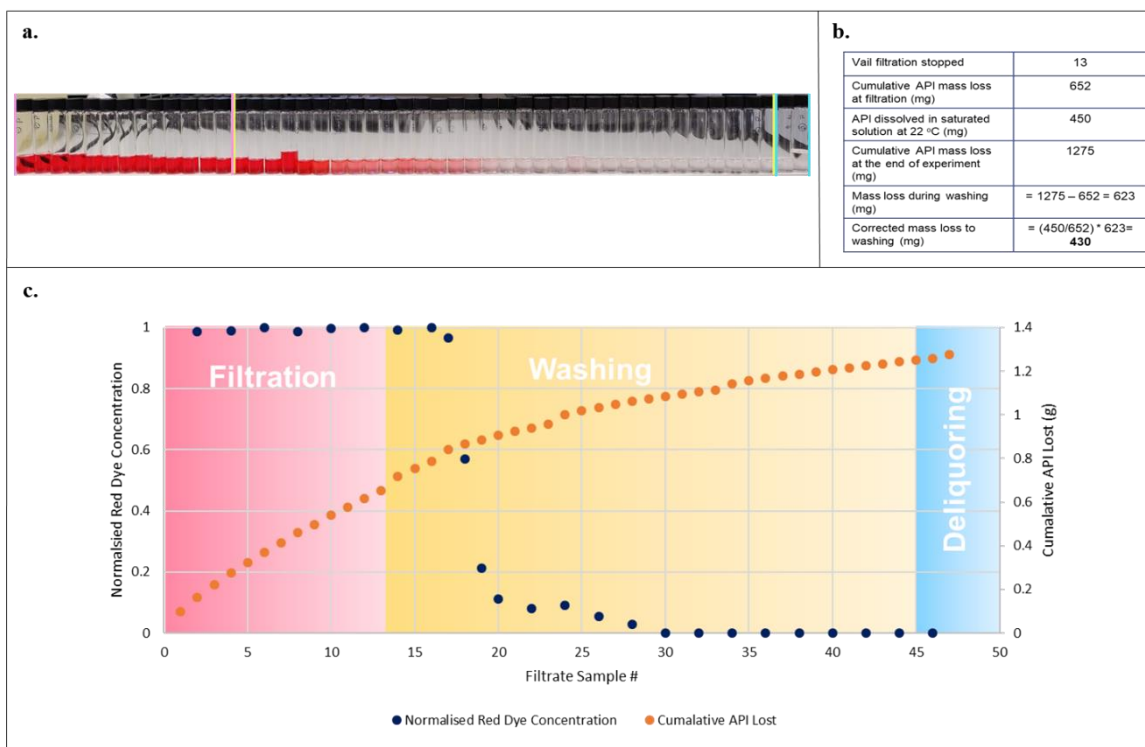


Figure C-20: Experiment R4. a.) Filtrate vails samples obtained, showing gradual decrease in red dye impurity concentration. b.) Calculation to correct for API loss during washing process due to isooctane presence in the dry filtrate vails. c.) Wash profile curve obtained for red dye impurity concentration and the cumulative API lost graph obtained for the experiment.

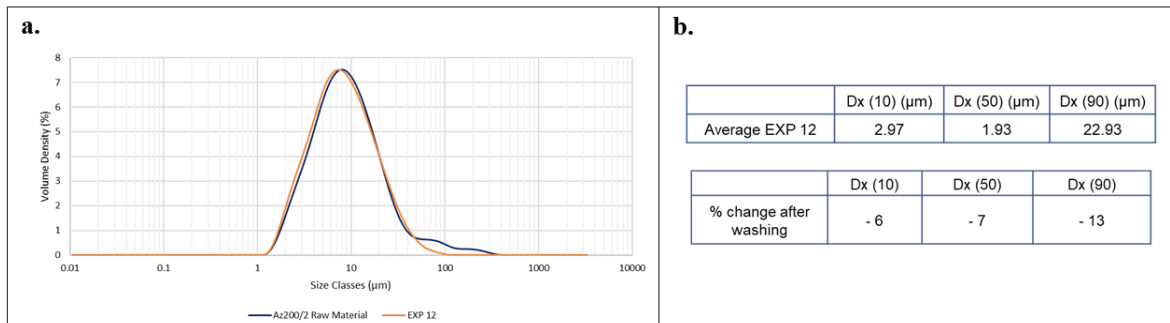


Figure C-21: Experiment R4. a.) Particle size distribution of the raw AZC1 API material and the washed cake sample obtained at the end of the experiment. b.) Particle size distribution comparison of the washed material obtained vs the raw material started with.

Appendix D - Investigating particle size distribution of agglomerates formed during washing process

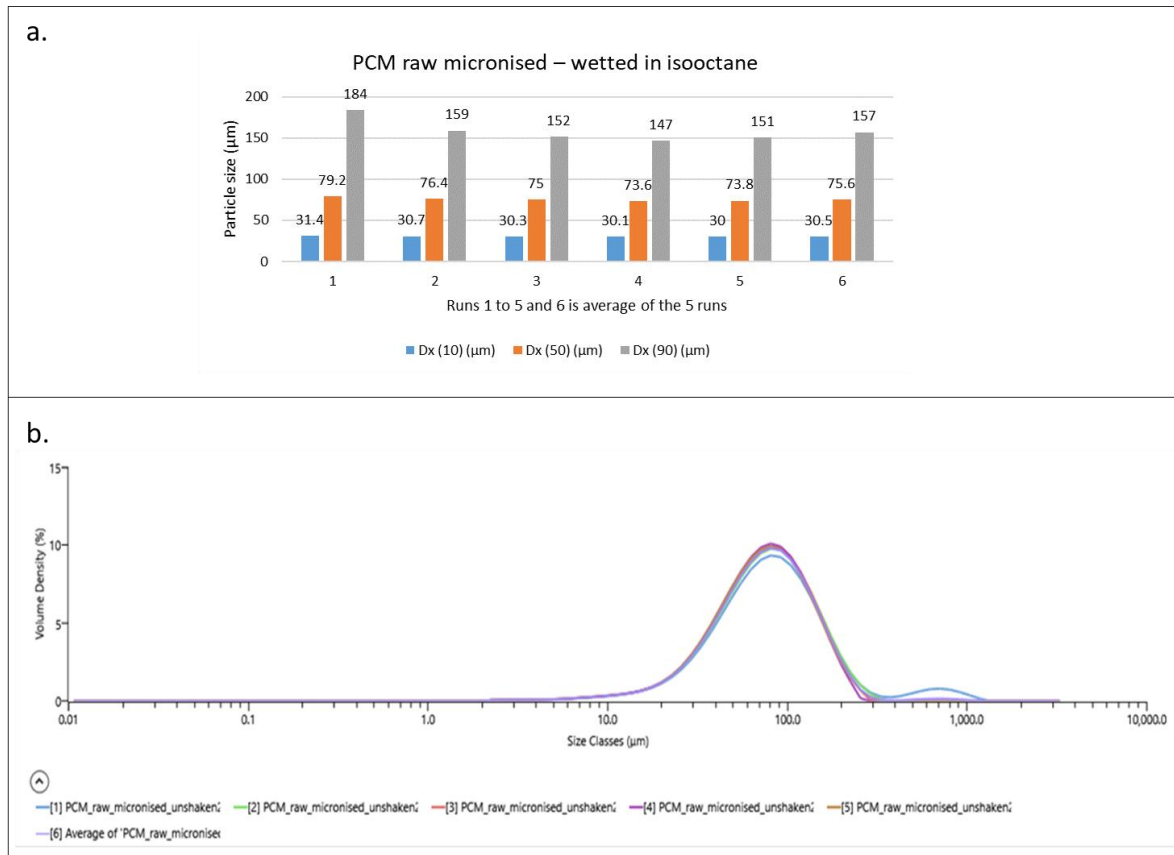


Figure D-1: Mastersizer analysis of micronised PCM using isooctane as dispersant after raw micronised PCM left in isooctane over the weekend. a.) D10, D50 and D90 values obtained for the 5 mastersizer runs 1-5 and 6 is the average value of the 5 runs. b.) Particle size distribution obtained for the 5 runs from mastersizer software.

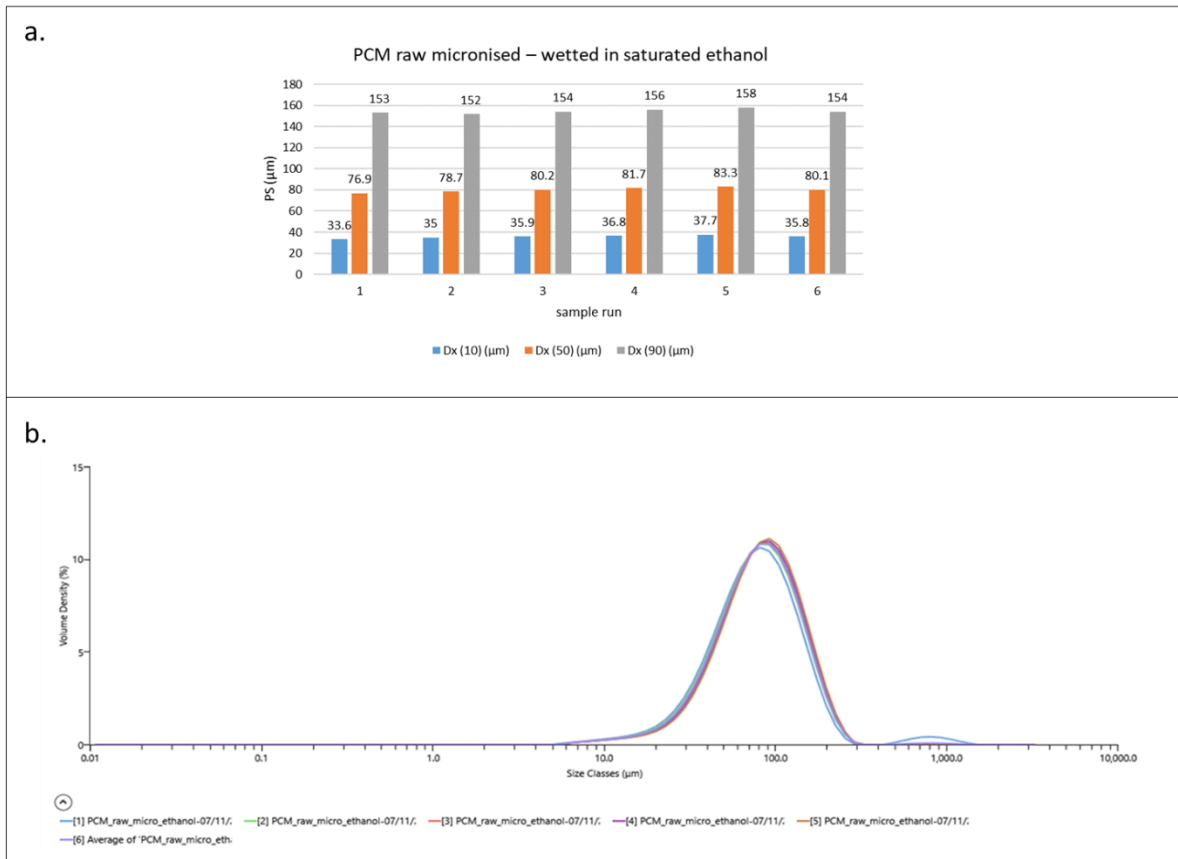


Figure D-2: Mastersizer analysis of micronised PCM using saturated ethanol as dispersant after raw micronised PCM left in saturated ethanol over the weekend. a.) D10, D50 and D90 values obtained for the 5 mastersizer runs 1-5 and 6 is the average value of the 5 runs. b.) Particle size distribution obtained for the 5 runs from mastersizer software.

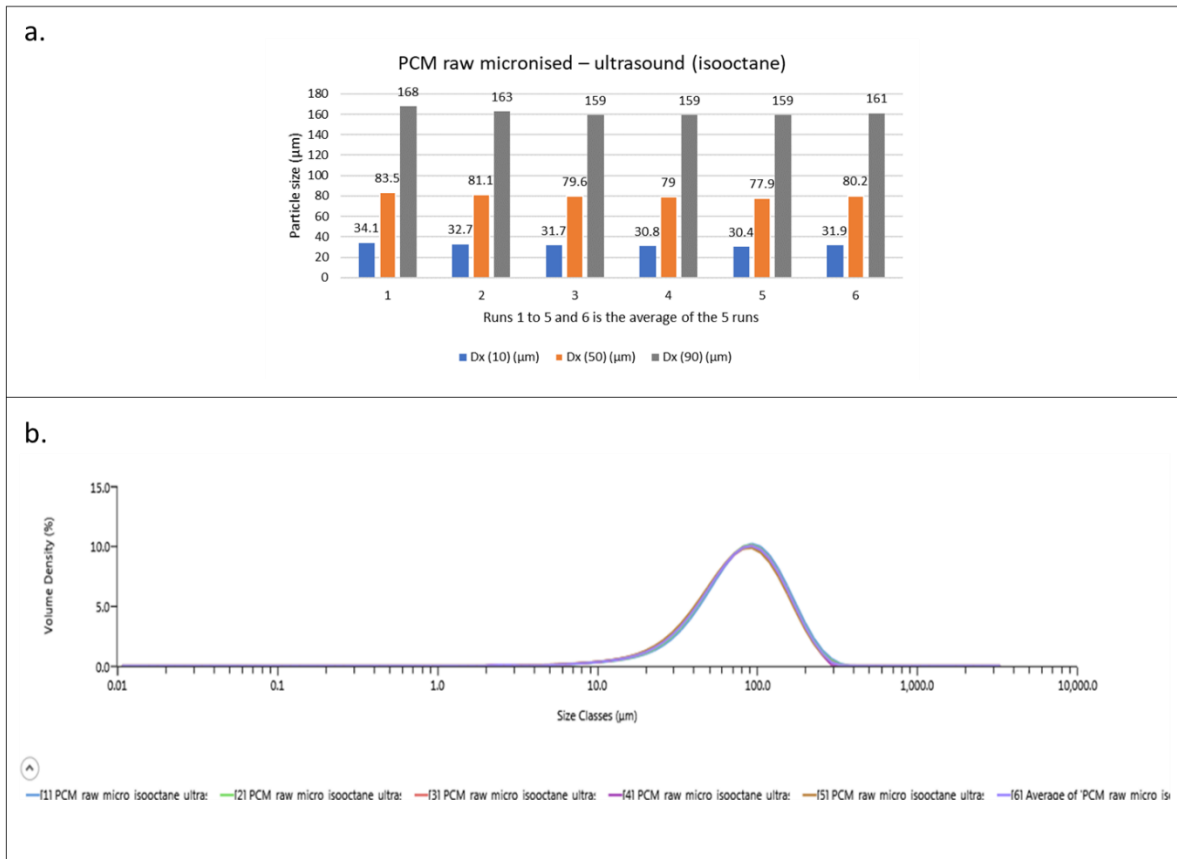


Figure D-3: Mastersizer analysis of micronised PCM using isooctane as dispersant after raw micronised PCM left ultrasound for 5 minutes at 30 kHz power. a.) D10, D50 and D90 values obtained for the 5 mastersizer runs 1-5 and 6 is the average value of the 5 runs. b.) Particle size distribution obtained for the 5 runs from mastersizer software.

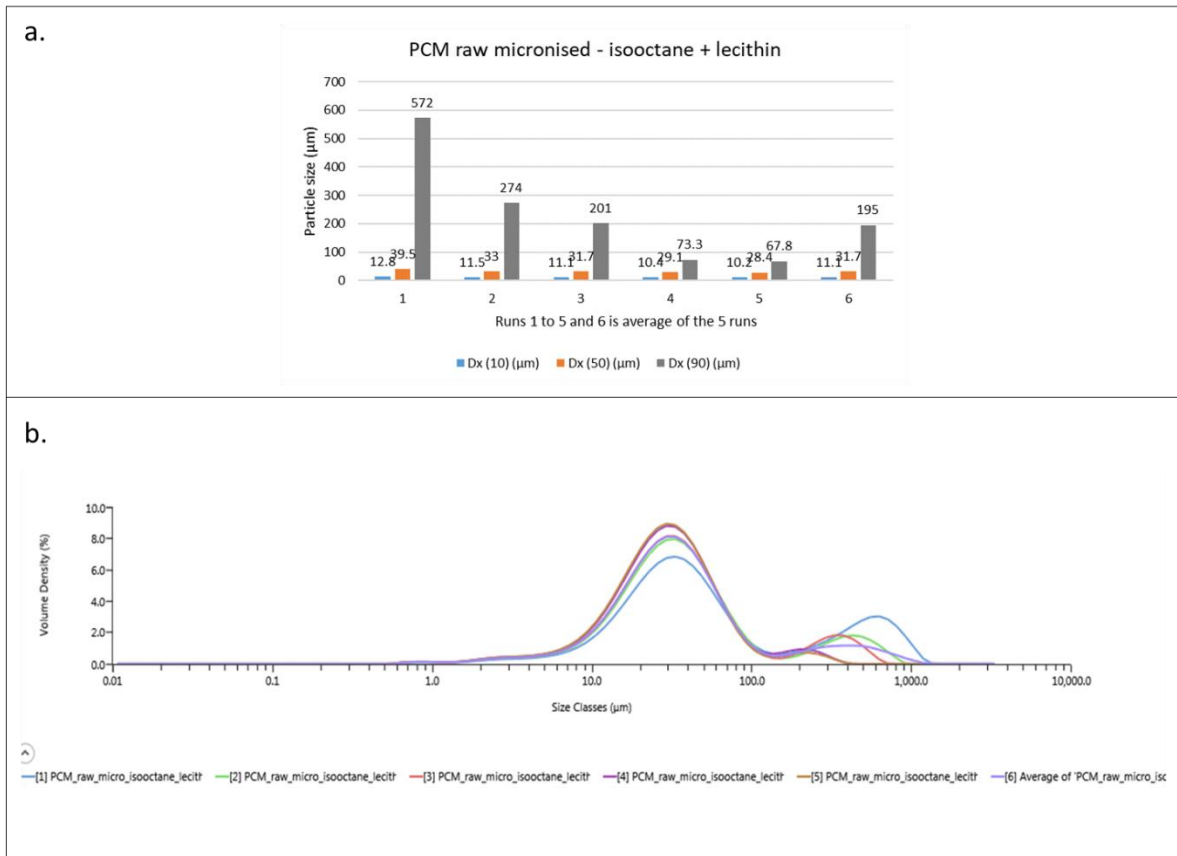


Figure D-4: Mastersizer analysis of micronised PCM using isooctane as dispersant with lecithin added to isooctane as surfactant. a.) D10, D50 and D90 values obtained for the 5 mastersizer runs 1-5 and 6 is the average value of the 5 runs. b.) Particle size distribution obtained for the 5 runs from mastersizer software.

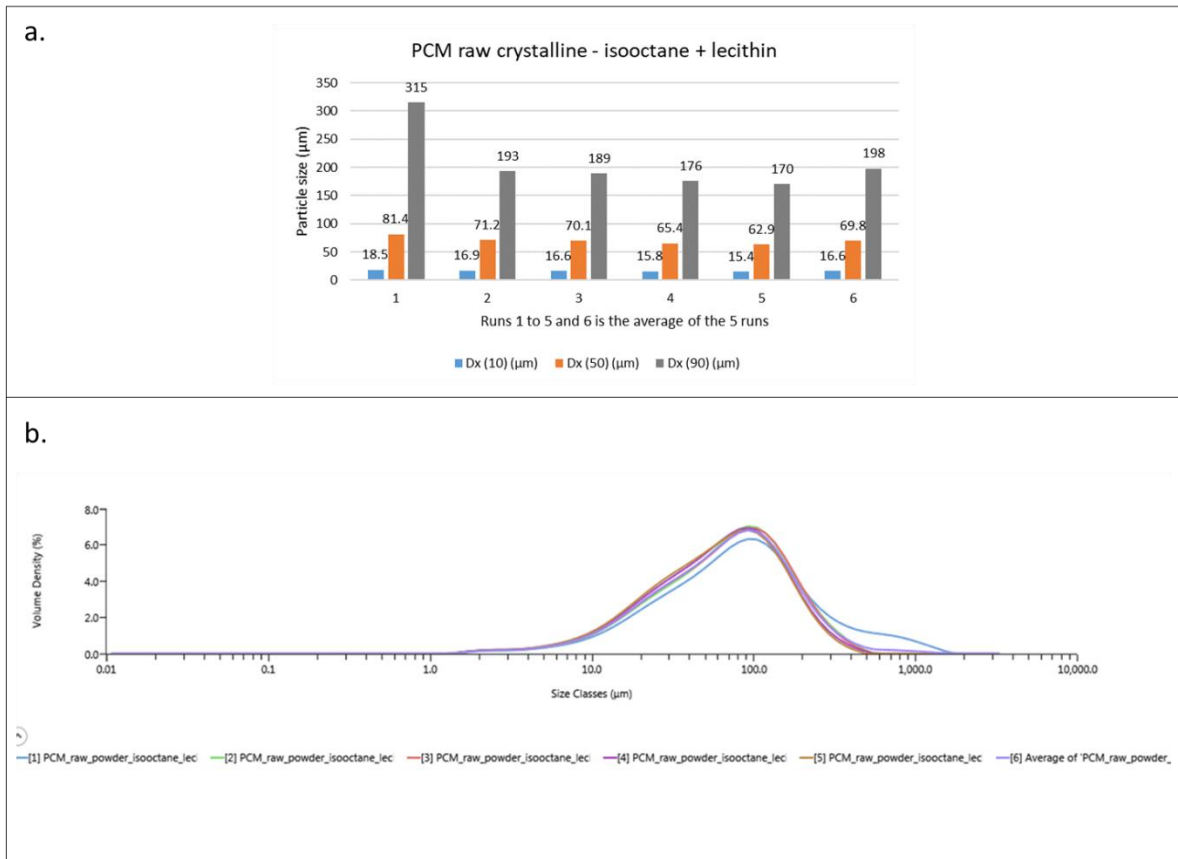


Figure D-5: Mastersizer analysis of crystalline PCM using isooctane as dispersant with lecithin added to isooctane as surfactant. a.) D10, D50 and D90 values obtained for the 5 mastersizer runs 1-5 and 6 is the average value of the 5 runs. b.) Particle size distribution obtained for the 5 runs from mastersizer software.

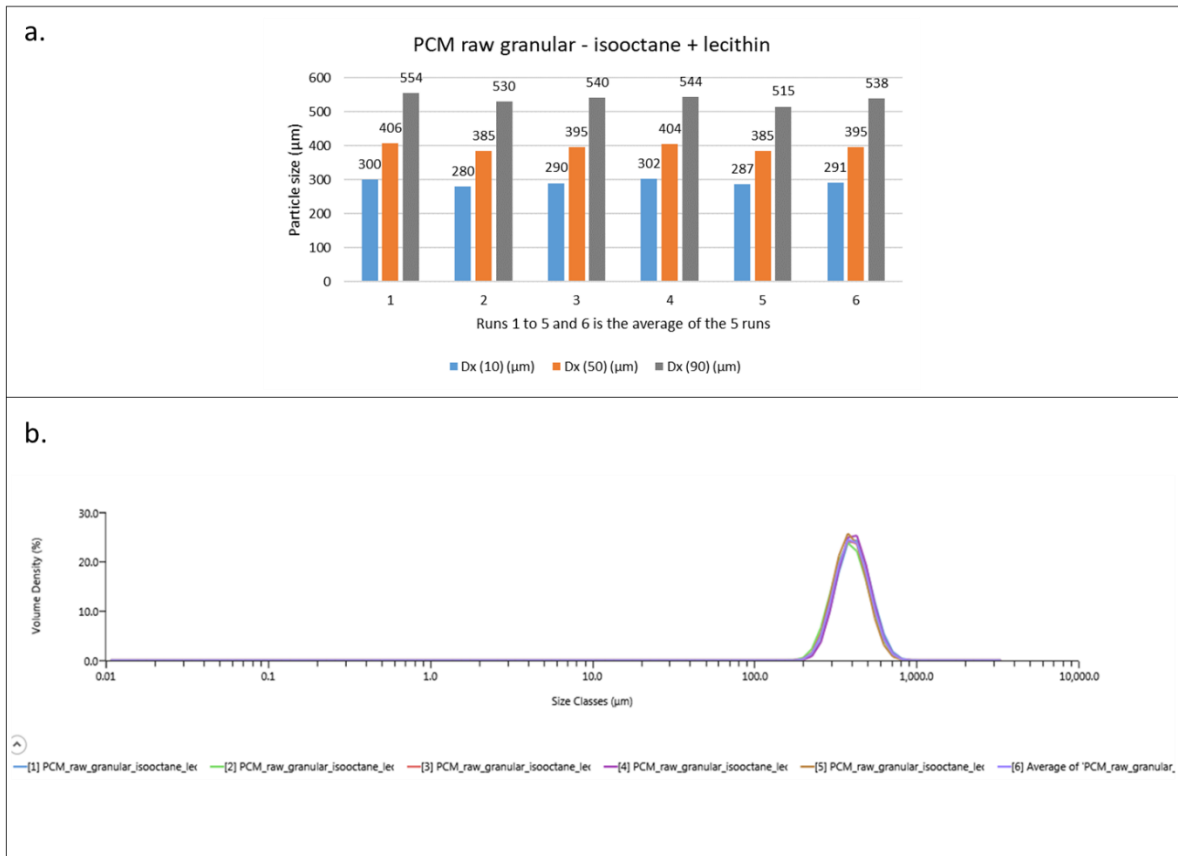


Figure D-6: Mastersizer analysis of granular PCM using isooctane as dispersant with lecithin added to isooctane as surfactant. a.) D10, D50 and D90 values obtained for the 5 mastersizer runs 1-5 and 6 is the average value of the 5 runs. b.) Particle size distribution obtained for the 5 runs from mastersizer software.

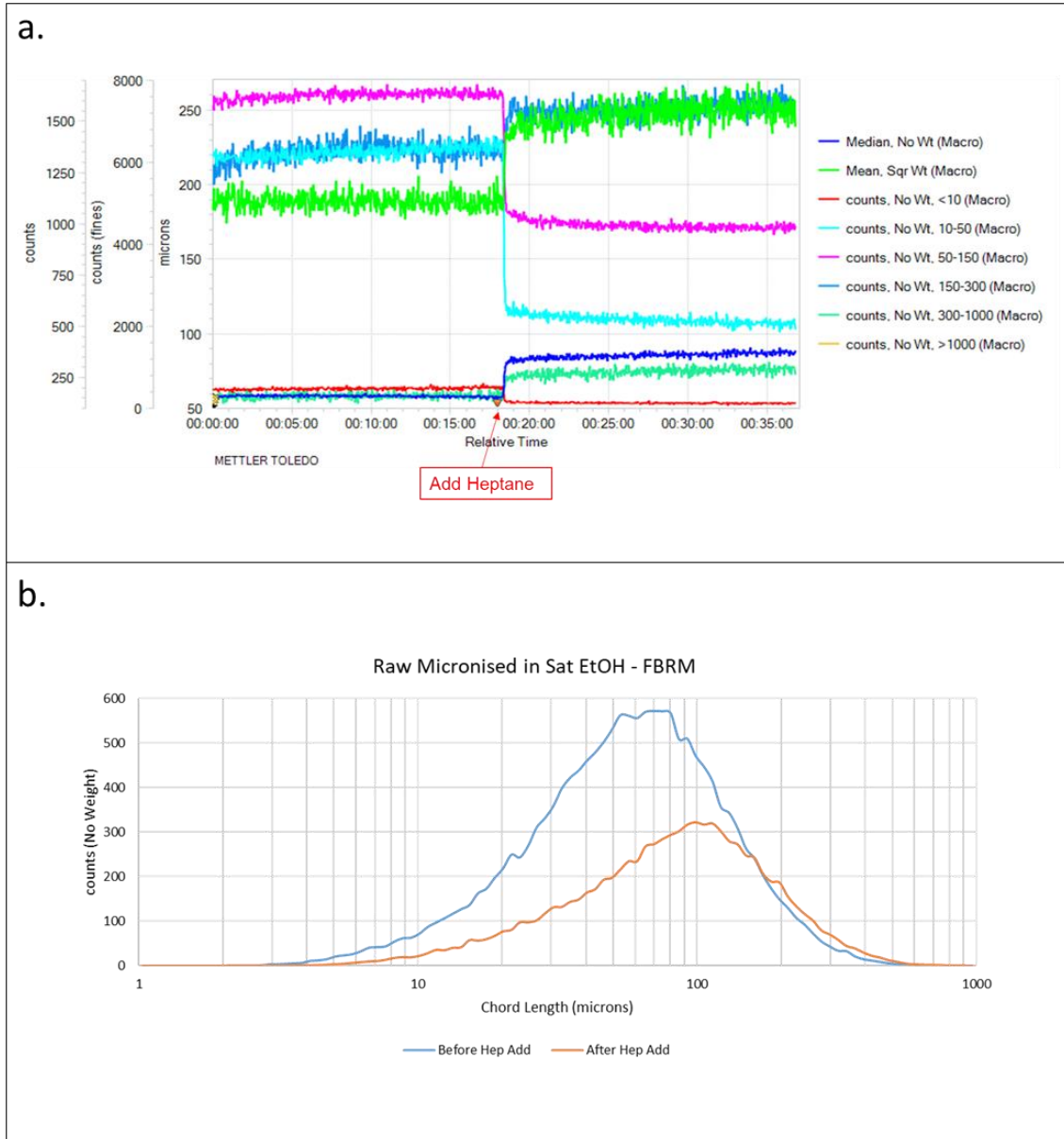


Figure D-7: a.) Particle size trend obtained from FBRM probe for raw micronised PCM in saturated ethanol, before and after heptane addition. b.) Chord length distribution obtained for raw micronised PCM in saturated ethanol, before and after heptane addition.

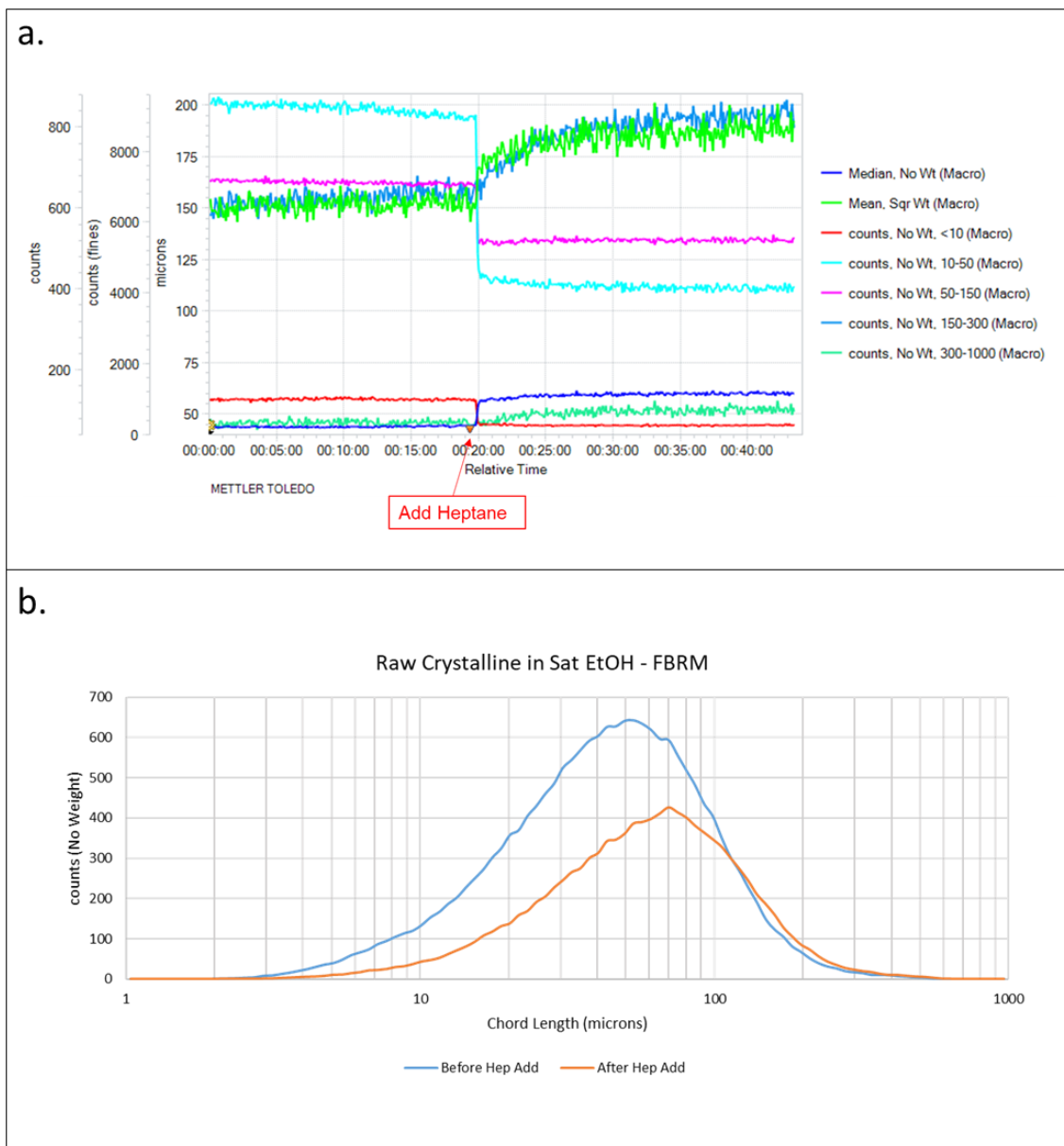


Figure D-8: a.) Particle size trend obtained from FBRM probe for raw crystalline PCM in saturated ethanol, before and after heptane addition. b.) Chord length distribution obtained for raw crystalline PCM in saturated ethanol, before and after heptane addition.

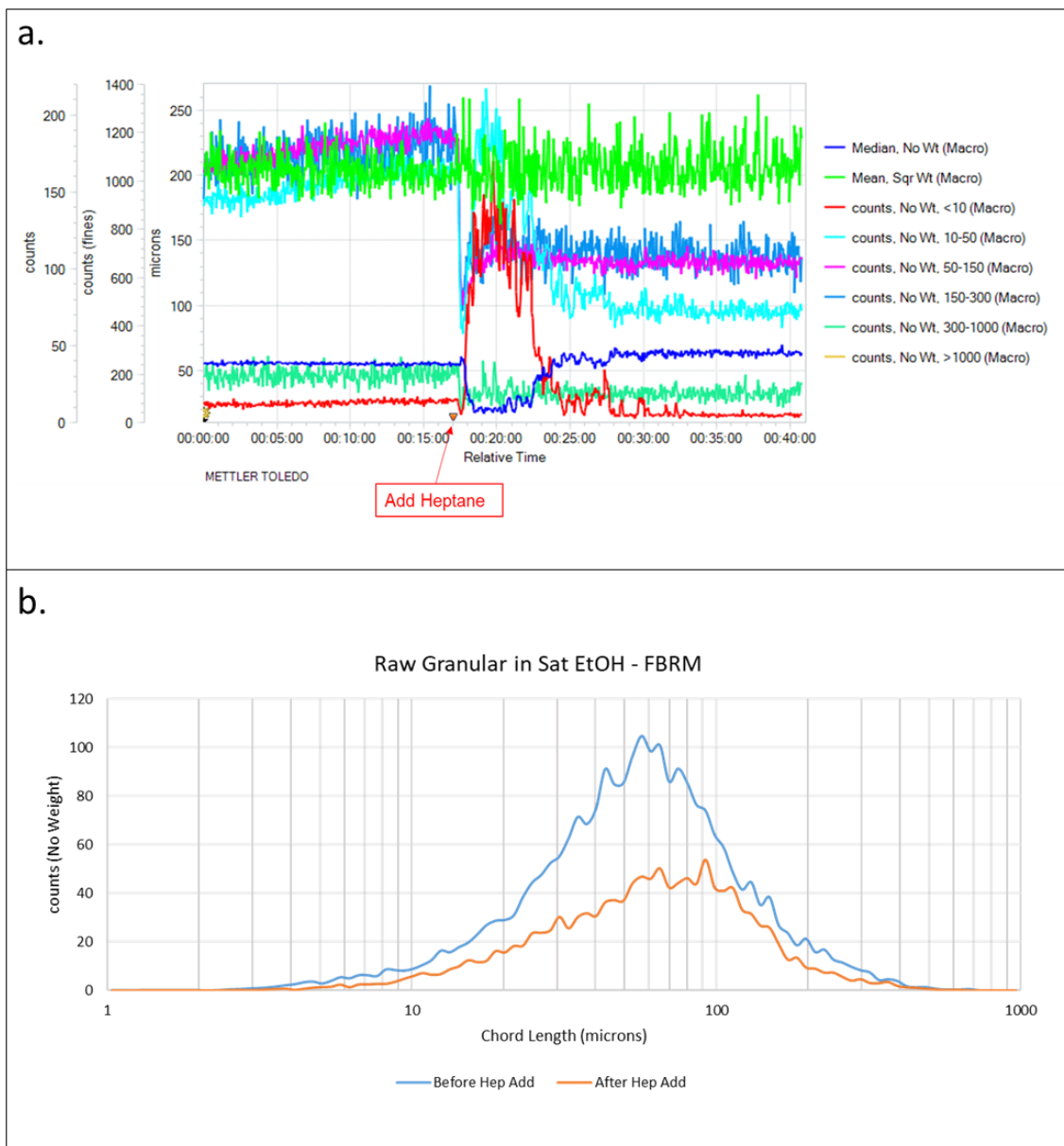


Figure D-9: a.) Particle size trend obtained from FBRM probe for raw granular PCM in saturated ethanol, before and after heptane addition. b.) Chord length distribution obtained for raw granular PCM in saturated ethanol, before and after heptane addition.

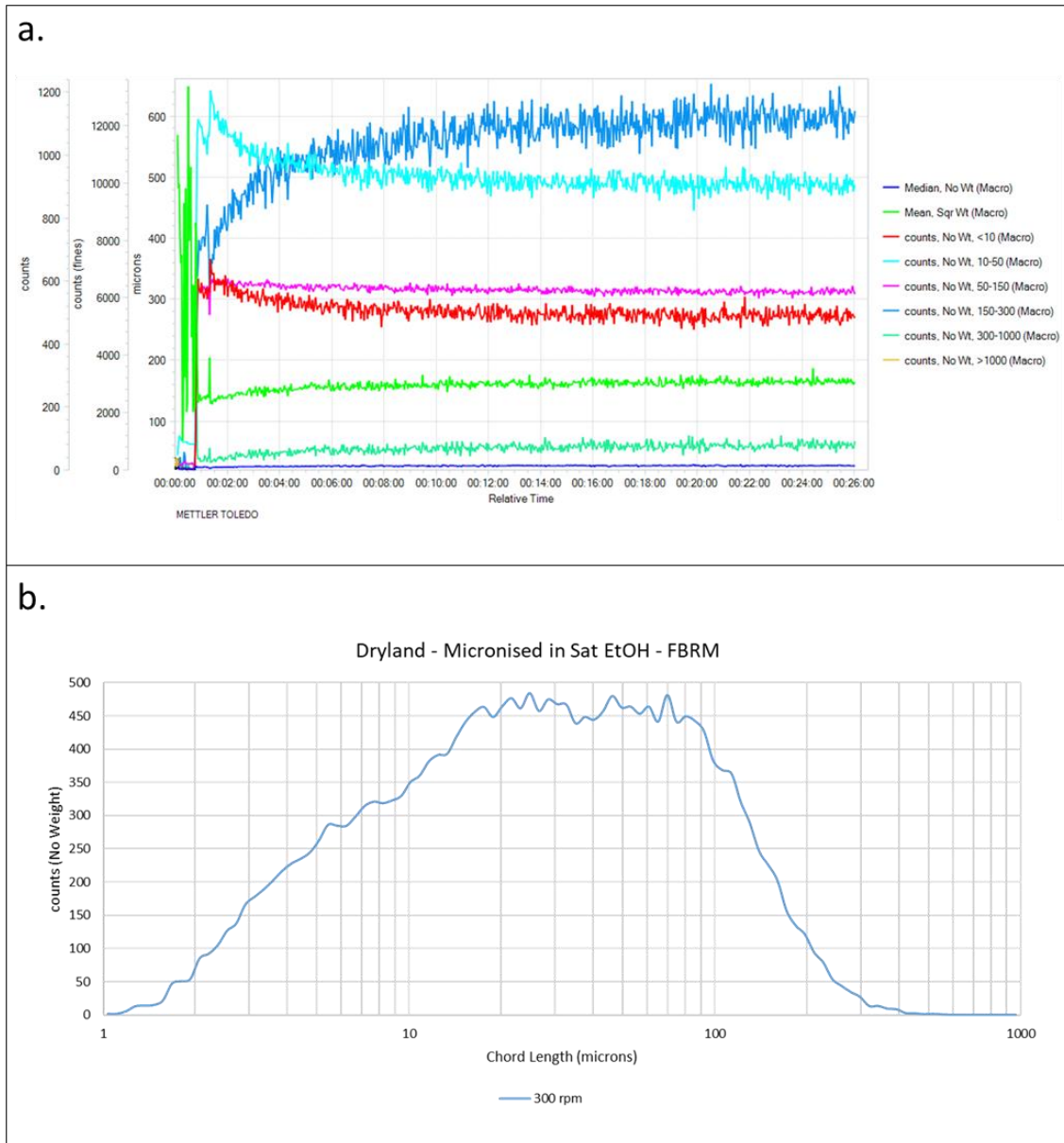


Figure D-10: a.) Particle size trend obtained from FBRM probe for filtered micronised PCM in saturated ethanol. b.) Chord length distribution obtained for filtered micronised PCM in saturated ethanol.

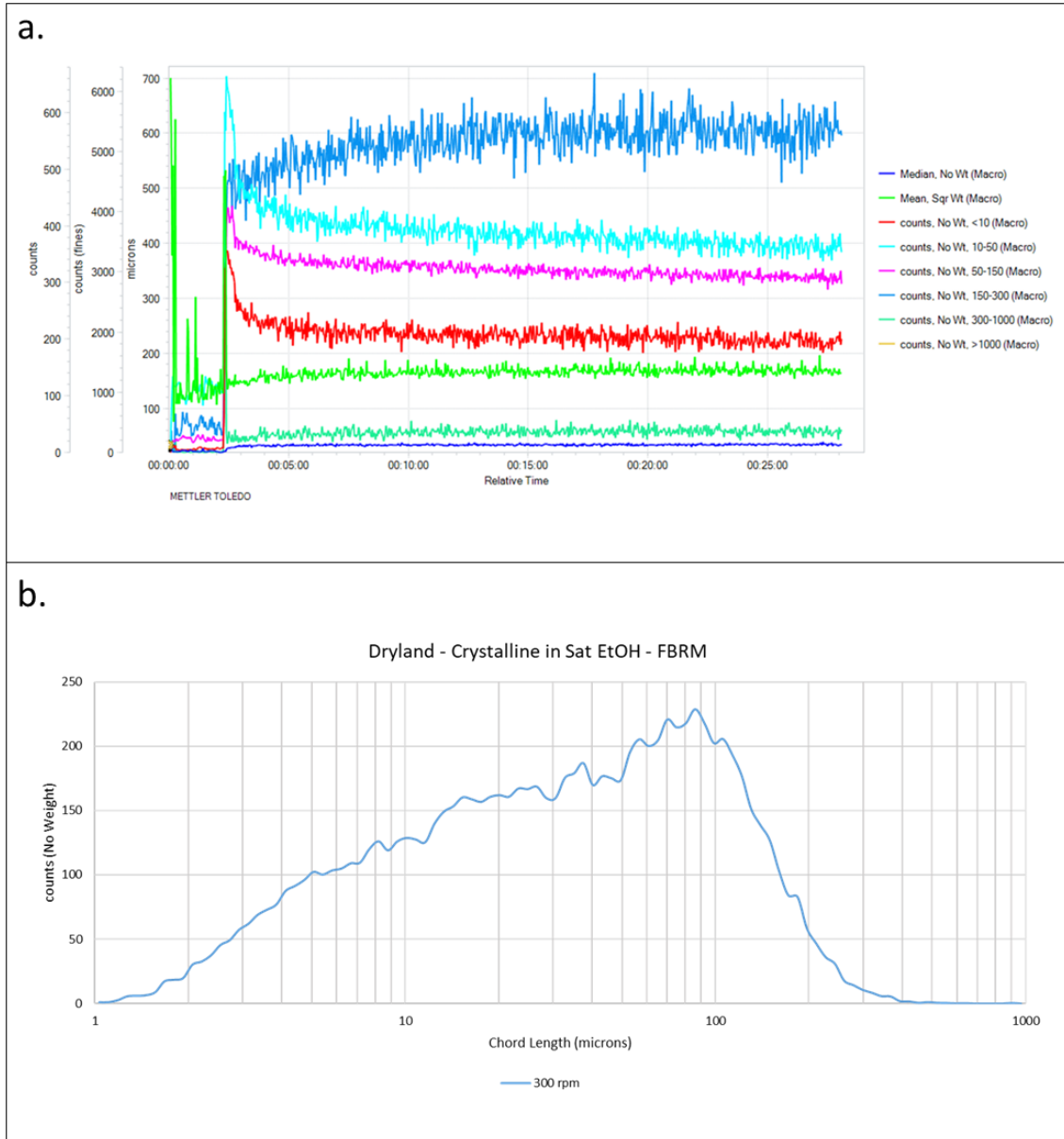


Figure D-11: a.) Particle size trend obtained from FBRM probe for filtered crystalline PCM in saturated ethanol. b.) Chord length distribution obtained for filtered crystalline PCM in saturated ethanol.

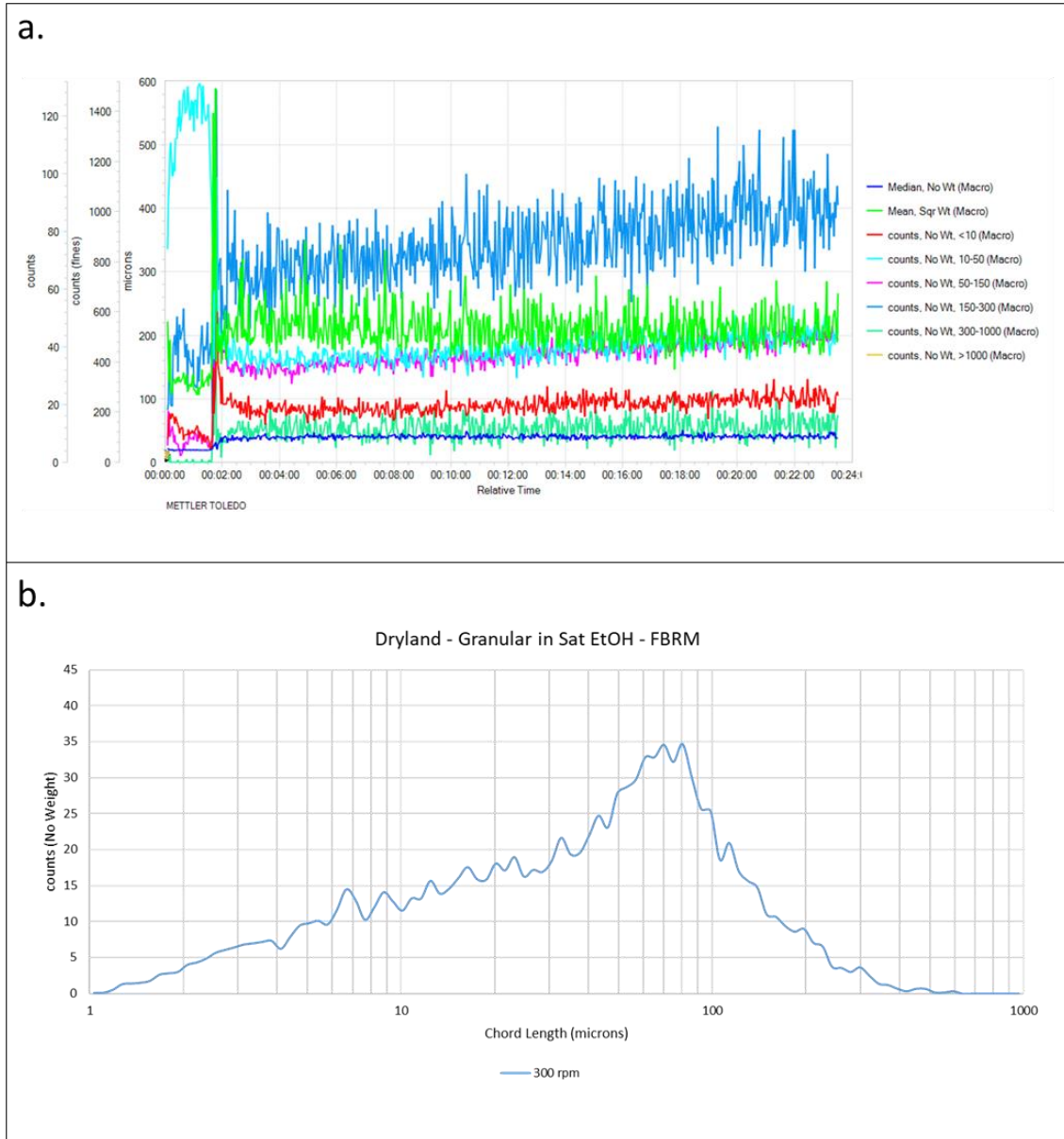


Figure D-12: a.) Particle size trend obtained from FBRM probe for filtered granular PCM in saturated ethanol. b.) Chord length distribution obtained for filtered granular PCM in saturated ethanol.

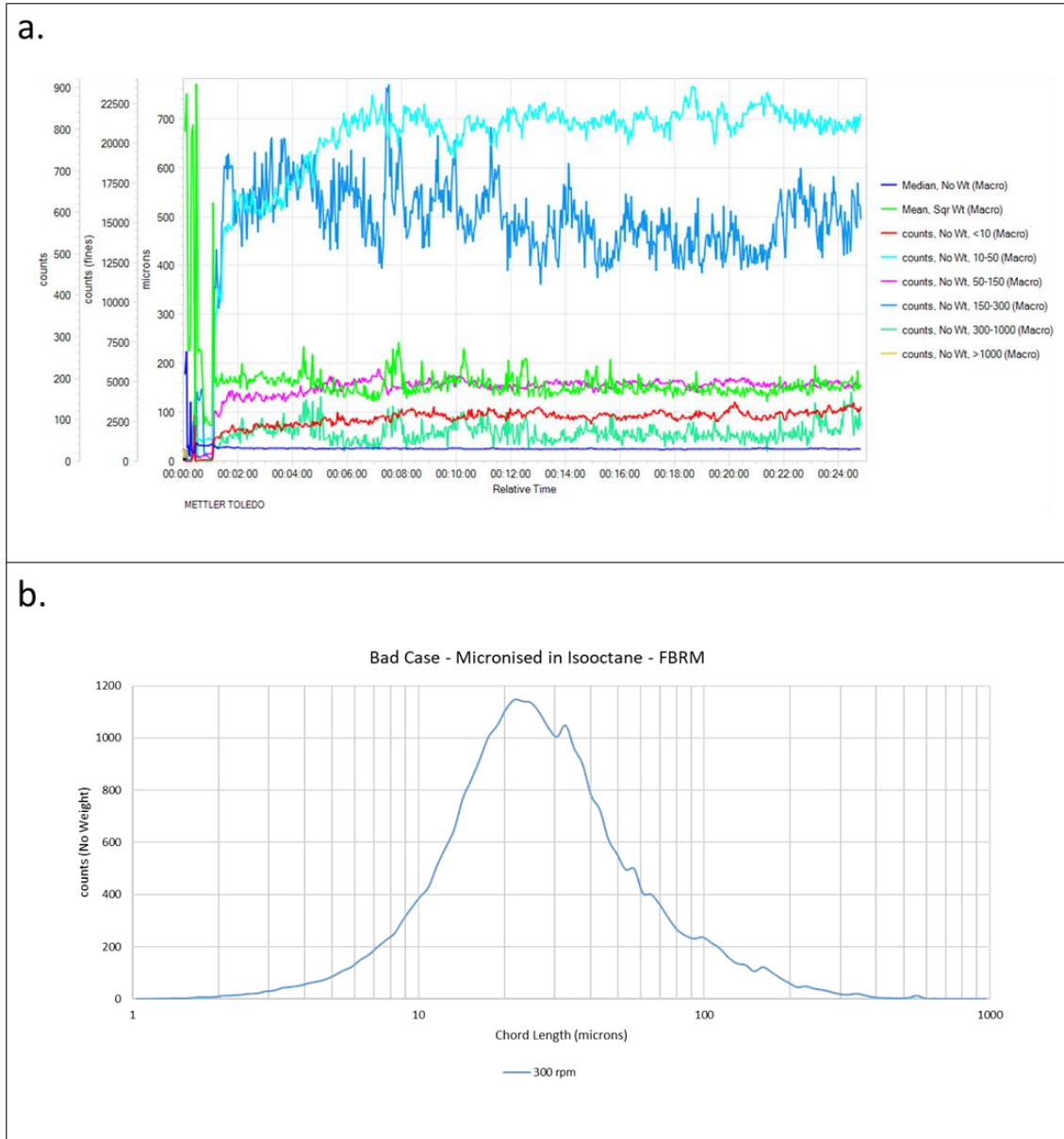


Figure D-13: a.) Particle size trend obtained from FBRM probe for micronised PCM washed cake – bad case scenario in isooctane. b.) Chord length distribution obtained for micronised PCM washed cake – bad case scenario in isooctane.

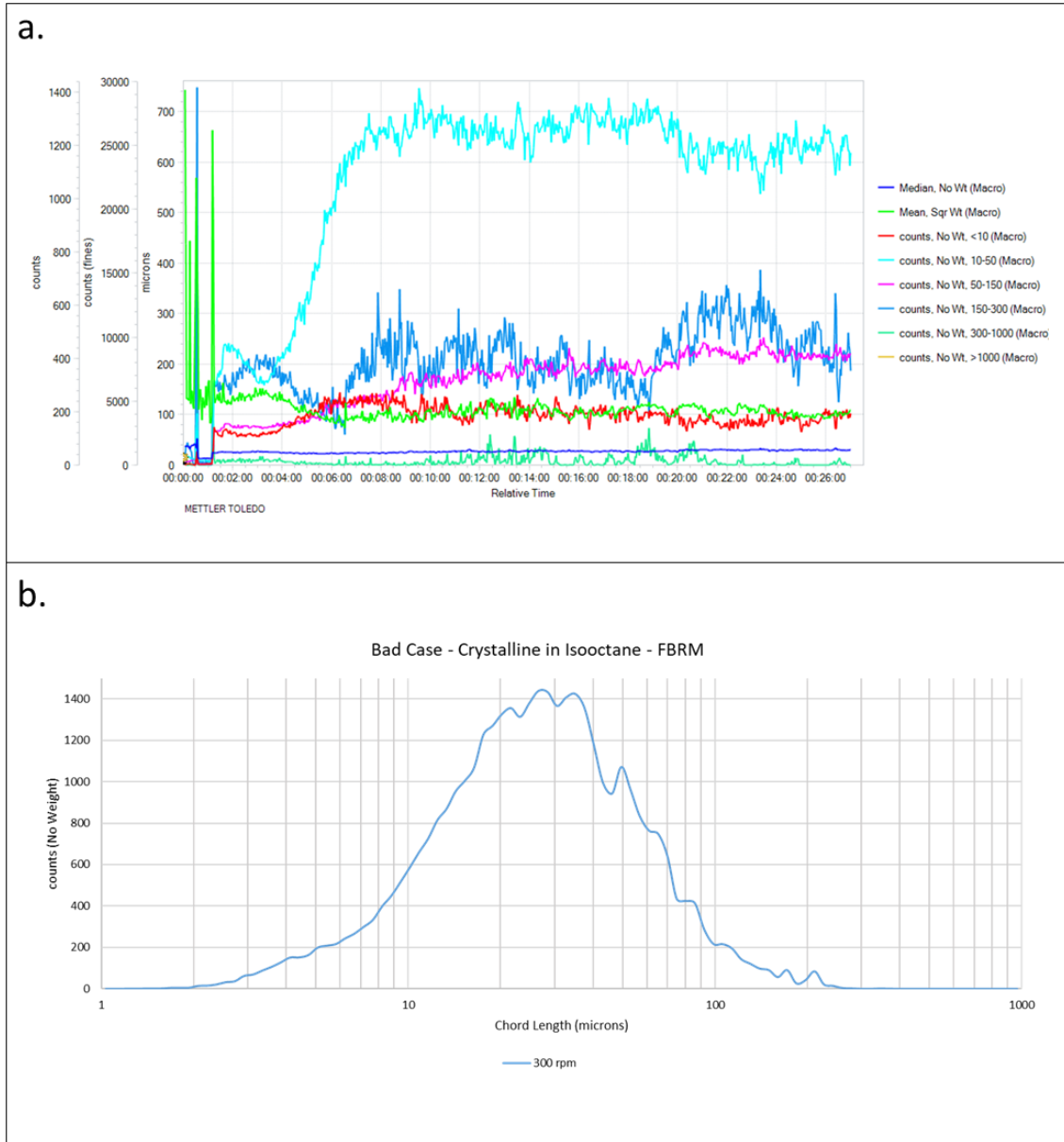


Figure D-14: a.) Particle size trend obtained from FBRM probe for crystalline PCM washed cake – bad case scenario in isooctane. b.) Chord length distribution obtained for crystalline PCM washed cake – bad case scenario in isooctane.

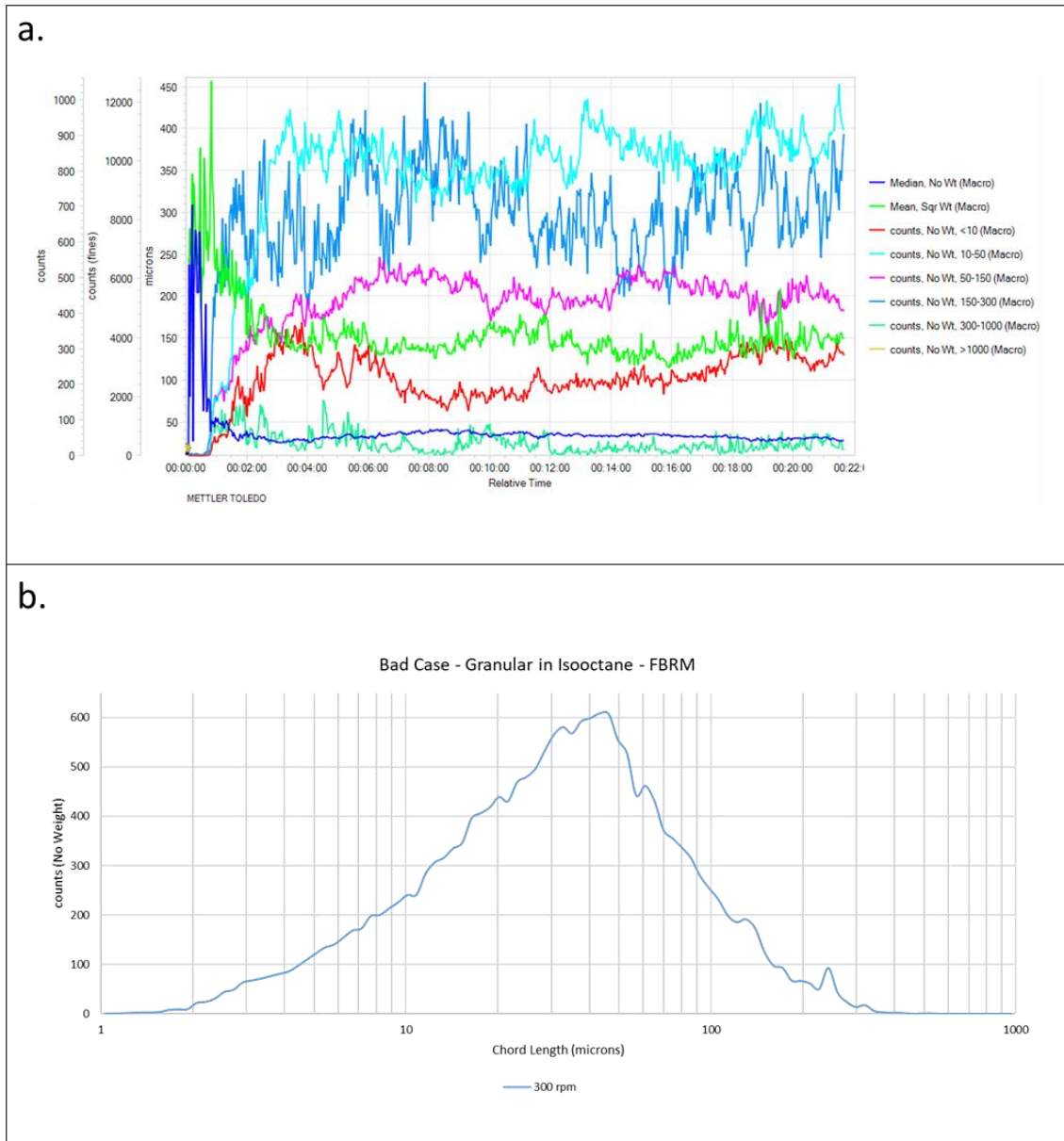


Figure D-15: a.) Particle size trend obtained from FBRM probe for granular PCM washed cake – bad case scenario in isooctane. b.) Chord length distribution obtained for granular PCM washed cake – bad case scenario in isooctane.

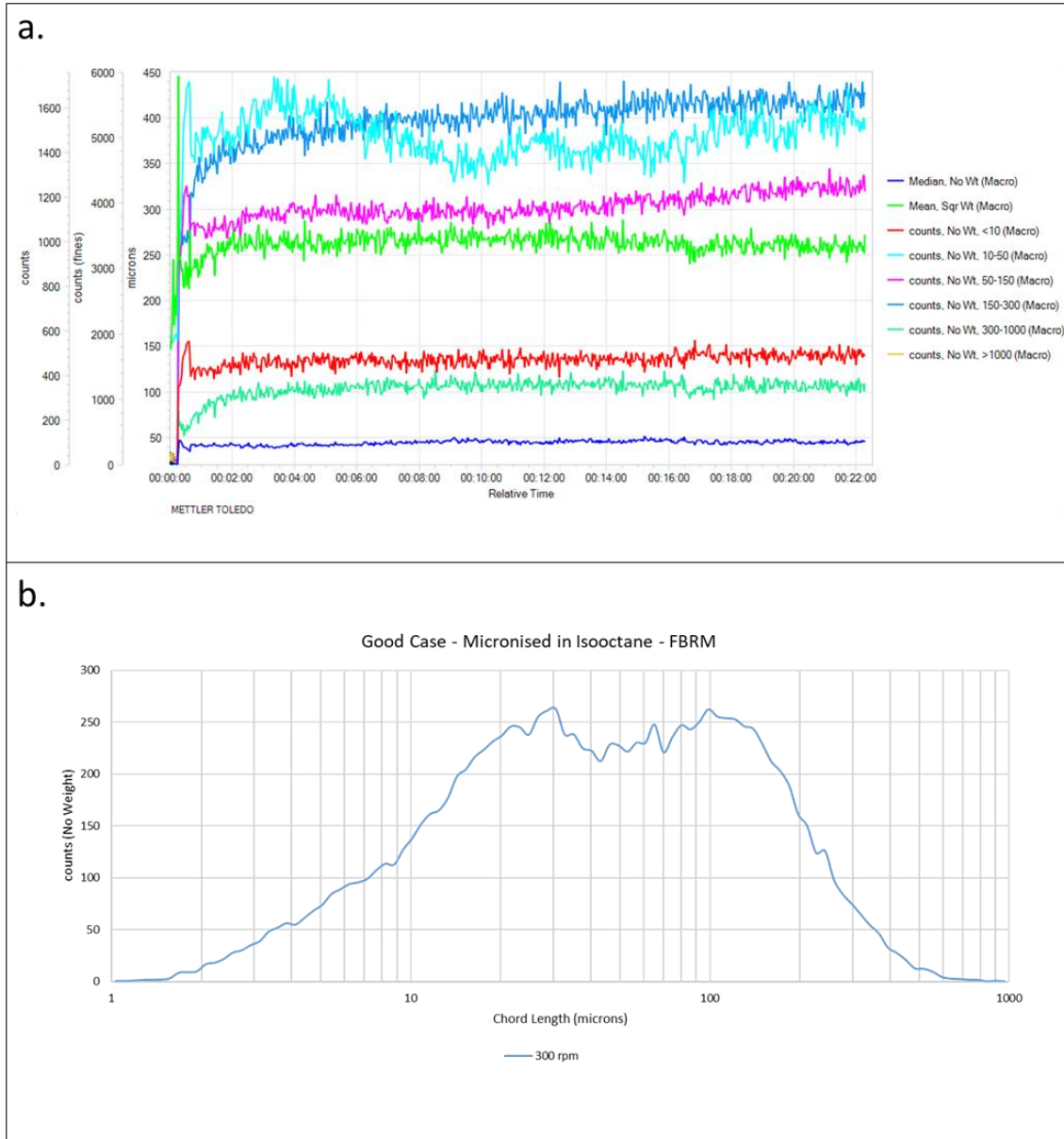


Figure D-16: a.) Particle size trend obtained from FBRM probe for micronised PCM washed cake – good case scenario in isooctane. b.) Chord length distribution obtained for micronised PCM washed cake – good case scenario in isooctane.

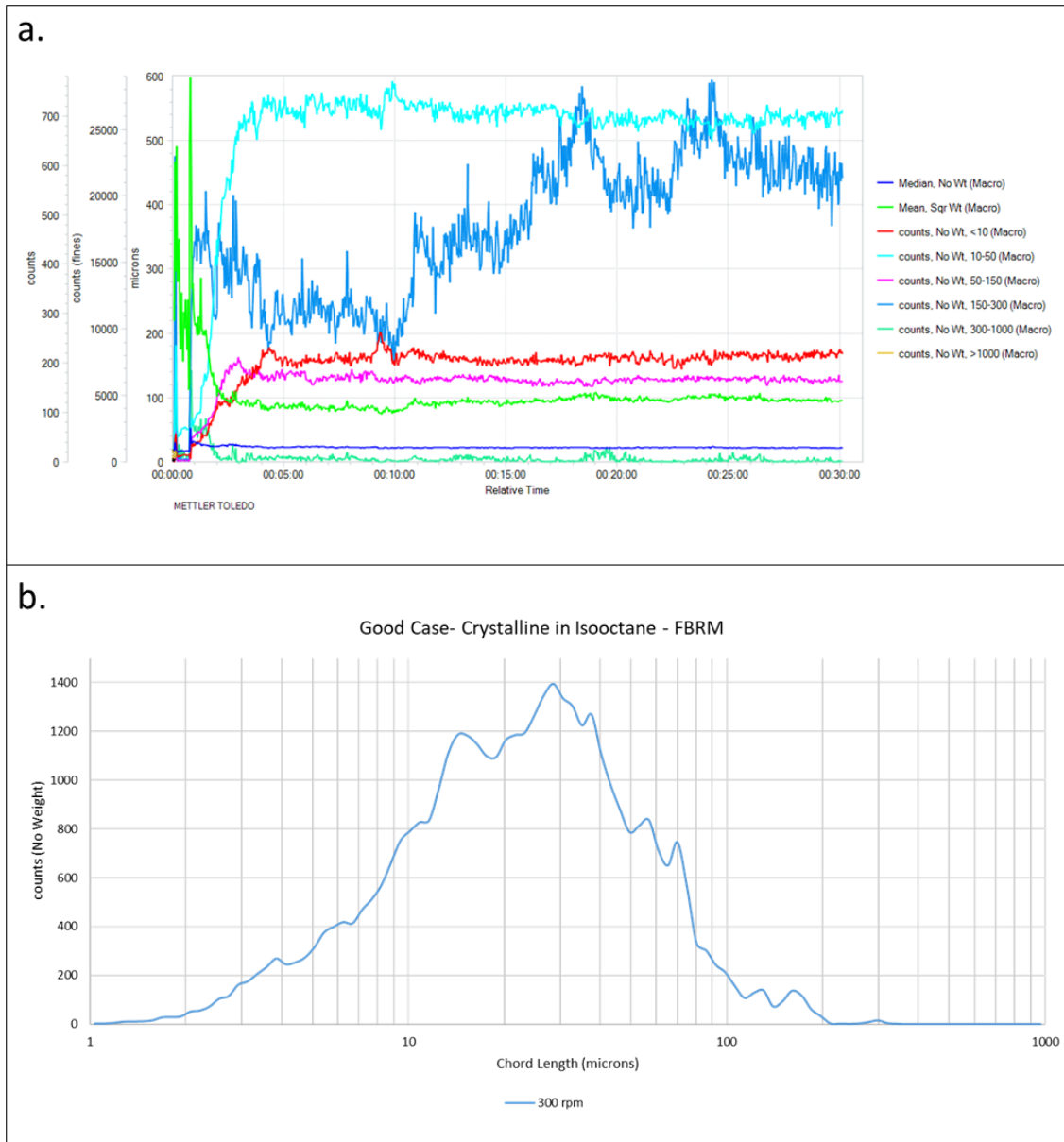


Figure D-17: a.) Particle size trend obtained from FBRM probe for crystalline PCM washed cake – good case scenario in isooctane. b.) Chord length distribution obtained for crystalline PCM washed cake – good case scenario in isooctane.

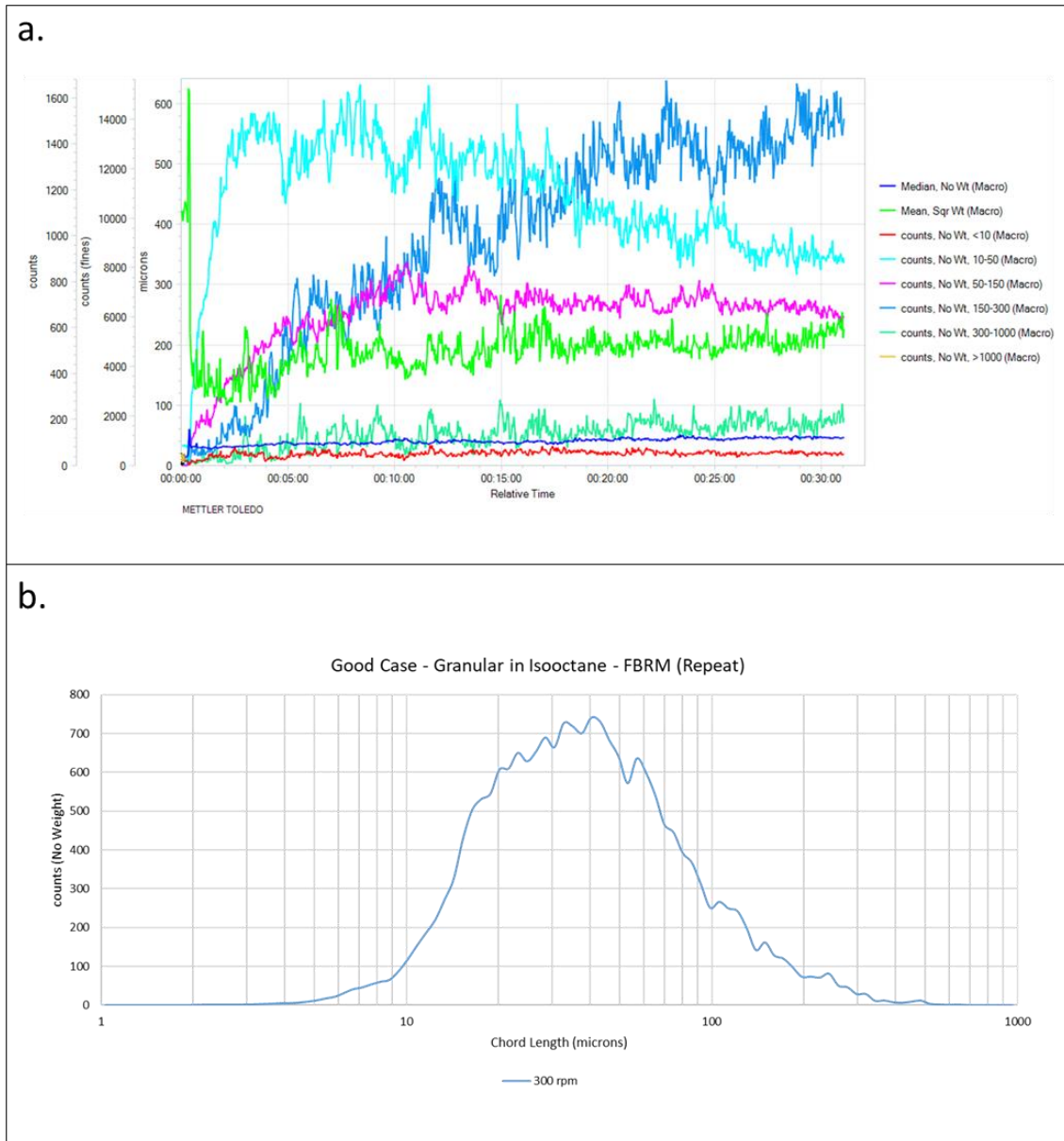


Figure D-18: a.) Particle size trend obtained from FBRM probe for granular PCM washed cake – good case scenario in isooctane. b.) Chord length distribution obtained for granular PCM washed cake – good case scenario in isooctane.

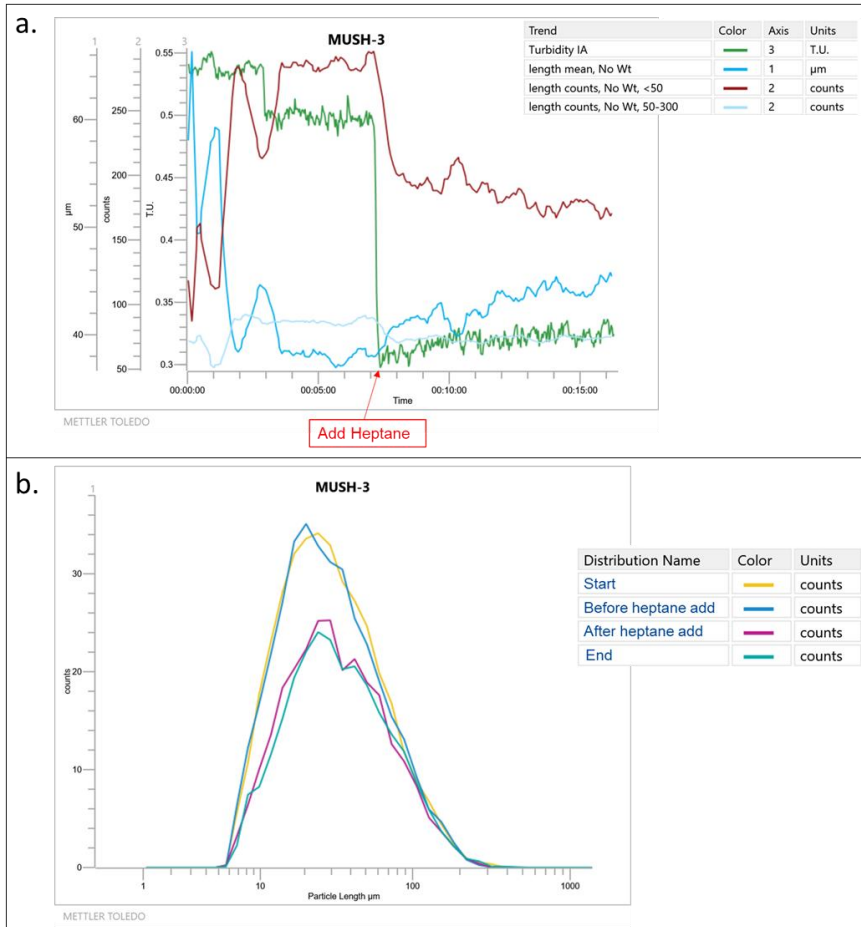


Figure D-19: Graphs obtained from crystalline PCM run carried out using easy viewer provided by Mettler Toledo. a.) Trend for turbidity and chord length obtained during the crystalline PSD analysis run. b.) Chord length distribution obtained for crystalline PCM during the different stages of the run.

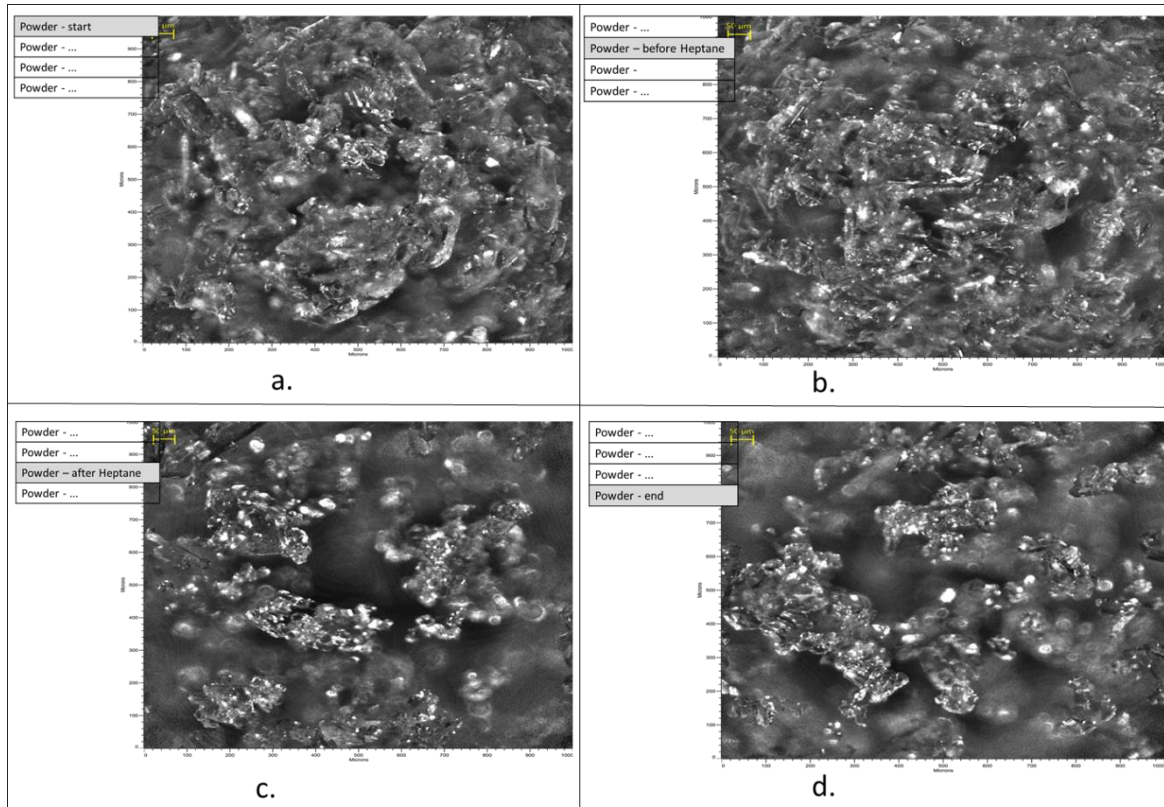


Figure D-20: Images obtained from easy viewer for crystalline PCM at different stages of the run. a.) Image of crystalline PCM particles at the start of analysis dispersed in saturated ethanol. b.) Image of crystalline PCM particles at the start of analysis dispersed in saturated ethanol before heptane addition. c.) Image of crystalline PCM particles after heptane addition to the slurry mixture, causing aggregation. d.) Image of crystalline PCM at the end of the run.

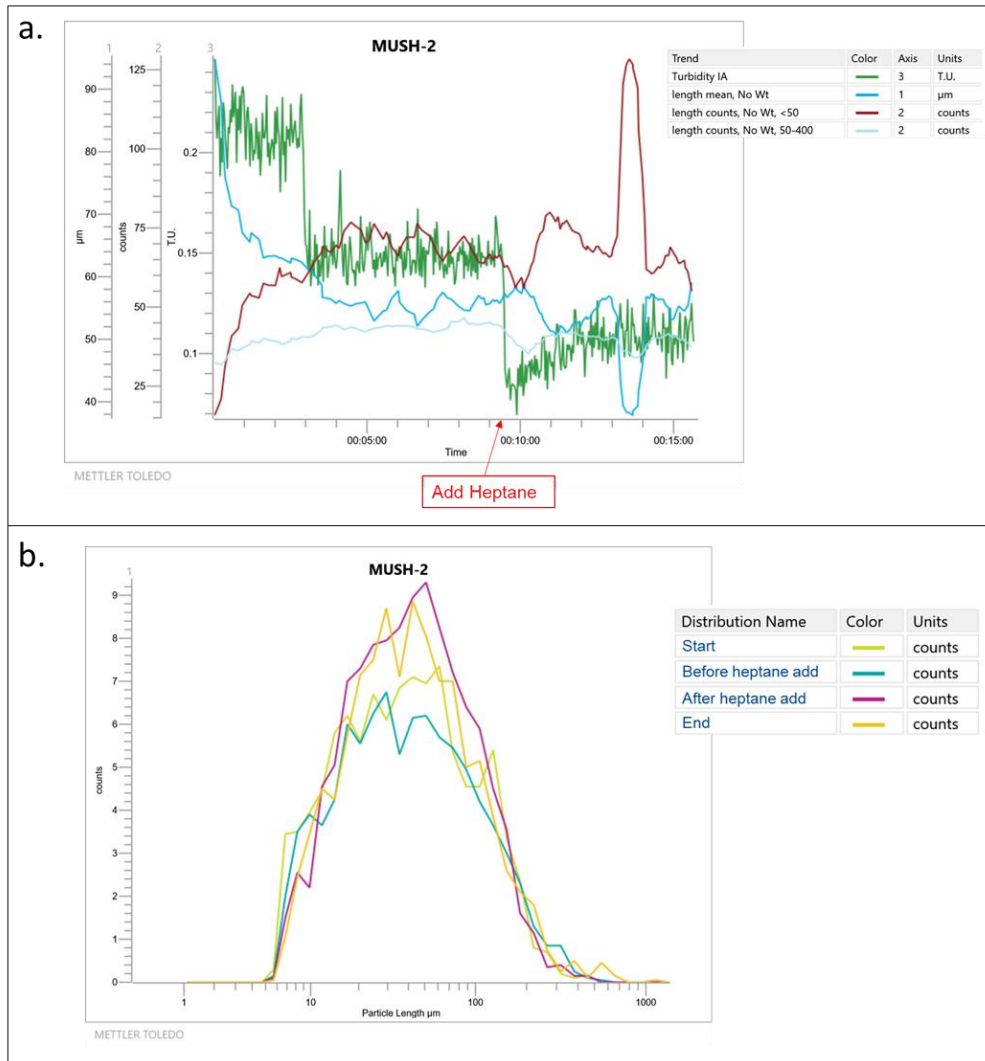


Figure D-21: Graphs obtained from granular PCM run carried out using easy viewer provided by Mettler Toledo. a.) Trend for turbidity and chord length obtained during the granular PCM PSD analysis run. b.) Chord length distribution obtained for granular PCM during the different stages of the run.

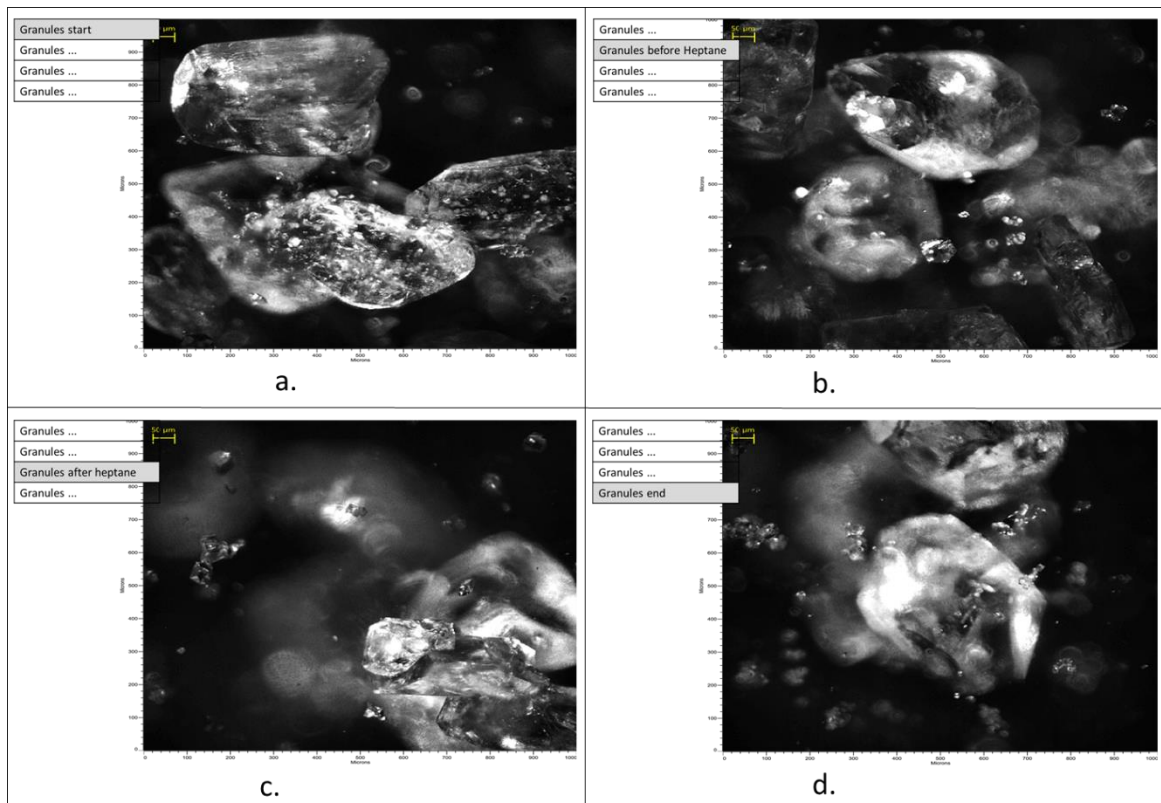


Figure D-22: Images obtained from easy viewer for granular PCM at different stages of the run. a.) Image of granular PCM particles at the start of analysis dispersed in saturated ethanol. b.) Image of granular PCM particles at the start of analysis dispersed in saturated ethanol before heptane addition. c.) Image of granular PCM particles after heptane addition to the slurry mixture, with some evidence that the smallest particles have aggregated slightly. d.) Image of granular PCM at the end of the run.